Investigation of host factors involved in *Legionella pneumophila* virulence

Sze Ying Ong

Submitted in total fulfilment of the requirements of the degree of Doctor of Philosophy

October 2017

Department of Microbiology and Immunology

The University of Melbourne

at the Peter Doherty Institute of Infection and Immunity

Produced on archival quality paper

ABSTRACT

Legionella pneumophila is an environmental organism that can become accidental bacterial pathogen when inhaled into the lungs of humans. On entering the lungs, *L. pneumophila* is phagocytosed by alveolar macrophages. However, instead of being removed accordingly by the host immune system, the bacteria rapidly establish a *Legionella*-containing vacuole (LCV) and replicate intracellularly. The ability to establish the LCV relies on a type IV secretion system, also known as the Dot/Icm system. The Dot/Icm system is essential for virulence and delivers a large repertoire (> 300) of effector proteins into infected host cells. These effector proteins modulate a wide range of host processes such as vesicle trafficking, host protein translation, regulation of GTPases and apoptosis.

Despite the phenomenal number (one of the highest among known bacterial pathogens) of effector proteins translocated by *L. pneumophila* into host cells, effector secretion is not detected until the bacterium contacts a host cell. This is in contrast to other bacterial pathogens such as enteropathogenic *Escherichia coli* or *Salmonella* sp., which can be induced to secrete effector proteins via a type III secretion system into liquid bacteriological cultures. The interactions that occur between the host cells and *L. pneumophila* in order to activate the Dot/Icm system are poorly understood.

In this study, we used an RNAi approach to screen for host factors that contribute to Dot/Icm effector protein translocation. A genome-wide siRNA screen was performed that individually silenced each protein-coding gene in the human genome (~ 18 000 genes) and monitored for any changes in translocation of the prototypic effector protein, RalF, after *L. pneumophila* infection. This screen identified 119 genes whose silencing resulted in increased translocation of RalF while knockdown of 321 genes resulted in decreased translocation. Strikingly, we found that genes in the ubiquitination pathway were significantly over-represented among the factors that contribute to the efficiency of RalF translocation during *L. pneumophila* infection. We further showed these ubiquitination factors also influence translocation of another effector protein, SidB. This suggested that the host ubiquitination pathway was important in mediating Dot/Icm effector protein translocation. Interestingly, we also found that two of the host ubiquitination factors that facilitated effector protein translocation were also important for *L. pneumophila* intracellular replication. These

were UBE2E1 and CUL7; an E2-conjugating enzyme and E3 ligase respectively. On top of host ubiquitination factors, this screen also identified many other host factors that were not previously appreciated as having possible roles in Dot/Icm mediated effector protein translocation.

Given the finding that ubiquitination is important for Dot/Icm effector protein translocation and that the LCV is an ER-like compartment, we hypothesised that this process occurred in a manner equivalent to retrotranslocation, a process that moves ubiquitinated protein substrates from within the ER into the cytoplasm. Unfortunately, we were not able to conclude this as silencing gene expression of the ATPase, p97, which drives this process, resulted in significant host cell death. To this end, the significance of ubiquitination pathways on Dot/Icm mediated effector protein translocation is yet to be elucidated. Nevertheless, this study has contributed significantly to our understanding of host-*Legionella* interactions and provided much new information about the plausible interplay between the host cell and the Dot/Icm system. Finally, we demonstrated the utility of genome-wide high-throughput screening in human cells to study *L. pneumophila* pathogenesis.

DECLARATION

This is to certify that:

i. This thesis comprises only my original work towards the Doctor of Philosophy except where indicated in the preface
ii. Due acknowledgement has been made in the text to all other material used
iii. This thesis is fewer than 100,000 words in length, exclusive of tables, maps, bibliographies and appendices

Sze Ying Ong
Department of Microbiology and Immunology,
The University of Melbourne,
at the Peter Doherty Institute for Infection and Immunity

PREFACE

In accordance with the regulations of The University of Melbourne, I acknowledge that some of the work presented in this thesis was collaborative. Specifically:

In chapter 3, optimisation of the genome-wide RNAi screen was performed with the assistance of Ralf Schülen.

In chapter 3, the pXDC61:LseA and pXDC61:LseB constructs were made by Ralf Schülen.

In chapters 3, 4 and 5, the pXDC61:RalF construct was made by Ralf Schülen.

In chapter 4, the genome-wide RNAi screen was performed with the assistance of Ralf Schülen. Operation of transfection robot was performed by Daniel Thomas while data was analysed with assistance from Piyush Madhamshettiwar (Victorian Centre for Functional Genomics, Peter MacCallum Cancer Centre).

In chapter 5, the *L. pneumophila* 130b Δ*icmSW* was constructed by Ralf Schülen.

The remainder of this thesis comprises only my original work.

LIST OF PUBLICATIONS ARISING FROM THIS THESIS

This thesis contains material that is published or is currently in preparation for publication:

Ong SY, Schülen R, Thomas D, Madhamshettiwar P, Luu J, Handoko Y, Freytag S, Bahlo M, Simpson KJ, Hartland EL (2017). Genome-wide RNAi screen identified host ubiquitination as important for *Legionella pneumophila* Dot/Icm mediated effector translocation.

ACKNOWLEDGEMENTS

Completion of this PhD will not be possible without the help, support and guidance of many people, all of whom needs to be properly acknowledged.

Firstly, thank you Liz for taking me on as a research assistant in 2010. Back then, I really appreciated the opportunity you gave me even though I came fresh out of Honours without any real experience in Microbiology. Even more surprising for me is when you fully supported and encouraged me to complete a PhD in your lab 2 years later. I really appreciate the confidence you had in me and I am extremely grateful that you allowed me to take on such a big and crazy project in my PhD. Thank you for all your guidance and encouragement over the years, for giving me confidence to do and take on so many things that I otherwise will have been too scared to do. Your little timely push always does the trick in making me get over myself and get on with the task. I have grown and learnt so much under your supervision during my PhD, be it how to think and run experiments as a scientist to enthusiasm for science. Till now, I still think that I am extremely lucky that we crossed paths many years ago and you graciously took me on. So once again, a big THANK YOU!

Thank you also to my second supervisor, Ralf. You have taught me all that I ever know about molecular biology and *Legionella*. You are an incredibly patient man who always had time for me and answered all my naive questions. Your meticulous approach to science is something that I truly admire and I am indebted to you for all the guidance you gave me. Without you, the RNAi screen will have been a lot harder, both physically and mentally! The daily trips to Peter Mac were more enjoyable with your company and those sneaky lunches that we squeeze in are something I looked forward to. I have learnt a lot from you and you had a significant role in making me the scientist (and person) I am today. I really couldn't have asked for a better lab supervisor. Finally, thank you also for your friendship. It helped me get through PhD without going insane.

Thank you also to Shivani for the guidance towards the end of my PhD. You made sure my thesis drafts were not an embarrassment before they were submitted to Liz.

They could have been torn to shreds if you hadn't so generously given up some of your time to help me.

To my PhD buddies in the Hartland lab – Cristina, Tania and Ying Z, thank you for 'being in it' together! It was fantastic having company and people who are going through the same thing together. You girls motivate me to work harder and push me to do things which I would not have done if I did not have you guys doing it with me together. Being the last in the gang to write up, I also probably had the easiest job putting my thesis together as I had all your theses to look at as a guide/template. Thank you for all the thesis help! Cristina, thank you for making me sit down and submit my 80-word summary. I would still have been umm-ing and ahh-ing about it if you hadn't put your foot down and got me to submit it. Also, thank you for all the free rides I get at the end of the day so that I don't have to go onto the dreaded tram to get home! Finally, our birthday celebrations, dinners and drinking sessions were critical in helping me make it to the end of my PhD, so thank you for all the fun over the years too! We might have gone on different paths now, but this experience together is something that will stay with us forever.

Ka Yee, thank you for being my listening ear in the lab. You are the best lab bench buddy and I can truly say that no one else had been able to replace you since you left the lab. You had the wisdom of making it through a PhD and always give me intelligent opinions in my scientific dilemmas. You never fail to put things into perspective and making me feel like I actually know something! Of course, you and Ying Z always have the best gossip on asian celebrities and TV shows to keep me up-to-date. So, thank you for everything over the years and the friendship we formed.

A big thank you to all past and present Hartland lab members for welcoming me into the lab. The ski trips, dinners, Friday drinks and Thursday badminton were highlights of my PhD. Gina thank you for being the unlikely friend, I really appreciate it! Clare thank you for making sure the lab functions.

Thank you to everyone at VCFG. Kaylene, thank you for your knowledge and guidance in setting up the RNAi screen. Dan, Jennii and Yanny, thank you for running the robots, for always fitting us into your schedule and all your help in

making sure our experiments are performed without much delay all the time. Piyush and Kate in helping me analyse all the data. Thank you also to Odilia and Hayley, who were on my PhD committee and provided me with useful suggestions and guidance over the years.

Last but definitely not least, THANK YOU to my family and friends. Even though you didn't understand the science world, you were always happy for my achievements and supportive of me. Thank you to my big brother Alex and the sis-in-law Arielle for everything. I know that I would not have the luxury of a life away from home, pursuing my own interests, if I did not know that you would be there for the family in times of needs. Thank you to my sister, Hwee Hwee. As much as you annoy me with your mess at home and lack of cooking skills, it was as much fun sitting on the couch and watching stupid TV shows while snacking on chips at the end of every day. I wouldn't have asked for another person to be my housemate. Also, thank you for showing me all those funny dog videos and other fun times, I really needed those laughs! Thank you to the larrikin of the family, my baby brother Matthew. While you stressed me out with your carefree nature, it helped me looked at the lighter side of things. Lastly, thank you to my mom and dad who go above and beyond in everything you do, and for always supporting me in whatever I do. You instilled hard work in me since young and it is this very virtue that has truly seen me through this PhD. Even though I know that you prefer having me closer to you guys in Singapore, you are un-selfish and even encourage me to go see the world and spread my wings. I am very appreciative that you had given me with the opportunity to go to university, which you both did not have. And to allow me to go to an overseas university when I was only 16, this is something I will forever be indebted to you. I hope this PhD will make you proud. Thank you.

ABBREVIATIONS

The following abbreviations have been used throughout the thesis:

%	Percentage
°C	Degrees Celsius
~	Approximate
ACES	N-(2-acetamido)-2-aminoethanesulfonic acid
ADP	Adenosine diphosphate
AEC	Airway epithelial cell
AIM2	Absent in melanoma 2
AMP	Adenosine monophosphate
ARF	ADP ribosylation factor
ATP	Adenosine triphosphate
BCYE	Buffered charcoal yeast extract
BiP	Binding protein
BNIP3	BCL2 Interacting Protein 3
bp	Base pair
cAMP	Cyclic AMP
CCV	*Coxiella* containing vacuole
CFU	Colony forming unit
CRISPR	Clustered regularly interspaced short palindromic repeats
CV	Coefficient of variation
DC	Dendritic cell
DFA	Direct fluorescent antibody
dH_2O	Distilled water
DNA	Deoxyribonucleic acid
dNTP	Deoxynucleotide triphosphate
dsRNA	Double-stranded RNA
DUB	Deubiquitinating enzyme
EHEC	Enterohemorrhagic *E. coli*
EPEC	Enteropathogenic *E. coli*
ERAD	ER associated degradation
ER	Endoplasmic reticulum
FBS	Fetal bovine serum
FRET	Fluorescence resonance energy transfer
GAP	GTPase activating protein
GDP	Guanosine diphosphate
GEF	Guanine nucleotide exchange factor
GRIP	Golgin-97, RanBP2alpha, Imh1p and p230/golgin-245
GTP	Guanosine triphosphate

h	Hour(s)
IFA	Indirect fluorescent antibody
IFN	Interferon
IκB	Inhibitor of NF-κB
IL	Interleukin
JNK	c-Jun N-terminal kinase
kDA	Kilodalton
LAMP-1	Lysosomal-associated membrane protein 1
LB	Luria-Bertani
LC3	Autophagy specific light chain 3
LCV	*Legionella* containing vacuole
LPS	Lipopolysaccharide
LRR	Leucine-rich repeat
MAPK	Mitogen-activated protein kinase
MHC	Major histocompatibility
miRNA	MicroRNA
min	Minute(s)
MOI	Multiplicity of infection
mRNA	Messenger RNA
MVB	Multivesicular body
MyD88	Myeloid differentiation primary response gene 88
NDP52	Nuclear dot protein 52kDa
NEL	Novel E3 ligase
NK	Natural killer
NF-κB	Nuclear factor kappa-light-chain-enhancer of activated B
Nle	Non-lee encoded effector
NLR	Nod-like receptor
OD	Optical density
OPTN	Optineurin
PAL	Peptidoglycan-associated lipoprotein
PAMP	Pathogen-associated molecular pattern
PCR	Polymerase chain reaction
PI3K	Phosphatidylinositol-3 kinase
$PI(3,4)P_2$	Phosphatidylinositol (3,4)-bisphosphate
$PI(3,4,5)P_3$	Phosphatidylinositol (3,4,5)-trisphosphate
PI(4)P	Phosphatidylinositol 4-phosphate
ppGpp	Guanosine 3',5' bispyrophosphate
PRR	Pattern recognition receptor
PTM	Post-translational modification
qRT-PCR	Quantitative real-time PCR
RING	Really interest new gene

RISC	RNA-induced silencing complex
RNA	Ribonucleic acid
RNAi	RNA inteference
RT	Room temperature
SCV	*Salmonella* containing vacuole
SEM	Standard error mean
Ser	Serine
shRNA	Small hairpin RNA
siRNA	Short interfering RNA
SNARE	Soluble N-ethylmaleimide-sensitive factor activating protein
RNA	Ribonucleic acid
rRNA	Ribosomal RNA
T2SS	Type II secretion system
T3SS	Type III secretion system
T4SS	Type IV secretion system
Tat	Twin arginine translocation
TLR	Toll-like receptor
TNF	Tumour necrosis factor
Thr	Threonine
Ub	Ubiquitin
UPR	Unfolded protein response
Vip	Vacuole protein sorting inhibitor protein
v/v	Volume/volume
Z’	Z-prime

TABLE OF CONTENTS

LIST OF TABLES AND FIGURES

CHAPTER 1: LITERATURE REVIEW

1.1 Historical Perspective

In 1976, 182 attendees of the American Legion convention in Pennsylvania, Philadelphia, suffered from a severe form of pneumonia (1). 29 of these individuals eventually died from respiratory failure (1). After an extensive investigation, a Gram-negative bacillus was isolated from lung tissues in four of the fatal cases by inoculation into guinea pigs (2). The newly identified infectious organism responsible for this outbreak was termed *Legionella pneumophila* (*Legionella* for the Legionnaires who attended the convention and *pneumophila* for lung loving) (3). The pattern of transmission appeared to be air-borne without any apparent person-person spread (1).

The discovery of this novel bacterium subsequently allowed the aetiological agent of several pre-1976 outbreaks to be retrospectively identified. For example, using indirect fluorescent antibody (IFA) testing to compare *L. pneumophila* isolated from the 1976 Philadelphia outbreak, a previously unsolved outbreak that occurred at St. Elizabeth's Hospital in 1965 was linked to *L. pneumophila* (4). Furthermore, investigations into a Pontiac fever outbreak in 1968, also found *Legionella* bacteria to be the causative agent (5). Subsequent to discovery of the bacterium as a cause of human infection, strategies to isolate and culture *L. pneumophila* were rapidly developed where charcoal-yeast extract agar was found to best support growth (6, 7).

1.2 Characteristics of *Legionella* bacteria

Following rigorous isolation and identification of the bacteria from the outbreak in 1976, the genus *Legionella* was later described in 1979 (3). *Legionella* belongs to the *Legionellaceae* family which forms a monophyletic subgroup within the γ-2 subdivision of the Proteobacteria (8). Its closest phylogenetic relative is *Coxiella burnetii,* the causative agent of Q fever (9). To date, ~60 species of *Legionella* and 70 serotypes have been identified, with new species still being discovered today (10). As recently as 2012, a new species, *Legionella nagasakiensis* sp. nov., was defined (11). Strains of this new species were isolated from water well in Nagasaki Japan, a cooling tower in Australia and a patient in the United States (11).

Morphologically, *Legionella* species are rod-shaped, Gram-negative, and typically measure 0.3-0.9 μM in diameter and 2-20 μM in length (2, 12, 13). Electron microscopy shows that they possess multiple pili with a monopolar flagellum also present in some species, such as *L. pneumophila* (14, 15).

Despite the large number of species and serogroups in the *Legionella* genus, only around half are pathogenic in humans (16). *L. pneumophila* is the leading cause of Legionnaires' disease worldwide (~90%) with serogroup 1 being responsible for 84% of these cases (17). In Australia however, only ~50% of Legionnaires' disease is caused by *L. pneumophila* serogroup 1 (17), whereas *L. longbeachae* is the aetiological agent found in > 80% of the reported cases in South and West Australia (18, 19). Australia's largest outbreak of Legionnaires' disease occurred in 2000 at the newly constructed Melbourne Aquarium where *L. pneumophila* contaminated aerosols generated from the aquarium's newly commissioned cooling towers were inadvertently inhaled by patrons and passers-by (20).

1.3 Legionellosis – Legionnaire's disease and Pontiac fever

1.3.1 Clinical manifestation

Legionellosis refers to two clinically distinct diseases – Legionnaires' disease and Pontiac fever, caused by *Legionella spp*. Regardless of either forms of Legionellosis, infections by *Legionella* are most often efficiently cleared by immunocompetent hosts (21). Individuals who smoke or who have poor immune function such as the elderly, neonates and the immunocompromised are more susceptible to infections (22, 23).

Legionnaires' disease is a severe, acute pneumonia with typical incubation period of between 2-10 days (16). Early symptoms of the disease include malaise, muscle ache, headache and a non-productive cough accompanied by chest pain (1, 16). This is followed by a rapidly rising fever with chills over 3 days, with temperatures reaching up to 40°C (1). While pneumonia caused by *L. pneumophila* is almost indistinguishable from other community acquired pneumonia, features that are more pronounced in a *Legionella* infection include diarrhea, severe hyponatremia, elevation in serum creatine kinase levels and delirium (24, 25). On the other hand, Pontiac fever is an acute, self-limiting, flu-like disease without pneumonia with a very short incubation time of 24 – 48 h and full recovery is usually achieved within 5 days (26, 27). Symptoms of Pontiac fever predominately include mild fever, dry cough,

headache and malaise but can also include vomiting, thoracic pain and diarrhea (27). An investigation into an outbreak of Pontiac fever in 1995 found viable *L. pneumophila* from one of the affected children, thus showing that live bacteria can cause either disease forms (28). However, it still remains unclear why the infection from one bacterial source can result in two distinctly different disease presentations (29). Possible explanations include the amount of bacteria inhaled, mixture of live and dead bacteria as well as different host immune responses and susceptibility (29-31).

1.3.2 Diagnosis strategies

Legionnaires' disease is often misdiagnosed as an exotic plague (16, 32). This is because both its clinical presentation and chest x-rays do not appear to show any significant difference from other forms of pneumonia (32). Despite advances in diagnostic methods for Legionnaires' disease since its discovery, these are still highly insensitive and slow in leading to accurate diagnosis (32). One of the most popular methods is the commercially available urinary antigen test that rapidly detects soluble *Legionella* antigen in urine samples, allowing for rapid diagnosis (33). These kits have been designed to detect is lipopolysaccharide in the cell wall of *L. pneumophila* serogroup 1 (16). While this test is highly specific (with a specificity of ~100%), the major disadvantage is that it is restricted to detecting only *L. pneumophila* serogroup 1 (34). In addition, the test is not highly sensitive (with a sensitivity of ~80%), and so many positive cases are missed. Therefore, even though *L. pneumophila* serogroup 1 is known as the causative agent of Legionnaires' disease in most cases, it has been predicted that up to 40% of cases are misdiagnosed due to the limitations of the urinary antigen detection method (16).

In order to overcome the limitations of the urinary antigen detection test, multiple other methods have been employed. Direct fluorescent antibody (DFA) staining was the first method developed for detecting *Legionella* in both lung tissues and respiratory secretions (16). Results from such a test are available within 2-4 h, but the advantage of this quick turnaround time is offset by the fact that it requires high technical expertise and occurrence of cross-reactivity with other bacterial species, such as *Pseudomonas* species (32). Serology testing for antibodies is a very useful tool for epidemiology studies, but relevance in terms of clinical settings such as treatment options is questionable (32). This is because results can take up to 10 weeks

to be available and it is important to test both the acute and convalescent phases of infection (32). Due to the above deficiencies in giving accurate diagnosis of Legionnaires' disease in a timely manner, strategies that involve amplifying DNA of *Legionella* are starting to emerge. Even though the first of such assays was rapidly removed from the market due to high incidence of false positives, recent advancements have proved more promising (35). More specifically, this real-time PCR technique targets the 23s-5s rRNA intergenic spacer region and therefore allows for the detection of all *Legionella* species and accurate discrimination from *L. pneumophila* (36). Culture diagnosis of lower respiratory tract secretion remains the definitive method for diagnosis, with *Legionella* colonies growing on special buffered charcoal yeast extract (BCYE) agar supplemented with α-ketogluratate after 3-5 days of incubation in appropriate conditions (32, 36). With the large repertoire of different diagnostic methods available, the accurate diagnosis of *Legionella* infection will usually require a positive result from a combination of two or more of the above mentioned methods.

1.3.3 Treatment

Knowledge for treating Legionellosis has been largely based on the outbreak in Philadelphia in 1976 whereby individuals treated with erythromycin or tetracycline demonstrated 50% higher survival rate compared to patients treated with β-lactams (37). As a consequence, *Legionella* infection has been predominantly treated with erythromycin, despite recent evidence of treatment failures, negative side-effects and contraindications with the metabolism of other drugs (1, 38, 39). Newer macrolides (azithromycin, clarithromycin, roxithromycin) and quinolones developed in the 1990s has allowed for alternative therapeutic options (38). Whether macrolides or quinolones provide the best treatment for Legionnaire's disease is still under debate and the recommended antimicrobials for *Legionella* infection at present are azithromycin (a macrolide) or levofloxacin (a quinolone) (38-41). For individuals with a mild to moderate display of pneumonia there appeared to be no significant therapeutic advantage between the two drugs terms of duration of hospital stay, defervescence, complication rate and eventual recovery (39-41). For patients with severe forms of pneumonia, using levofloxacin results in shorter hospital stays and a lower rate of complications compared to azithromycin (40, 42). Finally, as quinolones do not contraindicate other drugs; levofloxacin is recommended for patients who are

also using other drugs for instance, immunosuppressive drugs (43). Nonetheless, more investigation to determine the best treatment plan for Legionnaires' disease is required, such as dosage and route of drug administration.

1.4 *Legionella* – an opportunistic human pathogen

1.4.1 Ecology

In the environment, *Legionella* are ubiquitous, aquatic micro-organisms capable of surviving in a range of extreme conditions. The bacteria are traditionally found in freshwater water bodies such as rivers and lakes as well as unconventional aquatic environments such as mud and soils (44-46). However, modern advances in technology and water use have allowed the growth and prevalence of the bacteria to include artificial water sources. These sources include cooling towers, whirlpools, spas, fountains, ice machines, dental equipments and shower heads (44, 47-51). The practice of composting plant waste matter has also created an ideal niche for *Legionella* to multiply in (52).

Protozoan hosts are crucial for *Legionella* growth in the environment as they provide the ideal habitat for environmental survival and proliferation of the bacteria (44). Amoebae from the genera *Acanthamoeba* and *Naegleria* found in soil and freshwater environments were the first protozoa identified that enable the replication of *L. pneumophila* (53). Since then, other protozoan hosts that support *L. pneumophila* replication include *Dictyostelium discoideum*, *Cyclidium* spp., *Tetrahymena pyriformis* and many more amoebae species such as *Hartmannella* was identified (54-56). Even though protozoa such as *Acanthamoeba* ingest *L. pneumophila* as a food source, the bacteria can ultimately kill the protozoa after replication within the LCV (57, 58). Protozoa are good environmental reservoirs in other ways because they protect *Legionella* from harsh conditions such as high temperatures, chlorination and biocidal compounds (59). Importantly, *L. pneumophila* appears to infect both mammalian and protozoan cells in a very similar manner, using the same genes for both the initial infection and subsequent bacterial replication (60-62). It is widely speculated that the ability of *Legionella* spp. to infect higher order mammalian host such as humans has evolved from their adaptation to survive in these primitive eukaryotic hosts (59). In fact, Brieland *et al*. showed that *L. pneumophila* infected *Hartmannella vermiformis* were not only infectious to mice, but actually more so than

L. pneumophila alone or a co-inoculum of *L. pneumophila* and uninfected amoebae (63). Additionally, Barker and Brown demonstrated that *L. pneumophila* that had replicated in amoebae displayed increased resistance to antimicrobials compared to bacteria grown *in vitro* on agar plates (64). Hence, *L. pneumophila* growth within amoebae might have led to increased virulence in humans.

1.4.2 Transmission

Despite the large amount of natural water in the environment, *Legionella* found in natural water bodies do not usually cause outbreaks with the exception of hot springs (65). The reason is that water found in the natural environment does not usually provide the ideal conditions for *Legionella* to replicate to high enough numbers to cause an infection. In contrast, it is man-made water sources that are notoriously linked to outbreaks of legionellosis, in locations ranging from homes and hotels to hospitals and cruise ships (44). In particular, switching on cooling towers that have been sitting un-used for a substantial period of time has been linked to major outbreaks of legionellosis (66, 67). In the man-made systems, utilising water at elevated temperatures in combination with providing nutrients, such as iron which is essential for *Legionella* survival and growth, allow the bacteria to proliferate to dangerous numbers (68). Another factor aiding *Legionella* growth is aquatic biofilms found both in natural and man-made environments. In synergy with the large diversity of bacterial populations in the biofilm, *Legionella* is able to form microcolonies in existing biofilms (44, 69). In fact, it has been found that at 40°C, up to 50% of total biofilm flora on plastic water piping is made up of *L. pneumophila* (69). The risk of *Legionella* infection from dental practice has also been documented as biofilms form particularly well on dental apparatus and together with aerosols generated during the procedure provide ideal growth and transmission for the bacteria (44, 47, 70). *Legionella* is also capable of necrotrophic growth, thriving on dead microbial cells found in biofilms and heat-treated water systems (71). The ability of *Legionella* to thrive in such challenging environments highlights the difficulty of removing the bacteria from water systems.

Man-made water systems held at higher than ambient temperature provide the ideal growth conditions and with protozoa providing an environmental reservoir, *Legionella* has emerged as an opportunistic human pathogen. Transmission of

Legionella typically occurs via the inhalation of contaminated aerosols from artificial water systems. Particularly systems that generate a lot of aerosols pose a significant risk. These aerosols can contain free bacteria, bacteria contained in vesicles that have been released from infected protozoa or live amoebae containing *Legionella* (59, 63, 72). No human-to-human transmission has been reported to date.

1.4.3 Life cycle

Given that *L. pneumophila* can persist as a free-living microbe and also has the ability to replicate in amoebae in the natural environment, it is no surprise that the bacterium alternates between a biphasic life-cycle in order to successfully adapt to different environments. *L. pneumophila* alternates between an infectious stationary phase and an intracellular replicative phase. Studies have shown that close to half of the genes in the bacterial genome are expressed differently between the phases (73). In the replicative phase, rod-shaped bacteria appear aflagellated, long and filamentous, and do not express transmission traits (74). This form eventually matures into short flagellated rods in the stationary phase allowing for motility and transmission into new hosts (74). *In vitro* modelling of the biphasic life cycle can be achieved using bacterial broth cultures. Exponential phase cultures represent the replicative phase where the bacteria do not transmit to other hosts while post-exponential phase cultures represent the stationary phase and express transmission factors (75).

The availability of nutrients is an important factor in determining the phase in which the bacteria persist. Where nutrients are readily available, the replicative phase is induced as *L. pneumophila* commits to replication. As nutrient availability diminishes, the bacteria switch to the virulent stationary phase and exit the host cell ready to survive as free-living microbes in the aquatic environment, and infect new host cells (74). In nutrient depleted conditions, *L. pneumophila* also produces guanosine 3',5' bispyrophosphate (ppGpp), a trigger for the bacteria to switch to the stationary phase and express genes required for exiting the host (76). Results from infection studies are also consistent with results obtained from broth cultures. During *A. castellanii* infection, genes used for amino acid catabolism and the Entner-Doudoroff pathway are up-regulated during the replicative phase, indicating that intracellular *L. pneumophila* scavenges both proteins and carbohydrates from the host as nutrients for replication (73). On the other hand, genes up-regulated during the stationary phase

include those required for transmission, invasion, motility and type IV pilus machinery as well as effectors of the Dot/Icm system (73).

In addition to nutrient availability, other regulators important for controlling the transition from replicative to stationary phase include LetA/LetS (*Legionella* transmission activator and sensor). Before phagocytosis, LetA/LetS relieve CsrA, a protein that is a pivotal repressor of transmission traits, allowing *L. pneumophila* to evade lysosomes and establish a replicative vacuole (77). In contrast, CsrA repression has to be restored before the bacteria can replicate intracellularly (77). This is an example of how *L. pneumophila* is capable of self-regulating between the two different phases depending on the environmental conditions.

1.5 *L. pneumophila* infection strategy

To cause disease in humans, *L. pneumophila*-contaminated aerosols are inhaled into the lungs. The bacteria then infect alveolar macrophages where they proliferate and propagate, a process that appears to have evolved from their ability to infect primitive amoebae in the natural environment. In fact, there are many similarities in the way the bacteria invade, replicate and eventually egress from human macrophages and amoebae. The three main processes of infection by the bacteria are 1) attachment and entry 2) establishment of a *Legionella*-containing replicative vacuole and 3) exit from host cell for further transmission.

1.5.1 Entry into macrophages

In order for *L. pneumophila* to successfully replicate intracellularly, it is vital that the bacteria are internalised by amoebae and macrophages. To date, the mechanism of entry is still under debate. Two mechanisms of entry have been observed: conventional phagocytosis and coiling phagocytosis (Figure 1.1). Horwitz first showed in 1984 that *L. pneumophila* could be internalised by a novel uptake method termed 'coiling phagocytosis' by alveolar macrophages, human monocytes and polymorphonuclear leukocytes (78). Coiling phagocytosis does not discriminate between live or dead *L. pneumophila* and occurs by engulfing the bacterium into a pseudopod coil as it is internalised (78). Similarly, studies in *A. castellanii* showed that uptake of *L. pneumophila* into amoebae could occur via coiling phagocytosis (79). The complement system had also been implicated in the phagocytosis of

L. pneumophila where complement receptors (CR1 and CR3) were found to mediate the uptake of complement coated bacterium (80). Conversely, when these receptors were blocked, adherence was decreased and thus subsequent entry also reduced (80). However, the role of complement in the attachment of the bacteria to host cells is still debatable as levels of complement are generally low in the lungs (81). The involvement of phosphatidylinositol-3 kinase (PI3K) in *L. pneumophila* phagocytosis has also been studied; however opposing results have been observed. Using wortmannin, a PI3K inhibitor, one study concluded that PI3K does not play a role in the phagocytosis of wild-type *L. pneumophila* (82). This is supported by another study using *Dictyostelium*. When the two isoforms of PI3K – PI3K1 and PI3K2 in *Dictyostelium* were genetically inactivated, phagocytosis of wild-type *L. pneumophila* was unaffected (83). A similar observation was made when PI3K inhibitors were used to treat the *Dictyostelium* (83). However, using similar pharmacological methods, another study claimed that PI3K was essential for phagocytosis of non-opsonised *L. pneumophila* in macrophages (84). As reviewed above, what is known about host factors that contribute to the process of *L. pneumophila* uptake is still not well elucidated.

To add another layer of complexity, several *L. pneumophila* proteins have been implicated in entry into host cells as *L. pneumophila* strains lacking these proteins are unable to enter host cells as efficiently. Examples of these proteins are: EnhC, LvhB2 and RtxA (85-87). *L. pneumophila* Δ*enhC* and *L. pneumophila* Δ*rtxA* mutants display a significant defect in entry into Hep-2 epithelial cells and THP-1 macrophages (86). EnhC and RtxA contain similar repeats to a Sel-1 protein and a structural toxin protein of *Caenorhabditis elegans* respectively (86). On top of its role in invasion, RtxA is also an important virulence factor as *L. pneumophila* lacking RtxA do not replicate as efficiently and show decreased virulence in mice (85). LvhB2 is a particularly unique entry protein as it appears to affect *L. pneumophila* infection of host cells in a temperature-dependent manner (87). *L. pneumophila* Δ*lvhB2* grown at 30°C, but not 37°C, are less efficient in entry into host cells (87). It is still unclear whether the process of *L. pneumophila* entry into host cells is directed mainly by the pathogen or the host, even though both host and bacterial factors clearly play a part.

1.5.2 Formation of the Legionella-containing vacuole

Traditionally, the endocytic pathway delivers phagosomes to the lysosomal network to degrade phagocytosed material. Intracellular pathogens have evolved different ways to avoid this fate; such as evasion of phago-lysosome fusion, escape to host cytosol, resistance to lysosomal digestion and regulation of pH in the phagosome to create an environment conducive for bacterial survival (88). *L. pneumophila* efficiently avoids phago-lysosome fusion and instead sets up a replicative vacuole termed the *Legionella*-containing vacuole (LCV) which does not undergo normal acidification (Figure 1.2) (89, 90). The ability to avoid phago-lysosome trafficking allows the bacteria to persist and proliferate in a favourable niche.

Horwitz *et al*. examined the process of LCV establishment in human monocytes and found that formation of the LCV occurs within 4-8 h after bacterial uptake (91). Initially, the vacuole is surrounded by plasma membrane; but within minutes smooth vesicles derived from the host appear to fuse to the vacuolar membrane and mitochondria are also transiently recruited to the vacuole (91). Interestingly, these vacuoles will usually only contain up to two bacteria until approximately 8 h after uptake, suggesting that *L. pneumophila* does not start replicating until LCV biogenesis is complete (91). By 4 h, the smooth vesicles and mitochondria start to disappear from the vacuolar membrane and ribosomes begin to associate with the LCV (91). A study using labelled endoplasmic reticulum (ER) luminal binding protein (BiP), indicated that the LCV is associated with membrane derived from the ER and that the ribosomes that line the cytoplasmic face of the vacuole are also ER derived and not from the cytoplasmic pool (92). By 8 h after bacterial uptake, the biogenesis of the LCV is generally complete and bacterial replication commences, at a doubling rate of approximately 2 h during mid-log phase (93, 94). After 15-24 h, the host cell undergoes lysis, allowing for the infection of new neighbouring macrophages to occur (93, 94). The infection and replication process of *L. pneumophila* is shown graphically in Figure 1.1.

In addition to host derived organelles, host factors are also involved in the process of setting up the ER-like replicative niche for *L. pneumophila*. The families of Rab and soluble N-ethylmaleimide-sensitive factor activating protein receptor (SNARE) proteins play important roles in membrane trafficking. Specifically, Rabs are involved

in regulation of vesicle movements and SNAREs are involved in vesicle fusion to the target membrane (95, 96). Rab1 is rapidly recruited to the surface of a significant proportion of LCVs; and is believed to enhance ER vesicle recruitment (97, 98). In support of this, inhibiting Rab1 function using a dominant interfering protein results in abrogated intracellular growth of *L. pneumophila* (97, 98). Rab1 subsequently recruits other host factors that are required for the fusion of recruited ER vesicles to the target membrane (99, 100). Sec22b is a v-SNARE found on the ER-derived vesicles membrane and is important in the membrane fusion process, allowing for the biogenesis of the LCV (98, 101, 102). Recent studies found that *L. pneumophila* effector proteins directly control Rab1 dynamics on the LCV. In host cells, Rab1 is maintained in a GDP-bound inactive state. The effector SidM/DrrA is a multifunctional enzyme that first recruits Rab1 to the LCV by displacing GDP association inhibitors from the pool of inactive Rab1 in the cell cytosol (103, 104). Guanine nucleotide exchange factor (GEF) activity of SidM/DrrA then catalyses GDP-to-GTP, thereby activating Rab1 (103). Subsequently, SidM/DrrA AMPylates a tyrosine residue of Rab1, blocking the access of GTPase-activating protein, thus keeping Rab1 in an active state (105, 106). As the LCV matures, SidM/DrrA and Rab1 begin to cycle off the LCV surface (107). Rab1 removal is also mediated by *L. pneumophila* effectors. SidD deAMPylates Rab1, allowing for another effector, LepB, a Rab1 GTPase activating protein (GAP) to inactivate Rab1 via GTP hydrolysis (105, 107, 108). SidD and LepB essentially act as antagonist of SidM/DrrA. Further control is provided by the effector pair AnkX and Lem3, which respectively phosphocholinate Rab1 to activate it and dephosphocholinate to allow GAP binding (109, 110) Finally, *L. pneumophila* also hijacks the host ubiquitination system to decorate the LCV surface with polyubiquitin conjugates (111). The process for establishing the LCV is highly sophisticated and, like entry into macrophages, involves both factors derived from the host and the bacteria.

1.5.3 Exit from macrophages

Following replication in host macrophages, the next step in the infection cycle requires the bacteria to exit the original host cells and disseminate to infect new host cells (Figure 1.1). The exact mechanism facilitating the exit process of *L. pneumophila* is unknown, however, theories have been proposed. In protozoan hosts, *L. pneumophila* may not egress through the induction of cell death (112), but

rather, *L. pneumophila* forms pores in the membrane and induces cytolysis of infected *A. polyphaga* (112). However, the factors driving this are unknown. Two *L. pneumophila* effectors, LepA and LepB were initially implicated in promoting non-lytic release of the bacteria by fusing the intact LCV to the protozoan membrane (113). It is still unclear if the Rab1 GAP role of LepB is directly involved in this process. Removal of Rab1 from the LCV by LepB is perhaps a trigger to direct the LCV for release and infection of neighbouring cells. In mammalian hosts, it is proposed that *L. pneumophila* escapes from host cells via similar pore-formation induced lysis (114, 115). Although LepA and LepB were associated with bacterial release from protozoan host cells (113), they are not important for egress from human and mouse phagocytic cells (113).

When infected with intracellular pathogens, many host cells undergo apoptosis as a defence mechanism to expel the invading organisms (116). To avoid this, *L. pneumophila* has developed ways to preserve survival of the host cell after infection so that it can fully utilise the host for its own replication. At a low multiplicity of infection, a Dot/Icm-dependent activation of caspase-3 within the host cell can be detected during the early and exponential stages of replication (117, 118). Despite caspase-3 being a critical component of the apoptosis cascade, apoptosis is delayed and happens only when bacterial replication is completed (117). The apoptotic role of caspase-3 is halted by *L. pneumophila*, by up-regulating 12 human anti-apoptotic genes, including NF-κB (119, 120). Specifically, the effector LegK1 of *L. pneumophila* contains eukaryotic-like Ser/Thr kinase activity that directly stimulates NF-κB activation, thereby up-regulating anti-apoptotic factors during infection (120). The *L. pneumophila* effector, SidF, also contribute to inhibition of apoptosis during infection by inhibiting the functions of 2 pro-apoptotic proteins, BNIP3 and Bcl-rambo (121). Recently, SidF was characterised as a phosphatidylinositol polyphosphate 3-phosphatase which hydrolyses the D3 phosphate group of $PI(3,4)P_2$ and $PI(3,4,5)P_3$ (122). This converts the LCV into an organelle enriched with PI(4)P on the surface, thus allowing PI(4)P-binding effectors such as SidM/DrrA to anchor onto the LCV surface (122). Considering SidM/DrrA plays a role in biogenesis and maintenance of the LCV, SidF likely supplement its anti-apoptotic role by also spatially regulating other effectors that are important for *L. pneumophila* replication during early stages of infection. Like entry and replication,

escape of *L. pneumophila* from infected cells is likely to involve both host and bacterial factors.

1.6 Protein secretion systems of *L. pneumophila*

Many bacterial pathogens use protein secretion systems to deliver effector proteins across surrounding membranes into host cells. These effectors manipulate many host processes, such as antimicrobial responses and signalling cascades, thus creating an environment that facilitates survival of the pathogen (123, 124). The release of effector proteins by secretion systems is a major virulence attribute during *L. pneumophila* infection (125) and *L. pneumophila* harbours multiple secretion systems.

1.6.1 The Lsp Type II secretion system and its substrates

The secretion pathway, Lsp, is a type II secretion system (T2SS) that is primarily important for environmental survival of *L. pneumophila* (126, 127). T2SSs are found in many Gram-negative bacteria and are typically involved in the export and release of toxins, proteases and other enzymes (128). The Lsp is made up of 12 different components including 6 pseudopilin proteins (129); a prepilin peptidase which processes the pilin of both the type II pseudopilins and type IV pili (130); an outer membrane secretin; an ATPase; and 3 proteins predicted to promote secretion (129). Several Lsp proteins are important in intracellular replication of *L. pneumophila* and *L. pneumophila* strains lacking several Lsp components display drastic reduction in replication within *A. castellanii* and *H. vermiformis* (131, 132). Similar phenotypes are also seen when *L. pneumophila lsp* mutant strains are used to infect A/J mice compared to wild-type bacteria (129). The Lsp secretion system also plays a role in enabling *L. pneumophila* to survive in temperatures as low as 4°C in aquatic environments, presumably by secreting factors such as a peptidyl-prolyl *cis-trans* isomerise, known to facilitate *L. pneumophila* persistence in low temperature (127, 133). Finally, when U937 macrophages and A549 epithelial cells are infected with *lsp* mutants, they show higher levels of interleukin-6 (IL6), IL8, TNFα and IL1β compared to cells infected with wild-type bacteria. This suggests that Lsp is involved in blocking the cytokine response during infection.

Cianciotto *et al*. utilised a proteomics approach to identify 27 proteins that were secreted by the Lsp secretion system (134). Examples of substrates secreted by this secretion system are ProA/Msp, a zinc metalloprotease; SrnA, an RNase and the chitinase enzyme ChiA (126, 134). ProA/Msp and SnrA are necessary for optimal *L. pneumophila* replication in *H. vermiformis* cells, and while ChiA appears to not be required for replication *in vitro*, but is important for persistence of the bacteria during *in vivo* infection (134-136). Other characterised substrates such as phospholipase C, the lipases LipA and LipB and the aminopeptidases LapA and LapB do not cause decreased replication even at low temperature (136-138). In addition, characterisation of Lsp substrates revealed that much functional redundancy is evident. For example, there are at least 15 proteins with phospholipase A and lysosomal phopholipase A activities (139, 140). Two of these proteins, PlaA and PlaC are proposed to be important for *L. pneumophila* virulence; however, mutants lacking these functions did not display a replication defect in macrophages and amoebae (139, 140). Interestingly, IcmX and LvrE are two secreted substrates of the Lsp system that potentially suggest a link with other secretion systems in *L. pneumophila* (134). Both these proteins have been detected in culture supernatants with IcmX being described as a component of the type IV Dot/Icm secretion system that is important for the formation of the LCV. LvrE is linked to genes encoding the Lvh, type IVA secretion system of *L. pneumophila* (134, 141, 142). Interestingly, the M12 zinc metalloprotease is apparently first secreted by the Lsp system and then translocated into host cells via the Dot/Icm secretion system (134, 143). These results highlight that there may be substantial cross-talk between different secretion systems of *L. pneumophila*.

1.6.2 The Lss and Tat secretion systems

In comparison to the type II Lsp system, there are secretion systems in *L. pneumophila* that are not as well characterised. For example, the locus *lssXYZABD* carries the components of a type I secretion system (Lss) (144). To date, no substrates of the Lss have been identified and it does not appear to play a role in host-pathogen interactions and bacterial survival (144). However, it has been proposed that the Lss may be involved in secreting and transporting toxins produced by *L. pneumophila* across its membranes (144).

While the Lsp system secretes substrates to modulate *L. pneumophila* survival in the environment, a twin arginine translocation (Tat) secretory pathway transports substrates from bacteria to host cells. It typically does this by moving the protein across the inner membrane in a folded state (145). As shown using *tatB* and *tatC* mutants, the Tat pathway plays an important role in enabling *L. pneumophila* to form biofilms, it also facilitates intracellular replication in amoebae and macrophages and survival in low-iron conditions (142, 146). Several Tat pathway substrates have been confirmed, including phospholipase C, cytochrome c oxidase and even include components of the Lss system (142, 147, 148). *L. pneumophila* lacking both the Tat and Lsp systems exhibit a reduction in intracellular replication which is greater than that of the single mutants, thereby suggesting distinct activities (146). Hence, both of these secretion systems have important and independent roles in *L. pneumophila* virulence.

1.6.3 Type IV secretion system

Type IV secretion systems (T4SS) are essential for the pathogenesis of many pathogens, such as *Helicobacter pylori*, *C. burnetii* and *L. pneumophila*. Three main classes of T4SS have been identified: T4SSA, T4SSB, and genomic island-associated T4SS (GI-T4SS). *Legionella* carries two of these, the T4SSA and T4SSB (149, 150).

1.6.3.1 Lvh Type IVA secretion system

The *L. pneumophila* type IVA secretion system (Lvh) is encoded by 11 genes in which the locus is either integrated in the chromosome or exists as an extrachromosomal plasmid (151). The substrates of Lvh have not been identified, but Bandyopadhyay *et al*. suggested that the Lvh system complements the T4SSB Dot/Icm system (below) and is involved in aspects of pathogenesis such as host cell invasion (152).

1.6.3.2 The Dot/Icm TypeIVB secretion machinery

Despite the multiple secretion systems that *L. pneumophila* harbours, the Dot/Icm secretion system is undeniably the most well studied and is vital in the pathogenesis of the bacteria. Its roles range from supporting the formation of the LCV, to aiding *L. pneumophila* intracellular replication and the eventual egress from the host cell (115, 153). Mutations within the Dot/Icm system in *L. pneumophila* lead to formation

of a vacuole that fails to recruit ER vesicles and undergoes rapid endocytic maturation (154, 155). Two independent studies using a forward genetics approach identified 27 genes to be essential for *L. pneumophila* to both avoid the endocytic pathway and to establish a replicative vacuole (156-159). These genes have been named Dot (for defective in organelle trafficking) or Icm (for intracellular multiplication). They are found in two distinct regions on the chromosome. Region 1 comprises *dotDCB* and *dotA-icmVWX* while Region 2 comprises *icmTSRQPONMLKEGCDJBFH* (Figure 1.3A) (141, 160, 161). Together, these *dot*/*icm* genes encode proteins that make up the type IVB secretion system of *L. pneumophila* (Figure 1.3B). The majority of these proteins are found within the inner and/or outer membranes of the bacteria, with a handful existing as putative cytoplasmic adaptor proteins (Figure 1.3B). Although the role of each protein in the Dot/Icm system has not been completely established, several studies have attempted to define the roles of some complexes. For example, IcmGCDJBF has been implicated in killing macrophages (162) and the interaction between DotH, DotI and DotO was important for replication and evasion of lysosomal degradation (163). DotB is an essential protein which has been assigned the role of an ATPase, most likely providing the energy required for the function of the system (164). Shortly after this discovery, the same group utilised genetic methods to create 30 *dotB* allele mutants and provided the first evidence of DotB playing a role in aiding the secretion of a subset of effector proteins (165).

DotA was the first component of the Dot/Icm system found to play a role in establishing the LCV (154). DotA is an integral cytoplasmic membrane protein with 8 membrane spanning domains, 2 periplasmic membrane and a C-terminal cytoplasmic domain which is critical for virulence (166). Although DotA is a component of the Dot/Icm system, it has also been observed to be secreted into bacterial culture by the Dot/Icm system, forming a ring-shaped structure (167). This finding suggested that DotA was a substrate of the Dot/Icm system. However, this secretion has not been reported during intracellular infection of *L. pneumophila*. As *L. pneumophila* Δ*dotA* strains do not translocate effectors into host cells during infection, it is thought that DotA forms a channel to facilitate movement of vacuolar contents into host cells. However, further studies are required to confirm this.

Vincent *et al*. provided evidence that suggested the Dot/Icm machinery is formed by multiple proteins that span both the inner and out membrane of *L. pneumophila* cell

wall (168). The putative core complex of Dot/Icm contains DotC, DotD, DotH, DotG and DotF (168). DotC and DotD are outer membrane lipoproteins which recruit DotH to the outer membrane, forming a DotC-DotD-DotH outer membrane complex (168). DotG is a transmembrane protein with the C-terminal domain in the outer membrane complex, thus generating a core complex spanning both membranes (168). Proper embedment of DotG into the core complex is facilitated by DotF (169). It binds to the above 4 proteins, thereby aiding the formation and stabilising the core complex (168, 169).

Through structural analysis, IcmQ together with its chaperone IcmR were found to associate with the membrane, potentially acting as pore-forming proteins for the secretion system (170, 171). Although exactly where in the secretion process they operate is unclear. Similar to the type III secretion system (T3SS), translocation of bacterial effector proteins via the Dot/Icm system appeared to require cytoplasmic chaperone proteins, namely IcmS and IcmW (172). IcmS and IcmW are thought to exist as a heterodimer in order for them to function properly as translocation chaperone proteins (172). However, IcmS also appears to interact with another known *L. pneumophila* virulence factor, LvgA (172, 173). The putative chaperone proteins are proposed to bind to their substrates causing a conformational change in the substrates, exposing the translocation domain to the Dot/Icm system and thereby allowing effector protein translocation (174).

Although some Dot/Icm proteins have not been functionally characterised, how effector translocation proceeds is still unknown. In particular, no LCV membrane pore has been identified that explains the translocation of effectors across the LCV membrane. Not only is the Dot/Icm system critical for replication of *L. pneumophila* in the LCV, through the activity of the effector proteins that are translocated into host cells during infection, it is also associated with other aspects of pathogenesis. This includes the activation of host NF-kB and JNK/p38 mitogen-activated protein kinase signalling pathways (175, 176) and the inhibition of host cell apoptosis (117, 119, 177).

1.6.4 Substrates of the Dot/Icm system

The importance of a functional Dot/Icm system for the replication and virulence of *L. pneumophila* suggests that effector proteins are important in dictating how the

bacteria interact with host cells. Initial attempts to identify a single translocated effector took a substantial amount of time (88). However, the emergence of new strategies which combined technologies such as bioinformatics and proteomics with biochemical screening assays expedited the identification process and the number of identified effectors has since avalanched (88). Approaches employed for the identification process have included interaction with Dot/Icm apparatus components (IcmW/IcmS), using a Cre-lox site assay to identify the presence of the Dot/Icm translocation signal, interbacterial protein transfer, surveying *orfs* larger than 300 base pairs for Dot/Icm-dependant translocation using a TEM-1 β-lactamase quantitative assay and heterologous expression of *L. pneumophila* genes in *Saccharomyces cerevisiae* that cause a loss in viability and/or interference to secretory functions (160, 161, 172, 178-182).

In 2009, a genome-wide machine-learning study was carried out which successfully identified many new Dot/Icm effector proteins based on similar features to other known effectors (183). Other bioinformatic approaches have investigated protein sequences for the presence of eukaryotic-specific domains, post-translational modification motifs, presence of the E Block motif or other putative C-terminal Dot/Icm translocation motifs (151, 184-186). Collectively, these studies have identified ~300 different translocated Dot/Icm effector proteins, accounting for more than 10% of *L. pneumophila* protein-coding genes (125). Substantial functional redundancy exists due to the large repertoire of effectors and paralogues that exist among them. Unlike the loss of function of the Dot/Icm system, deletion of effector genes does not generally demonstrate a significant defect in replication and virulence. Functional redundancy has been suggested to assist the bacteria to avoid killing by different environmental hosts and allow them to infect different cells and protozoa. Effectors are translocated shortly after contact between the bacterium and the host cell and are found on both the cytoplasmic face of the LCV as well as associated with diverse vesicles and organelles of the host cell.

1.7 Modulation of host cell processes by Dot/Icm substrates

To date, only a comparatively small subset of *L. pneumophila* effector proteins mediated by the Dot/Icm system have been characterised. They target host cell processes ranging from the regulation of host vesicular trafficking pathways and host

GTPases to manipulate phosphatidylinositol interactions during LCV biogenesis. Effectors also inhibit host cell apoptosis and manipulate the stress response in infected host cells (125, 187).

1.7.1 Regulating host vesicular trafficking pathways

As previously described, *L. pneumophila* avoids the host endocytic pathway in a Dot/Icm dependant manner and several effector proteins facilitate this process. Deletion of *L. pneumophila* effector protein AnkX for example, results in a greater interaction between *L. pneumophila* and endocytic organelles (187). AnkX AMPylates the host proteins Rab1 and Rab35 via its Fic domain and was shown to be important for disrupting host vesicle transport (187, 188). Another *L. pneumophila* effector protein that has roles in the entry and lysosomal avoidance of the bacteria is LpnE (189). Curiously, while LpnE is apparently not secreted by the Dot/Icm system, its localisation to the LCV is Dot/Icm dependant (189, 190).

Using a yeast genetic screen, several groups collectively found 79 Dot/Icm effector proteins that interfere with host cell vesicular trafficking pathways, albeit the mode of action is yet to be determined for some (143, 178, 179, 182). One such effector, SetA, caused both a severe growth defect and decreased ER trafficking when expressed in yeast (182). When SetA was expressed in mammalian cells, it localised with the late endosomal markers Rab7 and lysosomal-associated membrane protein 1 (LAMP-1), providing support that SetA plays a part in bacterial evasion of the endocytic network (187). LAMP-1 is a glycoprotein that resides primarily on lysosomal membranes and characteristically co-localises with cargos that are destined for lysosomal degradation. Shohdy *et al*. identified additional *L. pneumophila* effectors termed Vips (vacuole protein sorting inhibitor protein) that interfere with lysosomal protein trafficking. VipA appears to interfere with carboxypeptidase Y in the Multivesicular body (MVB) pathway, and more recently was determined to be a bacterial actin nucleator that directly polymerises host microfilaments during infection of macrophages (179, 191). It is further speculated that this effector supports the intracellular life cycle of *L. pneumophila* by manipulating host cytoskeletal dynamics, and thus targeting important host cell pathways (191). VipD on the other hand inhibit multivesicular body formation and thus ER-to-Golgi trafficking (179).

Like many other intracellular pathogens, *L. pneumophila* targets host GTPases and regulates GTP cycling to manipulate host organelle trafficking events during LCV establishment (192). The first characterised Dot/Icm effector protein, RalF is an Arf specific GEF that is essential for the localisation of ADP ribosylation factor-1 (ARF-1) to the LCV surface (193). As ARF-1 is a GTPase that regulates vesicle trafficking between the ER and the Golgi, RalF redirects this trafficking to facilitate construction of the LCV (193). Despite the importance of RalF, the removal of its function does not affect the ability of the bacteria to replicate intracellularly in both mouse and human macrophages and the protozoan, *A. castellanii* (193).

As previously described in Section 1.5, effector SidM/DrrA is rapidly translocated upon *L. pneumophila* infection and acts as a potent Rab1 GEF that recruits and activates Rab1 (103, 194-196). SidM/DrrA then keeps Rab1 in an active state by adenylating it with adenosine monophosphate (AMP) (106). As such, SidM/DrrA is important for LCV establishment and maintenance. LidA is another effector protein that is critical for maintenance of the LCV as *L. pneumophila* lacking LidA displays reduced LAMP-1 avoidance (194). LidA plays a role in recruiting early secretory vesicles to the LCV during the early stages of establishment and works in synergy with SidM/DrrA (196). LidA binds directly to Rab1 and plays the role of an accessory protein to SidM/DrrA, increasing the efficiency of Rab1 recruitment to the LCV (195). In addition to Rab1, LidA also binds to other Rabs, such as Rab6 and Rab8 (195). While *lidA* mutants are not able to evade the endocytic pathway, *sidM*/*drrA* mutants of *L. pneumophila* are still able to replicate (195). Finally, both LidA and SidM/DrrA anchor to the LCV membrane via interactions with PI4P, a phosphatidylinositol (PI) derivative that is abundant on the surface of the LCV (197, 198). Another Dot/Icm effector protein SidC and its homologue, SdcA, are proposed to be vesicle fusion tethering factors that also anchor to the LCV via a similar mechanism (83, 180, 197). Recently, SidC/SdcA were found to modulate events early in LCV maturation, especially in the recruitment of ARF-1 and ubiquitination of Rab1 (199). As a result, *L. pneumophila sidC*/*sdcA* deletion mutants show a delay in LCV formation and in the appearance of ubiquitin on the LCV (199). Structural studies have revealed a N-terminal domain of SidC that harbours unique ubiquitin E3 ligase activity that assists LCV formation and remodelling, specifically in the recruitment of ER-derived

vesicles and polyubiquitinated proteins onto the cytoplasmic face of the LCV membrane (200).

In addition to activating Rab1, *L. pneumophila* effector proteins also inactivate Rab1 later in the infection process. SidD deAMPylates Rab1 so as to relieve Rab1 of being permanently activated and LepB subsequently inactivates and removes Rab1 from the surface of the LCV (105, 107, 108). AnkX and Lem3 also regulate Rab1 dynamics on the LCV surface. AnkX was initially identified as an ankyrin-repeat effector that interferes with host vesicular trafficking pathways when over-expressed (188). Subsequently, AnkX is further characterised as a phosphorylcholine transferase that covalently attaches a phosphocholine moiety onto the serine residue at position 76 of Rab1 (109, 110). This modification on Rab1 hinders the accessibility of LepB, and therefore prevents removal of Rab1 from the surface of the LCV (110). Interestingly, this is alleviated by another effector, Lem3 which removes the phosphocholine moiety from Rab1 (110). Lem3 therefore regulates the activity of AnkX.

These results suggest that as the needs of *L. pneumophila* change over different phases of infection, the bacteria are capable of regulating and dictating the fate of Rab1 through the actions of different effector proteins. Through this modulation of host vesicular trafficking, *L. pneumophila* is able to ensure the successful construction of the LCV.

1.7.2 Arrest of host protein synthesis

In addition to interfering with host vesicular transport, effector proteins of *L. pneumophila*, in particular SidI and Lgt1, are also capable of halting host protein translation. SidI does this by binding to the components of the protein synthesis elongation complex, eEF1A and eEF1Bγ, while Lgt1 post-translationally glycosylates eEF1A (201, 202). Putting host cell protein synthesis in arrest induces a response that might create an environment which is more favourable for bacterial replication (125). For example, the inhibition of translation elongation blocks the cell unfolded protein response which would normally result in host cell death (203). The halt in protein translation also affects the cytokine responses of infected cells (204). Interestingly, *L. pneumophila* strains lacking these genes do not display a defect in replication, which suggests that there might be more effectors that play the same role (201).

1.7.3 Inhibition of host cell apoptosis

L. pneumophila effectors are also able to inhibit the infected host cells from undergoing apoptosis, thus allowing the bacteria to exploit the host for replication for as long as possible. The effector protein, SidF, directly interacts and inhibits two proapoptotic proteins, BNIP3 and Bcl-rambo although the mechanism is unknown (121). Recently discovered phosphoinositide 3-phosphatase activity of SidF is thought to prevent $PI(3,4)P_2$ and $PI(3,4,5)P_3$ from being converted into PI(3)P, thus maintaining the LCV surface in a PI(4)P enriched state (122). As *Mycobacterium tuberculosis* phagosomes enriched with PI(3)P on the surface efficiently fuse to endosomes and lysosomes (205); preventing the accumulation of PI(3)P on the LCV surface likely allows *L. pneumophila* to avoid the endocytic degradation pathway.

SidF is a unique effector with dual roles that prevents infected host cell apoptosis while at the same time promoting bacterial replication intracellularly. Another effector protein, SdhA, also prevents host cell death in response to *L. pneumophila* infection by maintaining LCV integrity. Unlike infection with wild-type *L. pneumophila*, infection of macrophages with *sdhA* mutants results in host cell pyroptosis that is stimulated by activation of the host AIM2 (absent in melanoma 2) inflammasome (206). SdhA has a functional Golgi-targeting GRIP domain that is needed to prevent AIM2 activation (206). Although replication of *L. pneumophila* Δ*sdhA* in mouse bone marrow derived macrophages was attenuated compared to the wild-type strain (207), this phenomenon was less pronounced in *D. discoideum*, where a reduced replicative phenotype is rarely seen by removing just one effector protein (207). Indeed, deleting ~30% of known effector proteins from *L. pneumophila* did not result in a replication defect within macrophages, highlighting the fact that the *L. pneumophila ΔsdhA* phenotype is unusual and likely related to death of the host cell (208). SdhA stabilises and maintains the integrity of the LCV membrane during intracellular replication; creating a favourable vacoular environment that protects *L. pneumophila* from host cytosol factors that do not support the bacterium's replication (209). However, its biochemical mechanism of action is unknown.

While this is only a select list of known *L. pneumophila* effector proteins and their roles in infection, it is clear that many effectors facilitate survival of the bacteria within host cells. With the majority of effector proteins still uncharacterised, future

work will undoubtedly uncover further mechanisms by which *L. pneumophila* successfully establishes infection.

1.8 Host response to *L. pneumophila* infection

The immune system comprises multiple signalling processes that aid host clearance of invading pathogens. In mammals, this system consists of two main branches: the innate immune system and the adaptive immune system. Despite the fact that *L. pneumophila* sets up a specialised replicative vacuole that evades the traditional phago-lysosome fusion pathway, mouse models show that infection is usually efficiently resolved by a combination of both the innate and adaptive immune response. An early robust inflammatory response mediated via the innate immune response is important in controlling bacterial replication while the cell-mediated adaptive response is involved in the resolution and eventual clearance of infection (210). It is still unclear if these responses also apply to *L. pneumophila* infection in human as little has been studied in human.

1.8.1 Innate response

Upon infection, pathogens activate the innate immune response via pathogen-associated molecular patterns (PAMPs) which are recognised by different families of pattern recognition receptors (PRRs) on innate immune cells (211). In the case of *Legionella*, these PAMPs include lipopolysaccharide (LPS) and flagellin (212, 213). Studies show that *L. pneumophila* infection in MyD88-/- mice results in bacterial dissemination and eventual death. The dependence on MyD88 signalling for proinflammatory cytokine production within *in vitro* and *in vivo* models suggests that Toll-like receptors (TLRs) play an important role in controlling *Legionella* infection (214-216). Principally, stimulation of TLRs - particularly TLR2 and TLR5 initiate a cascade of host response to aid in recovery from *L. pneumophila* infection. Purified *Legionella* LPS does not activate TLR4 but instead activates TLR2-dependent signalling pathways (213, 217). Mice deficient in TLR2 have a decreased capacity for pulmonary bacterial clearance when compared to wild-type mice (218). In addition, peptidoglycan-associated lipoprotein (PAL) of *L. pneumophila* activates macrophages via TLR2, inducing proinflammatory cytokines IL6 and TNF (219). TLR5 typically recognizes an evolutionary conserved region of most bacterial flagellins, and subsequently elicits NF-κB activation (220). Hawn *et al*. confirmed activation by

Legionella flagellin and showed that a common polymorphism of TLR5 in humans, which abrogates function, leads to increased susceptibility to Legionnaires' disease (212).

The activation of TLRs by infected macrophages also produces pro-inflammatory cytokines such as IL12, IL18, TNFα and interferon gamma (IFNγ), leading to the recruitment of lymphocytes (221, 222). When compared to untreated mice, mice depleted in IL12 or IL12 knockout mice showed 100 times more pulmonary bacterial load, indicating that IL12 is important in bacterial clearance *in vivo* (223, 224). Together with IL18, IL12 also plays an important role in activating and eliciting IFNγ production from natural killer (NK) cells and T cells (223-225). IL12 and IL18 are induced within 24 h and 12 h after infection respectively, and depleting both in mice leads to a significant drop in IFNγ production, impairing the animal's ability to clear the infection (223, 225). IFNγ also activates infected macrophages, restricting further *L. pneumophila* replication, partly by limiting the availability of intracellular iron (226, 227). However, this may be only an *in vitro* phenomenon as IFNγ did not influence bacterial numbers in murine lung macrophages after infection (224). Likewise, together with IFNγ, TNF is able to restrict replication of *L. pneumophila* (228). Recently, IL1β was also implicated in the innate immune response against *L. pneumophila* infection. IL1β released by *L. pneumophila* infected macrophages induces chemokine production by nonhematopoietic cells such as airway epithelial cells (AECs) that line the airspace of lungs (229). This in turn results in recruitment of leukocytes to the site of infection, helping control the infection (229). Finally, intracellular Nod-like receptor (NLR) proteins capable of detecting bacterial products in the host cytosol also play an important role in immunity. Specifically, a genetic locus in mice that encodes Naip5 (a Nod protein family member) is important in restricting *L. pneumophila* replication by the Naip5/NLRC4 inflammasome that recognises bacterial flagellin and caspase-1 mediated cell death (230, 231).

1.8.2 Adaptive response

The adaptive immune system includes both antigen-specific humoral and cell-mediated immunity components. Dendritic cells (DCs) and macrophages play an important role in linking the innate and adaptive immune response. This is because their ability to present antigens on major histocompatibility (MHC) molecules in turn

stimulate antigen-specific T cell subsets (210). During an infection, immature DCs phagocytose *L. pneumophila* and allow the bacteria to establish an ER – derived vacuole but restrict bacterial replication in this compartment via apoptotic cell death mediated by caspase-3 (232, 233). After infection, the DCs are stimulated to mature and subsequently migrate to lymphatic organs (232). These mature DCs then present *Legionella* antigens on the surface, prime antigen-specific naïve T cells and finally make them into type 1 effector T cells which are capable of producing IFNγ upon sensing *Legionella* antigens presented on infected macrophages (232). IFNγ produced from the adaptive response or from the early innate response also activates monocyte-derived cells which help in bacterial clearance (224). CD4 and CD8 T cells are important in clearing *L. pneumophila* infection as mice deficient in CD4 and CD8 T cells have significantly lower survival rates compared to wild-type mice (234).

With respect to the humoral response, the frequent usage of seroconversion as a technique to diagnose Legionnaires' disease in humans has proved that antibodies are generated during *L. pneumophila* infection (210). Guinea pigs challenged with a sublethal dose of *Legionella* display a robust antibody response which then subsequently protects them against a lethal dose of bacteria, suggesting the development of adaptive immune memory (235, 236). Despite this, intracellular *Legionella* replication is not hindered in human macrophages when antibody is used to opsonise the bacteria (237). Therefore, it is still unclear if antibodies are important for controlling *Legionella* infections.

1.9 Eukaryotic ubiquitination system in bacterial infections

Post-translational modifications are widely used by eukaryotic cells in response to changes in environment, such as pathogenic infections. In particular, ubiquitination plays vital role in cell intrinsic immune defence against bacterial infections.

1.9.1 Basics of the eukaryotic ubiquitin system

Ubiquitination is a process whereby ubiquitin (Ub), a small 76 amino acid polypeptide is covalently conjugated to lysine residue on target proteins (238). This form of post-translational modification is highly conserved in eukaryotes and regulates different biological processes including tagging proteins for degradation, DNA repair, signal transduction, endocytosis and endosomal sorting and vesicle trafficking events (238-

243). Ubiquitination is a multi-enzyme process that requires E1 (Ub-activation enzyme), E2 (Ub-conjugating enzyme) and finally E3 (Ub ligase) (244). The activation of Ub by the E1 enzyme occurs in an ATP-dependent manner. Firstly, an Ub-adenylate intermediate is formed, which then reacts with a specific E1 cysteine residue to form a thioester linkage (245, 246). Following activation, Ub is transferred and covalently linked to a cysteine residue on the intermediate E2 enzyme (245). The final step in the ubiquitination cascade is facilitated by the E3 ligase, where the Ub is transferred to its target substrate protein and attached to a lysine residue via an amide isopeptide linkage, thereby modifying and tagging the protein for different destinations (243, 245, 246).

In humans, there are only two E1 enzymes, but over 40 E2 enzymes and an even greater number of E3 ligases (245, 247, 248). Historically, much attention has been placed on studying E3 ligases as they appear to dictate substrate specificity which is evident by the hundreds identified in humans (249, 250). The large number of E3 ligases can be loosely grouped into 2 major groups, HECT-type E3 ligases and the superfamily of RING finger and RING finger-like E3 enzymes (246, 251, 252). Up to 95% of known E3 ligases belong to the RING superfamily and these 2 groups differ in the mechanism by which they mediate the transfer of the Ub from the E2 conjugating enzyme to the substrate (249). For example, Ub is first transferred to HECT-type E3 before transfer to the substrate whereas RING E3 enzymes form a scaffold with the E2-Ub complex, bringing it in close proximity with the target substrate and allow the direct transfer of the Ub to the substrate, thereby circumventing E3 ligase-Ub binding (252).

Ubiquitination is a reversible process that is also regulated by a group of enzymes called the deubiquitinating enzymes (DUBs) (238, 246). DUBs have substrate specificity with more than 100 DUBs known in humans that recognise different forms of Ub modification (248, 253). They function by hydrolysing the bond between the Ub and its substrate, recycling the Ub for other uses, and as such counteract the downstream consequences of target protein ubiquitination (253).

1.9.2 Manipulation of host ubiquitin pathways by bacterial pathogens

During bacterial infections, the ubiquitination process is part of the host cell defence mechanism that senses the bacteria and subsequently activates the immune response

(246). Upon recognition of bacterial infection by host cell sensors, a cascade of signalling pathways occurs via ubiquitination events leading to the degradation of IκB, the inhibitor of NF-κB (254, 255). Activating NF-κB then triggers host inflammatory responses, which result in the limitation of bacterial replication (246). In addition, Ub-dependent autophagy has the potential to tag unwanted cellular components, such as bacteria-containing vacuoles for degradation (246).

In order to establish successful infections, many bacterial pathogens have evolved ways to disarm, manipulate and exploit the host ubiquitination machinery. In some instances, bacterial effector proteins are secreted to specifically co-opt the host ubiquitination systems resulting in cytoskeletal rearrangement, evasion of host defence, increased replication and scavenging host nutrients for growth (246, 256-259). One such example is seen in *Salmonella enterica* serovar Typhimurium, the causative agent of the gastroenteritis, Salmonellosis. During infection, ubiquitinated protein aggregates form on the surface of the *Salmonella* containing vacuole (SCV), which then triggers autophagy and destruction of the bacteria (246, 260, 261). However, the bacteria secrete an effector, SseL, which functions as a deubituitinating enzyme on the Ub aggregates, promoting SCV escape of autophagy and thereby allowing more bacterial replication (262). Another example of a bacterial DUB is YopJ of *Yersinia pseudotuberculosis*, the first bacterial effector protein discovered to have DUB activity (263). A catalytic cysteine residue of YopJ removes Ub from its target substrates (TRAF6, TRAF2 and IκBα), leading to inhibition of the NF-κB pathway and the mitogen-activated protein kinase (MAPK) pathway (263). In addition to its deubiquitinating activity, YopJ also possesses acetyltransferase activity which directly blocks phosphorylation of MAPK6 and thus prevents its activation (264, 265). The dual enzymatic activities of YopJ are thus both important in dampening the host immune response against *Y. pseudotuberculosis* infection.

As seen in *S*. Typhimurium, pathogens are also able to hijack the host ubiquitination system to regulate effector function. The SopB effector protein localises to different cellular compartments and plays distinct roles during different stages of infection depending on its ubiquitination state. During the early stages of infection, SopB is found on the plasma membrane where it has two roles. Firstly, SopB re-models the host cytoskeleton and membrane leading to increased *S*. Typhimurium invasion (266). Secondly, SopB activates Akt/protein kinase B leading to survival of *S*. Typhimurium

within epithelial cells (267). During later stages of the infection, SopB localises to the SCV where its role is to prevent lysosomal degradation of the bacteria via its phosphoinositide phosphatase activity (246). The movement of SopB from the plasma membrane to the SCV is mediated by monoubiquitination of its lysine residues, which acts as a signal for trafficking (268).

Despite the fact that bacteria lack the typical ubiquitination system found in eukaryotes, characterisation of bacterial effector proteins has found many to have eukaryotic E3 ligase-like domains and/or activities (269). These E3 ligase-like effector proteins mimic the host ubiquitination machinery so that host defences, cellular functions and signalling are disrupted. The SopA effector of *S*. Typhimurium T3SS-1 is a HECT-type E3 ligase that is found to regulate host inflammation even though the exact mechanism and target is yet to be determined (270, 271). Another newly described group of bacterial E3 ligases known as novel E3 ligases (NELs) are widely conserved among bacterial pathogens (246, 272) . Members of this group have a substrate recognising N-terminal leucine-rich repeat (LRR) domain and a conserved C-terminal domain containing a conserved cysteine residue important for E3 ligase activity (273). SspH1 of *S*. Typhimurium is an example of such an effector. SspH1 interacts with PKN1, a host serine/threonine protein kinase via the LRR domain and ubiquitinates PKN1 (274). This in turn causes PKN1 activity to increase and results in the reduction of NF-κB dependant gene expression, suggesting that this interaction plays a role in regulating host inflammatory responses during infection (274). Typically, the eukaryotic ubiquitination process is not implicated in survival of bacterial pathogens, but instead is involved in ubiquitin-proteasome degradation. For example, the SopE effector protein of *S*. Typhimurium is ubiquitinated by the host and degraded, rendering it inactive (275).

1.10 Ubiquitination is an important process in *L. pneumophila* infection

The eukaryotic ubiquitination system is also heavily implicated in *L. pneumophila* pathogenesis. This includes *L. pneumophila*-driven recruitment of polyubiquitinated proteins to the LCV and the identification of *L. pneumophila* effector proteins that function as E3 ligases and DUBs.

1.10.1 Polyubiquitination of the LCV

During *L. pneumophila* infection of mouse bone marrow derived macrophages, Dorer *et al*. first observed that shortly after formation, the cytoplasmic face of the LCV becomes decorated with polyubiquitinated proteins (111). More than 60% of the LCVs found in cells infected with wild-type *L. pneumophila* were positive for the presence of polyubiquitin within 1 h of infection, and this lasted throughout replication, until 14 h post-infection (111). The polyubiquitinated proteins were both K48- and K63- linked, with no particular preference for either (276). The accumulation of these ubiquitinated proteins also appeared to occur in a Dot/Icm dependant manner as *L. pneumophila* Δ*dotA* failed to stain with anti-polyubiquitin antibodies (111). When exposed to LPS, ubiquitin-rich dendritic cell aggresome-like structures (DALIS) contained aggregates of polyubiquitinated proteins as a result of TLR2 stimulation (277). During *L. pneumophila* infection, suppression of DALIS did not reduce the polyubiquitinated proteins on the surface of the LCV and DALIS formation was also not mediated by the bacteria (276); thereby eliminating DALIS as being responsible for the polyubiquitinated conjugates found on the LCV (277). The tight maintenance of the replication vacuole ensured that *L. pneumophila* replication was maximised.

L. pneumophila-driven polyubiquitination of its own replicative niche is an interesting phenomenon and many efforts have been made to ascertain the identity of the ubiquitinated proteins on the LCV surface. Employing a high-throughput proteomics approach, the ubiquitinated proteome of LCVs purified from human U937 macrophages infected with *L. pneumophila* Δ*ankB* and wild-type *L. pneumophila* were studied (278). AnkB is an effector protein that has been reported as essential for proliferation of *L. pneumophila* in both protozoa and human macrophages (279-281). AnkB anchors to the LCV surface through exploiting host lipidation machinery, interacts with the host SCF1 E3 ligase and mediates the accumulation of K48-linked polyubiquitinated proteins found on the LCV surface (282-285). LCVs from macrophages infected with *L. pneumophila* Δ*ankB* contain more proteins (1546 vs 1193) and slightly higher number of ubiquitinated ones (29 vs 24) when compared to wild-type *L. pneumophila* infected macrophages (278). While there are significant similarities, the ubiquitinated proteome of LCVs containing the two different strains of *L. pneumophila* are enriched for proteins of distinctly unique functions. For

instance, while both strains showed enrichment for protein transport and carbohydrate metabolism, Δ*ankB* LCVs were preferentially enriched for immune response factors (278). Similarly, differences were also seen in the identity of the ubiquitinated proteins found on the LCVs (278). Although the significance of this difference is yet to be confirmed, the absence of AnkB perhaps led to a more robust host immune response, consistent with the well-documented result of reduced replication phenotype seen in *L. pneumophila* Δ*ankB*.

Comparing ubiquitin profiles of host proteins from macrophages infected with wild-type *L. pneumophila* versus a *dot*/*icm* mutant strain revealed that only infection with the wild-type strain yielded ubiquitination-dependent downregulation of mTOR activity (286). Specifically, the PI3K-Akt-mTOR pathway is suppressed as PI3K, Akt and mTOR are ubiquitinated only in wild-type *L. pneumophila* infected macrophages (286). Ubiquitination of these positive regulators led to their degradation and therefore suppression of mTOR function. Among the processes that mTOR regulates is ribosome biogenesis and cap-dependent protein translation (287). Ivanov and Roy found that suppressing mTOR function by wild-type *L. pneumophila* led to inhibition of cap-dependent translation and this increased proinflammatory cytokine production. This Ub-dependent mechanism is thought to be how mammalian cells are able to mount an appropriate immune response to virulent pathogens whenever required.

1.10.2 L. pneumophila acquire nutrients from polyubiquitinated proteins

Through results obtained from studies of AnkB, the purpose for recruiting polyubiquitinated conjugates to the LCV was proposed to be for nutrient acquisition. More recently, Bruckert and Abu Kwaik reported that AnkB is itself also rapidly polyubiquitinated upon entering the host cell (288), and constitutes the first example of K11-linked polyubiquitination of a bacterial protein. The host proteasome rapidly degrades polyubiquitinated proteins accumulated on the LCV upon infection to increase the levels of available free amino acids required for intracellular replication of *L. pneumophila* (285). In particular, levels of free cysteine were ~25-fold greater in macrophages infected with wild-type *L. pneumophila* compared to *L. pneumophila* Δ*ankB* (285). Acquisition of host nutrients and utilising the host cell for replication and survival is a common strategy of facultative intracellular pathogens. For example, *M. tuberculosis* resides and multiplies within phagosomes found in macrophages by

utilising host-derived carbon such as glucose, cholesterol and triglycerides (289-292). Older studies have shown that the amount of free amino acids in host cells are below the levels sufficient for *L. pneumophila* to replicate intracellularly (293, 294) and while cysteine is the least abundant amino acid in eukaryotes, it is a very important amino acid for *L. pneumophila* replication. Not only is it one of the seven amino acids for which the bacteria are auxotrophic, it is also the metabolically preferred amino acid of *L. pneumophila* (295, 296). Therefore, it has been proposed that *L. pneumophila* drives the ubiquitination of the LCV in order to establish a favourable environment for nutrient acquisition and hence proliferation and survival.

1.10.3 The role of the host factor – Cdc48/p97 in L. pneumophila virulence

In addition to making the first observation of a polyubiquitinated LCV, Dorer *et al*. also found the host complex Cdc48/p97 was vital for intracellular replication of *L. pneumophila* in both *Drosophila* and human cells (111). Using immunofluorescence, Cdc48/p97 was also seen to co-localise to the surface of the LCV in a Dot/Icm dependant manner (111). Cdc48/p97 is a type II AAA (ATPases associated with various cellular activities) ATPase that plays a role in a wide range of different cellular functions (297). These include but are not limited to Golgi, ER movements and membrane reassembly (298, 299); DNA repair (300); ubiquitin proteasome degradation (301, 302) and ER associated degradation (ERAD) (303, 304). Interestingly, silencing the genes involved in the ERAD pathway, *Npl4*, *Ufd1*, *Ufd3*, *Dsk2*, *Pac10* and *CG32566* via RNAi reduces *L. pneumophila* replication significantly compared to wild-type cells (111). ERAD is part of normal cellular physiology where the complex transports and degrades misfolded proteins. While properly folded proteins leave the ER via transport vesicles, misfolded proteins within the ER are ubiquitinated and subsequently moved into the cytosol by the complex Cdc48/p97-Npl4-Ufd1 so that they can be destroyed by the proteasome (111, 305, 306). During *L. pneumophila* infection, this complex appears to remove the bacterial effector protein, LidA, from the LCV and reduces the amount of polyubiquitinated protein conjugates on the LCV (111).

In summary, ubiquitination is clearly an important process for the pathogenesis of *L. pneumophila*. However, it is still unclear whether the accumulation of polyubiquitinated proteins on the LCV surface is a mechanism that is solely driven by

the bacteria or whether it also involves the host cell. Moreover, the precise role of ERAD in LCV biogenesis requires more research.

1.11 Host autophagy in bacterial infection

Autophagy is an ancient, highly conserved cellular remodelling process that plays a number of roles in maintaining cellular homeostasis, including degradation and recycling of organelles and proteins (307). Autophagy is also involved in both the innate and adaptive immune responses (308). Traditionally regarded as a non-selective process, growing evidence suggests that ubiquitination determines selective autophagy in some substrates (309). Autophagic adaptor proteins such as p62 bind to both the Ub on target substrates and also to autophagy specific light chain 3 (LC3), directing the target substrate to become a mature autophagosome subject to degradation by lysosomes (309). An example of selective autophagy is xenophagy, which is the degradation of pathogen containing vacuoles (307, 308, 310).

1.11.1 Autophagy controls bacterial replication

In the case of *S*. Typhimurium, bacteria typically reside in the SCV, with a small number escaping into the host cell cytosol (311). Once in the cytosol, polyubiquitinated proteins rapidly bind to the bacteria, resulting in recruitment of p62, nuclear dot protein 52 kDa (NDP52) and optineurin (OPTN) to the bacterial surface (312, 313). Ubiquitin-dependent recruitment of these three autophagy receptors, p62, NDP52 and OPTN, to cytosolic *S*. Typhimurium ultimately leads to reduced proliferation of bacteria and LAMP-1 and LC3 mediated elimination of the bacteria (314, 315). Such infection control mechanisms are also important for control of other bacteria such as *M*. *tuberculosis*. Compared to autophagy-proficient mice, autophagy-deficient mice show increased susceptibility to *M*. *tuberculosis* infections (316) and it was proposed that autophagy is both antibacterial and anti-inflammatory since *M*. *tuberculosis* growth is higher and excessive pulmonary inflammation were seen in autophagy-deficient mice (316). These studies clearly demonstrate how autophagy may restrict and eliminate intracellular pathogens.

1.11.2 Legionella inhibits host autophagy

As many bacteria aim to survive and replicate within host cell, it is perhaps unsurprising that intracellular pathogens have evolved ways to evade the destructive

nature of autophagy and instead exploit this host mechanism to ensure their replication and survival. One such example is *L. pneumophila*. In addition to being polyubiquitinated, the LCV recruits the autophagy adaptors, LC3 and Atg7 (317). However, several Dot/Icm-secreted effector proteins, namely RavZ, LegA9 and *Lp*Spl enable *L. pneumophila* to curtail host autophagy via various mechanisms (318-320). RavZ is a cysteine protease that irreversibly deconjugates Atg8 proteins on early autophagosomes, rendering them inactive during *L. pneumophila* infection (319). As binding of Atg8 proteins, such as LC3, to autophagosomes is an essential initial step in autophagy, inactive Atg8 essentially inhibits the formation of autophagosomes and thereby halts progression of the pathway (321, 322). RavZ therefore interrupts autophagosome formation and thus ensures that the LCV does not fuse with lysosomes for degradation (317).

Recently, *Lp*Spl was identified as a sphingosine-1 phosphate lyase that modulates host sphingolipid metabolism (318). Specifically, *Lp*Spl prevents sphingosine biosynthesis, a by-product of sphingolipid metabolism. There was no significant p62 accumulation when catalytic inactive *Lp*Spl mutants were expressed in cells compared to active *Lp*Spl, indicating that this effector is also important for restraining autophagy during *L. pneumophila* infection (318).

Given the large number of effector proteins that *L. pneumophila* possesses, it is highly likely that there are further, as yet uncharacterised, effectors that modulate host autophagy for the benefit of the bacteria. Advances describing intimate relationship between ubiquitination and autophagy suggest that polyubiquitination of the LCV might provide another avenue for *L. pneumophila* to survive and replicate in eukaryotic cells.

1.12 Aims

Despite the Dot/Icm secretion system being a vital virulence factor of *L. pneumophila*, surprisingly little is known about the mechanism of effector translocation. To this end, only the make-up and role of the system is well-established. Even though the Dot/Icm system translocates one of the largest collections of bacterial effector proteins (> 300) into host cells during infection, the mechanism of the translocation process is poorly defined and modelled on unrelated systems such as T3SS. Intriguingly, unlike pathogens that translocate effector proteins via a T3SS or substrates of the *L. pneumophila* Lsp system, activating effector protein secretion function of the Dot/Icm system *in vitro* has not been reported. Although Dot/Icm effectors are not found in the culture supernatant collected from *L. pneumophila* grown in liquid culture medium (125), as soon as *L. pneumophila* infects an appropriate host cell, the effector proteins produced during the bacterial growth *in vitro*, are rapidly translocated from the bacteria into the infected host cell. The absolute requirement for a host cell in order for the Dot/Icm system to actively secrete effectors suggests that the host cell directly engages in Dot/Icm function and effector translocation.

The broad aim of this study was to perform a comprehensive systems based genetic screen to identify host factors important for Dot/Icm mediated translocation of effector proteins. The specific aims were to

1. To develop and perform a mammalian genome-wide RNAi screen coupled with a quantitative reporter assay that measures the amount of Dot/Icm mediated effector protein translocation
2. To identify individual host factors that when absent resulted in altered Dot/Icm effector translocation levels
3. To assess the role of selected host factors in other aspects of *L. pneumophila* pathogenesis, such as LCV biogenesis, replication and phagocytosis

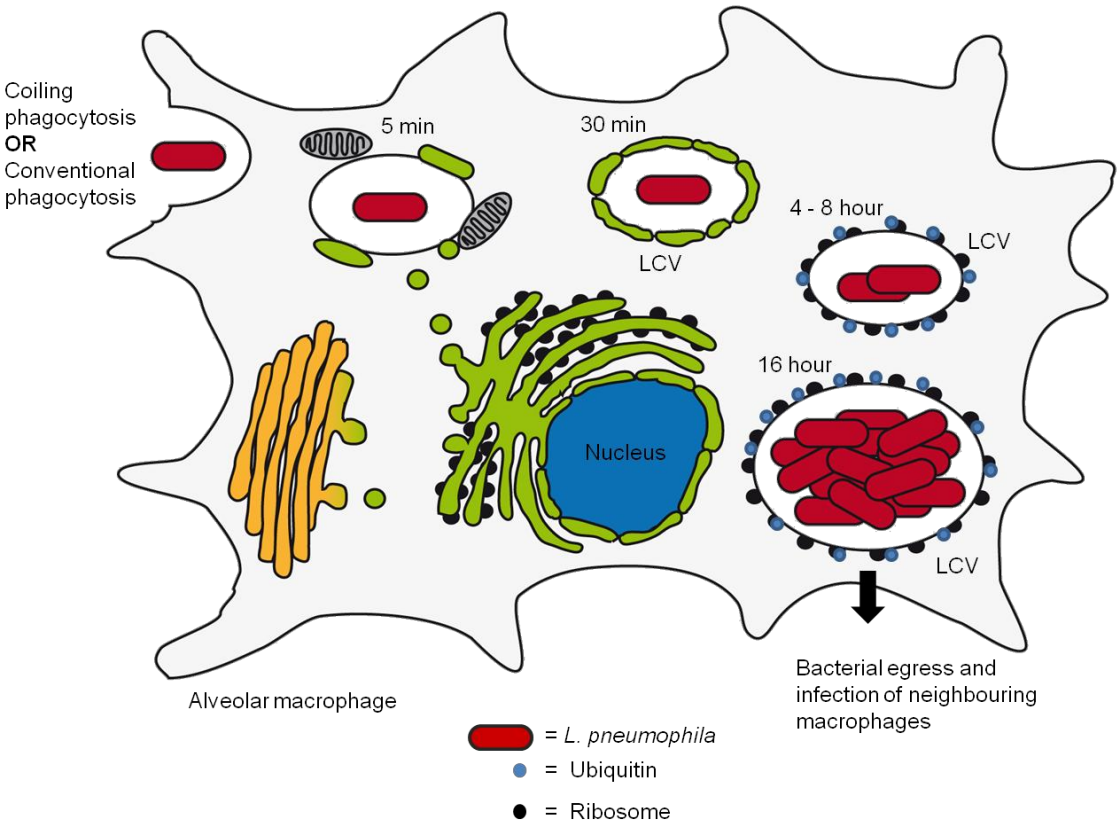

Figure 1.1 Infection process of *L. pneumophila*

Upon entry into alveolar macrophages via either coiling phagocytosis or conventional phagocytosis, the bacteria evade the degradative lysosomal fusion pathway and establish a specialised replicative vacuole – termed the ***L****egionella* **c**ontaining **v**acuole (LCV). Host mitochondria and ER-derived vesicles are rapidly recruited to the LCV surface after uptake of bacteria and a series of remodelling events occur in the next 4–6 h to establish the LCV. Once completed, bacterial replication initiates. *L. pneumophila* replicates to high numbers intracellularly and eventually egress by lysing the host cell.

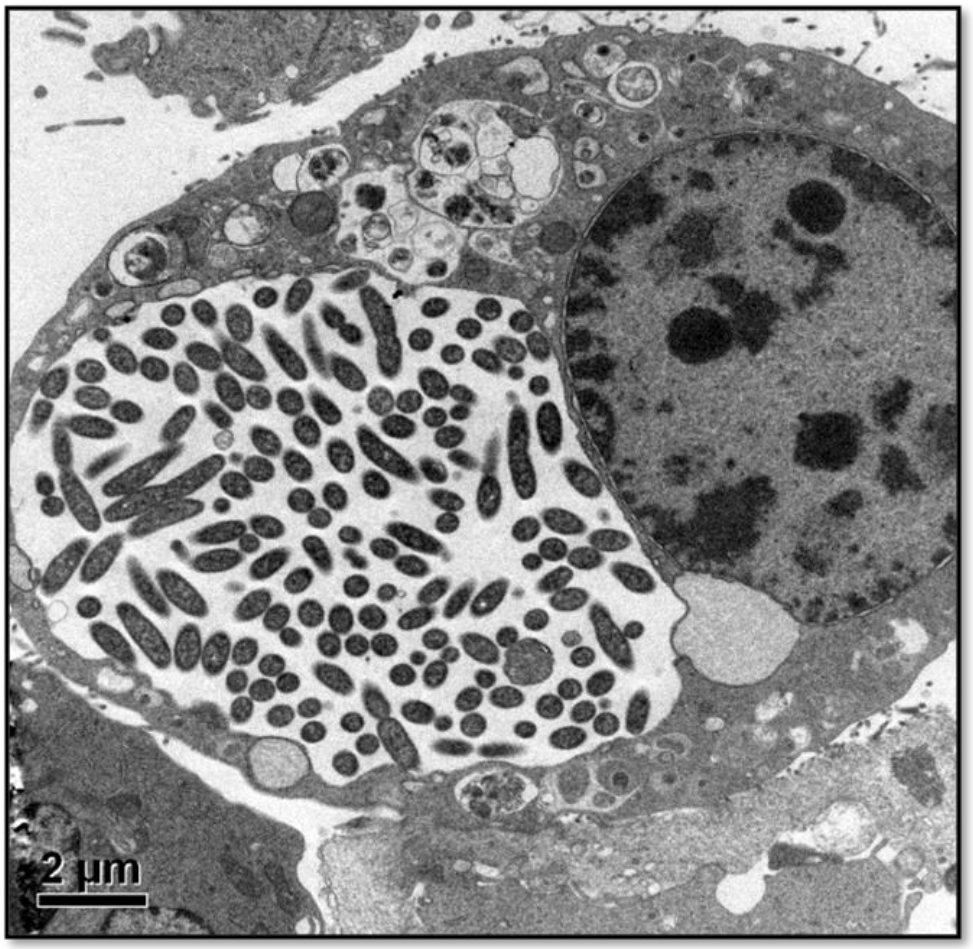

Figure 1.2 Electron micrograph of a macrophage infected with *L. pneumophila* for 24 h

Rod-shaped *L. pneumophila* is phagocytosed by macrophages during infection where the bacteria replicate in a LCV. Image courtesy of Vicki Bennett-Wood.

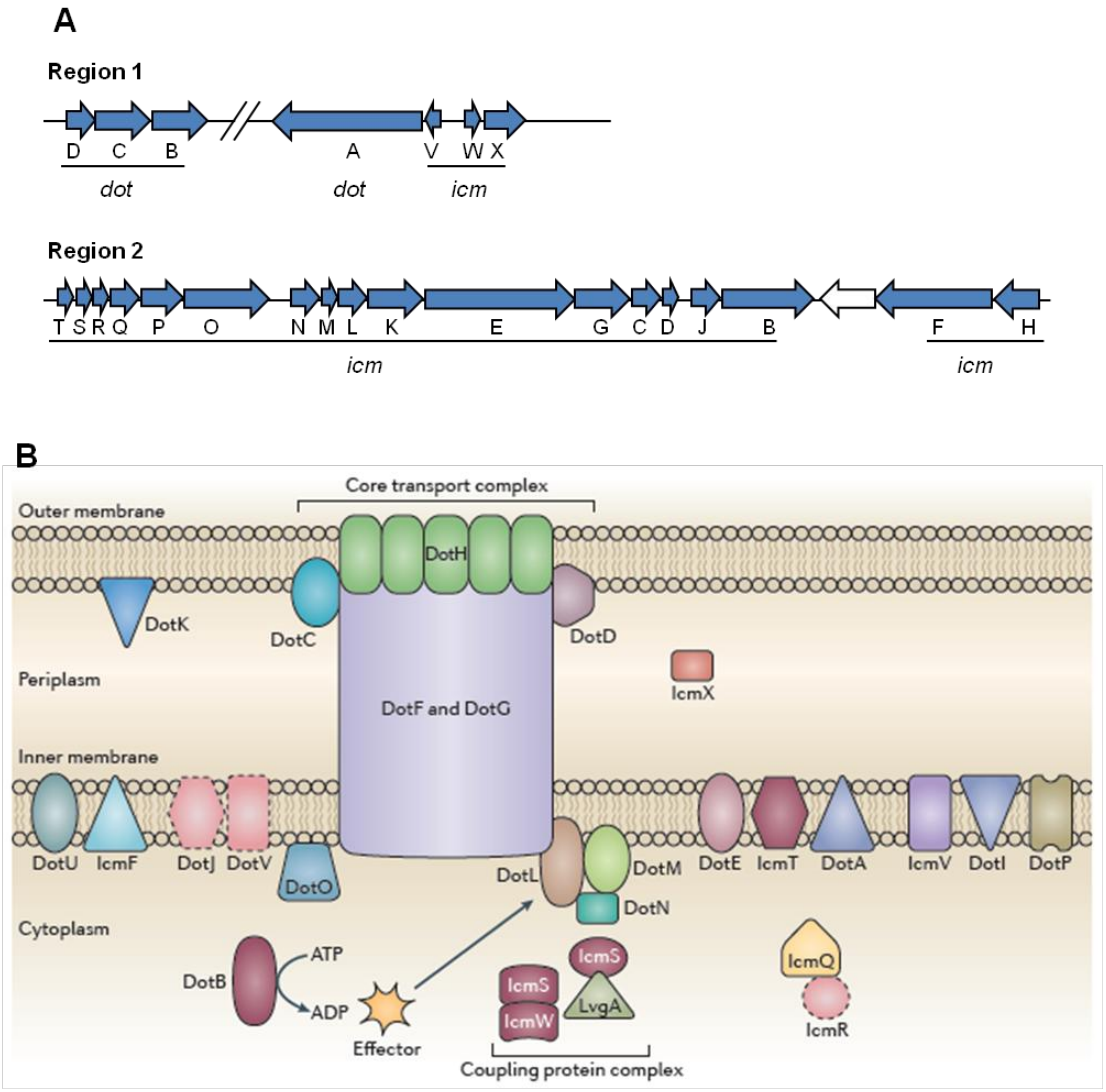

Figure 1.3 The Type IVB Dot/Icm secretion system of *L. pneumophila*

A. The two chromosomal regions of *L. pneumophila* that encode the 27 Dot/Icm secretion system genes showing gene organisation and direction of transcription, adapted from (323).

B. Overview of the *L. pneumophila* Dot/Icm secretion machinery showing the putative location of the 27 different protein components in the bacterial cytoplasm, periplasm or embedded in the inner or outer membrane, adapted from (324).

CHAPTER 2: MATERIALS AND METHODS

2.1 Chemicals and reagents

Unless otherwise stated, all common chemicals used in this study were purchased from Sigma Aldrich, Merck, Chem Supply or Amresco. Bacteriological media components were obtained from Oxoid or Sigma Aldrich, and antibiotics from Amresco, Invitrogen or Boehringer Ingelheim. Tissue culture media components were obtained from Life Technologies or Thermo Scientific.

2.2 Bacterial growth and storage conditions

All bacterial strains and plasmids used in this study are listed in Table 2.1. *E. coli* cultures were grown in either Luria-Bertani (LB) broth or agar supplemented with chloramphenicol (25 µg/mL) or kanamycin (100 µg/mL) when required. *L. pneumophila* strains were grown in either ACES [N-(2-acetamido)-2-aminoethanesulfonic acid]-buffered yeast extract (AYE) broth or on buffered charcoal yeast extract (BCYE) agar supplemented with chloramphenicol (6 µg/mL) or kanamycin (25 µg/mL) when required. *E. coli* strains cultured on LB agar were incubated aerobically at 37°C for 24 h while *L. pneumophila* strains cultured on BCYE agar were incubated aerobically at 37°C for 72 h. Liquid broth cultures of both *E. coli* and *L. pneumophila* were grown aerobically overnight at 37°C with agitation at 180 rpm. Long-term storage of both *E. coli* and *L. pneumophila* bacterial strains were in 50% glycerol broth kept at -70°C.

2.3 DNA isolation, purification and sequencing

2.3.1 Isolation of bacterial genomic DNA

A loopful of freshly streaked *L. pneumophila* cells was resuspended in 200 µL PBS containing Proteinase K enzyme (New England Biolabs (NEB)) at a final concentration of 1 mg/mL. The mixture was then incubated at 37°C for 10 min. Subsequently, *L. pneumophila* genomic DNA was then extracted using the Quick-gDNA™ MiniPrep Kit (Zymo Research Corp.) according to the manufacturer's instructions.

2.3.2 Isolation of plasmid DNA

Plasmid DNA was isolated using QIAprep Spin Miniprep kit (QIAGEN) according to manufacturer's instructions.

2.3.3 Purification of DNA

Whenever required, DNA was purified from agarose gel or PCR products using the Wizard SV gel and PCR Clean-Up System (Promega) according to manufacturer's instructions.

2.3.4 DNA sequencing and analysis

DNA was sequenced using ABI PRISM Big Dye Terminator v3.1 Cycle Sequencing kit. Electrophoresis reactions were carried out by either Centre for Translational Pathology (The University of Melbourne, Victoria, Australia) or Australian Genome Research Facility (Melbourne, Victoria, Australia). Finally, DNA sequence analyses were performed using Sequencher® version 5.0 software (Gene Codes Corporation). Sequencing oligonucleotides (Sigma Aldrich) used in this study are listed in Table 2.2.

2.4 DNA manipulations

2.4.1 DNA amplifications

Specific DNA segments were produced by polymerase chain reaction (PCR) using either AmpliTaq Gold® DNA polymerase (Applied Biosystems) or PCR Extender System (5 Prime) according to manufacturer's recommendations. PCR reactions generally consisted of 200 ng DNA template, 0.2 μM of each primer and 0.7 mM of each dNTP. PCR amplifications were performed using a G-Storm GS482 Thermal Cycler (G-STORM). PCR cycling conditions generally involved a denaturation step at 95°C for 30 sec, followed by annealing for 30 sec at a temperature dependent on the melting temperature of each oligonucleotide and finally an extension step at 72°C for 1 min per 1000 bp of PCR product. All oligonucleotides (Sigma Aldrich) used for DNA amplifications are listed in Table 2.2. PCR products were purified as described in Section 2.3.3 before insertion into plasmids of interest.

2.4.2 DNA ligations

To insert DNA fragments of interest into plasmid DNA, the plasmid was first cleaved using appropriate DNA-modifying restriction enzymes from NEB or Roche and purified as described in Section 2.3.3. Subsequently, DNA fragments were then ligated into the plasmid using a molar ratio of 3:1. In general, ligation reactions were performed using 1 µL of T4 DNA ligase (Promega) and incubated at 4°C overnight. Ligation into pGEM®-T-Easy vector (Promega) was performed according to manufacturer's instructions.

2.5 DNA transformation

2.5.1 Preparation of chemically competent E. coli

Chemically competent *E. coli* XL-1 Blue and DH5α cells were produced as described. A single colony of freshly grown bacteria was transferred from an LB agar plate to an LB broth and cultured overnight at 37°C with agitation. 1 mL of this overnight culture was sub-inoculated 1:100 into SOB and cultured at 16°C with agitation to an OD_{600} of 0.4 – 0.8. Cells were subsequently harvested by centrifugation (4°C, 15 min, 2500 rpm) and resuspended in ice-cold transformation buffer (10 mM PIPES, 15 mM $CaCl_2 \cdot 2H_2O$, 250 mM KCl). This was repeated once and the cells finally resuspended in an appropriate volume of ice-cold transformation buffer containing 7.5% (v/v) DMSO. Cells were then snap-frozen in 50 µL aliquots using a dry-ice ethanol bath before long-term storage at -70°C.

2.5.2 Chemical transformation

Pre-prepared frozen aliquots of chemically competent *E. coli* cells were first thawed on ice before addition of either plasmid DNA or ligation products. This mixture was incubated on ice for at least 30 min before subjection to heat-shock at 42°C for 90 sec and further incubation on ice for 2 min. Finally, cells were allowed to recover in 1 mL of SOC at 37°C with agitation for 75 min before being cultured on LB agar plates containing appropriate antibiotics to select for transformants.

2.5.3 Preparation of electrocompetent L. pneumophila

Freshly grown bacteria were transferred from BCYE agar plate to ice-cold dH_2O and adjusted to OD_{600} of 2. Cells were harvested by centrifugation (4°C, 10 min,

3000 rpm). This is repeated once before resuspension in an appropriate volume of ice-cold dH_2O containing 10% (v/v) glycerol, ready for immediate use.

2.5.4 Transformation by electroporation

100 µL of pre-prepared electrocompetent *L. pneumophila* cells were mixed with 500 ng of plasmid DNA before being transferred to a pre-chilled 0.2 cm gap electroporation cuvette (Cell Projects). Plasmids were then electroporated into *L. pneumophila* using a Micropuler electroporator (Bio-Rad) emitting an electric pulse of 2.3 kV at 200 Ω and 25 µF. Cells were allowed to recover for 5 h at 37°C with agitation in 1 mL of AYE broth before being cultured on BCYE agar plates containing appropriate antibiotics to select for successful transformants.

2.6 Genetic manipulation of *L. pneumophila*

2.6.1 Construction of L. pneumophila icmSW marker-less in-frame mutant

A *L. pneumophila* 130b marker-less in-frame double mutant of the *icmSW* genes was generated in a two- step mutagenesis strategy whereby *ΔicmS* was first constructed followed by *ΔicmW*. Upstream and downstream flanking regions of *icmS* were amplified by PCR using primer pairs $IcmS(U)_F$/$IcmS(U)_R$ and $IcmS(D)_F$/$IcmS(D)_R$ respectively. This was then inserted into the unique SalI restriction enzyme site of the mutagenesis vector, pSR47s which encodes kanamycin resistance and *sacB* of *Bacillus subtilis* to result in sucrose sensitivity (325). pSR47s with the desired insert was transformed into *L. pneumophila* as described in Section 2.5.4 and successful homologous recombination was determined by recovering transformants on BCYE agar plates supplemented with kanamycin (25 µg/mL). A second crossover event was subsequently selected by plating on BCYE supplemented with 5% sucrose. This resulted in either *L. pneumophila* wild-type or *ΔicmS*. A screening PCR using primer pair $IcmS_F$/$IcmS_R$ was used to confirm mutants. The double *L. pneumophila ΔicmSW* mutant was then constructed via the same strategy. Upstream and downstream flanking regions of *icmW* were amplified by PCR using primer pair $IcmW(U)_F$/$IcmW(U)_R$ and $IcmW(D)_F$/$IcmW(D)_R$ respectively. pSR47s with the desired insert was transformed into *L. pneumophila ΔicmS* and positive mutants confirmed by a screening PCR using primer pair $IcmW_F$/$IcmW_R$. This thus resulted in

a marker-less in-frame *L. pneumophila ΔicmSW*. Primers used for this purpose are listed in Table 2.2.

2.7 Construction of vectors to express TEM-1 β-lactamase and effector fusion proteins

2.7.1 Construction of pXDC61:RalF

The *ralF* (Lpw19971) gene was amplified by PCR from *L. pneumophila* 130b genomic DNA using the primer pair $RalF_{F(TEM)}$/ $RalF_{R(TEM)}$. The PCR product was digested with BamHI and XbaI and ligated into pXDC61 to produce an N-terminal TEM-1 β-lactamase fusion to RalF.

2.7.2 Construction of pXDC61:SdbB

The *sdbB* (Lpw27041) gene was amplified by PCR from *L. pneumophila* 130b genomic DNA using the primer pair $SdbB_{F(TEM)}$/ $SdbB_{R(TEM)}$. The PCR product was digested with BamHI and XbaI and ligated into pXDC61 to produce an N-terminal TEM-1 β-lactamase fusion to SdbB.

2.7.3 Construction of pXDC61:LseA

The *lseA* gene (Lpc2110) was amplified by PCR from *L. pneumophila* Corby genomic DNA using the primer pair $LseA_{F(TEM)}$/ $LseA_{R(TEM)}$. The PCR product was digested with BamHI and XbaI and ligated into pXDC61 to produce an N-terminal TEM-1 β-lactamase fusion to LseA.

2.7.4 Construction of pXDC61:LseB

The *lseB* gene (Lpc2109) was amplified by PCR from *L. pneumophila* Corby genomic DNA using the primer pair $LseB_{F(TEM)}$/ $LseB_{R(TEM)}$. The PCR product was digested with BamHI and XbaI and ligated into pXDC61 to produce an N-terminal TEM-1 β-lactamase fusion to LseB.

2.7.5 Construction of pXDC61:SidB

The *sidB* gene (Lpw16681) was amplified by PCR from *L. pneumophila* 130b genomic DNA using the primer pair $SidB_{F(TEM)}$/ $SidB_{R(TEM)}$. The PCR product was

digested with KpnI and BamHI and ligated into pXDC61 to produce an N-terminal TEM-1 β-lactamase fusion to SidB.

The above constructs were verified via DNA sequencing using primers $pXDC61_F$ and $pXDC61_R$. Verified constructs were then introduced into *L. pneumophila* 130b, *L. pneumophila* 130b Δ*dotA* or *L. pneumophila* 130b Δ*icmSW* strains via electroporation as described in Section 2.5.4. Protein expression of these constructs was confirmed via immunoblot before these strains were used for TEM-1 β-lactamase effector protein translocation assays.

2.8 Tissue culture

2.8.1 Maintenance of mammalian cell lines

HeLa cells, J774A.1 macrophages, immortalised bone marrow-derived mouse macrophages and HEK293Fcγ cells were maintained in DMEM with GlutaMax™ culture media (Gibco, Life Technologies) supplemented with 10% (v/v) heat-inactivated FBS (HyClone Laboratories, Thermo Fisher Scientific). Cells were incubated at 37°C, 5% CO_2 and passaged whenever cell growth reached ~90% confluency. To ensure optimal cell health and phenotype, a maximum of 40 passages were performed before new cell stocks are revived. To ensure consistency and reproducibility in the genome-wide RNAi screen, a new stock of cells was used for each screen run.

2.8.2 Reviving mammalian cells from frozen stocks

Stocks of HeLa cells, J774A.1 macrophages, immortalised bone marrow-derived mouse macrophages (iBMDMs) and HEK293Fcγ cells were obtained from cryogen and left to thaw at room temperature. Cells were then harvested by centrifugation (RT, 5 min, 1200 rpm), resuspended in 7 mL of culture medium and incubated at 37°C with 5% CO_2 as above.

2.9 siRNA induced knock-down of gene expression

2.9.1 siRNA transfection

Commercially purchased SMARTpool and duplex siRNA (GE Dharmacon) in lyophilised form were initially hydrated in sterile siRNA buffer (GE Dharmacon) to a

final concentration of 1 μM before use in transfections. DharmaFECT™ lipid-based transfection reagents (GE Dharmacon) were used to transfect J774A.1 macrophages, iBMDMs and HeLa cells with siRNA. For a 96 well format, the appropriate volume and formulation of DharmaFECT™ was mixed with OptiMEM (Life Technologies) to a final volume of 16 μL and incubated at RT for 5 min. Varying volumes and formulations of DharmaFECT were used as indicated. Subsequent chapters in this thesis will discuss the appropriate volume and formulation of DharmaFECT™ to use for each cell type. 40 nM of SMARTpool siRNA were next added to the above DharmaFECT™/OptiMEM mixture and left to incubate at RT for 20 min. 80 μL of cells made up to the appropriate concentration were then added to wells and the cells left to incubate at 37°C and 5% CO_2 for 24 h before the culture medium was replaced with 100 μL of fresh culture medium. Unless otherwise stated, cells were further incubated at 37°C, 5% CO_2 for 48 h before use in subsequent assays.

2.9.2 Automated siRNA transfection

To allow for high-throughput screening, the siRNA transfection process was automated in the genome-wide RNAi screen and wherever else stated such that 12 plates of cells could be simultaneously prepared. Automated siRNA transfection was performed at the Victorian Centre for Functional Genomics (VCFG), Peter MacCallum Cancer Centre. Firstly, 350 μL of DharmaFECT™4 or 175 μL of DharmaFECT™1 was incubated with 27.65 mL and 27.83 mL of OptiMEM respectively for 5 min at RT. DharmaFECT™4 was used for iBMDMs while DharmaFECT™1 was used for HeLa cells. Using a liquid dispensing robot (BioTek EL406), 16 μL of the above DharmaFECT™/OptiMEM mixture was dispensed into each well of a black, clear bottom 96 well assay plate (Corning). 4 μL of SMARTpool siRNA reagent was then added to appropriate well using the transfection robot (Calliper Sciclone ALH3000) and left to incubate for 20 min at RT. Following this, 80 μL of culture media containing 2.5 x 10^4 iBMDMs or 4 x 10^3 HeLa cells were dispensed into each well using BioTek EL406. This was then left to incubate at 37°C, 5% CO_2 for 24 h. After 24 h, culture medium was aspirated from each well using the aspirator manifold of BioTek EL406. To avoid cells from being removed during the automated aspiration process, the aspirator manifold was set to co-ordinates of x= 36 and y= 36. Finally, 100 μL of fresh culture medium was added to each well. Unless

otherwise stated, cells were further incubated at 37°C, 5% CO_2 for 48 h before use in subsequent assays.

2.9.3 Validation of knock-down via immunoblot

To confirm siRNA induced gene silencing, cell lysates were harvested after siRNA treatment as described above and analysed via immunoblot. Cells were lysed in ice-cold lysis buffer (50 mM Tris-HCl pH 7.4, 150 mM NaCl, 1 mM EDTA, 1% Triton X-100, 10 mM NaF, 1 mM PMSF, 2 mM Na_3VO_4, 1x EDTA-free Complete Protease Inhibitor Cocktail (Roche)) and cell debris removed by centrifugation at 12 000 rpm for 10 min at 4°C. Supernatant was collected and 5x SDS sample buffer added before boiling for 5 min and loaded onto 10% SDS-PAGE gels.

After SDS-PAGE, proteins were transferred onto nitrocellulose membranes (Pall). Membranes were subsequently blocked in Tris buffered saline (TBS) (50 mM Tris-HCl pH 7.5, 150 mM NaCl) containing 0.05% Tween 20 (Biochemicals) for 1 h. One of the following primary antibodies: horseradish peroxidise (HRP)- conjugated mouse monoclonal anti-β actin (Sigma Aldrich) or rabbit polyclonal anti-ATP6V0D1 (ProteinTech) was then incubated with the membrane overnight at 4°C to probe for the protein of interest. Primary antibodies were used at 1:1000 in TBS containing 5% bovine serum albumin (BSA) (Sigma Aldrich) and 0.05% Tween 20. Membranes were washed and HRP-conjugated anti-mouse or anti-rabbit (PerkinElmer) secondary antibodies were incubated with the membrane at 1:3000 in TBS containing 5% BSA and 0.05% Tween 20 for 1 h. Amersham ECL™ Western Blotting Detection Reagents (GE Healthcare) were used to develop immunoblots before detection using the DNR MF-ChemiBIS Bio Imaging System.

2.9.4 Validation of knock-down via qRT-PCR

To confirm siRNA induced gene silencing via qRT-PCR, cells were transfected with siRNA as described above for 48 h and RNA was subsequently extracted. Cells were first washed twice with ice-cold PBS and total RNA isolated using TRIsure (Bioline) according to manufacturer's instructions. In a total reaction volume of 20 µL, up to 4 µg of isolated RNA were subsequently treated with DNase I (Ambion) according to manufacturer's instructions. To synthesis cDNA, 1 µg of DNase-treated RNA was transcribed into cDNA using iScript cDNA synthesis kit (BioRad) in a reaction

volume of 20 µL according to manufacturer's instructions. cDNA was then diluted 1:7 and 2 µL utilised in qRT-PCR. In a 10 µL reaction, qRT-PCR was performed using SsoAdvanced Universal SYBR Green Supermix (BioRad) and 0.3 µM of each primer. Primer pairs $CUL7_F$/$CUL7_R$, $UBE2E1_F$/$UBE2E1_R$ and $18S_F$/$18S_R$ were used for qRT-PCR analysis of *CUL7*, *Ube2e1* and *RNA18S5* gene expression respectively. Relative mRNA levels of either *CUL7* or *Ube2e1* were analysed and normalised to the housekeeping gene *RNA18S5*. The equation fold change = $2^{-\Delta\Delta Ct}$ was used to calculate relative expression of *CUL7* and *Ube2e1*. All oligonucleotides used for qRT-PCR are listed in Table 2.2.

2.10 TEM-1 β-lactamase effector protein translocation assay

2.10.1 Infection of mammalian cells

Legionella pneumophila strains carrying N-terminal TEM-1 β-lactamase fusions to various effector proteins were cultured in AYE broth supplemented with 1 mM IPTG and 6 µg/mL chloramphenicol and grown at 37°C overnight with agitation at 180 rpm.

In general, 4 x 10^4 J774A.1 macrophages or iBMDMs and 4 x 10^4 HeLa or HeLa229 cells were seeded into black, clear bottom 96 well assay plates (Corning) and left to incubate at 37°C, 5% CO_2 for 24 h. Cells treated with siRNA were prepared as previously described in Section 2.9.1 into black, clear bottom 96 well assay plates before infection with appropriate *L. pneumophila* strains. J774A.1 macrophages and iBMDMs were then infected with *L. pneumophila* strains at multiplicity of infection (MOI) of 40 while HeLa and HeLa229 cells were infected at MOI of 125. MOI broadly indicates the number of bacteria infecting one mammalian cell. After addition of bacteria, infection was synchronised by centrifugation at 1700 rpm for 8 min, then left to incubate for 1 h at 37°C, 5% CO_2. After infection, cells were washed once with Hanks Balanced Salt Solution (HBSS) supplemented with 5% (v/v) HEPES (Sigma Aldrich). Subsequently, 100 µL of CCF2-AM LiveBLAzer™ substrate (Thermo Scientific) which was prepared according to manufacturer's instructions was added to each well and left to incubate for 1 h 30 min at RT in the dark. Finally, CCF2-AM LiveBLAzer™ substrate was removed and replaced with 100 µL of HBSS. TEM-1 β-lactamase activity in infected cells was then determined immediately by measuring the level of conversion of CCF2-AM to CCF2 with a FLUOStar® Omega or ClarioStar® microplate reader (BMG LABTECH). Microplate reader was set to

bottom-read mode with an excitation filter of 410 nm and detection of fluorescence intensity emitted at both 450 nm and 520 nm were detected

2.10.2 Data analysis

In general, ratiometric analysis was used to determine levels of TEM-1 β-lactamase activity. After measuring the fluorescent intensity emitted at 450 nm and 520 nm as described above, background fluorescence from wells containing no cells was subtracted from all sample wells to yield the net fluorescence intensity at each wavelength. Net fluorescence intensity at 520 nm was then divided by net fluorescence intensity at 450 nm to obtain the blue to green ratio for each sample. Finally, the response ratio was obtained by dividing the blue to green ratio of each sample by the average blue to green ratio of the negative control. Unless otherwise indicated, negative control refers to cells which are infected with *L. pneumophila* carrying the empty pXDC61 vector. Samples with response ratio of > 1 indicate the presence of TEM-1 β-lactamase activity.

Level of TEM-1 β-lactamase activity in siRNA treated cells in the genome-wide RNAi screen was determined by the net fluorescence intensity emitted at 520 nm. The fold change in levels of TEM-1 β-lactamase activity of each sample was obtained by dividing the net fluorescence intensity of each sample by the average of the net fluorescence intensity of the positive control. Unless otherwise stated, positive control refers to cells that were treated with OTP control siRNA.

2.11 Enumeration of viable cells in RNAi screen

To determine the number of cells for each sample in the genome-wide RNAi screen, cells were first fixed with 4% (w/v) paraformaldehyde (Sigma Aldrich) in PBS for 20 min at RT then stained with DRAQ5 (Thermo Fisher Scientific) diluted 1:1000 in PBS. DRAQ5 was incubated with cells for 30 min at RT and subsequently replaced with PBS before cells were enumerated. Enumeration was performed over 9 fields of cells taken using the 5x magnification on the automated high throughput Cellomics ArrayScan VTi microscope (Thermo Fisher Scientific).

2.12 *L. pneumophila* replication assays in siRNA treated cells

In 24 well plates (Corning), HeLa229 cells were first transfected with SMARTpool siRNA according to an adaptation of protocol described in Section 2.9.1. Briefly, 0.4 µL of DharmaFECT™1 was mixed with 63.6 µL of OptiMEM and incubated for 5 min at RT. Subsequently, 40 nM of appropriate siRNA was added and this mixture was further incubated for 20 min at RT. 1.5 x 10^4 HeLa229 cells were then added to the above mixture and incubated at 37°C, 5% CO_2 for 24 h before cells were replenished with fresh culture media. 48 h after transfection with siRNA, cells were infected with various *L. pneumophila* strains at MOI of 25. Infection was synchronised by centrifugation of the cells at 1000 rpm for 5 min at RT before cells were left to incubate at 37°C, 5% CO_2 for 2 h to allow for phagocytosis of bacteria. Following this, gentamicin (100 µg/mL) was added to the cells and left to incubate at 37°C, 5% CO_2 for 1 h to kill off non-phagocytosed *L. pneumophila*. Cells were then washed 3 times with warm PBS to remove gentamicin before fresh culture media was added to the cells and these were then further incubated at 37°C, 5% CO_2 until appropriate time-points.

At 3 h, 24 h, 48 h and 72 h post infection with *L. pneumophila*, cells were lysed by incubating 200 µL of 0.05% (w/v) digitonin (Sigma Aldrich) in PBS for 5 min at RT. This released all *L. pneumophila* that were replicating and residing within infected cells. These bacteria were collected and plated onto BCYE agar plates in 10-fold dilutions. After 72 h of incubation at 37°C, bacterial colony forming units (CFU) were counted. CFU for time-points 24 h, 48 h and 72 h post-infection were divided by CFU at 3 h to obtain *L. pneumophila* replication fold change.

2.13 Localisation of eukaryotic proteins during *L. pneumophila* infection by immunofluorescence microscopy

In order to study the localisation of eukaryotic proteins of interest during *L. pneumophila* infection, 5 x 10^4 HEK293Fcγ cells were seeded onto poly L-lysine (Sigma Aldrich) coated round glass coverslips in 24 well plates (Corning) and left to incubate at 37°C, 5% CO_2 for 24 h before infection with opsonized *L. pneumophila*. The following day, opsonised *L. pneumophila* were prepared by resuspending 10^8 bacterial cells in 1 mL of DMEM media supplemented with 10% FBS and incubating this with 1 µL of anti-*L. pneumophila* antibody (Meridian Life Sciences) at 37°C, 5%

CO_2 for 20 min with frequent mixing by hand. Cells were then infected with opsonized *L. pneumophila* at MOI of 1. Infection was synchronised by centrifugation at 1000 rpm for 5 min at RT and infected cells left to incubate at 37°C, 5% CO_2 until appropriate time-points. Following infection, cells were fixed with 4% (w/v) paraformaldehyde (Sigma Aldrich) in PBS for 20 min at RT. After fixation, cells were then permeabilised with 190 mM ammonium chloride (BDH) in PBS for 20 min at RT followed by 0.2% Triton X-100 (Sigma Aldrich) for 5 min at RT. After 30 min blocking of permeabilised cells in 3% BSA in PBS, appropriate primary antibodies prepared in 3% BSA in PSB were added to each sample and left to incubate for 1 h at RT. Primary antibodies used in this study include: mouse monoclonal anti-UBE2E1 (Santa Cruz Biotechnology), mouse monoclonal anti-CUL7 (Santa Cruz Biotechnology) and rabbit anti-*L. pneumophila* (Meridian Life Sciences), used at dilutions of 1:75, 1:75 and 1:250 respectively. Appropriate secondary antibodies prepared in 3% BSA in PBS were then added to each sample at 1:2000 and left to incubate for 45 min at RT in the dark. Secondary antibodies used in this study include: Alexa-Fluor® 568 goat anti-rabbit IgG (H+L) (Invitrogen) and Alexa-Fluor® 488 goat anti-mouse IgG (H+L) (Invitrogen). Samples were subsequently stained with Hoechst diluted in PBS to 1:4000 for 5 min at RT in the dark. Finally, coverslips were mounted onto microscope slides using ProLong Gold anti-fade mounting medium (Invitrogen). Images were acquired on Zeiss LSM710 confocal laser scanning microscope with a 63x/EC Epiplan-Apochromat oil immersion objective.

2.14 Statistical analysis

2.14.1 General experimental analysis

Statistical analyses of data were performed using GraphPad Prism 6.0 (GraphPad In Stat Software Inc.). When required, an unpaired, two-tailed student t-test or one-way ANOVA with Dunnett post-test was applied to determine statistical significance of experimental data.

2.14.2 RNAi screen analysis

To ensure that data obtained from the genome-wide RNAi screen was not skewed due to technical reasons, two different Z' factors were generated for each screen plate. To

control for the siRNA transfection process, the number of viable cells obtained after OTP and siPLK transfection was entered into the formula below:

Z' = 1 – ((3(SD of OTP + SD of siPLK))/(mean of OTP – mean of siPLK))

To control for *L. pneumophila* infection efficiency, the levels of blue fluorescence of infected OTP treated cells versus uninfected OTP treated cells were entered into the formula below:

Z' = 1 – ((3(SD of OTP-infected + SD of OTP-uninfected))/(mean of OTP-infected – mean of OTP-uninfected))

Robust z-score was generated to determine statistical significance of data obtained from the genome-wide RNAi screen. This was done by normalising the blue fluorescence of each sample against the median of the entire population. A cut-off of ± 3 was applied to identify potential hits.

Table 2.1 Bacterial strains and plasmids used in this study

Strain/Plasmid	Characteristics	Source/Reference
E. coli XL1-Blue	*recA1 endA1 gyrA96 thi-1 hsdR17 supE44 relA1 lac* [*F' proAB lacI*q*ZΔM15 Tn10* (Tet^R)]	Stratagene
L. pneumophila 130b	Serogroup 1, Clinical isolate (USA), ATCC BAA-74	(326)
L. pneumophila 130b *ΔdotA*	*dotA* in-frame deletion mutant of 130b	(327)
L. pneumophila 130b *ΔicmSW*	*icmSW* in-frame deletion mutant of 130b	This study
pXDC61	N-terminal TEM-1 β-lactamase expression vector	(328)
pXDC61:RalF	*ralF* from *L. pneumophila* 130b in pXDC61	This study
pXDC61:LseA	*lseA* from *L. pneumophila* Corby in pXDC61	This study
pXDC61:LseB	*lseB* from *L. pneumophila* Corby in pXDC61	This study
pXDC61:SdbB	*sdbB* from *L. pneumophila* 130b in pXDC61	This study
pXDC61:SidB	*sidB* from *L. pneumophila* 130b in pXDC61	This study

Table 2.2 List of primers used in this study

Name	Primer sequence (5' - 3')
$IcmS(U)_F$	AGCTAGGTCGACCCGGGTTACTAACACTTAGG
$IcmS(U)_R$	ACACTTGCTAATATCTCGCTC
$IcmS(D)_F$	GAGCGAGATATTAGCAAGTGTACTCCCCTGGATGAGTTAATG
$IcmS(D)_R$	AGCTAGGTCGACTGATAATTTGAAACCACGTTCC
$IcmS_F$	CTAATATGTTAGGGATATCATC
$IcmS_R$	AACAGCATTTGTAAAAATCACTG
$IcmW(U)_F$	AGCTAGGTCGACTTTAACGGTACATCCCAATTTAC
$IcmW(U)_R$	CTTCATGGCTTAAATCAGGCAT
$IcmW(D)_F$	ATGCCTGATTTAAGCCATGAAGCACTCGAAGGGGATGAATAA
$IcmW(D)_R$	AGCTAGGTCGACCTGTAATCCGGGGTTCCC
$IcmW_F$	GACCGTAATAGCTAATTTATTC
$IcmW_R$	GATAGTTGAGTTTACAATCGG
$RalF_{F(TEM)}$	ACGTATGGATCCATGCATCCAGAAATTGAAAAGG
$RalF_{R(TEM)}$	TCCATTCTAGATTATTTCTTATAACTGGATCTAC
$SdbB_{F(TEM)}$	GAGGATCCATGGCCAAAACTATTACAAAAG
$SdbB_{R(TEM)}$	GTTCTAGATTACATAGAGATGCTTTTACCTATTGTATTATCG
$LseA_{F(TEM)}$	ACGTATGGATCCATGAAGAAAAACAGCAGTACTAA
$LseA_{R(TEM)}$	TCCATTCTAGATTACATCAAGAAACAGCTTGAC
$LseB_{F(TEM)}$	ACGTATGGATCCATGTTTCCTCCATTACAAGATC
$LseB_{R(TEM)}$	ATCCATTCTAGATTAATTTGAAAAGGCATTTGAAG
$SidB_{F(TEM)}$	CGTGGTACCATGGTTAAAATTTATAATG
$SidB_{R(TEM)}$	CCAGGATCCCTAATTTATTTCTGGTATAC
$pXDC61_F$	CTACACGACGGGGAGTCAG
$pXDC61_R$	AGGCAAATTCTGTTTTATC
$RalF_{397,398F}$	GATGAAAGTAGATCCAGTTATAGGAGATAATCTAGATAAGCTTGGCTG
$RalF_{397,398R}$	CAGCCAAGCTTATCTAGATTATCTCCTATAACTGGATCTACTTTCATC
$RalF_{353F}$	CGCCCAATAAAAATATGGTAATTAGGGGGAGTATGTTCAG
$RalF_{353R}$	CTGAACATACTCCCCCTAATTACCATATTTTTATTGGGCG
$RalF_{369F}$	CGCTGAACAACAAGAAACTTCAAGATCTGCAACAAGAACGG
$RalF_{369R}$	CCGTTCTTGTTGCAGATCTTGAAGTTTCTTGTTGTTCAGCG
$RalF_{389F}$	CGAGGATACAGTGACTAGAAGAGATGAAAGTAGATCC
$RalF_{389R}$	GGATCTACTTTCATCTCTTCTAGTCACTGTATCCTCG
$CUL7_F$	GAGGGGCACTTTGAACAGATACT
$CUL7_R$	CTTCAGGTCGTTGAGATACAGCA
$UBE2E1_F$	ATCCGTGTATGAGGGTGGTG

$UBE2E1_R$	TGTCCAAGCAAATAACACCTTG
$18S_F$	CGGCTACCACATCCAAGGAA
$18S_R$	GCTGGAATTACCGCGGCT

CHAPTER 3: Developing a genome-wide RNAi screen in mammalian cells for studying Dot/Icm effector translocation

3.1 INTRODUCTION

For many pathogens, direct interaction with the host cell is vital in ensuring successful infection and disease propagation. Historically, the function of eukaryotic host factors in disease has been studied by gene over-expression which does not always reflect the endogenous function of the gene. For a long time, loss-of-function studies have been challenging to perform in mammalian cells due to the lack of genetic manipulation tools. However, advances in forward genetics has led to new genome editing methods such as RNA interference (RNAi) (329), zinc finger nucleases (330), transcription activator-like effector nucleases (331) and very recently clustered regularly interspaced short palindromic repeats/Cas system (CRISPR/Cas) (332). These now make it relatively easily to manipulate the genetic material of eukaryotic cells.

Since the discovery of RNAi in *C. elegans* 20 years ago, this natural process has been exploited by many researchers as a tool for loss-of-function studies in mammalian cells (333). A wide range of eukaryotic organisms including protozoans, invertebrates, vertebrates, plants, fungi and algae all utilise this endogenous cellular process to turn-off unwanted gene expression (334). In RNAi silencing, long dsRNA is first diced into short interfering RNAs (siRNA), which are shorter sequences of ~20 nucleotides. Following incorporation of the guide strand of siRNA into the RNA-induced silencing complex (RISC), the siRNA then binds to complementary messenger RNA (mRNA) target sequence, leading to cleavage of the mRNA (Figure 3.1). As a research tool, RNAi allows for precise and systematic suppression of genes via introduction of exogenous RNAi reagents (such as synthetic siRNAs or microRNA) into mammalian cells or whole animal (Figure 3.1). Advances in RNAi technology, such as the development of genome-scale libraries of RNAi reagents, have made it relatively easy to carry out systematic functional screens in human and mouse cells, tissues and whole organisms such as *Drosophila melanogaster* and *C. elegans* (335). To date, hundreds of large-scale RNAi high-throughput screens (HTS) have been performed and these have helped in identifying new genes and networks involved in diverse

biological processes ranging from cancer biology to host responses in pathogenic infections.

As is often the case with screening approaches, reports of widespread off-target effects arising from imperfect base pair matching of siRNA to mRNA quickly led to a decline in enthusiasm in using this technology (336, 337). In addition to that, the observation that only three genes out of ~800 identified were common across three independent but highly similar RNAi screens screening for host factors required in HIV replication discouraged researchers from embracing RNAi (338-341). While it is impossible to completely eliminate such effects from screening studies, strategies have been adopted to better manage this as understanding of the RNAi mechanism increased. This includes the use of bioinformatics to flag potential off-target effects as well as the development of reagents that are more specific (336).

In this study, we embarked on developing a systematic siRNA-based genome level screen to interrogate the influence of individual host genes on the translocation of *L. pneumophila* Dot/Icm effector proteins. Vital in achieving a successful RNAi screen is the precise and meticulous development of the screen itself. After extensive optimisation in three mammalian cell lines (two murine macrophage and HeLa), we eventually chose to perform a genome-wide RNAi screen in HeLa cells. The optimisation phase involved establishing the parameters necessary for two entities of the screen, the phenotypic readout assay to measure Dot/Icm activity and effective RNAi knockdown of target host genes. Optimal conditions for infecting HeLa cells with *L. pneumophila* that ensured high levels of translocation of the Dot/Icm effector RalF were determined as well as the conditions for achieving a consistent and high level of siRNA-mediated RNAi in HeLa cells for a high-throughput screen with little cellular toxicity.

3.2 RESULTS

3.2.1 *L. pneumophila* infection conditions in J774A.1 macrophages

During mammalian infection, *L. pneumophila* predominately translocates Dot/Icm effector proteins into macrophages (342). J774A.1 is a murine macrophage cell line commonly used for *L. pneumophila* studies; and so we investigated their suitability for siRNA screening (343, 344). A fluorescence resonance energy transfer (FRET) - based assay was employed to determine optimal conditions for detection and quantification of Dot/Icm mediated effector protein translocation in J774A.1 cells. Initially established by Charpentier *et al*. (345), Felipe *et al*. subsequently modified this system to allow quantification of Dot/Icm mediated effector translocation, where a β-lactamase (TEM-1) lacking a signal peptide for secretion is fused to the N-terminus of an effector protein and this is introduced into *L. pneumophila* (143). As the Dot/Icm translocation signal of *L. pneumophila* effector proteins is believed to reside in the C-terminus, TEM-1 β-lactamase is fused to the N-terminus to avoid masking this signal (Figure 3.2A) (346). Successful Dot/Icm mediated translocation of these effector proteins during infection allows the TEM-1 β-lactamase fusion protein to cleave the CCF2-AM substrate, resulting in a shift in fluorescence emission from 520 nm to 450 nm (Figure 3.2B). The ratio of the fluorescence intensity at 450 nm to that at 520 nm is expressed as the response ratio which positively correlates to the level of translocation of each effector protein.

Here *L. pneumophila* strain 130b was transformed to express TEM-1 β-lactamase fused to either the RalF or SdbB effectors and used to infect J774A.1 macrophages at five different multiplicity of infection (MOI), 1, 5, 10, 20 or 40. *L. pneumophila* 130b expressing only the TEM-1 β-lactamase (empty pXDC61), with a normalised response ratio of 1, was used as a negative control for each MOI. A response ratio > 1 represents translocation of the effector proteins into the J774A.1 macrophages during infection.

At the lowest MOI of 1, no significant level of RalF translocation was detected (Figure 3.3). However, when the MOI was increased to 5, significant levels of translocation of both SdbB and RalF were observed. The level of translocation also steadily increased as the MOI increased. The observation that the effector proteins were reliably translocated by *L. pneumophila* into J774A.1 macrophages supported

the suitability of these cells for use in screening. We concluded that the ideal MOI for J774A.1 cells was 40 due to the unambiguous detection of effector protein translocation.

3.2.2 Optimisation of siRNA transfection protocol in J774A.1 macrophages

As the strategy in this study is to use RNAi through the introduction of siRNA, high siRNA transfection efficiency is important to achieve significant and selective gene silencing. While most cell lines can quite easily be transfected with siRNA, the parameters to achieve a high level of coverage and knockdown vary from one cell line to the next. Factors that influence the success of RNAi include the type and volume of transfection reagent, cell density and amount of siRNA supplemented.

3.2.2.1 Minimising toxicity induced by transfection reagent

siRNA carries a net negative charge as does the lipid bilayer of the target cell membrane, making it challenging to introduce into target cells. Thus, different methods, such as lipid based transfection, have been developed to circumvent this complication. During transfection, siRNA is encapsulated within positively charged liposomes and this complex is allowed to traverse the target cell membrane, ensuring efficient entry of the siRNA. While cationic lipid based transfection reagents are able to facilitate the efficient delivery of siRNA into target cells, many of these also elicit an undesired cellular cytotoxic effect at the same time. Optimising siRNA transfection conditions is therefore a complex act of fine-tuning the volume of transfection reagent relative to cell densities to ensure high transfection efficiency, giving a high level of gene silencing with minimal cell toxicity.

According to the manufacturer (Dharmacon™), 90% of gene silencing in J774A.1 macrophages was attained when siRNA targeting the GAPDH gene was transfected into 1 x 10^4 cells using 0.2 µL of the transfection reagent DharmaFECT™4. These conditions were used as a recommended starting guideline for optimising siRNA transfection of the J774A.1 cell line. Here, we first evaluated different conditions to address the issue of transfection reagent induced toxicity. To measure cell toxicity, an alamarBlue® assay was used. This resazurin-based reagent is usually a non-fluorescent indicator dye; however, metabolically active cells readily reduce it to

resorufin, which produces a bright-red fluorescence that linearly reflects the number of viable cells.

Three cell densities of J774A.1 macrophages were mock transfected using 4 different volumes of DharmaFECT™4 and left to incubate for 24 h before an alamarBlue® cell viability assay was performed (Table 3.1). The level of fluorescence emission by resorufin was measured and compared to the respective untreated negative control. As shown in Figure 3.4, the recommended guideline for one well of a 96 well plate (0.2 µL of DharmaFECT™4 and 1 x 10^4 cells) proved to be toxic for the J774A.1 macrophage line used here as indicated by a significant reduction in viable cells when compared to the untreated control. Similarly, a significant amount of cell death was observed when 0.3 µL of DharmaFECT™4 was used regardless of cell densities (Figure 3.4). Using 0.2 µL of DharmaFECT™4 did not affect cell viability for both 2.5 x 10^4 and 3 x 10^4 of cells. However, the latter exceeded the limit of the eventual phenotypic assay for quantifying effector protein translocation, and thus later attention was focused solely on optimising the parameters for obtaining high transfection efficiency of siRNA into 2.5 x 10^4 J774A.1 macrophages per well of a 96 well plate.

3.2.2.2 Conditions to achieve high siRNA transfection efficiency

With the cell density chosen above and using DharmaFECT™4 for the transfection of siRNA into J774A.1 macrophages, the final parameter to optimise was the amount of transfection reagent required to effectively deliver siRNA into these cells. The fluorescent transfection indicator, siGLO, was employed for this purpose. Formulated by Dharmacon™, siGLO is a siRNA that does not target any gene in the genome and in addition, carries a red fluorescent tag. This unique property of siGLO allows qualitative visual assessment of transfection efficiency. This is because only cells that have successfully taken up the siGLO appear red when viewed under a fluorescence microscope while untransfected cells remain colourless.

To investigate the parameters for obtaining high siRNA transfection efficiency, Conditions 5 – 8 listed in Table 3.1 were again used to transfect 40 nM of siGLO. 72 h later, these were viewed under a fluorescence microscope and the level of successful transfection determined by the number of red fluorescent cells (Figure 3.5). Very low numbers of viable cells remained when 0.3 µL of DharmaFECT™4 was used which is consistent with that previously observed in the alamarBlue® assay

(Figure 3.4), suggesting that the cell death observed was most likely due to toxicity from the transfection reagent. However, ~80% of red fluorescent cells were observed when any of 0.1 µL, 0.15 µL or 0.2 µL of DharmaFECT™4 was used (Figure 3.5). Hence, a method that more definitively differentiates the best condition out of these three for achieving high siRNA transfection efficiency was required.

To assess siRNA knockdown efficiency, levels of target protein expression were analysed using immunoblots of cell lysates collected from siRNA-treated J774A.1 cells. Cells were transfected with siRNA targeting the β-actin gene using the 3 different volumes of DharmaFECT™4. Also included were mock transfected controls as well as an untransfected negative control. A reduction of β-actin protein levels could be seen when comparing the siRNA treated samples to the respective mock controls when 0.15 µL or 0.2 µL of DharmaFECT™4 was used (Figure 3.6A). However, the loading control undesirably showed less total cellular protein in the 0.2 µL but not the 0.15 µL sample, indicating cell loss. When a similar experiment was performed using siRNA targeting the vATPase gene, a similar pattern was observed (Figure 3.6B). Thus, in a 96 well plate format, 0.15 µL of DharmaFECT™4 could be used to efficiently transfect siRNAs into 2.5 x 10^4 J774A.1 macrophages as indicated by both the high number of siGLO transfected cells and high knockdown in expression of the siRNA targeted genes.

3.2.3 Negative impact on viability observed for J774A.1 macrophages treated with siRNA

Even though the parameters required for yielding good siRNA transfection and knockdown efficiency were established, it was also important to ensure that the transfection outcome produced low variability and high reproducibility to reduce the likelihood of identifying false positives. Using the parameters described above, two plates (A and B), each containing 48 replicates of J774A.1 macrophages transfected with the non-targeting siRNA, OTP and 24 replicates of untransfected controls were prepared. The cell viability alamarBlue® assay was then performed. Fluorescence intensity emitted at 590 nm was measured and represented as a percentage of the average for each set of replicates. Surprisingly, unlike the untransfected control group, the number of viable cells within the OTP replicates of both plates varied significantly (Figure 3.7). In order to statistically measure this dispersion, the coefficient of

variation (CV) for this was determined (Table 3.2). The CV for plates A and B were 88% and 83% respectively, indicating high variability in the number of viable cells within the OTP replicates. In contrast, the CV for plates A and B were only 9% and 16% for the untransfected control group, indicating low variability in the number of viable cells within the untransfected replicates. Unfortunately, this highly variable response of J774A.1 macrophages to the siRNA transfection process made this cell line unsuitable for use in a high-throughput screen.

3.2.4 *L. pneumophila* infection conditions in immortalised mouse bone marrow derived macrophages (iBMDM)

Due to the shortcomings of the J774A.1 cell line, immortalised bone marrow derived macrophages (iBMDM) from C57BL/6 mice were next tested for suitability for use in the RNAi screen. Again, it was important that the Dot/Icm mediated secretion of *L. pneumophila* effector proteins could be effectively quantified using the TEM-1 β-lactamase assay previously described. To confirm this, iBMDM were infected with *L. pneumophila* strains carrying N-terminal TEM-1 β-lactamase fusions with either RalF or SdbB and the level of translocation of each effector protein was quantified and presented as response ratio (Figure 3.8). Very low levels of both effectors were secreted at an MOI of 1 and 5, and this was significantly higher (as indicated by the higher response ratio) when the MOI was increased to ≥ 10 (Figure 3.8). This was especially true for RalF, where a response ratio of ~30 was recorded at MOI of 40 (Figure 3.8). Similar to the J774A.1 macrophages, infecting iBMDM with *L. pneumophila* at a high MOI of 40 was optimal for studying Dot/Icm mediated effector protein translocation.

3.2.5 Optimising siRNA transfection conditions in iBMDM

Despite having optimised the siRNA transfection conditions in J774A.1 macrophages, these were not entirely transferable to iBMDM. This is because different cell lines have different requirements for achieving good siRNA transfection efficiency with minimal cell toxicity.

For the purpose of optimising these conditions in the iBMDM cell line, a cytotoxic transfection indicator siRNA (siPLK) was utilised. As a result of silencing the polo-like kinase (PLK) gene, cells rapidly undergo apoptosis as this gene has an important

role in cell cycle regulation. Due to restrictions on cell densities dictated by the TEM-1 β-lactamase assay, we chose to use the same density determined for J774A.1 (2.5 x 10^4 cells per well of a 96 well plate). Three different amounts of DharmaFECT™4 were used to transfect siPLK into this density of iBMDM cells and a PrestoBlue® cell viability assay that functions in similar fashion to the alamarBlue® assay, was performed. The fluorescence intensity was presented as a percentage of the mean of the non-targeting OTP control (Figure 3.9A). In comparison to the respective OTP control, 80%, 50% and 25% of cells remained viable when 0.14 μL, 0.16 μL and 0.2 μL of DharmaFECT™4 were used respectively to transfect the cytotoxic siPLK (Figure 3.9A). This highlighted that a higher volume of transfection reagent was required to efficiently deliver siRNA into iBMDM compared to J774A.1.

To further confirm the optimal transfection conditions, immunoblots were performed to determine protein levels of siRNA treated samples versus various negative controls. Results suggested that using 0.2 μL DharmaFECT™4 to transfect siRNA targeting β-actin into iBMDM led to almost complete elimination of the protein while β-actin could still be detected when 0.16 μL was used (Figure 3.9B). The silencing of vATPase was also examined. Similar to that observed for β-actin, reduction of vATPase production was observed in siRNA treated samples using 0.2 μL of transfection reagent (Figure 3.9C). This demonstrated that for each well of a 96 well plate, using 0.2 μL of DharmaFECT™4 resulted in optimal delivery of siRNA into 2.5 x 10^4 iBMDM.

3.2.6 Cell death of iBMDM treated with targeting siRNA

J774A.1 macrophages were previously shown to have a highly variable cellular response when transfected with non-targeting siRNA in a 96 well format, rendering them unsuitable for use in a genome-scale screen. For this reason, iBMDM were also monitored for any adverse cell viability responses post transfection. 24 replicates of iBMDM were transfected with non-targeting siRNA, OTP and 8 replicates left as untransfected controls before assessment of cell viability using the PrestoBlue® assay. The fluorescence intensity emitted at 590 nm was expressed as a percentage relative to the average of each group of replicates. In contrast to J774A.1, both plates displayed low variability in cell viability after treatment with OTP siRNA (Figure 3.10). This was also evident from the low CV (Table 3.3). The level of cell viability

of the OTP-treated group was also consistent with the untransfected group, showing no negative impact on cell viability due to siRNA transfection.

From this perspective, iBMDM appeared to be an ideal cell line for use in the siRNA based genome-wide high-throughput screen. As such, an initial screen was performed using the first 12 plates from the mouse siRNA library (Plate number: 14001 - 14012). Each plate consists of 80 distinct SMARTpool siRNA that each targets a different gene in the mouse genome and includes cytotoxic siPLK and OTP siRNA as controls. These were transfected into iBMDM using the previously determined siRNA transfection conditions. On visual inspection 72 h after siRNA treatment, wide-spread cell death was sighted in samples that were transfected with targeted siRNA but not in any of the controls. In order to quantitatively verify this phenomenon, a fluorescent DNA probe – DRAQ5 was used to stain cellular DNA. This allowed the number of cells present in each siRNA treated sample to be enumerated and normalised to that of the OTP control. Indeed, transfection of iBMDM with siRNAs found in all the 12 plates resulted in a very low level of viable cells (< 0.5) (Figure 3.11). This confirmed that there was a significant adverse effect on cell viability upon the introduction of target siRNAs into iBMDM. The negative outcome of this initial screen showed that these cells were also not suitable for use in a siRNA-based genome screen.

3.2.7 Optimising siRNA transfection conditions in HeLa cells

The inconsistencies in cell viability observed for two different macrophage cell lines as a consequence of siRNA treatment hinted that an alternative cell line was needed. The epithelial cell line, HeLa, had been shown by Dharmacon™ to be easily transfected with siRNA with effective results. HeLa cells had also been regularly documented as the cell line used in various large-scale RNAi screens, giving added confidence that technical difficulties would not be the limiting factor (347, 348).

Once again, parameters for obtaining optimal siRNA transfection efficiency had to be established for the HeLa cell line. Based on recommendations by Dharmacon™ for one well of a 96 well plate, 3 different volumes of the transfection reagent DharmaFECT™1 - 0.1 µL, 0.2 µL or 0.3 µL were paired with 3 different cell plating densities of 3500, 4000 or 4500 cells. To determine the best parameters for obtaining a high level of siRNA-mediated target gene knock-down in HeLa cells with minimal impact on cell viability, siTOX, a cytotoxic siRNA similar to siPLK was transfected

into HeLa cells using the nine different transfection conditions listed in Table 3.4. Non-targeting OTP siRNA, mock and untreated control samples were also prepared for each of the tested conditions. 72 h after transfection, DRAQ5 was used to fluorescently stain the cell nucleus to allow for enumeration of dead vs. viable cells.

The first three conditions tested resulted in relatively high number of live cells after treatment with siTOX, while Conditions 4 – 9 all resulted in significantly fewer (~1000) viable cells compared to OTP. This indicated poor siRNA transfection efficiency using Conditions 1 – 3 (Figure 3.12). By comparing the mock samples to the untransfected controls, there were significantly fewer viable cells only when 0.3 µL of the transfection reagent was used (Figure 3.12). This undesirable effect was not observed for the lower volumes of reagent used, suggesting that 0.3 µL induces toxicity. With the aim of achieving high levels of siRNA transfection efficiency without negatively impacting cell viability, Condition 4 (0.1 µL DharmaFECT™1; 4000 cells) was chosen as having the ideal parameters in achieving this balance. While Conditions 5, 7 and 8 also displayed similar results to Condition 4, they were not preferred solely for economic reasons.

3.2.8 HeLa cell survival upon treatment with targeting siRNA

iBMDM cells were previously shown to suffer from cell viability loss when transfected on a large scale with target siRNAs. To be certain that this undesirable effect did not also occur in HeLa cells, 240 SMARTpool siRNAs each targeting a different gene in the human genome were randomly selected from the library and transfected into HeLa cells. These were equally divided into 3 library plates (Plate number: 11019, 11020 and 11021) which also contained the non-targeting OTP, the cytotoxic siPLK and mock controls. As before, 72 h after siRNA treatment, cell nuclei were fluorescently stained with DRAQ5 and the number of dead vs. viable cells subsequently enumerated. As shown in Figure 3.13, by comparison to the OTP controls, most of the samples that had been transfected with target siRNAs yielded comparable number of live cells post-transfection. This is in contrast to that observed for iBMDM cells (Figure 3.9) and provided promising evidence that HeLa cells were suitable for use in a large scale siRNA-based screen. The cytotoxic siPLK treated controls yielded only < 10% of viable cells compared to the OTP controls, further verifying that there was efficient transfection of siRNAs into HeLa cells.

3.2.9 Effector protein translocation into HeLa cells during *L. pneumophila* infection

After optimising the siRNA transfection parameters of HeLa cells, the next step was to determine whether *L. pneumophila* can successfully infect these cells and translocate effector proteins via the Dot/Icm system.

To this end, three *L. pneumophila* 130b strains, each expressing N-terminal fusions of TEM-1 β-lactamase to one of three effector proteins (RalF, LseA or LseB) were used separately to infect HeLa cells for 1 h. Five MOIs, (40, 70, 100, 125 and 150) were tested. The TEM-1 β-lactamase assay was then performed to quantify the level of translocation of each effector protein. Results revealed that as the MOI increased, the level of effector protein translocation also increased correspondingly (Figure 3.14). This confirmed that *L. pneumophila* is able to infect HeLa cells and also effectively translocates Dot/Icm effector proteins during infection. In addition, the results showed that out of the three effector proteins tested, RalF was the most highly translocated, followed by LseB and finally LseA (Figure 3.14). We exploited this phenomenon to mimic the range of phenotypes in Dot/Icm mediated effector translocation that might be expected when different host genes were silenced. Differences in the secretion levels of RalF, LseA and LseB were statistically analysed. In particular, the Z' factor was evaluated as it quantitatively measures the quality of the TEM-1 β-lactamase assay. Z' statistics analyse the separation between the positive and negative controls of an assay and indicates likelihood of scoring false positives and negatives. Pair-wise comparisons were performed and the corresponding Z' factor values are listed in Table 3.5. These pairs were chosen to ensure that the TEM-1 β-lactamase assay was not only able to indicate presence or absence of translocation, but, were also capable of confidently differentiating between different amounts of effector protein translocation.

A Z' factor of 0.5 – 1 represents an excellent assay; 0.3 – 0.5 indicates an above average assay while 0 – 0.3 represents an assay that is on the margin of being acceptable. A value of less than 0 is interpreted as having too much overlap with the compared pair. In this case, the assay would not be recommended for use as the phenotypic readout would likely result in false positives and negatives As evident from Table 3.5, the amount of effector protein translocation into HeLa cells when

infected with *L. pneumophila* at MOI 40, 70, 100 and 150 did not result in a good Z' factor value for the TEM-1 β-lactamase assay, thereby eliminating them as good assay parameters. Using an MOI of 125, excellent Z' factor values were obtained for all the 3 comparisons performed, suggesting that these are the optimal conditions for infection of HeLa cells with *L. pneumophila* (Table 3.5). This would allow for identification of host genes that when silenced, influence Dot/Icm effector translocation.

3.3 Discussion

Macrophages are a diverse population of cells that make up part of the innate immune system. They are found in almost all tissues throughout the body, from microglia of the central nervous system to Langerhans cells of the skin (349). During the innate response, these phagocytic cells are capable of engulfing invading pathogens and digesting them, thereby eliciting a quick and immediate defence against infectious agents (349). Macrophages also present antigens to T cells, thus initiating the highly-specific adaptive immune response against the invading pathogen (350).

Despite this, a remarkable number of microbial pathogens, including *L. pneumophila* have evolved mechanisms to not only evade destruction by host macrophages, but to also use the cells as an intracellular replicative niche (349). *L. pneumophila* typically infects and replicates within alveolar macrophages found in the lung. As such, we initially attempted to develop an RNAi screen in a macrophage cell line. However, achieving good siRNA-induced RNAi in macrophages proved to be technically challenging. Our results showed that transfecting siRNAs into murine J774A.1 monocyte macrophages and iBMDM resulted in unexpected, large-scale cytotoxicity. For J774A.1, even non-targeting siRNA (OTP) resulted in significant cell death. Thus, we were unable to further use this cell line in our study. While iBMDM initially tolerated OTP siRNA, we subsequently found that transfecting targeting siRNA into these cells also resulted in widespread cell death.

Other studies have also found that macrophage cell lines such as RAW 264.7, J774A.1 and THP-1 are particularly troublesome when trying to transfect foreign DNA or RNA into them (351). Hence, it is perhaps not surprising that we faced these setbacks when transfecting exogenous siRNA into macrophages. In terms of harnessing RNAi as a research tool in macrophages, gene silencing levels can be relatively inefficient in macrophages and vary greatly from gene to gene (352). There are many possible reasons for this, such as these cells inherently carry enzymes that destroy non-self nucleic acids (353, 354). Indeed, only moderate levels of gene expression knock-down were observed when we transfected THP-1 macrophages with target siRNA (data not shown). Furthermore, high toxicity levels are usually associated with lipid-based method of transfection; though this was not the cause of

the toxicity we observed for J774A.1 macrophages and iBMDM in our study as mock treated cells did not exhibit widespread cell death (351, 355).

The widespread cytotoxicity we observed could be attributed to the exogenous siRNA itself causing an immune reaction within the cells. Long dsRNAs are well-documented as triggers of non-target-related induction of type I interferon (356-358). As such, siRNAs need to be designed so that they avoid this reaction. siRNAs that are < 30 bp in length are generally believed to not cause adverse cellular immune reactions such as recognition by Toll-like receptor (TLR) 3, and activation of protein kinase R, which generally lead to suppression of protein synthesis (356, 357, 359, 360). However, one study found that in five cell lines, DU 145, HEK293, HeLa, HeLa S3 and MCF7, siRNA of only 23 bp in length could lead to activation of potent interferon responses, which was associated with varying degrees of cell death in cultured cells (361). More importantly, Reynolds *et al*. further elaborated that instead of there being a fixed length threshold for siRNA that induces interferon responses and cellular toxicity, this varies from cell type to cell type (361). In addition, siRNAs with high GU content are thought to bind to and activate TLR7 in plasmacytoid dendritic cells, leading to interferon alpha induction and, ultimately cell death (356). All of these reasons are possible causes of the widespread toxicity we observed when siRNAs were transfected into macrophages. Even though the exact mechanism was not determined, the deleterious consequences on cell viability meant that we did not further pursue macrophages as the cell line of choice for our genome-wide RNAi study.

Recent studies have employed new protocols to efficiently transfect macrophages with siRNA. For example, the Amaxa Nucleofactor 96 well Shuttle System was proposed to be suitable for use in medium to high-throughput RNAi studies in RAW264.7 and J774A.1 macrophages (352). Despite this, to our knowledge, there is only one published genome-wide RNAi screen performed in macrophages. This study revealed that CD137 is a host factor important for clearance of *Francisella tularensis* in THP-1 macrophages (362). Since macrophages play a key role in the innate response to pathogens, it is clear that improvements in reliable genome-wide screening methods such as CRISPR/Cas9 will allow us to better understand these processes.

Currently, genome-wide siRNA screens aiming to study the phenotype of macrophages or macrophages-like cells are predominantly performed in *Drosophila* cells (363). In particular, the *Drosophila* Schneider 2 (S2) cell line is popular as it was derived from a macrophage-like lineage and thus, is regularly used as a model system for macrophage-related studies (364-366). As opposed to mammalian macrophage cells, *Drosophila* S2 cells not only passively take up dsRNA from the culture medium, bypassing complications involved with deliberate transfection, they also lack a strong innate immune response upon dsRNA introduction (367, 368). Hence, their susceptibility to genetic manipulations through RNAi has been useful for genome-wide RNAi screens that have identified new components of the metazoan secretory pathway and lysosome motility regulation (369, 370). While *Drosophila* S2 cells are a good substitute for macrophages, being able to consistently and reliably genetically manipulate the macrophage itself will no doubt be embraced by researchers.

In contrast to macrophages, other mammalian cell lines such as fibroblasts, epithelial cells or mesenchymal cell lines are more tolerant of exogenous siRNAs and also more responsive to the effects of siRNA-induced gene silencing. In our study, we overcame the technical challenges posed by macrophages by utilising HeLa cells. As previously discussed, the *Drosophila* S2 cell line may be used instead. Indeed, it was previously used to study *L. pneumophila*-host interactions (368). However, differences still exist between insect and mammalian cells and thus, the relevance of results achieved from insect cells remained questionable.

HeLa cells have been extensively used for genome-wide siRNA-based RNAi screens, including screens studying host-pathogen interactions. A genome-scale RNAi screen found 72 proteins to be involved in different stages of *Salmonella* invasion during infection, from initial attachment to host cells through to maturation of the *Salmonella*-containing vacuole (371). In our study, we were successful in transfecting HeLa cells with siRNAs in a high-throughput manner with consistently high levels of target gene knock-down and no adverse cellular responses such as the siRNA-induced widespread toxicity. In addition, previous studies have found that virulent *L. pneumophila* strains are not only able of efficiently invading HeLa cells, but also replicate intracellularly within an LCV (372-374). Prior to this study, the translocation of *L. pneumophila* effector proteins into HeLa cells during infection had not been thoroughly characterised. Using TEM-1 β-lactamase as a reporter, we found that three

characterised Dot/Icm mediated effector proteins, RalF, LseA and LseB were translocated into HeLa cells during infection. This further verified that HeLa cells were a good candidate cell line for studying *L. pneumophila* pathogenesis.

In summary, after extensive optimisation, we developed an RNAi strategy to systematically screen the entire human genome for host factors that are important for the *L. pneumophila* Dot/Icm system to translocate effector proteins. We utilised HeLa cells over conventional cell types such as macrophages in our screening study as we found them to more reliable and consistent for the purposes of this RNAi approach. We were able to relatively easily transfect siRNA into HeLa cells and achieved a high level of target gene knock-down. More importantly, we confirmed that *L. pneumophila* translocates Dot/Icm effectors into HeLa cells during infection, thereby, allowing us to reliably quantify differences in the level of Dot/Icm effector translocation.

Table 3.1 Conditions evaluated in J774A.1 and iBMDM for optimal siRNA transfection efficiency

Condition	Cell Number [a]	Volume of DharmaFECT™4 [a] (μL)
1	1×10^4	0.1
2	1×10^4	0.15
3	1×10^4	0.2
4	1×10^4	0.3
5	2.5×10^4	0.1
6	2.5×10^4	0.15
7	2.5×10^4	0.2
8	2.5×10^4	0.3
9	3×10^4	0.1
10	3×10^4	0.15
11	3×10^4	0.2
12	3×10^4	0.3

[a] per well of a 96 well plate

Table 3.2 Coefficient of variance (CV) for J774A.1 macrophages transfected with OTP

	Coefficient of Variance (%)	
	OTP [a]	Untransfected
Plate A	88	9
Plate B	83	16

[a] non-targeting control siRNA

Table 3.3 Coefficient of variance (CV) for iBMDM transfected with OTP

	Coefficient of Variance (%)	
	OTP [a]	Untransfected
Plate A	5	10
Plate B	14	7

[a] non-targeting control siRNA

Table 3.4 Conditions evaluated in HeLa cells for optimal siRNA transfection efficiency

Condition	Cell Number [a]	Volume of DharmaFECT™1 [a] (μL)
1	3500	0.1
2	3500	0.2
3	3500	0.3
4	4000	0.1
5	4000	0.2
6	4000	0.3
7	4500	0.1
8	4500	0.2
9	4500	0.3

[a] per well of a 96 well plate

Table 3.5 Z' factor values comparing levels of translocation of 3 different *L. pneumophila* effector proteins

Pair-wise comparisions	Multiplicity of Infection (MOI)				
	40	**70**	**100**	**125**	**150**
Ralf vs pXDC61	0.42	0.85	0.60	0.94	0.82
RalF vs LseB	0.90	-7.20	-4.04	0.92	0.73
LseB vs LseA	0.42	-0.66	-0.46	0.55	-0.70

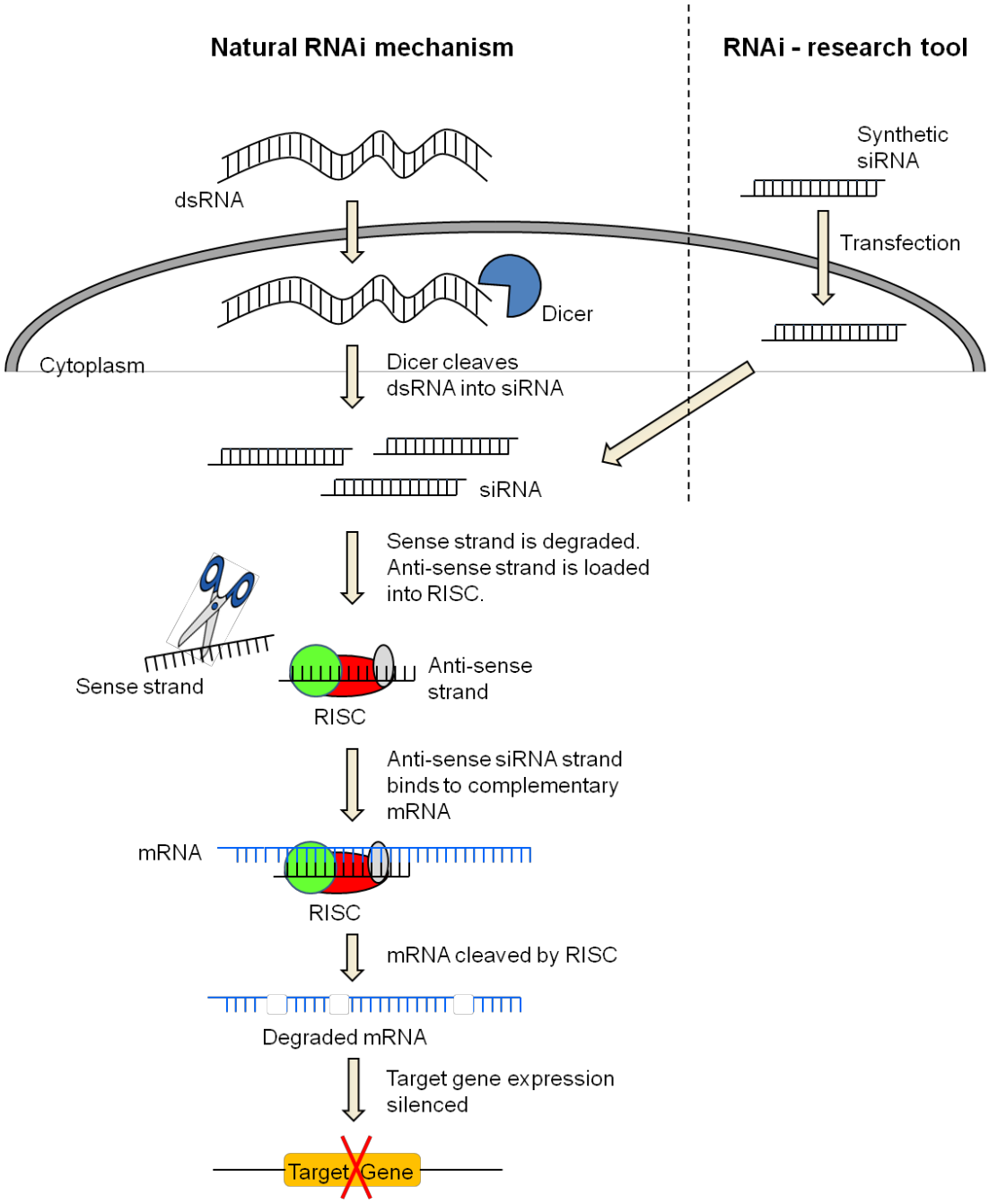

Figure 3.1 Mechanism of RNAi gene silencing

RNAi is a natural biological phenomenon seen in a wide diversity of organisms. It suppresses the expression of target genes when dsRNA specifically target mRNA for degradation. It is also a valuable research tool whereby synthetic siRNA are designed and introduced into cells to silence specific gene of interest by hijacking the endogenous RNAi machinery. Adapted from Gu *et al*. (375).

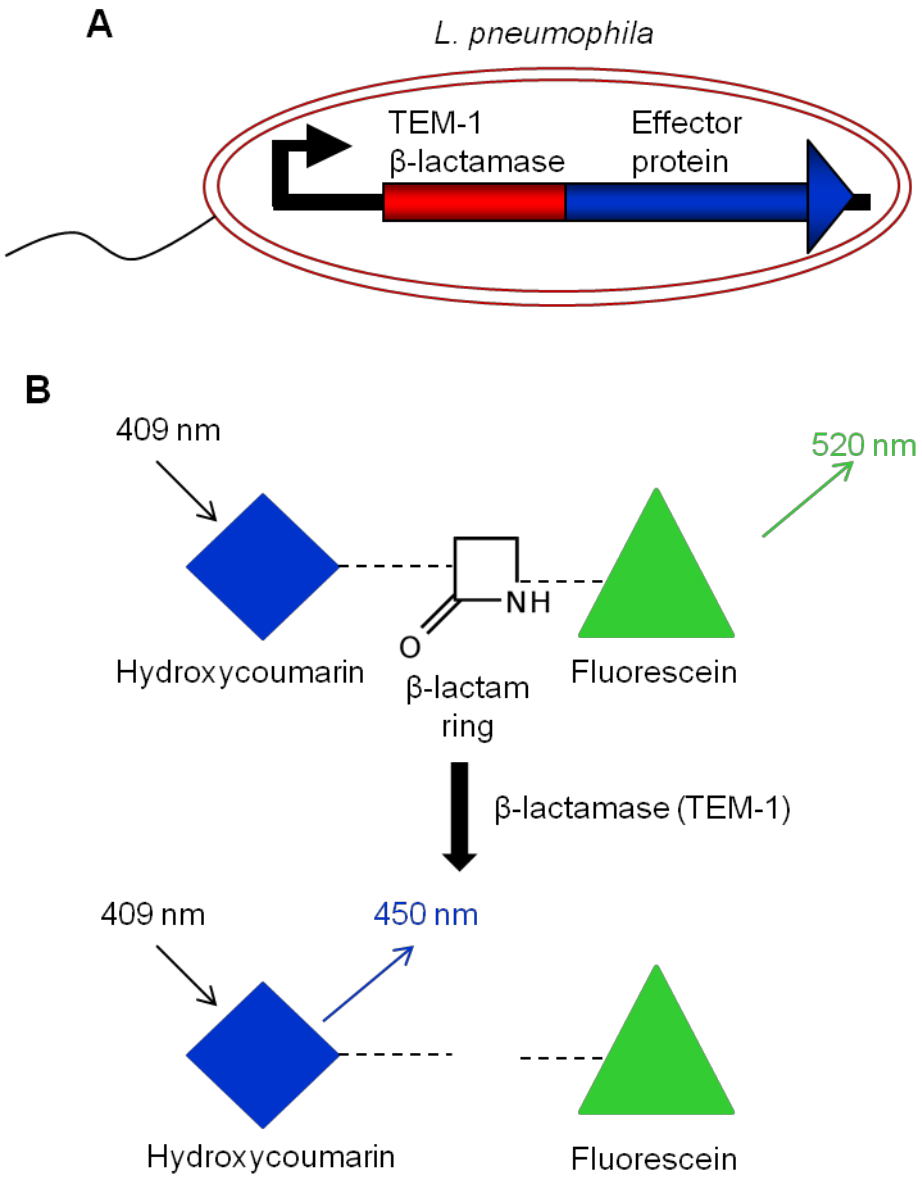

Figure 3.2 TEM-1 β-lactamase reporter assay

A. *L. pneumophila* strains over-expressing effector proteins carrying a TEM-1 β-lactamase fused to the N-terminus were constructed. These strains are used in the TEM-1 β-lactamase assay for quantifying translocation of effector protein of interest.

B. Uncleaved CCF2-AM exist with the hydroxycoumarin and fluorescein entities joined via a β-lactam ring, and emit a green fluorescence when excited using a wavelength of 409 nm. When loaded into cells that contain β-lactamase (TEM-1) in the cytoplasm, the β-lactam ring is cleaved, resulting in separation of the hydroxycoumarin from the fluorescein entity. This cleaved product emits a blue fluorescence instead.

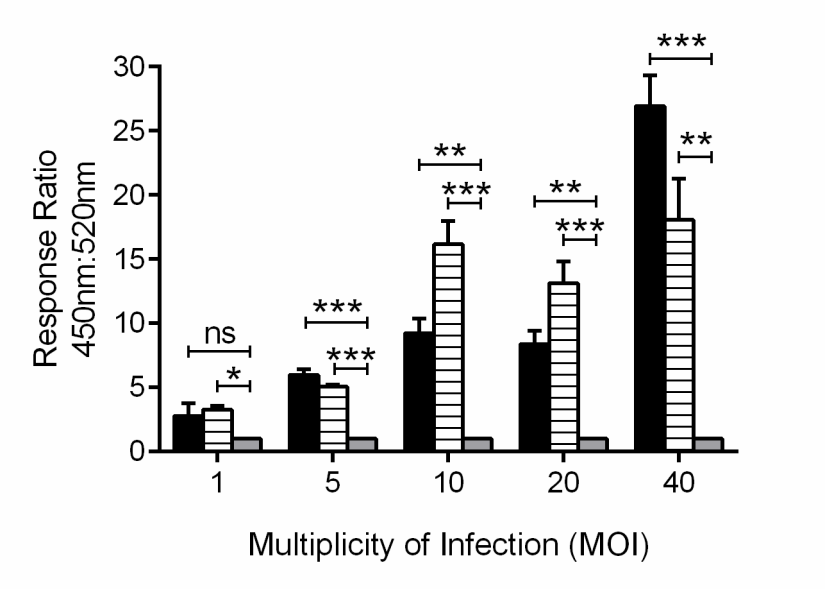

Figure 3.3 J774A.1 macrophages infected at different MOI with *L. pneumophila*

J774A.1 macrophages were infected with *L. pneumophila* carrying either pXDC61:RalF (■) or pXDC61:SdbB (⊟) at five different MOI and the level of translocation of each effector was quantified using the TEM-1 β-lactamase translocation assay. By normalising the fluorescence ratio to that of the negative control, L. pneumophila carrying pXDC61 (▣), the response ratio of each sample was generated. Results are the mean ± SEM of four independent experiments carried out in triplicate. *Significantly different to negative control of respective MOI (*$p \leq 0.05$, **$p \leq 0.01$, ***$p \leq 0.001$, ns = $p > 0.05$ one way ANOVA with Dunnett post test).

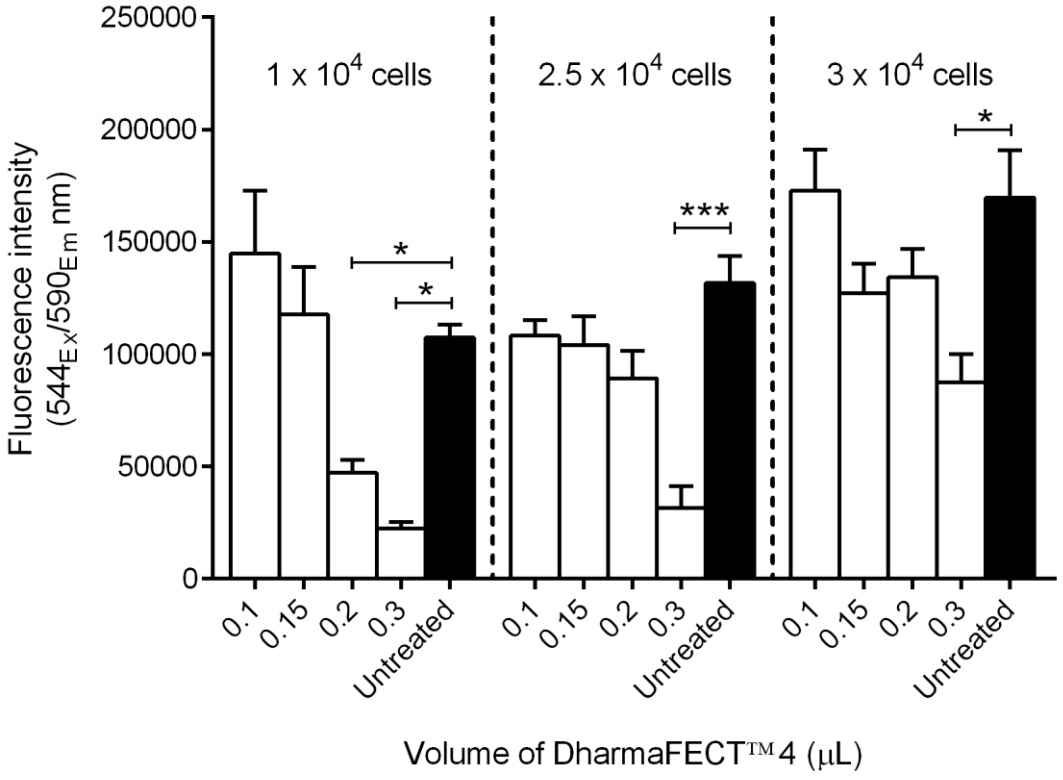

Figure 3.4 Evaluation of transfection reagent toxicity in J774A.1 macrophages

3 different densities of J774A.1 macrophages were treated with various volumes of DharmaFECT™4 transfection reagent and cell viability measured with alamarBlue®. Also shown are untreated controls (■) for each of the 3 cell plating densities evaluated. Levels of cell viability are expressed as fluorescence intensity emitted at 590 nm. Results are the mean ± SEM of three independent experiments performed in triplicate. *Significantly different to respective untreated controls (*$p \leq 0.05$, ***$p \leq 0.001$, one way ANOVA with Dunnett post test).

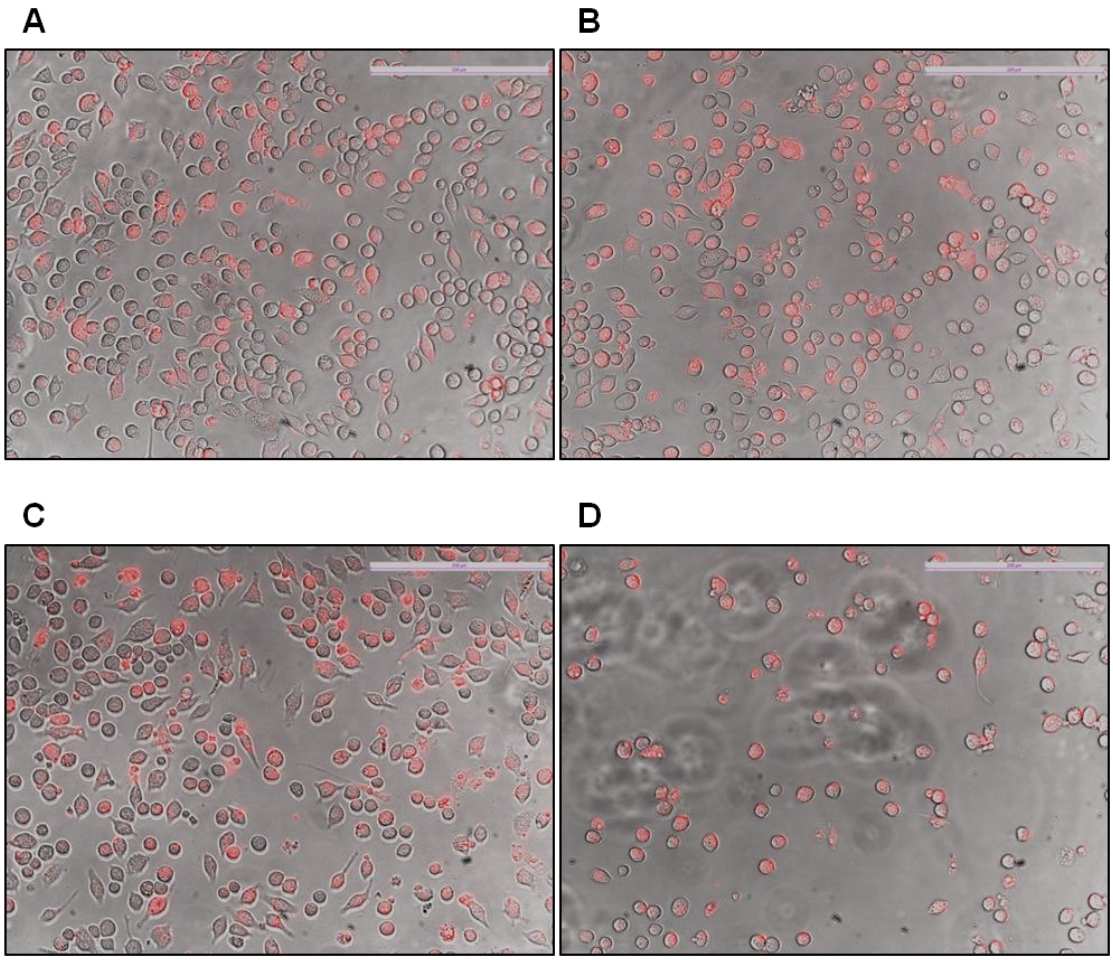

Figure 3.5 Visual determination of siRNA transfection efficiency using siGLO

siGLO was transfected into J774A.1 for 72 h with different volumes of DharmaFECT™4, 0.1 µL (**A**); 0.15 µL (**B**); 0.2 µL (**C**); 0.3 µL (**D**). Successful siRNA transfection efficiency was determined by visually examining the percentage of red fluorescent cells. Clear toxicity was also observed when 0.3 µL of DharmaFECT™4 used. A representative image from three independent experiments is shown here.

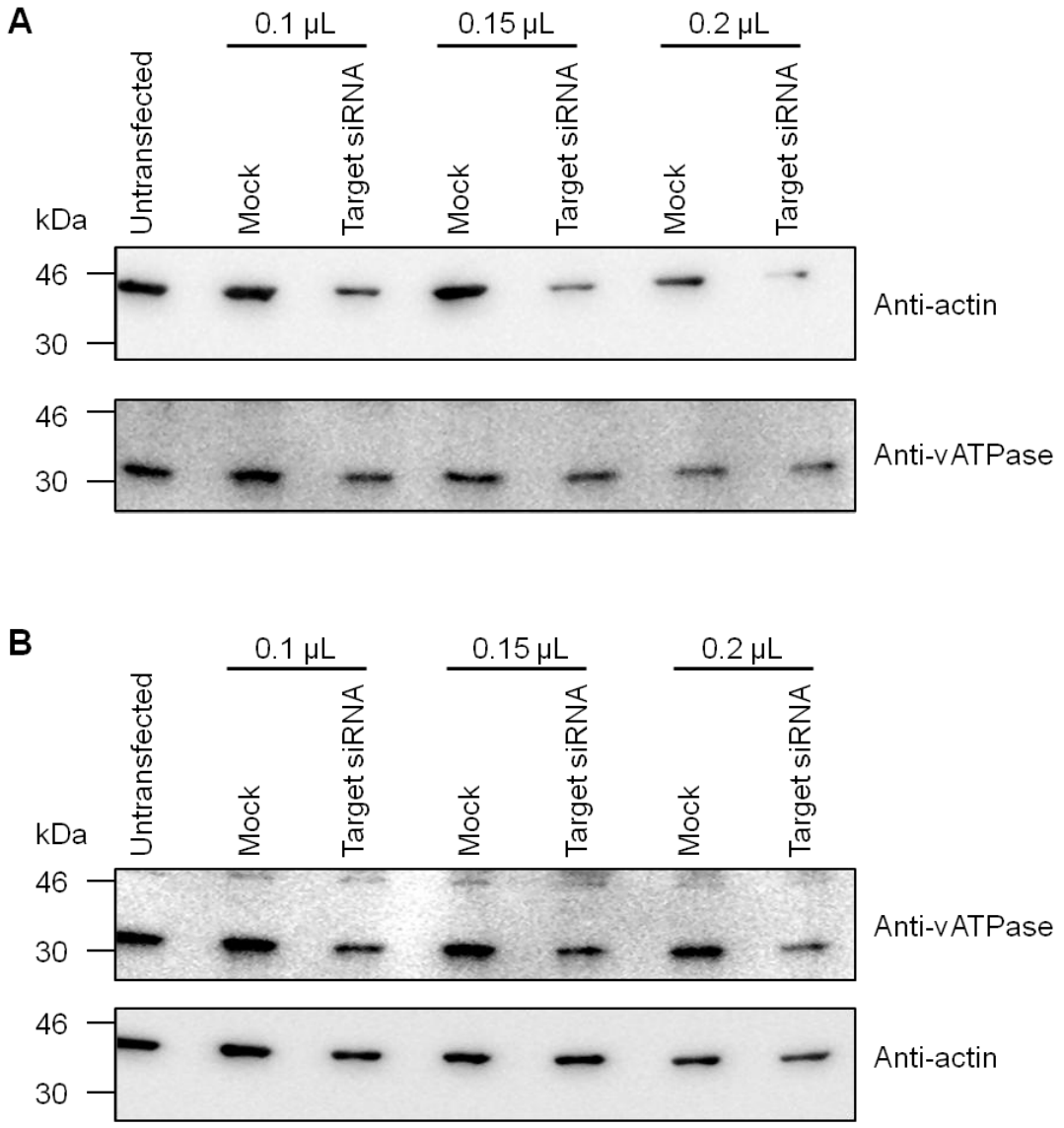

Figure 3.6 Western blot analysis of siRNA induced target protein knock-down in J774A.1 macrophages

siRNA targeting β-actin (**A**) and vATPase (**B**) was transfected into J774A.1 using three different amounts of DharmaFECT™4. 72 h later, cell lysates were harvested for analysis of β-actin (**A**) and vATPase (**B**) protein levels by immunoblot using anti-actin and anti-vATPase antibodies respectively. Mock treated controls were also included for each condition tested. Antibodies to vATPase (**A**) or β-actin (**B**) were used as a loading control for β-actin and vATPase knockdowns respectively. Representative immunoblot of at least three independent experiments.

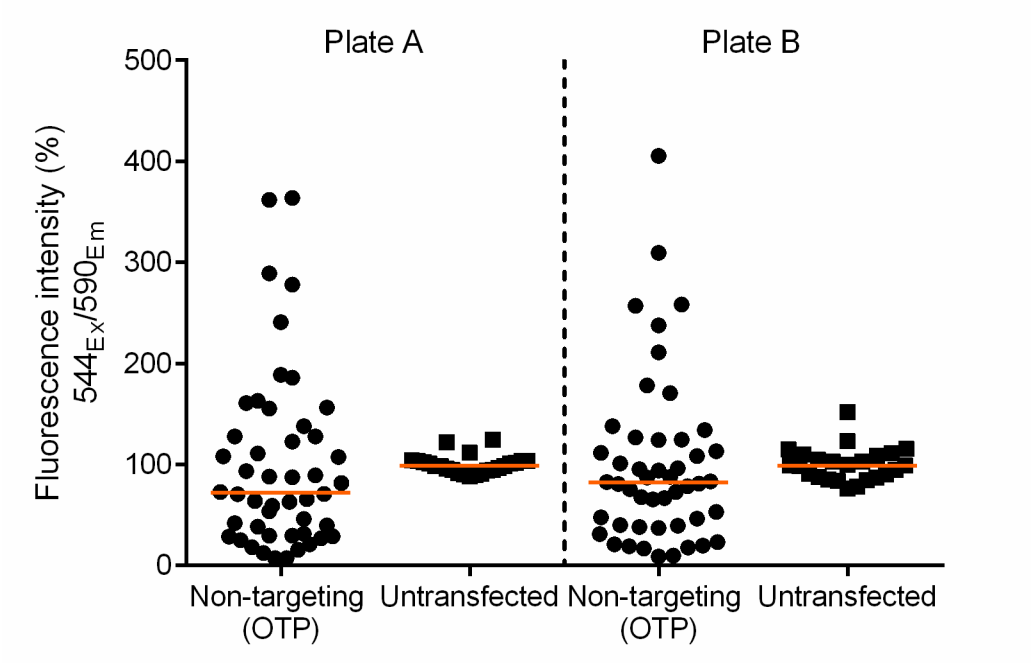

Figure 3.7 Inconsistent cell viability observed in J774A.1 macrophages post non-targeting siRNA transfection

alamarBlue® Cell Viability assay was performed on two 96 well plates (A and B), each containing 48 replicates of J774A.1 macrophages transfected with the non-targeting siRNA, OTP and 24 replicates of untransfected controls. Fluorescence intensity emitted at 590 nm was quantified and the result for each replicate is expressed as the percentage of the mean of each group of samples. The median of each sample group is represented by the orange line (—).

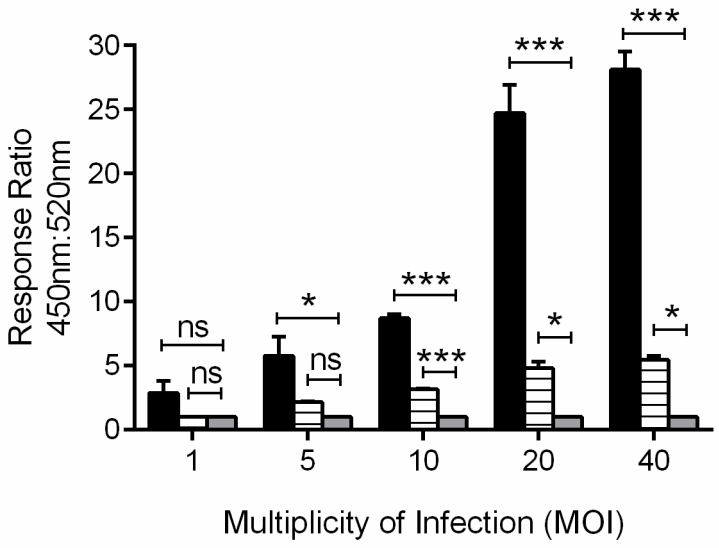

Figure 3.8 iBMDM macrophages infected at different MOI with *L. pneumophila*

iBMDM were infected with *L. pneumophila* carrying either pXDC61:RalF (■) or pXDC61:SdbB (⊟) at five different MOI and the level of translocation of each effector was quantified using the TEM-1 β-lactamase translocation assay. By normalising the fluorescence ratio to that of the negative control, *L. pneumophila* carrying pXDC61 (▭), the response ratio of each sample was generated. Results are the mean ± SEM of four independent experiments carried out in triplicate. *Significantly different to negative control of respective MOI (*$p \leq 0.05$, ***$p \leq 0.001$, ns = $p > 0.05$ one way ANOVA with Dunnett post test).

A

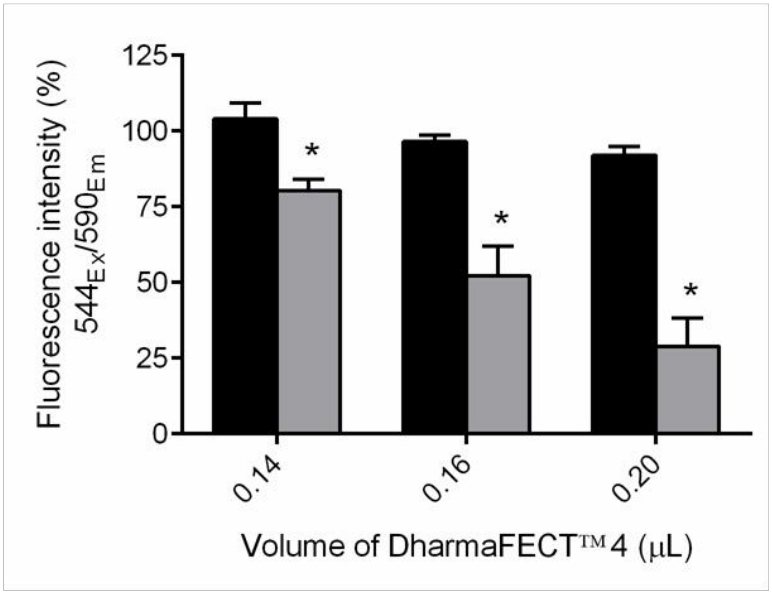
Fluorescence intensity (%)
544EX/590Em
125
100
75
50
25
0
*
*
*
0.14
0.16
0.20
Volume of DharmaFECT™ 4 (µL)

B

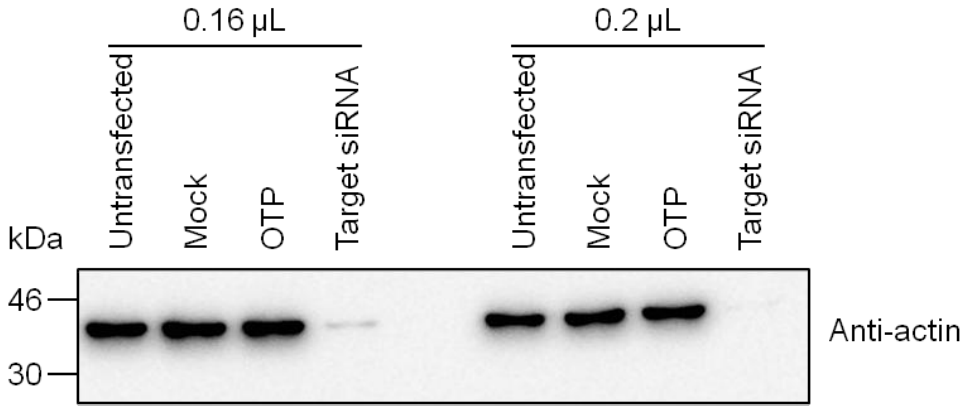
0.16 µL
0.2 µL
Untransfected
Mock
OTP
Target siRNA
Untransfected
Mock
OTP
Target siRNA
kDa
46
30
Anti-actin

C

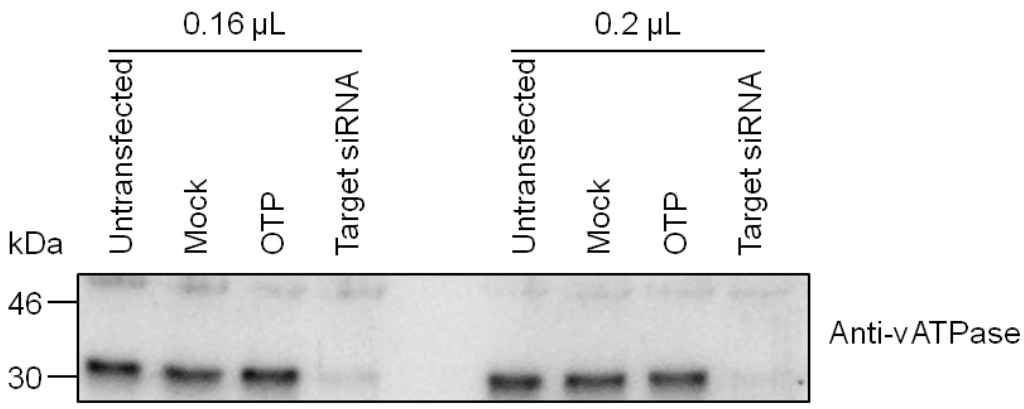
0.16 µL
0.2 µL
Untransfected
Mock
OTP
Target siRNA
Untransfected
Mock
OTP
Target siRNA
kDa
46
30
Anti-vATPase

Figure 3.9 Cell viability assay and immunoblot used to optimise siRNA transfection efficiency in iBMDM

A. Non-targeting OTP siRNA (■) or siRNA targeting PLK (▭) was transfected into iBMDM using 3 different volumes of DharmaFECT™4 transfection reagent. 72 h later, a PrestoBlue® Cell Viability assay was performed and the level of fluorescence intensity emitted at 590 nm was quantified. Results are expressed as percentage relative to the mean of each respective OTP control. Results are the mean ± SEM of three independent experiments carried out in triplicate. *Significantly different to corresponding OTP controls (*$p \leq 0.05$, one way ANOVA with Dunnett post test).

B and C. siRNA targeting β-actin (**A**) or vATPase (**B**) was transfected into iBMDMs using two different amounts of DharmaFECT™4. 72 h later, cell lysates were harvested for analysis of β-actin (**A**) and vATPase (**B**) protein levels by immunoblot using anti-actin and anti-vATPase antibodies respectively. Mock treated controls were also included for each condition tested. Representative immunoblot of at least three independent experiments.

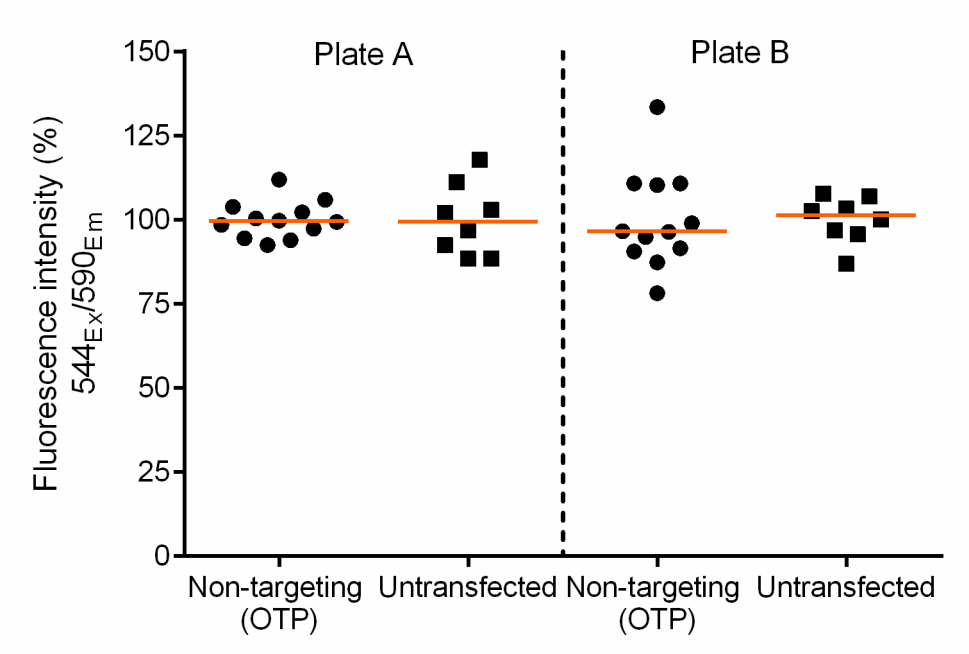

Figure 3.10 iBMDM cell viability remains unaffected after transfection with non-targeting siRNA

A PrestoBlue® Cell Viability assay was performed on two 96 well plates (A and B), each containing 12 replicates of iBMDMs transfected with the non-targeting OTP siRNA and 8 replicates of untransfected controls. Fluorescence intensity emitted at 590 nM was quantified and result for each replicate is expressed as the percentage of the mean of each group of samples. The median of each sample group is represented by the orange line (—).

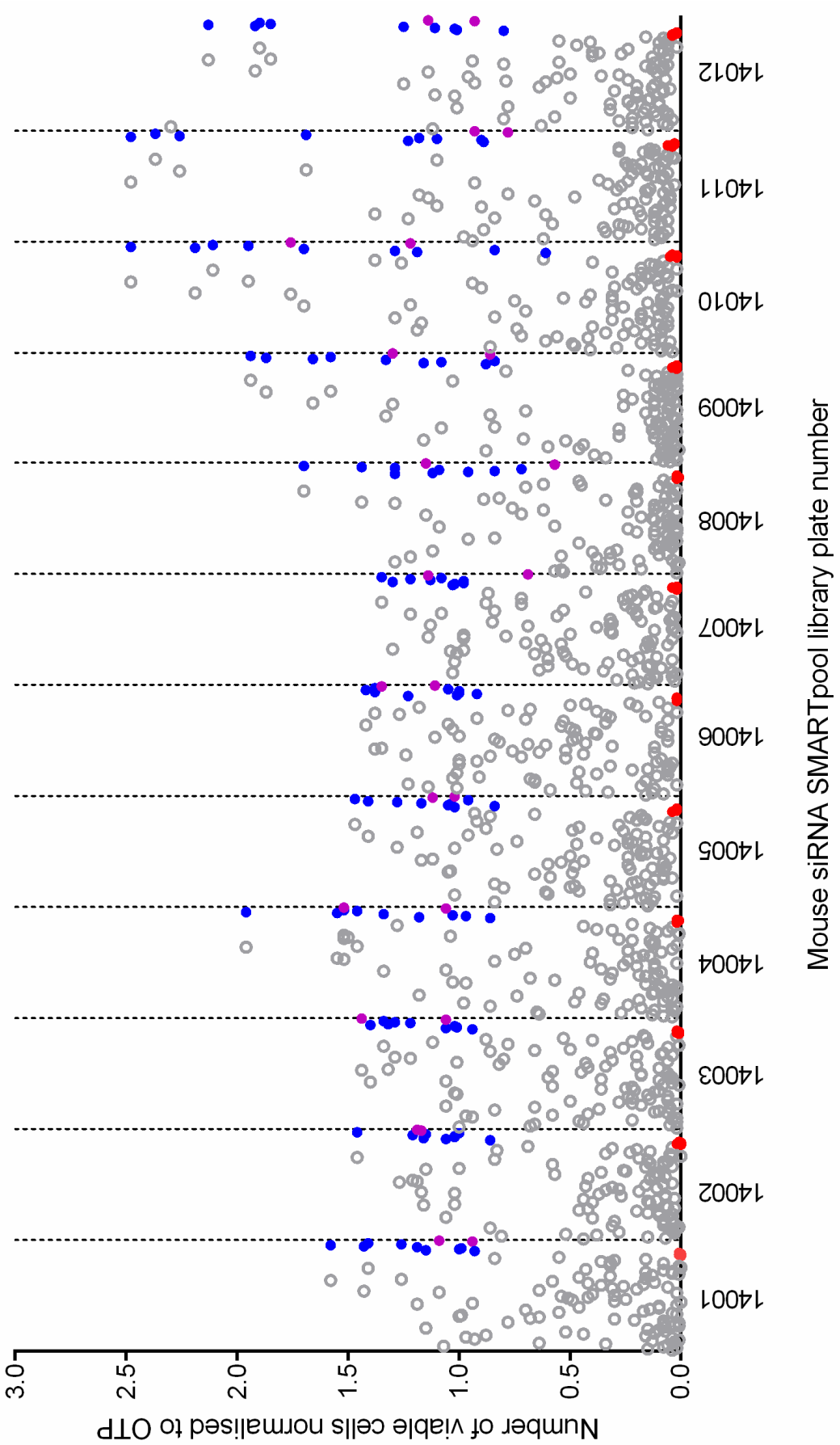
Number of viable cells normalised to OTP
3.0
2.5
2.0
1.5
1.0
0.5
0.0
14001
14002
14003
14004
14005
14006
14007
14008
14009
14010
14011
14012
Mouse siRNA SMARTpool library plate number

Figure 3.11 Target siRNA transfection led to unexpected large-scale cell death in iBMDM

12 randomly selected library plates (No.: 14001 to 14012) - each containing 80 different SMARTpool siRNAs targeting a gene of interest (○) were transfected into iBMDM for 72 h. Also included are controls transfected with either non-targeting OTP siRNA (●), cytotoxic siPLK (●) or mock (●). Cells were then subsequently stained with DRAQ5, and the number of cells in each well enumerated. This was normalised to that of the mean of the OTP controls in each respective plate.

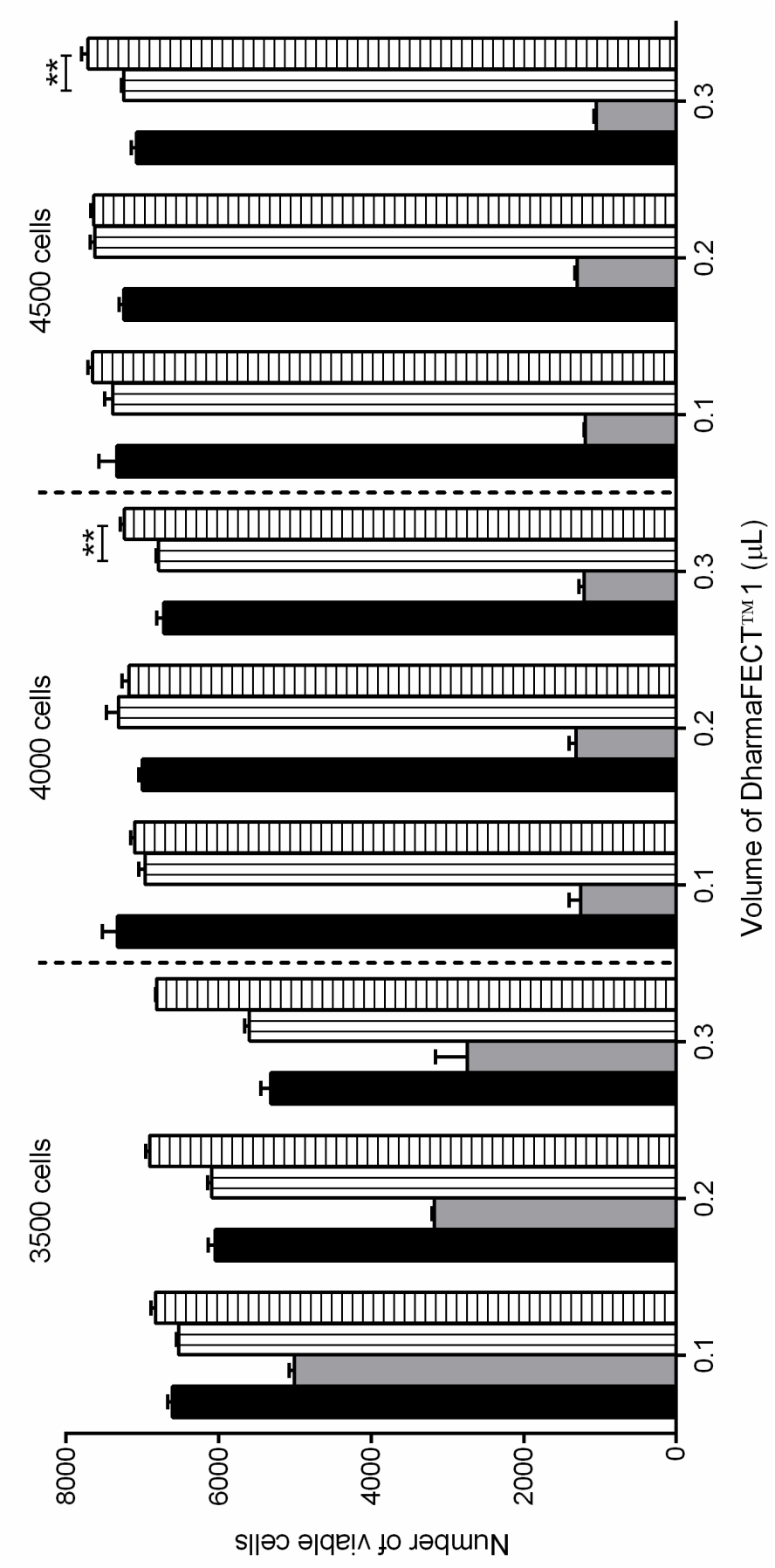
Number of viable cells
8000
6000
4000
2000
0
3500 cells
4000 cells
4500 cells
0.1
0.2
0.3
**
**
Volume of DharmaFECT™ 1 (µL)

Figure 3.12 Optimal conditions for siRNA transfection of HeLa cells

HeLa cells were transfected with either cytotoxic siTOX (▭) or non-targeting OTP (■) for 72 h using cell number and volume of DharmaFECT™1 as shown. Also included are mock (▯) and untreated (⊟) controls. Cell nuclei were then stained with DRAQ5 and number of viable cells enumerated. Results are the mean ± SEM of three independent experiments performed in triplicate. *Significantly different to respective untreated controls (**$p \leq 0.01$, one way ANOVA with Dunnett post test).

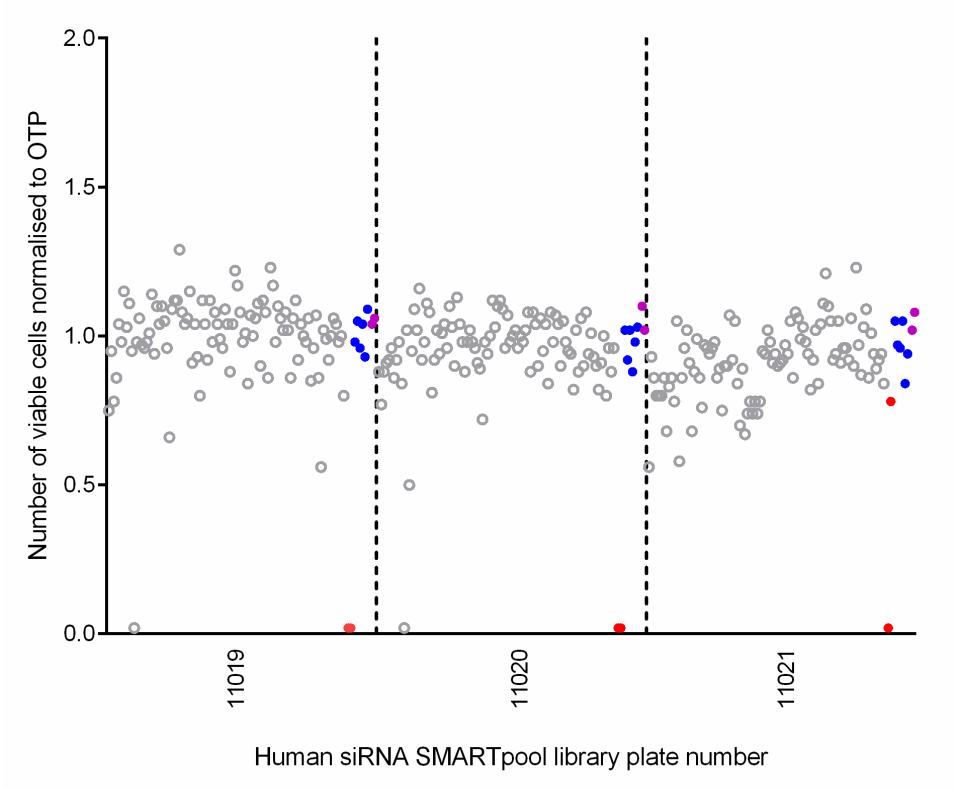

Figure 3.13 Target siRNA transfection did not lead to cell death in HeLa cell line

Three randomly selected library plates (No.: 11019, 11020 and 11021) - each containing 80 different SMARTpool siRNAs targeting a gene of interest (○) were transfected into HeLa cells for 72 h. Also included are controls transfected with either non-targeting OTP siRNA (●), cytotoxic siPLK (●) or mock (●). Cells were then subsequently stained with DRAQ5, and the number of cells in each well enumerated. This is normalised to that of the mean of the OTP controls in each respective plate.

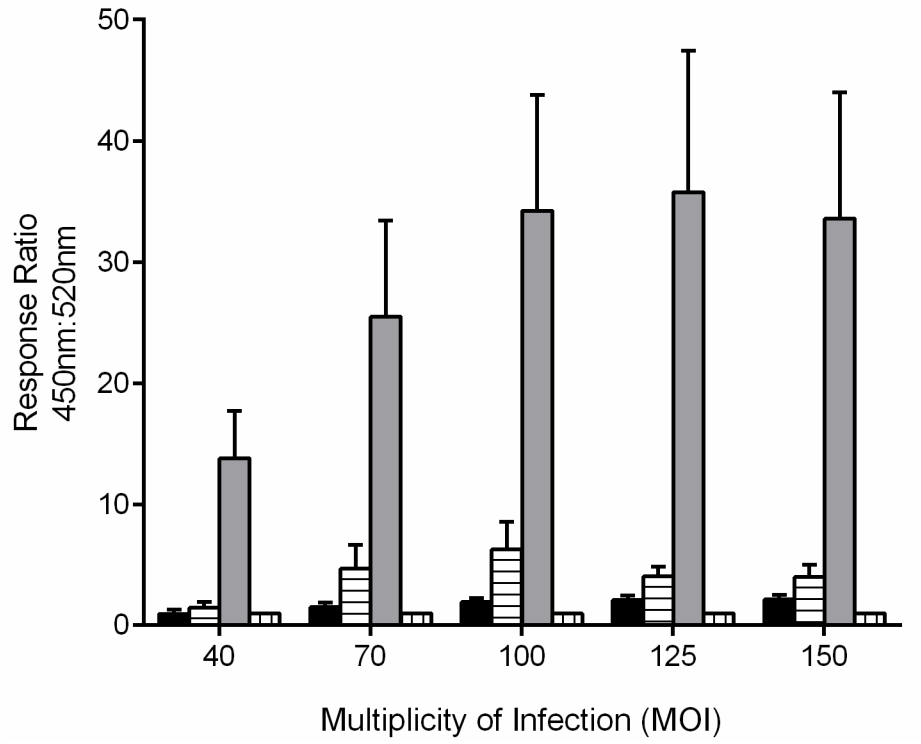

Figure 3.14 HeLa cells infected at different MOI with *L. pneumophila*

HeLa cells were infected with *L. pneumophila* carrying either pXDC61:LseA (■), pXDC61:LseB (▭) or pXDC61:RalF (▭) at five different MOI and the level of translocation of each effector was quantified using the TEM-1 β-lactamase translocation assay. By normalising the fluorescence ratio to that of the negative control, *L. pneumophila* carrying pXDC61 (▭), the response ratio of each sample was generated. Results are the mean ± SEM of three independent experiments carried out in triplicate.

CHAPTER 4: Genome wide siRNA screen identifies host ubiquitination genes that contribute to *L. pneumophila* Dot/Icm effector translocation

4.1 Introduction

The successful sequencing of multiple complete *L. pneumophila* and *L. longbeachae* genomes has resulted in significant advances in the field of *Legionella* research (151, 376-379). Through the use of molecular genetics and bioinformatics, *L. pneumophila* is now known to possess one of the largest repertoires of effector proteins (at least 330) known for any bacterium; albeit the roles of many of these are yet to be elucidated (380). This is in part due to the large number and functional redundancies among them (380). To date, clear biochemical activity has been determined for only ~10% of *Legionella* effectors (381). These interfere with diverse host pathways and modify various eukaryotic host proteins in order to ensure bacterial intracellular replication.

Recently, research on *L. pneumophila* pathogenesis has deepened our understanding of the interactions of *Legionella* with host cells. For example, LegU1 and LegAU13, which are F-box-domain-containing Dot/Icm effectors, form complexes with human SKP1 and CUL1 (382). Forming these complexes with Skp-Cullin-F-box confers E3 ligase roles for LegU1 and LegAU13 as they support polyubiquitination *in vitro* (382). LegU1 in particular direct ubiquitination of BAT3, a host chaperone protein (382). As BAT3 is involved in host cell cycle and ER stress response, it was proposed that *L. pneumophila* translocate effectors that directly interact with host proteins in order to perhaps modulate host response to infection (382). Using yeast as a model system, Heidtman *et al*. screened a total of 127 Dot/Icm translocated effector proteins and characterised SetA to be a putative bacterial glycosyltransferase that interfere with host cell vesicle trafficking to aid biogenesis of the LCV (182). While the above examples were successful in understanding how individual effector protein interact with host cells, the large number of effectors makes it far too laborious to identify host factors and/or processes that are important for *L. pneumophila* pathogenesis via probing each one individually. In addition, it is also likely that there are more bacterial effectors yet to be identified.

A comprehensive investigation can also be achieved by screening host factors for their effect on *L. pneumophila* pathogenesis using methods such as RNAi. Thus far, only one study to our knowledge has performed such investigation. Dorer *et al*. individually screened a subset of host genes involved in membrane trafficking between the ER and Golgi to identify those that are involved in LCV formation (111). This study paved the way for similar studies where the manipulation of individual host genes was monitored for perturbations to specific *L. pneumophila*-dependent phenotypes.

In this study, we aimed to identify host factors that regulate Dot/Icm effector translocation. Despite its importance in allowing intracellular replication of the bacteria, the host factors that participate in the function of this system are still unknown. The approach we undertook was to knock down the expression of individual genes in the entire human genome using RNAi in HeLa cells and inspect how the absence of each gene altered the levels of Dot/Icm effector translocation. As an indicator of Dot/Icm system function, we measured the levels of RalF translocated into siRNA treated HeLa cells. From this genome-wide screen, we found a significant number of genes involved in eukaryotic ubiquitination pathways. The silencing of these by RNAi led to decreased translocation of RalF.

4.2 Results

4.2.1 Implementation of the genome-scale RNAi screen for host proteins involved in Dot/Icm function

Previously, we optimised conditions for transfecting siRNA into HeLa cells and for infecting HeLa cells with *L. pneumophila*. Here we performed a siRNA-based RNAi screen of the entire human genome for host factors that influenced levels of RalF translocation. This screen was carried out in collaboration with the Victorian Centre for Functional Genomics (VCFG) at the Peter MacCallum Cancer Centre. With the aid of various liquid- and plate- handling robots at VCFG, SMARTpool siRNA was first transfected into HeLa cells and incubated for 72 h in a 96 well plate format to allow gene silencing to take effect (Figure 4.1A). SMARTpool siRNA contains a mixed pool of four different siRNAs designed to specifically target different regions of individual genes, thereby maximising the likelihood of target gene silencing. It is worth noting that only one set of the pooled siRNA is introduced per transfection episode and so only one gene per well is assumed to be silenced. Plates containing siRNA treated HeLa cells were infected with *L. pneumophila* expressing the TEM-1β-lactamase-RalF fusion protein at a MOI of 125 for 1 h before the TEM-1β-lactamase reporter assay was performed (Figure 4.1B). The level of blue fluorescence emitted by the cleaved CCF2-AM substrate was measured on a CLARIOstar® microplate reader to indicate the amount of RalF translocated by the bacteria into the HeLa cells. For the purpose of the screen, the well-characterised RalF effector protein was selected as a representative effector protein due to its high levels of translocation into eukaryotic host cells during *L. pneumophila* infection. Finally, the nuclei of cells were stained with DRAQ5 and viable cells enumerated (Figure 4.1B). The primary SMARTpool screen of the human genome initially probed a total of 18,120 protein coding genes, of which 520 were identified from our data analysis pipeline as significant hits and thus selected for re-testing in a secondary screen (Figure 4.1C). Eight of those validated targets that were eventually characterised further in biologically relevant validation studies (Figure 4.1C).

4.2.2 Quality control of the screen

Considering the large number of genes screened in this study, it was crucial to perform quality controls to ensure that the data generated was robust enough to select

for high confident hits. In this screen, two parameters were controlled for quality, including the transfection efficiency of siRNA into HeLa cells, and subsequent *L. pneumophila* infection for the TEM-1β-lactamase effector translocation assay.

To control for siRNA transfection efficiency, 16 controls were distributed throughout columns 1 and 12 of each 96 well screen plate (Figure 4.2A). These included cells transfected with either non-targeting siRNA (OTP) or cytotoxic siRNA (siPLK). Also included were mock transfected controls where cells were treated with an appropriate amount of transfection lipid without addition of siRNA. Comparing cell numbers between OTP and mock controls enabled us to monitor any unexpected cell toxicity issues, while observing cell death in siPLK controls reassured us that the siRNA transfection process was efficient. During the process of assessing siRNA transfection efficiency, the enumerated cell number for each control was divided by the mean of all the OTP values within a plate. Significant differences in the normalised cell number between the OTP and siPLK treated controls within each plate confirmed good siRNA transfection efficiency (Figure 4.2B). This was because cells which successfully take up siPLK undergo apoptosis. In contrast, no significant differences in cell numbers observed between OTP and mock controls confirmed that no adverse cell toxicity occurred due to siRNA treatment (Figure 4.2B). At the conclusion of the genome-wide screen, the Z' factor was computed to statistically determine performance of the siRNA transfection process for the entire screen. An average Z' factor of ~0.7 was obtained for the pair of controls (OTP versus siPLK), indicating excellent transfection efficiency (Figure 4.2D).

To control for *L. pneumophila* infection efficiency and the TEM-1β-lactamase effector protein translocation assay, 6 out of 10 OTP transfected controls were infected with *L. pneumophila* while the rest remained uninfected. Comparing the levels of blue fluorescence between the infected and uninfected OTP controls allowed us to determine whether the infection was successful. Uninfected controls did not have the TEM-1 β-lactamase necessary for cleaving CCF2-AM and thus did not emit blue fluorescence. Infected controls on the other hand emitted high levels of blue fluorescence when TEM-1 β-lactamase tagged RalF was translocated from the bacteria into the cells. The blue fluorescence levels of each control was normalised to the mean of all the infected OTP within each plate (Figure 4.2C). Normalised blue fluorescence of ≤ 0.2 was obtained for the uninfected wells compared to infected

wells (~1) (Figure 4.2C). This significant difference verified that both infection with *L. pneumophila* and the Dot/Icm dependent translocation of RalF were successful. The Z' factor was again computed to statistically determine the performance of *L. pneumophila* infection and the TEM-1 β-lactamase assay for the entire screen. Comparing the normalised blue fluorescence of the pair of controls (uninfected versus infected) yielded an average Z' factor of ~0.7, indicating excellent assay quality (Figure 4.2E).

4.2.3 Data analysis and hit-selection for further validation

After obtaining genome wide data from the primary screen in which each gene is tested in duplicate, we developed a data analysis and subsequent hit-identification strategy together with the group at VCFG (Figure 4.3). Analysis began with subtracting the background blue fluorescence from each sample, resulting in the net blue fluorescence which was then normalised to the median of all the OTP controls within each plate. For each sample, an average of the two replicates was taken and used for further analysis and hit selection.

The first step in hit selection involved generating a robust z-score for each sample (Figure 4.3A). This was done by comparing the normalised blue fluorescence of each sample against the median of the entire population. The robust z-score is a measure of median ± median absolute deviation that is routinely used for hit identification in large-scale screen datasets (383). While ± 2 is traditionally the threshold for identifying targets, the cut-off was initially set at ± 3 in our study to increase stringency and provide added confidence to the identified targets (Figure 4.3A). A robust z-score of ≤ -3 meant that the silencing those human genes led to a reduction in RalF translocation during *L. pneumophila* infection. Conversely, a robust z-score of ≥ 3 represented genes that lead to an increase in RalF translocation when silenced.

The next step was to further categorise target genes into ones where siRNA treatment affected cell viability (Figure 4.3A). Cell viability post siRNA treatment was included as one of the hit selection parameters to account for those host genes that are essential for viability, therefore discounting the possibility of identifying false positives. Enumerated cell numbers for each sample were normalised to the median of all the OTP controls within each plate. Targets with a normalised cell number of < 0.5 were

discarded while those ≥ 0.5 were retained as potential hits that warranted further validation (Figure 4.3A).

Applying aforementioned hit selection criteria, 321 out of the 18 120 genes screened had a robust z-score of ≤ -3 while 119 genes had a robust z-score ≥ 3, yielding a total of 440 potential genes of interest (Figure 4.3B).

4.2.4 Over-representation of host ubiquitination genes in identified targets

In order to systematically organise positive hits from the primary screen, a gene set enrichment analysis was performed in collaboration with Dr. Melanie Bahlo and Dr. Saskia Freytag at The Walter and Eliza Hall Institute (WEHI). Together we statistically assessed the possible enrichment of genes in a particular biological pathway. Data was partitioned into either the hit (potential gene target) group or the control group based on z-score. The traditional threshold of a robust z-score ± 2 was used for this partitioning. Hence, the hit group comprised genes with a robust z-score between ≤ 2 and ≥ 2, while the control group comprised all the remaining genes. Subsequent bioinformatic analysis was performed using the ConsensusPathDB, and specifically five pathway databases – Reactome, KEGG, WikiPathways, PID and BioCarta.

To provide statistical significance, p-values and q-values were evaluated. All results with a p-value < 0.01 are shown and only q-values < 0.05 are reported and ranked according to significance (Table 4.1). 'Set size' refers to the total number of genes in a particular pathway while 'Candidates contained' refers to the number of genes identified from the screen as a potential target. This analysis found six pathways were overrepresented. The top 2 were eukaryotic ubiquitination related pathways and the next three were involved in antigen presentation and immunity (Table 4.1). The significant over-representation of human genes involved in ubiquitination was a striking result from the primary screen.

We next classified the 440 genes identified from the hit selection process according to their molecular functions and roles in biological processes. Approximately 25% of those targets that reduced RalF translocation (84 out of 321 genes) were found to be involved in the eukaryotic ubiquitination system (Figure 4.4A). In comparison, only

~2% of targets identified to increase RalF translocation (2 out of 119 genes) were ubiquitin-related genes (Figure 4.4B).

The functional analysis done thus far had implied that the host ubiquitin pathway had a significant role to play in Dot/Icm effector translocation. Therefore, we decided to loosen the cut-off for genes that have roles in ubiquitination to ± a robust z-score of 2.5. This allowed for more genes to pass through the hit selection filter and be assessed in a secondary validation screen. Allowing for this, the gene list increased from 321 to 401 with ubiquitin-related genes increasing from 84 to 146 for targets leading to a reduction in RalF translocation upon silencing (Figure 4.4C). Interestingly, no change occurred in the group that led to an increase in translocation of RalF. After various rounds of hit selection and analysis, a total of 520 genes from the primary screen were chosen for further validation in the secondary screen. These genes are listed in Appendix 1 together with the result of the blue fluorescence robust z-score. Genes that when silenced led to reduced RalF translocation (negative robust z-score) are listed first followed by genes that led to an increase (positive robust z-score).

4.2.5 Validation of potential targets in secondary screen

As with many high-throughput screens, potential hits from the primary screen were further verified to ensure only high confident targets were pursued. In this study, the secondary validation screen was again performed in collaboration with the VCFG. For the secondary screen, the SMARTpool siRNA used in the primary screen was deconvoluted into the 4 individual siRNA duplexes and then transfected into HeLa cells separately in a same manner as the primary screen (Figure 4.5). The subsequent effector quantification TEM-1 β-lactamase assay and cell viability assessment was carried out exactly as for the primary screen (Figure 4.1B). The blue fluorescence obtained for each duplex siRNA was normalised to the average of the OTP controls within each plate. The average of the normalised values was then used to evaluate the effect of each siRNA duplex on the translocation of RalF (Figure 4.6A). Duplexes with a normalised blue fluorescence value of 0.75 – 1.2 were considered not to have a significant impact on RalF translocation; while < 0.75 indicated duplexes that led to a decrease in RalF translocation. Values > 1.2 indicated an increase in RalF translocation (Figure 4.6A). Finally, cell viability was assessed as before. Duplex

siRNAs which when transfected into HeLa cells resulted in < 0.5 viable cells were discarded and not analysed further. The numbers of individual siRNA duplex/s that successfully passed the analysis strategy for each gene were used to classify the hits identified into different confidence levels. This increased the stringency of the hit selection process. The number of individual duplexes that validated each gene indicated the level of confidence. Genes that had either 2 or more duplexes validated were designated as 'high confidence' targets (Figure 4.6B). Those that displayed only 1 validated duplex were regarded as poor or low confidence targets, and thus not pursued further.

Of the 520 genes that were subjected to the secondary screen, 70 were designated 'high confidence' targets. These are shown in Figure 4.7 where they are organised according to their known functions or cellular localisation. Appendix 2 shows the complete list of genes that were investigated in the secondary screen and their respective validation outcome. A selection of genes out of the 70 'high confidence' targets was tested further in functional studies for their role in *L. pneumophila* infection (Chapter 5).

4.3 Discussion

Studies in bacterial pathogenesis have increasingly turned to RNAi to obtain insights into how perturbations of host gene expression affect pathogenesis and infection. Here we report the first genome-wide RNAi screen of host factors required for Dot/Icm mediated pathogenesis of *L. pneumophila* where we showed that optimal translocation of the Dot/Icm effector, RalF, was dependent on host factors. Results from our screen further highlighted the interplay between host and bacteria during infections. From the primary screen, we initially identified 520 human protein-coding genes that potentially influenced the function of the Dot/Icm secretion system of *L. pneumophila*. More specifically, a large proportion of these genes (401 genes) facilitated effector translocation as opposed to those that hindered it (119 genes). Of the 520 genes identified from the primary screen, 70 (~ 15%) were later successfully validated in a secondary screen. Categorising these validated targets determined that they were found in many different compartments of the cell including the ER and nucleus, and had diverse functions from GTPase activity to ubiquitination. In particular, we identified factors involved in actin cytoskeletal rearrangement such as profilin-1 and myosin-IC. Profilin-1 regulates actin polymerisation during phagocytosis (384) and this hit is consistent with findings that evaluated translocation of the *L. pneumophila* effector protein LepA into cells in the presence of small molecule inhibitors (328). Using a library of ~ 2500 chemical compounds to inhibit the functions of host factors, Charpentier *et al*. found that inhibition of host factors involved in phagocytosis such as phosphoinositide 3-kinases, actin and tubulin led to decreased translocation of the effector protein LepA into mouse J774A macrophages (328). In addition, inhibition of the host factors CD45 and CD148 also reduced *L. pneumophila* phagocytosis and subsequent effector translocation (328). Findings from both our work and Charpentier *et al*. support the idea that phagocytosis of *L. pneumophila* into host cells is an important requirement for efficient effector translocation during infection (328).

In addition to factors involved in phagocytosis and cytoskeletal organisation, the function and localisation of other targets identified from our screen suggested they could be potentially interesting host factors to characterise further. These included factors involved in GTPase activity and vesicular transport. GTPases are hydrolase enzymes that are strongly implicated in *L. pneumophila* infection (385). For example,

once secreted into the cytoplasm, RalF rapidly activates ARF-1, a host GTPase involved in early secretory vesicle trafficking (386). While the functions of the three GTPases (SERGEF, DENND2C and ACAP1) identified from our screen are not well-characterised, the protein SERGEF (Secretion Regulating Guanine Nucleotide Exchange Factor) is particularly interesting as it is a putative guanine nucleotide exchange factor that interacts with Sec5, a protein regulating vesicular transport in the secretory pathway (387, 388). We also identified a protein involved in ER to Golgi vesicle-mediated transport, FBXO43, also known as ERP1 (389). FBXO43 is an integral component of the ER membrane and regulates protein movement through the ER (390). Modulating the host early secretory pathway and hijacking host vesicles to remodel the LCV is a vital process during *L. pneumophila* infection. Thus, it is logical that silencing factors involved in vesicular secretion and transport led to decreased RalF translocation. Though still poorly characterised, these host proteins are certainly interesting targets for further analysis, as they may have novel roles in *L. pneumophila* infection.

The most striking finding from our RNAi screen was the identification of multiple genes involved in the eukaryotic ubiquitination system. Specifically, RNAi knock-down of 146 ubiquitination-related genes using siRNA led to a significant reduction in RalF translocation. In comparison, knock-down of only two genes with ubiquitin ligase activity (KMT2C and UBE4B) led to significant increase in RalF translocation. Consistent with previous studies, this observation strongly suggested that optimal Dot/Icm effector translocation requires engagement from the host ubiquitination system. Ubiquitination was first implicated in *L. pneumophila* pathogenesis when polyubiquitinated proteins were discovered to decorate the cytoplasmic face of the LCV shortly after infection and this did not occur in cells infected with a Dot/Icm mutant strain of *L. pneumophila* (111). Furthermore, infection of mouse macrophages with wild-type *L. pneumophila* caused ubiquitination of positive regulators of the central metabolic checkpoint kinase mTOR, thereby diminishing its function (286). Again, this was not seen for *L. pneumophila* lacking a functional Dot/Icm system (286). Reduced mTOR function eventually results in the downstream effects of increased inflammation and autophagy, presumably allowing the host to respond appropriately to the invading pathogen (391). Hence, even though the exact reason for modulating the host ubiquitination process during *L. pneumophila* infection is yet to

be clearly defined, a functional Dot/Icm system is imperative for LCV ubiquitination to occur. Interestingly, the collection of ubiquitination-related genes we identified did not classify into any specific biological networks. These findings thus suggested that the host ubiquitination system might be an important process that is hijacked by *L. pneumophila* to ensure its effector proteins are efficiently translocated into infected host cells.

Comparing the results of our RNAi screen and the chemical genetics screen by Charpentier *et al*. raises some interesting differences. These can most likely be explained by the different host cell perturbation strategies employed for each study. Firstly, out of the 2500 small molecule inhibitors used by Charpentier *et al*., none specifically targeted ubiquitination-related factors, essentially meaning the effect of ubiquitination on Dot/Icm effector translocation was not tested (328). Before the emergence of eukaryotic gene editing tools such as RNAi and more recently CRISPR/Cas9, small molecule inhibitor screens were limited by target specificity and availability (392). Our genome-wide RNAi strategy addressed this obstacle and indeed identified host factors previously not known to be important for *L. pneumophila* Dot/Icm function.

However, RNAi screening also has disadvantages. In our screen, the final 70 validated targets were selected by having at least two single siRNA duplexes leading to a > 25% reduction or > 20% increase in translocation of RalF. Setting a threshold to exclude genes that did not have at least two siRNA duplexes validating a phenotype is standard practice in pooled siRNA screens to minimise the risk of identifying false positives (393). False positives are notoriously common in pooled screens as off-target effects are more prevalent when multiple siRNA duplexes are used in a single transfection event (337, 393). Despite this, pooled siRNA is still commonly used for genome-scale primary siRNA screens to save time and reagents (394). Moreover, compared to individual siRNA duplex, pooled siRNA typically yields more efficient silencing of target gene expression (394). As it is difficult for individual siRNA duplexes to achieve high levels of silencing, it is perhaps not surprising that a large proportion of genes were not validated in our secondary screen. Hence, selecting hits following siRNA screening is a fine balance between including false positives in the pooled primary screen and dismissing false negatives in the validation screen (395, 396). Nevertheless, performing deconvoluted siRNA duplex validation is still

important to follow-up pooled primary screens. Having in place stringent hit selection and validation criteria ensured that the genes identified from the screen were *bona fide* host targets that influenced levels of RalF translocation. Regardless of these potential technical limitations, our RNAi screen was highly successful and identified a large group of ubiquitination-related gene targets.

In summary, our results revealed that even though the Dot/Icm secretion system is a virulence factor of *L. pneumophila*, it is unable to function optimally as an independent entity separate from the host cell. Following the RNAi screen which identified multiple host factors as important for efficient RalF translocation, more studies will be required to characterise their mechanisms of action. Hence, further work was performed to investigate the roles of selected ubiquitination-related host genes in *L. pneumophila* infection.

Table 4.1 Functional pathways over-represented among significant hits identified from the primary siRNA genome screen

Pathway	Set Size	Candidates Contained	Percentage Candidates	p-value [a]	q-value [b]
Antigen processing: Ubiquitination & Proteasome degradation	158	87	55.1%	6.56 E-46	1.33 E-42
Ubiquitin mediated proteolysis	135	72	53.3%	7.75 E-37	5.58 E-34
Class I MHC mediated antigen processing	202	89	44.1%	8.23 E-37	5.58 E-34
Adaptive Immune System	499	118	23.6%	9.67 E-20	4.91 E-17
Immune System	915	155	16.9%	1.12 E-11	4.56 E-9
Activation of Matrix Metalloproteinases	30	11	36.7%	9.31 E-05	0.0315

[a] calculated using Fisher's exact test with the entries in the 2 by 2 contingency table having a hypergeometric distribution

[b] calculated by empirical false discovery rates to correct for multiple testing

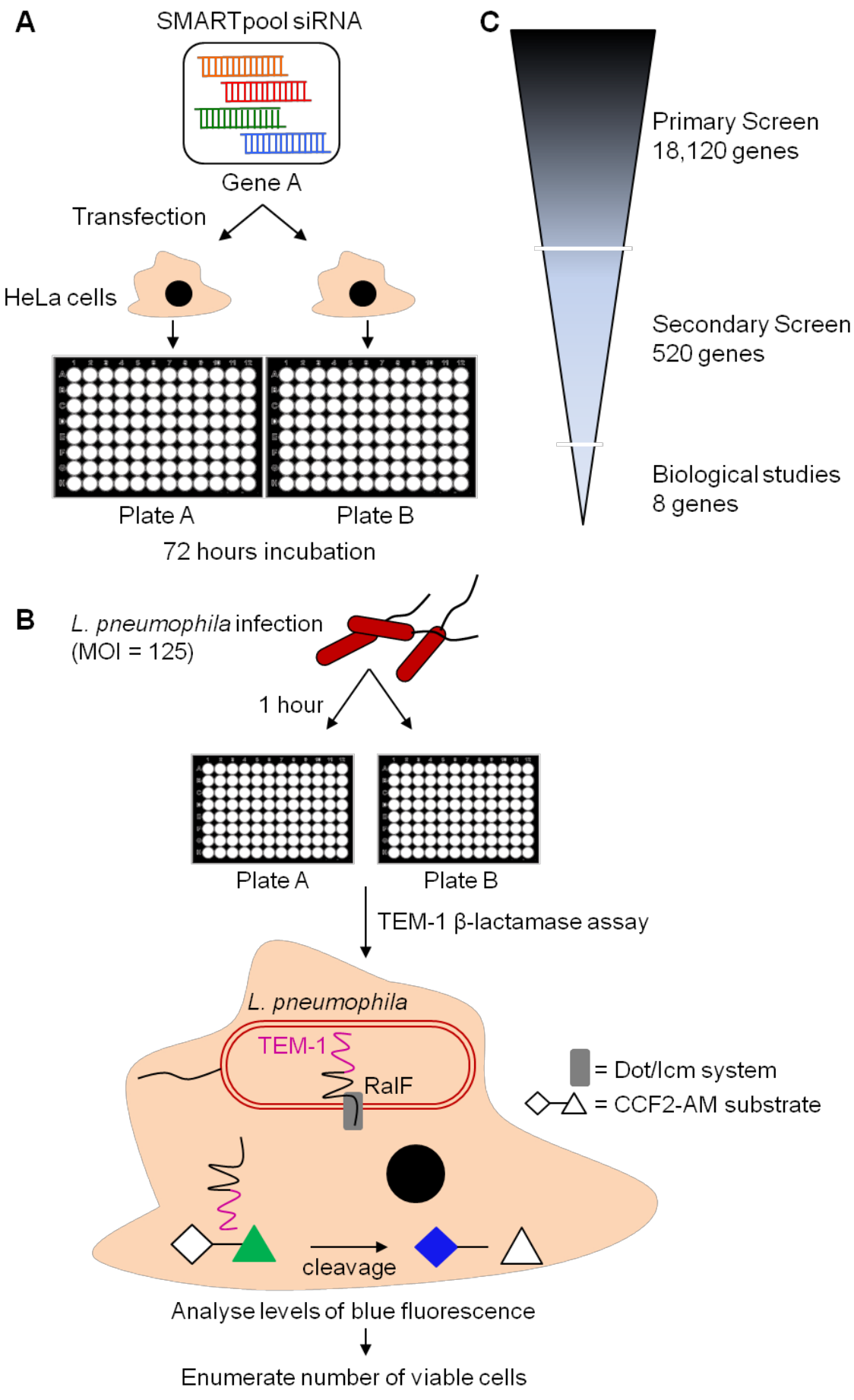
A
SMARTpool siRNA
Gene A
Transfection
HeLa cells
Plate A
Plate B
72 hours incubation
C
Primary Screen
18,120 genes
Secondary Screen
520 genes
Biological studies
8 genes
B
L. pneumophila infection
(MOI = 125)
1 hour
Plate A
Plate B
TEM-1 β-lactamase assay
L. pneumophila
TEM-1
RalF
= Dot/Icm system
= CCF2-AM substrate
cleavage
Analyse levels of blue fluorescence
Enumerate number of viable cells

Figure 4.1 Outline of the experimental design of the primary genome-wide RNAi screen

A. Using liquid handling robots, HeLa cells were transfected with SMARTpool siRNAs in duplicate 96 well plates and incubated for 72 h for siRNA induced RNAi to take effect.

B. 72 h after siRNA treatment, cells were infected with *L. pneumophila* carrying pXDC61:RalF at MOI of 125 for 1 h and translocation of TEM-1 β-lactamase fused RalF was detected. The level of blue fluorescence emitted by cleaved CCF2-AM was measured to indicate the amount of RalF translocated into the HeLa cells. Cells were finally stained with DRAQ5 and total cell number enumerated using an automated microscope.

C. Summary of the number of genes studied during each stage of the screening process.

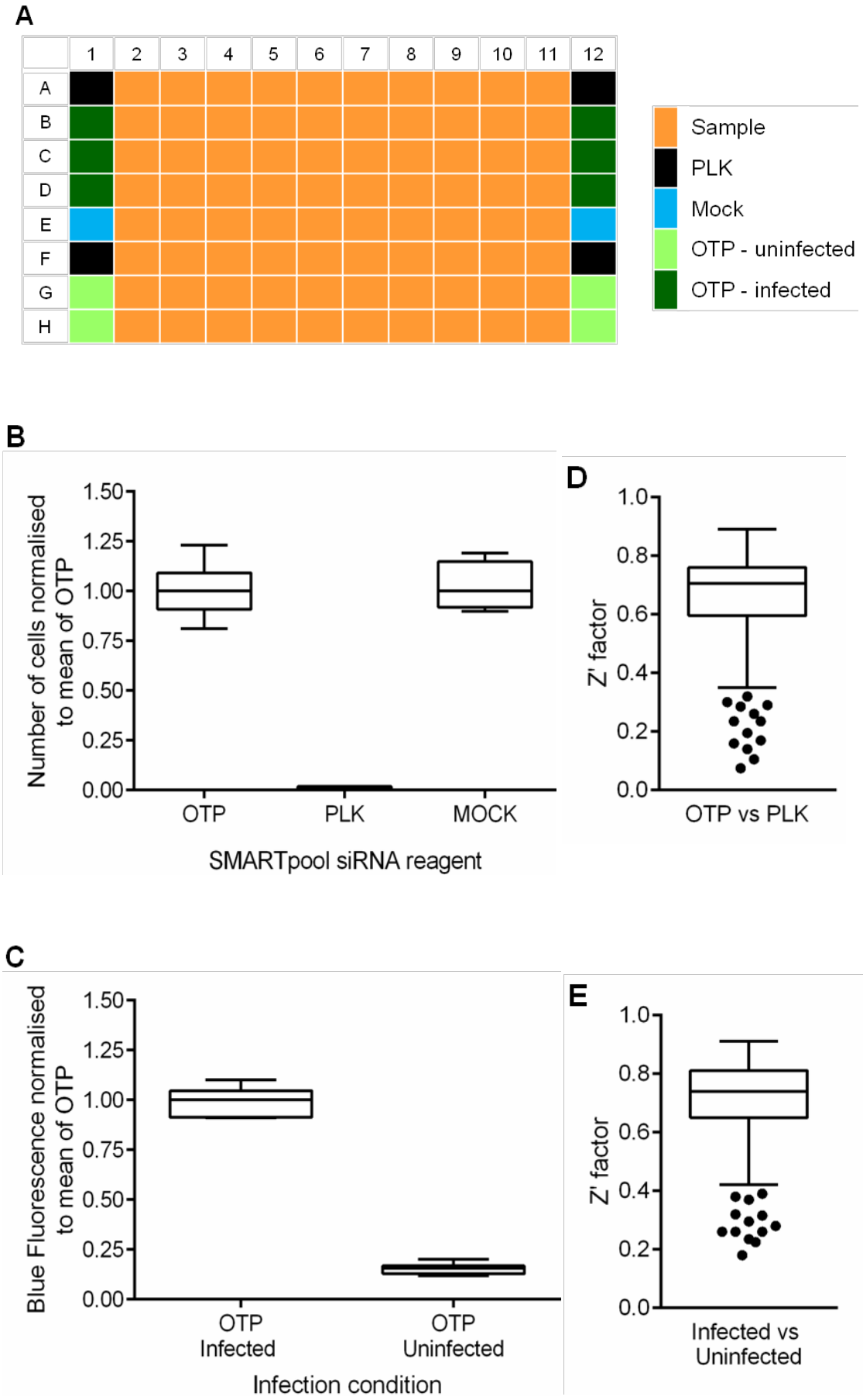
A
1
2
3
4
5
6
7
8
9
10
11
12
A
B
C
D
E
F
G
H
Sample
PLK
Mock
OTP - uninfected
OTP - infected
B
Number of cells normalised to mean of OTP
1.50
1.25
1.00
0.75
0.50
0.25
0.00
OTP
PLK
MOCK
SMARTpool siRNA reagent
D
Z' factor
1.0
0.8
0.6
0.4
0.2
0.0
OTP vs PLK
C
Blue Fluorescence normalised to mean of OTP
1.50
1.25
1.00
0.75
0.50
0.25
0.00
OTP Infected
OTP Uninfected
Infection condition
E
Z' factor
1.0
0.8
0.6
0.4
0.2
0.0
Infected vs Uninfected

Figure 4.2 Quality control of the screen

A. Primary genome screen plate design. A representative 96 well plate is shown, illustrating the layout of the sample and control siRNAs within each plate. Control siRNAs were distributed in columns 1 and 12. Transfection controls were represented by cells treated with siPLK, mock and OTP. TEM-1 β-lactamase assay controls were represented by infected and uninfected OTP wells. SMARTpool sample siRNAs, each targeting a different gene in the human genome were located in columns 2 to 11.

B. Box plot illustrating assessment of siRNA transfection of one representative screen plate. Cell numbers for the transfection controls – siPLK, mock and OTP treated cells were normalised to the mean of all the OTP controls within each assay plate.

C. Box plot illustrating assessment of TEM-1 β-lactamase assay of one representative screen plate. The blue fluorescence emitted from the infected and uninfected OTP controls were normalised to the mean of the 6 infected, OTP controls within each assay plate.

D and E. Z' factor evaluating quality of siRNA transfection (**D**) and TEM-1 β-lactamase assay (**E**) for the primary screen where a total of 464 assay plates were studied.

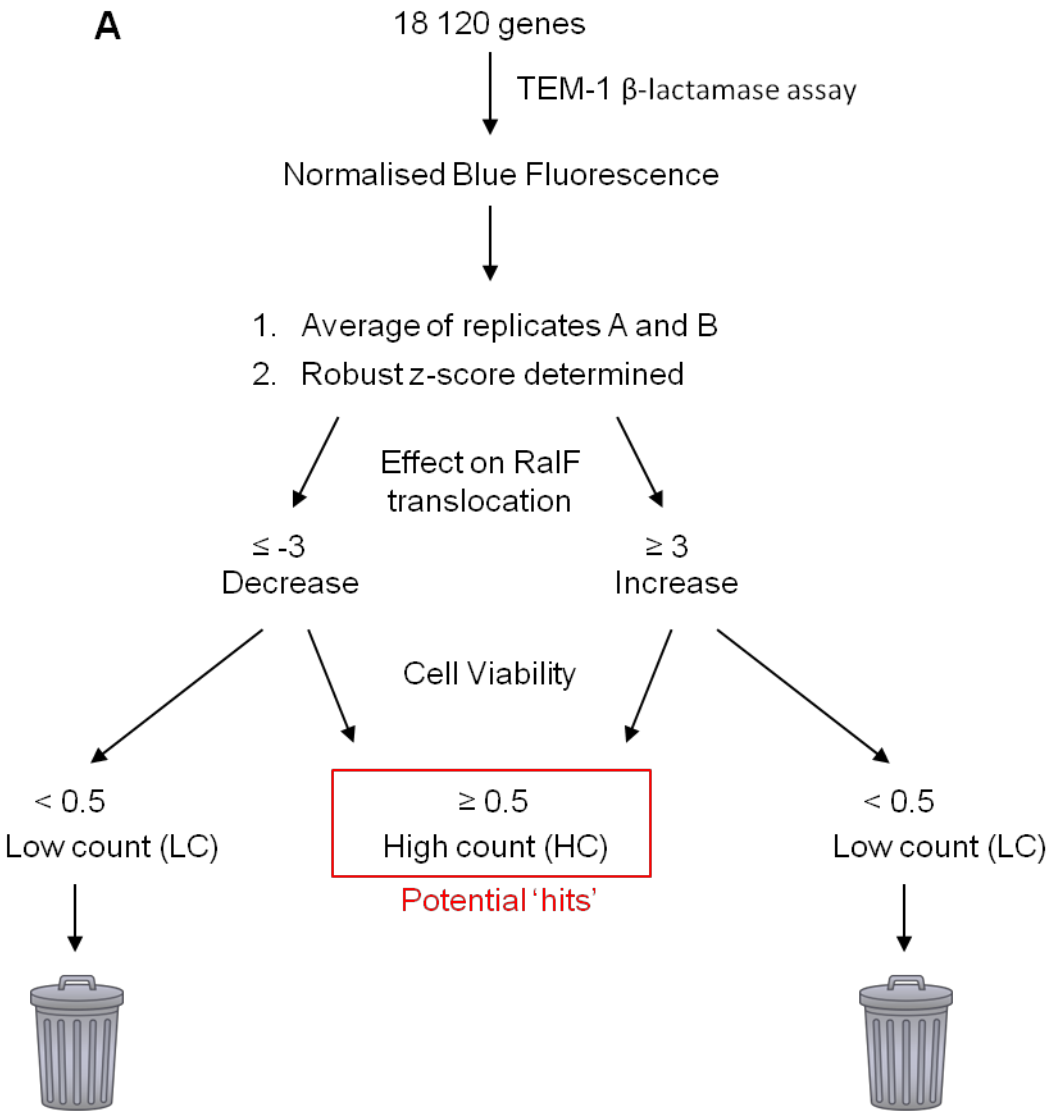
A
18 120 genes
TEM-1 β-lactamase assay
Normalised Blue Fluorescence
1. Average of replicates A and B
2. Robust z-score determined
Effect on RalF translocation
≤ -3
Decrease
≥ 3
Increase
Cell Viability
< 0.5
Low count (LC)
≥ 0.5
High count (HC)
Potential 'hits'
< 0.5
Low count (LC)

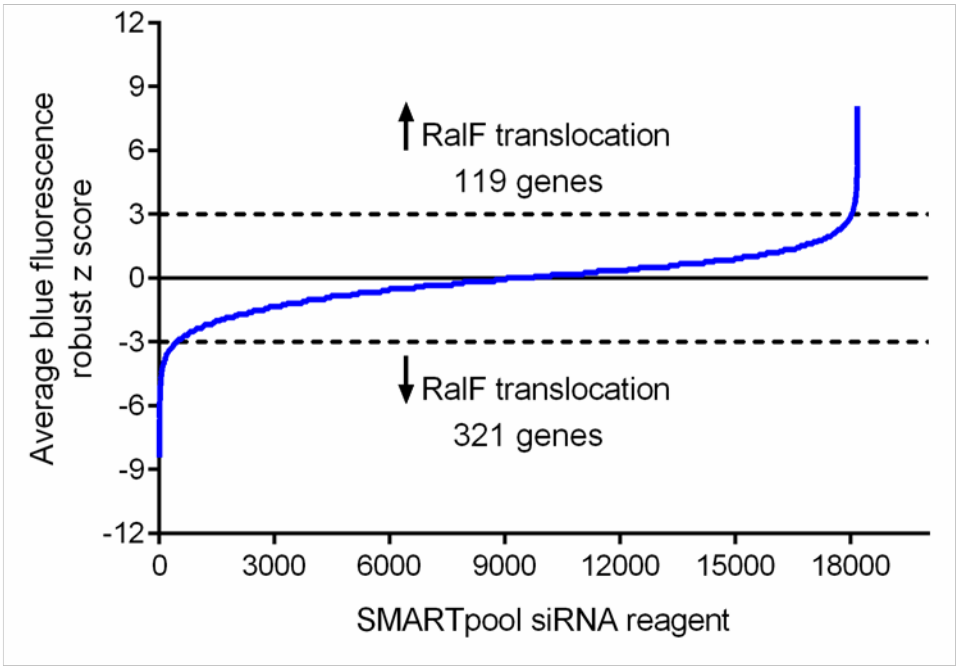
B
Average blue fluorescence robust z score
12
9
6
3
0
-3
-6
-9
-12
RalF translocation
119 genes
RalF translocation
321 genes
0
3000
6000
9000
12000
15000
18000
SMARTpool siRNA reagent

Figure 4.3 Identification of potential hits from the primary genome screen

A. Flowchart of hit selection strategy. Potential hits were indicated by genes that were not important for cell viability and significantly altered the amount of RalF translocation compared to the OTP-treated controls.

B. Number of hits identified. 119 targets found to increase RalF translocation when silenced with siRNA and conversely 321 led to a decrease.

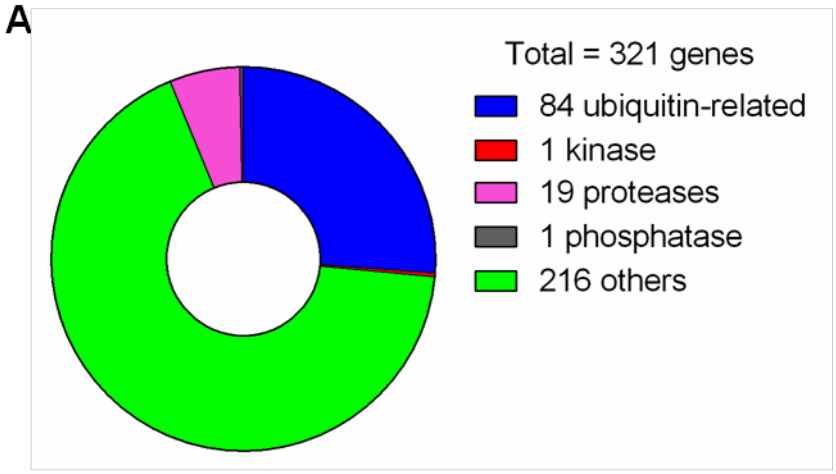
A
Total = 321 genes
84 ubiquitin-related
1 kinase
19 proteases
1 phosphatase
216 others

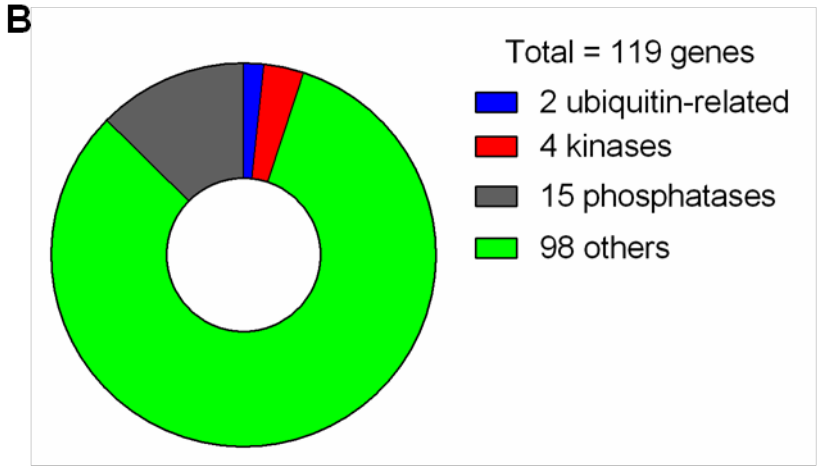
B
Total = 119 genes
2 ubiquitin-related
4 kinases
15 phosphatases
98 others

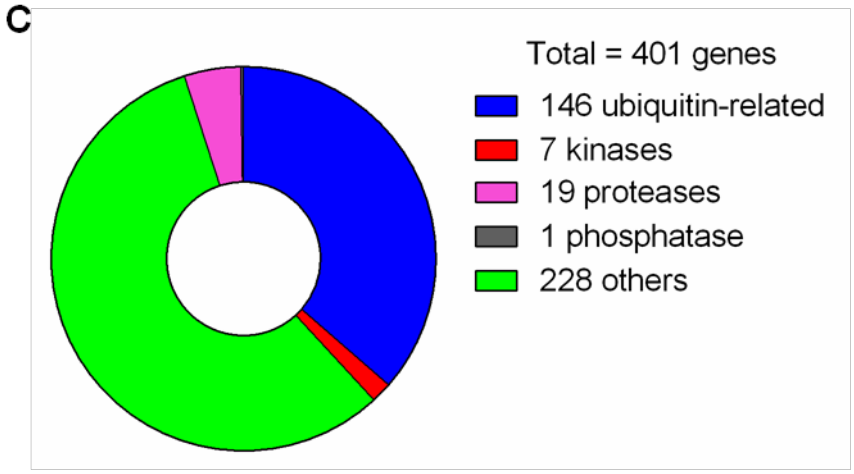
C
Total = 401 genes
146 ubiquitin-related
7 kinases
19 proteases
1 phosphatase
228 others

Figure 4.4 Predicted function of targets identified from primary screen

A. and B. Based on gene ontology, identified targets were categorised into 4 broad biological functional groups. Targets that resulted in decreased RalF translocation (**A**) and targets that resulted in increased RalF translocation (**B**).

C. Updated functional analysis pie chart after including more ubiquitination-related genes, based on a z-score of ± 2.

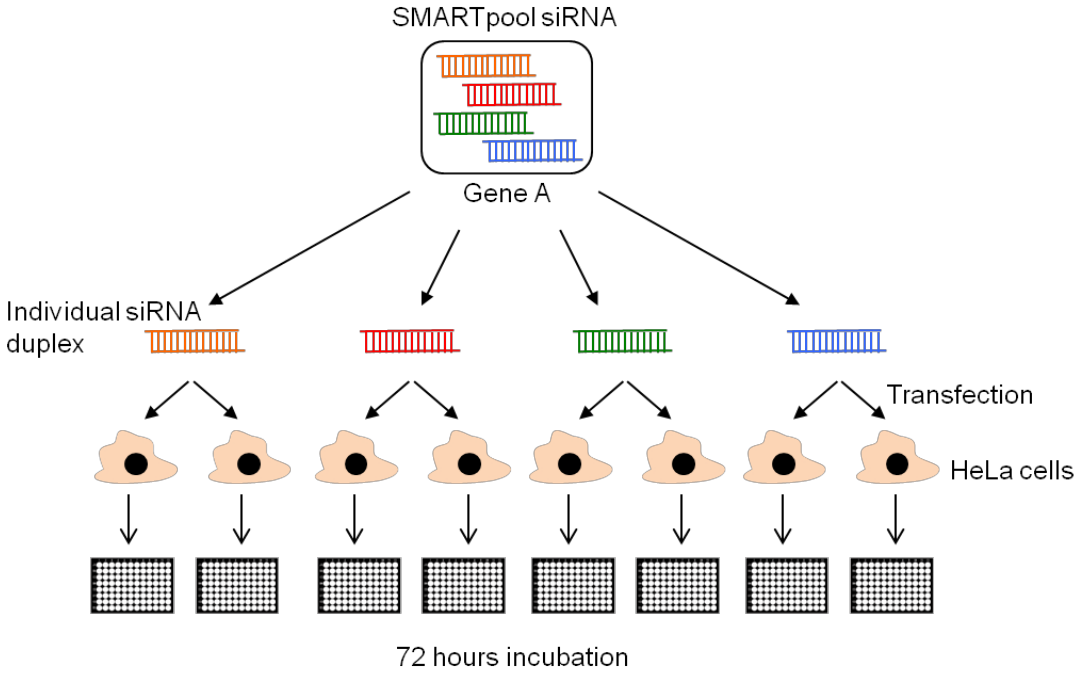

Figure 4.5 Outline of experimental design for the secondary validation screen

SMARTpool siRNAs used in the primary genome screen were deconvoluted into the 4 individual siRNA duplexes and these were transfected into HeLa cells in duplicate for 72 h. The transfection protocol was identical to that of the primary screen. Subsequent secondary screening procedures were identical to that for the primary screen.

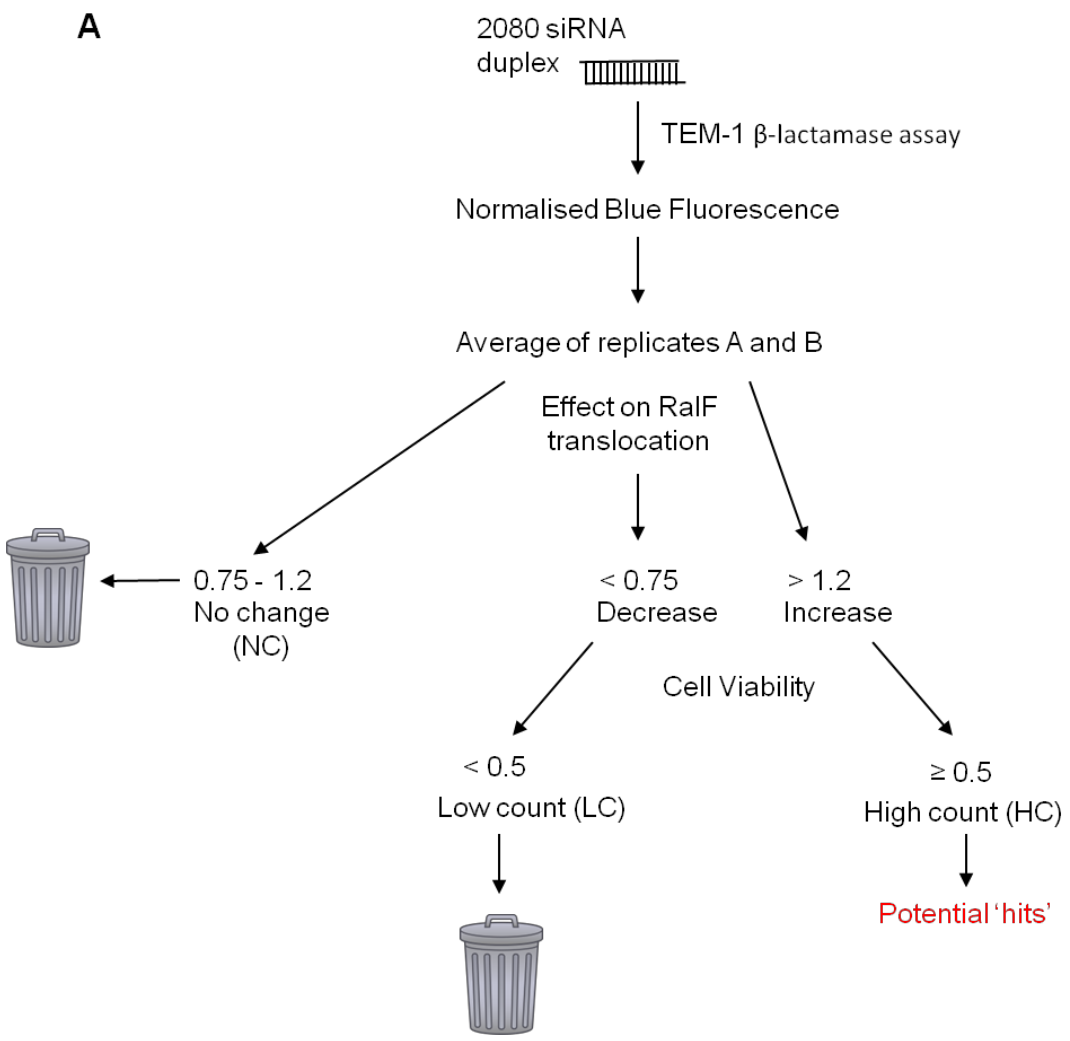
A
2080 siRNA duplex
TEM-1 β-lactamase assay
Normalised Blue Fluorescence
Average of replicates A and B
Effect on RalF translocation
0.75 - 1.2
No change (NC)
< 0.75
Decrease
> 1.2
Increase
Cell Viability
< 0.5
Low count (LC)
≥ 0.5
High count (HC)
Potential 'hits'

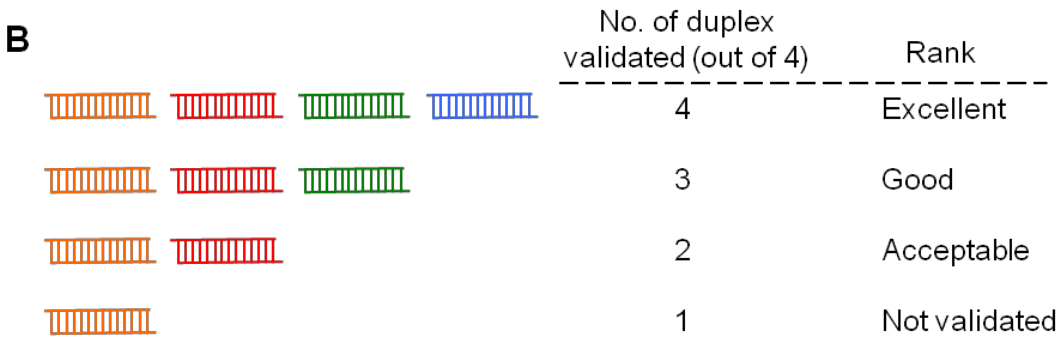
B
No. of duplex validated (out of 4)
Rank
4
Excellent
3
Good
2
Acceptable
1
Not validated

Figure 4.6 Data analysis strategy for validating hits in the secondary screen

A. Flowchart of hit validation process. Cells treated with individual siRNA duplex which resulted in significantly different amount of RalF translocation compared to OTP-treated controls were further categorised according to their cell viability.

B. Hits identified from the primary screen which had ≥ 2 individual siRNA duplexes successful in the secondary screen were considered successfully validated.

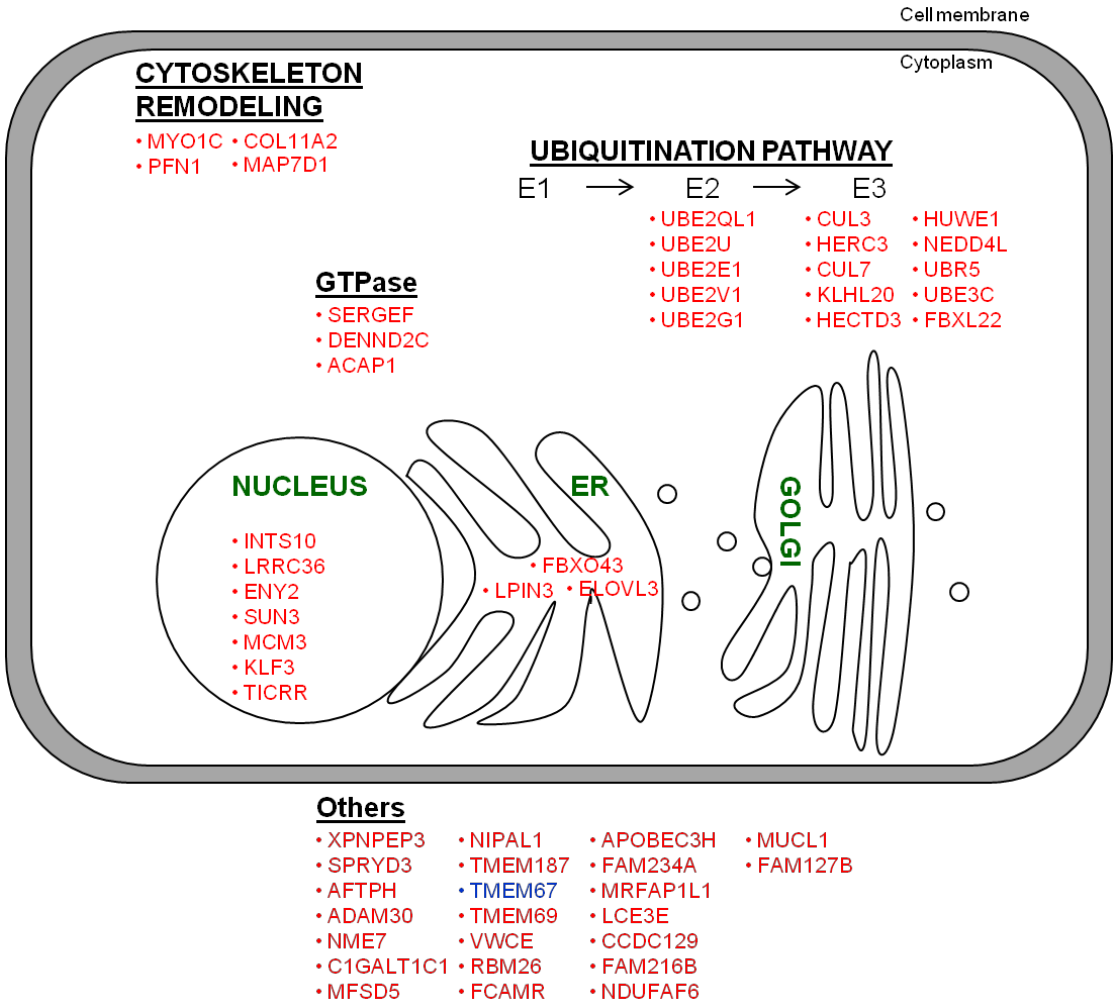

Figure 4.7 Targets validated from the secondary screen

Seventy targets were confidently validated with 2 or more siRNA duplexes. These were organised according to their known functions and/or cellular localisation. Silenced genes leading to an increase in RalF translocation are coloured blue while silenced genes leading to a decrease in RalF translocation are coloured in red.

CHAPTER 5: Further characterisation of the host E2 and E3 ubiquitination factors that mediate translocation of *L. pneumophila* effector proteins

5.1 Introduction

In humans, there are ~25,000 protein-coding genes in the genome, but over 1 million proteins in the proteome (397, 398). The large disparity between the number of genes and proteins contradicts the one gene-one enzyme hypothesis proposed by George Wells Beadle in 1941 (399). One of the reasons for the functional diversity seen in proteins is the discovery of post-translational modifications (PTMs) that regulate protein function. To date, over 200 types of PTMs have been identified; all of which specifically modify proteins via addition of chemical groups (e.g. phosphorylation), complex molecules (e.g. lipidation) and small proteins (e.g. ubiquitination), as well as proteolysis (398, 400, 401). PTMs are involved in the regulation of all forms of cell biology including the localisation, stability, activation and degradation of proteins. Until recently it was believed this process was restricted to eukaryotes (402).

Bacteria are often viewed as only requiring basic cellular processes for survival. However, advances in the last decade, such as bioinformatics predictions based on bacterial genome sequences, the development of assays to identify PTMs in the context of host-pathogen interactions and specialised quantitative proteomics approaches have facilitated research on PTMs in bacteria (403-405). Together, these strategies have shown that bacteria in fact possess the ability to perform a large diversity of PTMs, including modifications previously not seen in eukaryotes. For example, *Shigella flexneri*, a bacterial pathogen that causes bacillary dysentery was found to possess a newly characterised PTM called eliminylation (406, 407). The OspF effector protein functions as a phosphothreonine lyase that interferes with host MAPK signalling so that a phosphate group is irreversibly removed from a phosphorylated threonine residue (406, 407). This type of modification leads to dampening of the host immune response to infection by bacterial-driven down-regulation of host immune gene expression (406, 408). Overall, bacterial PTMs help bacteria adapt and survive in changing environments, and have been implicated in the subversion of host pathways and defence mechanisms, as in the case of OspF.

Furthermore, it also shows that translocated bacterial effector proteins facilitate PTMs in bacteria.

Being an intravacuolar pathogen, *L. pneumophila* also possesses the ability to carry out PTMs on target host proteins for the benefit of the pathogen (402). Many of these PTMs are performed by effector proteins with eukaryotic-like domains that are translocated into host cells during infection. *L. pneumophila* carries an extended array of eukaryotic-like effectors (~75 proteins) that are thought to have been acquired through horizontal gene transfer during co-evolution with multiple species of protozoa (151, 379, 409). For example, a recent study found that the *L. pneumophila* Dot/Icm effector protein, GobX carries a mammalian-like U-box domain, allowing it to act as an E3 ligase in the eukaryotic ubiquitination pathway (410). Interestingly, GobX also demonstrated evidence of exploiting host cell-catalysed S-palmitoylation to ensure it specifically localises to the Golgi (410). The types of PTMs that are catalysed by *Legionella* effectors include ubiquitination, prenylation, methylation, phosphorylation, glycosylation, AMPylation and deAMPylation, phosphocholination and dephosphocholincation (402). Through these PTMs, *L. pneumophila* alters the fate of host proteins in order to avoid being degraded by the host defence system, thereby allowing successful replication and finally lysis of the host cells when appropriate for bacterial egress (187, 238, 402).

Ubiquitination in particular, is important for a wide-range of eukaryotic cellular processes. This process describes the covalent attachment of Ub to target proteins, thereby altering their cellular fate (411). This process typically occurs in three sequential steps, namely activation, conjugation and ligation, with a different enzyme catalysing each reaction step. Ubiquitination can lead to the attachment of either one ubiquitin molecule (monoubiquitination), or a chain of multiple Ub molecules (polyubiquitination) to target proteins. K48- and K29- linked polyubiquitination are traditionally linked to tagging proteins for degradation while other polyubiquitination chains, such as K63- linked and monoubiquitination are involved in regulating inflammation (411, 412). Eukaryotic ubiquitination has been implicated in modulating host defence pathways during viral, bacterial and parasitic infections (246, 413, 414).

As ubiquitination dictates the function of PAMP receptors such as TLRs and therefore orchestrates immune signalling against pathogens, bacteria have developed counter-

measures to modulate this host PTM in order to avoid degradation by the host ubiquitination system (415). For example, the effector protein CHBP from the intracellular pathogen *Burkholderia pseudomallei* directly modifies Ub molecules, rendering them unable to form chains (416). Some bacteria, including *L. pneumophila* encode their own deubiquitinating enzymes (DUBs) to remove Ub from the surface of the LCV to prevent degradation by the proteasome (415, 417).

Since the discovery of polyubiquitin chains on the surface of the LCV and further analysis showing that this seems critical for *L. pneumophila* replication, recent studies have attempted to elucidate the purpose of ubiquitination for infection (111). A recent study by Price *et al*. claimed that *L. pneumophila* makes use of the pool of free amino acids generated when ubiquitinated proteins are degraded by the proteasome to supply their intracellular replication lifestyle (418). However, this does not completely explain the phenomenon that we observed in our screen. In this part of the study, we aimed to further characterise the reason a large proportion of host ubiquitination factors facilitated *L. pneumophila* RalF effector translocation. Here we focused on the host E2 and E3 ligases identified from the siRNA screen that appeared to influence RalF translocation levels. This validation was performed using a variant of the HeLa cell line, called HeLa229, as subsequent to the screening we discovered that HeLa229 cells were more susceptible to *L. pneumophila* infection. Specifically, we found that certain E2-conjugating enzymes and E3 ligases were important for *L. pneumophila* effector protein translocation and for supporting intracellular bacterial replication. Interestingly, these ubiquitination factors also rapidly co-localised with the LCV.

5.2 Results

5.2.1 Translocation of an IcmSW-dependent effector upon silencing of host ubiquitination factors

5.2.1.1 Identification of L. pneumophila effector proteins dependent on IcmSW for efficient translocation

To confirm that the changes in RalF translocation observed in the genome wide siRNA screen were not effector protein specific, the translocation levels of a different effector was measured when the candidate E2 and E3 host genes were silenced. Some Dot/Icm translocated effector proteins require two cytosolic proteins, IcmS and IcmW, to act as chaperones in order to be efficiently translocated by *L. pneumophila* into eukaryotic host cells (172, 419). RalF is not IcmSW dependent (172), and so we decided to select an IcmSW-dependent effector to substantiate our genome screen results. Previous studies that utilised a cAMP reporter assay reported that SidB is an IcmSW-dependent *L. pneumophila* effector protein (174). To verify that SidB was indeed a Dot/Icm substrate that is translocated in an IcmSW-dependent manner, an N-terminal fusion of TEM-1 β-lactamase and SidB was constructed and expressed in *L. pneumophila* 130b, and isogenic Δ*dotA* and Δ*icmSW* mutants. HeLa cells were infected with these *L. pneumophila* strains at a MOI 125 and TEM-1 β-lactamase-SidB translocation levels were measured. *L. pneumophila* 130b strain expressing only TEM-1 β-lactamase was included as negative control. SidB was translocated from wild-type 130b into HeLa cells, as indicated by the response ratio of ~7 (response ratio > 1 indicates positive translocation) (Figure 5.1). When SidB was expressed in *L. pneumophila* lacking either *icmSW* or *dotA*, the response ratio decreased to ~1, a level similar to the negative control (Figure 5.1). This confirmed that SidB is a Dot/Icm substrate and it also requires IcmSW for translocation.

5.2.1.2 Influence of host E2 and E3 ubiquitination factors on the translocation of both RalF and SidB

To investigate if the host ubiquitination factors identified from the genome screen also played a role in the translocation of SidB, siRNA was used to silence their expression. SMARTpool siRNA targeting five E2 enzymes, UBE2QL1, UBE2V1, UBE2E1, UBE2U and UBE2G1, were individually transfected into HeLa229 cells for 72 h.

Cells were subsequently infected with *L. pneumophila* 130b expressing N-terminal TEM-1 β-lactamase fusions with either RalF or SidB. Following this, the TEM-1 β-lactamase assay and analysis were performed in exactly the same manner as the genome screen. Blue fluorescence emitted from the cleavage of CCF2-AM by TEM-1 β-lactamase was quantified for each target host gene and this was normalised to the non-targeting OTP control. Silencing of UBE2QL1, UBE2V1 and UBE2E1 led to a significant reduction in the translocation of RalF into infected HeLa229 cells, while UBE2U and UBE2G1 did not appear to have any effect (Figure 5.2A). This discrepancy was perhaps due to the change in cell line from HeLa used in the genome screen to HeLa229 in this chapter. Similar trends were observed for SidB translocation; where the silencing of UBE2QL1, UBE2V1 and UBE2E1 led to a significant reduction in SidB translocation while silencing of UBE2U and UBE2G1 did not (Figure 5.2B).

The ten E3 ligases identified from the genome screen as having an influence on RalF translocation were also investigated for their effect on IcmSW-dependent translocation of SidB. SMARTpool siRNA targeting HECTD3, CUL7, HERC3, CUL3, KLHL20, UBR5, NEDD4L, HUWE1, FBXL22 and UBE3C were individually transfected into HeLa229 cells for 72 h before cells were infected with *L. pneumophila* 130b expressing N-terminal TEM-1 β-lactamase fusions with either RalF or SidB. The TEM-1 β-lactamase assay and analysis were performed in exactly the same manner as for the E2 ligases. There was a significant decrease in the translocation of RalF in cells that had one of HECTD3, CUL7, HERC3, CUL3, KLHL20 or UBR5 silenced (Figure 5.3A). In contrast to the results obtained from the genome screen, silencing of NEDD4L, HUWE1, FBXL22 or UBE3C in HeLa229 cells had no effect on translocation of RalF (Figure 5.3A). Silencing of CUL7, HERC3, CUL3 and KLHL20 also resulted in a significant reduction in SidB translocation (Figure 5.3B). In addition to the four E3 ligases that did not affect RalF translocation, HECTD3 and UBR5 also had no effect on SidB translocation (Figure 5.3B).

Together, these results strongly suggested that the reduction in RalF translocation observed when these host ubiquitination factors were silenced was not specific to one effector protein nor was it dependent on IcmSW.

5.2.2 Impact of silencing of UBE2E1 and CUL7 on *L. pneumophila* intracellular replication

Successful infection by *L. pneumophila* requires the effective translocation of effector proteins into eukaryotic host cells, and subsequent replication of the bacteria. Until now, we have focused on studying how modulating the expression of specific host ubiquitination genes affected the level of Dot/Icm effector translocation. In order to further probe the biological relevance of these host factors on the pathogenesis of *L. pneumophila*, expression of these genes was individually silenced and intracellular replication of the bacteria was monitored.

5.2.2.1 The E2-conjugating enzyme UBE2E1 is important for sustaining L. pneumophila replication

As UBE2QL1, UBE2V1 and UBE2E1 were previously validated as important for the translocation of Dot/Icm effectors, SMARTpool siRNAs targeting these three E2 conjugating enzymes were individually transfected into HeLa229 cells. 48 h later, these cells were infected with *L. pneumophila* 130b at MOI 25 and total bacterial CFU at 3 h, 24 h, 48 h and 72 h post-infection was enumerated. HeLa229 cells transfected with non-targeting OTP were also included as a control. The number of bacteria at 24 h, 48 h and 72 h was normalised to that at 3 h post-infection to indicate fold increase in replication of *L. pneumophila* following phagocytosis. As evident from the data in Figure 5.4A, no significant difference in the fold increase in replication compared to3 h was evident in HeLa229 cells that were treated with SMARTpool siRNA targeting UBE2V1 and those treated with OTP. A similar observation was made for HeLa229 cells in which UBE2QL1 expression was silenced, except at 48 h post-infection where the fold increase in replication was significantly lower in UBE2QL1 depleted cells (Figure 5.4B). Interestingly, when HeLa229 cells were treated with SMARTpool siRNA targeting UBE2E1, a significantly lower bacterial load was observed from 24 h through to 72 h post-infection compared to cells treated with OTP (Figure 5.4C).

5.2.2.2 Host E3 ligase CUL7 is important for sustaining L. pneumophila replication

Similar to the E2-conjugating enzymes above, the four E3 ligases (CUL7, HERC3, CUL3 and UBR5) that were important in allowing efficient translocation of RalF and SidB were tested for their impact on *L. pneumophila* replication. HeLa229 cells where CUL7 gene expression was silenced with SMARTpool siRNA showed significantly lower fold increase in bacterial replication at 24 h, 48 h and 72 h post-infection compared to OTP controls (Figure 5.5A). In contrast, HERC3 and CUL3 did not appear to impact the replication of *L. pneumophila* during infection (Figure 5.5B and C). Treating HeLa229 cells with SMARTpool siRNA targeting UBR5 resulted in significantly lower fold increase in bacterial replication at 48 h post-infection compared to OTP, but not at 24 h or at 72 h (Figure 5.5D). Together with the results of the E2-conjugating enzymes, this work suggests that some host factors have roles in both aiding Dot/Icm effector translocation as well as subsequent replication of *L. pneumophila*.

5.2.2.3 Knock-down of target gene expression was sustained throughout replication assay

As the *L. pneumophila* replication assays performed above extended until 5 days after siRNA treatment, we ensured that knock-down of target gene expression was maintained throughout the course of the assay. This was because siRNA-induced RNAi is a transient mechanism where mRNA levels sometimes recover 4–5 days after siRNA treatment (420).

To confirm that the gene expression was silenced throughout the entire replication assay, normalised mRNA levels of UBE2E1 and CUL7 were quantified via qRT-PCR of mRNA from HeLa229 cells transfected with siUBE2E1 and siCUL7 respectively. Results were expressed relative to OTP-treated HeLa229 cells to quantify target gene silencing. At the time of *L. pneumophila* infection (48 h after transfection with siUBE2E1), expression levels of UBE2E1 were only 0.1 fold of the control cells (Figure 5.6A). This significant reduction in gene expression was observed up until 5 days post-treatment with siRNA, confirming that the phenotype of reduced bacterial replication was consistent with the absence of UBE2E1 (Figure 5.6A).

Similarly, at 48 h, 72 h, 4 days and 5 days post-treatment with siCUL7, significantly reduced expression of CUL7 was recorded compared to OTP (Figure 5.6B). Therefore, the phenotype of reduced *L. pneumophila* replication could also be attributed to silencing of CUL7.

5.2.3 Decreased *L. pneumophila* replication was not due to impaired phagocytosis

In the replication assay performed above (Section 5.2.2), bacteria recovered from HeLa229 cells at 3 h post-infection with *L. pneumophila* were considered to be the number of bacteria that were successfully phagocytosed by the host cells. Only these internalised bacteria would then replicate and disseminate to other cells over the course of infection. As such, it was important to determine if the reduced replication seen in cells treated with UBE2E1 and CUL7 siRNA was due to reduced bacterial internalisation. For this, bacterial CFU obtained at 3 h post-infection was enumerated and expressed as a percentage of the total number in the starting inoculum (Figure 5.7). There was no significant difference in the number of *L. pneumophila* recovered from HeLa229 cells that were treated with siUBE2E1 or siCUL7 compared to OTP (Figure 5.7). This demonstrated that the reduced *L. pneumophila* replication observed in the absence of UBE2E1 and CUL7 was a *bona fide* defect, and not due to fewer bacteria successfully entering the cells.

5.2.4 Host ubiquitin factors required for both Dot/Icm activity and replication of *L. pneumophila* co-localise with the bacteria during infection

So far, the biological studies aiming to characterise the eukaryotic targets identified from the genome screen had focused on knocking-down expression of genes of interest to examine phenotypic changes in Dot/Icm effector translocation and *L. pneumophila* replication. We had shown through knock-down studies that the E2 conjugating enzyme UBE2E1 and E3 ligase CUL7 appeared to be host factors important in *L. pneumophila* infection. We were next interested to know if these host proteins form intimate interactions with the LCV during an infection. This was investigated via immunofluorescence, staining for localisation of the endogenous proteins in Hek293 FcγR-expressing cells infected with opsonised *L. pneumophila*.

Confocal laser scanning microscopy analysis of cells 3 h, 8 h and 18 h post-infection revealed that UBE2E1 was recruited from the host cytoplasm and associated tightly

with the LCV shortly after infection at 3 h and this was maintained until 8 h later (Figure 5.8). However, after 18 h, UBE2E1 co-localisation with the bacteria was no longer evident with most of the protein re-distributing throughout the cell (Figure 5.8). Similar to that observed for UBE2E1, CUL7 was also found to clearly associate with the LCV at 3 h and 8 h post-infection (Figure 5.9). While CUL7 was still found to be in the vicinity of the LCV 18 h after infection, the tight association seen earlier during infection had diminished (Figure 5.9). Hence, we concluded that both UBE2E1 and CUL7 closely interact with the LCV early during infection, most likely to modulate LCV biogenesis.

5.3 Discussion

From our initial genome-wide screen, several human Ub-conjugating enzymes (E2s) and Ub-ligases (E3s) were identified as being important in ensuring that the *L. pneumophila* Dot/Icm effector, RalF, was efficiently translocated during infection.

Here, we further showed that silencing of the E2-conjugating enzymes (UBE2QL1, UBE2V1 and UBE2E1) and E3 ligases (CUL7, HERC3, CUL3 and UBR5) resulted in reduced translocation of not only RalF, but also another *L. pneumophila* effector, SidB. Like RalF, SidB is translocated into host cells via the Dot/Icm system. However, SidB also requires the additional IcmSW cytoplasmic chaperone complex for translocation into host cells whereas RalF does not. The exact reason why certain Dot/Icm mediated effectors, such as SidB associate with IcmSW; while others, such as RalF do not, is still unknown. Our findings that a knock-down in expression of the E2 and E3-encoding genes described above resulted in a similar reduction in translocation levels of both RalF and SidB effector proteins, suggested that host ubiquitination factors were not required to mimic the chaperone functions of IcmSW. Rather, these enzymes were more likely to constitute additional factors hijacked by *L. pneumophila* to ensure that the Dot/Icm system translocates effectors at maximum capacity. Chaperone proteins such as IcmSW aid in the function of the Dot/Icm system and the effector proteins that they translocate into host cells have important roles in various stages of infection. For example, SidC is an effector protein that is translocated in an IcmSW-dependent manner (174). It functions as a unique bacterial E3 ligase that is important for the ubiquitination of host Rab1 and remodelling of the LCV through the recruitment of host-derived ER proteins and polyubiquitin conjugates to the cytoplasmic face of the LCV (199, 200).

Given that the presence of the Dot/Icm system is vital for *L. pneumophila* replication, the next obvious step in this study was to investigate whether host ubiquitination factors that were important for effector translocation also contributed to bacterial proliferation. Results from our intracellular replication assays in HeLa229 cells revealed that only one E2-conjugating enzyme (UBE2E1) and one E3 ligase (CUL7) were clearly involved in supporting *L. pneumophila* replication throughout a 72 h infection period. Silencing the expression of these factors did not significantly hinder *L. pneumophila* from being taken up/entering HeLa229 cells during initial stage of the

infection, thereby eliminating the possibility that the reduced replication phenotype could be attributed to a lower number of bacteria initially within the host cell. Hence, UBE2E1 and CUL7 both appeared to play important roles in controlling effector protein translocation as well as sustaining intracellular replication of *L. pneumophila*.

Reduced intracellular replication of *L. pneumophila* may arise for different reasons. One possibility is that the bacteria lose the ability to avoid lysosomal degradation pathway, and are therefore readily killed by the host cell before replication can occur (155, 157, 163, 421). Another possibility is that the bacteria retain the ability to form an LCV, but cannot replicate due to deficiencies in nutrient acquisition and utilisation, nucleotide biosynthesis and chromosome replication (422, 423). In this study, we did not further dissect the mechanism leading to the decreased replicative phenotype resulting from the loss-of-function of these host ubiquitination factors. However, this is certainly an exciting avenue for future studies because there remains a lack of understanding on how different host factors may influence intracellular replication of the bacteria.

Host factors that modulate replication of other intracellular pathogens, such as *S*. Typhimurium, have also been extensively studied. For example, a genome-wide RNAi screen found that numerous host factors promote *S*. Typhimurium replication within HeLa cells (424). These included factors involved in vesicle trafficking, vacuole acidification, signal transduction, lipid synthesis and metabolism, ubiquitination and transport (424). The implication of so many pathways in the replication of *S*. Typhimurium suggests that, similar to the Dot/Icm system, intracellular replication of *L. pneumophila* most likely involves a wide-range of host factors.

Unfortunately, our network analyses did not find UBE2E1 and CUL7 to be jointly involved in any common biological pathways. UBE2E1 is an E2-conjugating enzyme that typically mediates degradation of aberrant cellular proteins and K48-linked polyubiquitination, while CUL7 is a component of the RING-E3 ubiquitin-protein ligase complex that is reported to bind and attenuate the tumour suppressor gene, p53 (425, 426). Even though both have no known involvement in intracellular bacterial infections to date, findings from this study might pave the way for uncovering novel cellular roles for these host proteins.

Our study was entirely based on monitoring phenotypic perturbations to Dot/Icm effector translocation as a result of artificially induced RNAi of individual human genes. While this loss-of-function strategy proved effective in identifying two host factors that are important for Dot/Icm translocation and *L. pneumophila* intracellular replication, it is also important to understand the interactions that occur in a normal, unperturbed cellular state. Our co-localisation studies showed that both endogenous UBE2E1 and CUL7 associated intimately with the LCV within 3 h after bacterial uptake and this interaction was maintained throughout bacterial replication. However, as replication ceased over time, UBE2E1 and CUL7 appeared to re-distribute throughout the cytoplasm. Our finding that host ubiquitination factors associated with replicating *L. pneumophila* is consistent with a previous study that profiled the ubiquitinated host-derived proteome of LCVs isolated from *L. pneumophila* infected human macrophages (278). This study found that of the 1193 host-derived proteins found on the LCV, eight were E3 ligases and four were E2 conjugating enzymes (278). One of these E2 enzymes, UBE2V1, was also identified in our work as important for RalF and SidB translocation. However, it was not involved in bacterial replication. This highlights that different host factors are likely to be involved in different stages of *L. pneumophila* infection. While some are only involved in one aspect of pathogenesis, others such as UBE2E1 and CUL7 may have multiple roles. It was interesting to observe the close interaction of UBE2E1 and CUL7 with the LCV, and thus strategies to pursue this mechanism of action such as exploring interacting partners (both host and bacteria) using pull-downs will be the obvious next steps in this study.

L. pneumophila hijacks the host ubiquitination machinery in many ways, for different purposes. It has long been established that the LCV is decorated with polyubiquitinated proteins very shortly after infection and this is linked to efficient *L. pneumophila* replication (111). This process occurs in a Dot/Icm dependent manner with the effector protein, AnkB, allegedly driving the recruitment of these polyubiquitin conjugates (280, 281, 382). Studies performed in human cells and amoeba suggested that K-48 linked polyubiquitin tagged proteins recruited to the LCV are degraded via the ubiquitin-dependent proteolysis pathway (282). This in turn generates a large pool of free amino acids that feeds into the LCV, serving as carbon and energy sources for *L. pneumophila* during intracellular replication (282). While

this explanation offered possible roles for the polyubiquitinated proteins found on the LCV, it is unlikely that providing a nutrient source entirely accounts for the participation of host ubiquitination in *L. pneumophila* infection. It is even more unlikely that one effector protein, AnkB, dominates this process.

In eukaryotic cellular physiology, response to protein homeostasis and ER stress is through the induction of the unfolded protein response (UPR), leading to retardation of mRNA translation and a higher rate of protein folding (427). A critical consequence of the UPR is up-regulation of ER associated degradation (ERAD) to dispose of misfolded proteins (427). In ERAD, misfolded proteins are transported across the ER membrane and into the cytoplasm for degradation via a process called retrotranslocation (427, 428). The mechanism of retrotranslocation is not clearly defined, however it is believed that p97 binds and moves target substrates into the cytoplasm through a membrane channel such as Derlin1 (429). p97 is an AAA-ATPase chaperone protein that localises to the cytoplasmic surface of the ER membrane, and is proposed to actively pull out ubiquitinated ERAD substrates into the cytosol, for presentation to the proteasome (430).

Considering the enrichment of different host ubiquitination processes resulting from our RNAi screen and that p97 also localises to the LCV membrane in a Dot/Icm manner (111), it seems possible that Ub itself might play a molecular role in the translocation of Dot/Icm effector proteins. As silencing p97 gene expression using siRNA led to cell death, we were unable to determine if absence of p97 modulated translocation of RalF. Despite this, taking together the aforementioned findings regarding p97 and knowledge that the LCV is an ER-derived vacuole, we hypothesize that *L. pneumophila* may hijack host p97 and the process of retrotranslocation to translocate effector proteins across the LCV membrane. However, it is not yet clear if effector proteins themselves are ubiquitinated to facilitate their transport across the LCV membrane, although p97 appears to be necessary for optimal translocation of the Dot/Icm effectors, LidA and SidC (111). Using an ubiquitination prediction tool, UbPred, we found that 213 out of 249 Dot/Icm effector proteins we tested contained lysine residues that were predicted with at least medium confidence, as sites for ubiquitination. Interestingly, many effectors of *L. pneumophila*, such as SidC, are well-characterised bacterial E3 ubiquitination ligases that may potentiate the process. To explore this hypothesis, further work is required. For example, the effects of

inhibiting the functions of p97 on Dot/Icm effector translocation can be examined using reversible chemical inhibitor, DBeQ, although care must be taken as in our hands DBeQ also induced significant host cell death.

Another bacterial pathogen that utilises retrotranslocation for delivering toxins is *Vibrio cholerae*. During *V. cholerae* infection, cholera toxin (CT) is secreted by the bacteria, and then taken up by host intestinal cells where it enters the ER (431). Within the ER, CT undergoes repackaging before the A1 chain retrotranslocates across the ER membrane into the host cell cytoplasm where it ADP-ribosylates a trimeric G-protein, leading to secretion of chloride and water and eventually profuse, watery diarrhoea (431-433). Interestingly, CT is not ubiquitinated at any stage during the retrotranslocation process (432). In fact, it is proposed that the lack of ubiquitination helps CT avoid recognition from the proteasome and thus degradation (432). This suggests that the mode of retrotranslocation exploited by bacterial pathogens can differ from that typically observed in eukaryotes. As such, the question of whether *L. pneumophila* translocates Dot/Icm effector proteins into host cells via a process similar to regular retrotranslocation remains to be elucidated.

In summary, as silencing of a significant number of human ubiquitination factors led to reduced RalF translocation during *L. pneumophila* infection, we further validated and characterised their biological relevance. We found that effector proteins requiring IcmSW also depended on the E2-conjugating and E3-ligase host genes identified here for efficient translocation. In addition to being important for effector protein translocation, UBE2E1 and CUL7 were also important for ensuring high intracellular bacterial replication. While much still remains to be mechanistically understood and proven experimentally, we propose that the translocation of effector proteins via the Dot/Icm system may mimic the process of retrotranslocation, which requires Ub, and this may or may not require the effector proteins themselves to be ubiquitinated. Previous chemical compound screening performed by Charpentier *et al*. (328) found that phagocytosis facilitates effector translocation; therefore, whether the host ubiquitin system contribute to phagocytosis and inadvertently enhance effector translocation also remains to be determined. Availability of a hyperactive ubiquitin cell model system will also answer if effector translocation increases correspondingly.

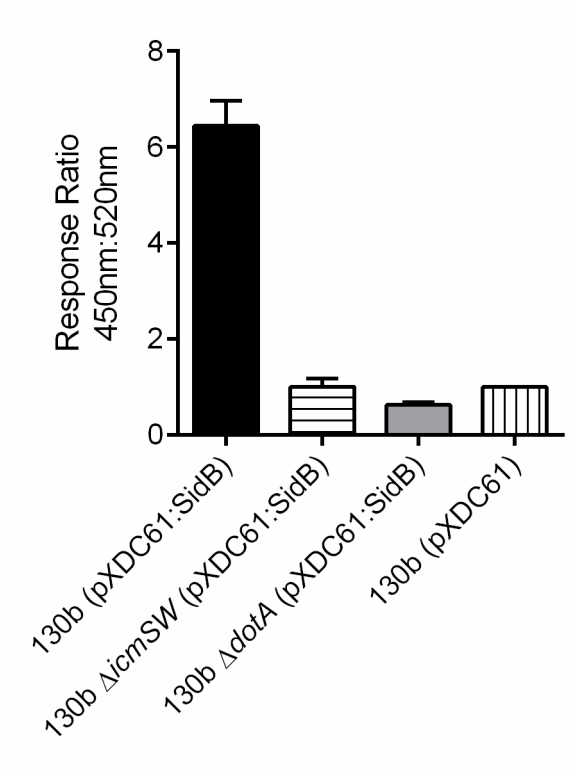

Figure 5.1 Translocation of the IcmSW-dependent effector SidB

HeLa229 cells were infected with *L. pneumophila* 130b (■), *L. pneumophila* 130b Δ*icmSW* (▭) or *L. pneumophila* 130b Δ*dotA* (▭), each carrying the plasmid pXDC61:SidB. The TEM-1 β-lactamase assay was subsequently performed and the response ratio determined to indicate amount of SidB translocation from each bacteria strain in infected host cells. *L. pneumophila* carrying the empty pXDC61 (▭) served as the negative control. Results are the mean ± SEM of three independent experiments carried out in triplicate.

A

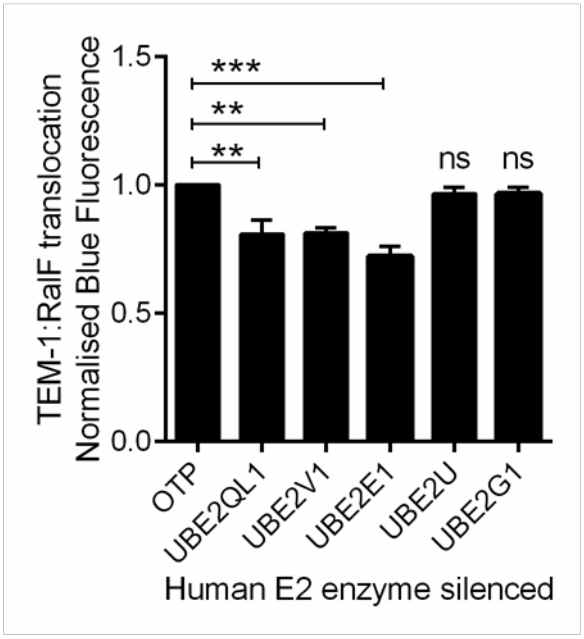
TEM-1:RalF translocation
Normalised Blue Fluorescence
1.5
1.0
0.5
0.0
***
**
**
ns
ns
OTP
UBE2QL1
UBE2V1
UBE2E1
UBE2U
UBE2G1
Human E2 enzyme silenced

B

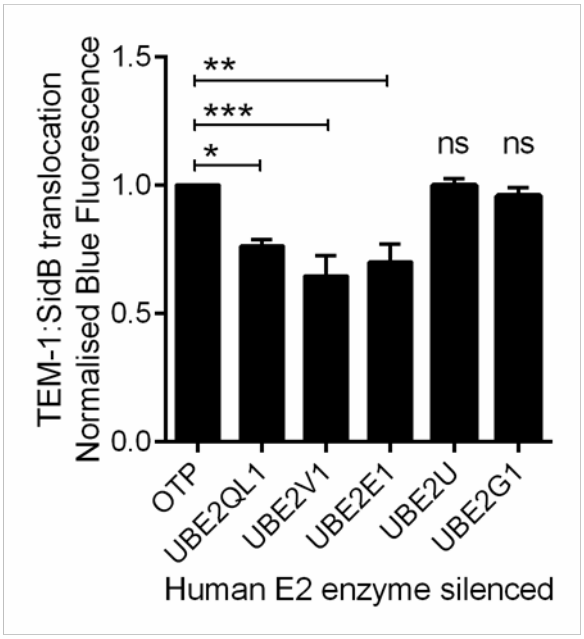
TEM-1:SidB translocation
Normalised Blue Fluorescence
1.5
1.0
0.5
0.0
**
***
*
ns
ns
OTP
UBE2QL1
UBE2V1
UBE2E1
UBE2U
UBE2G1
Human E2 enzyme silenced

Figure 5.2 Effects of silencing expression of five E2 ubiquitin conjugating enzymes on translocation of RalF and SidB

HeLa229 cells were transfected with siRNA targeting UBE2QL1, UBE2V1, UBE2E1, UBE2U, UBE2G1 or non-targeting OTP before being infected with *L. pneumophila* carrying pXDC61:RalF (**A**) or pXDC61:SidB (**B**). The TEM-1 β-lactamase assay was then performed and the blue fluorescence levels quantified for each were normalised to that of control cells (OTP). Results are the mean ± SEM of four independent experiments carried out in duplicates.*Significantly different to OTP control (*p ≤ 0.05, **p ≤ 0.01, ***p ≤ 0.001 one way ANOVA with Dunnett post test).

A

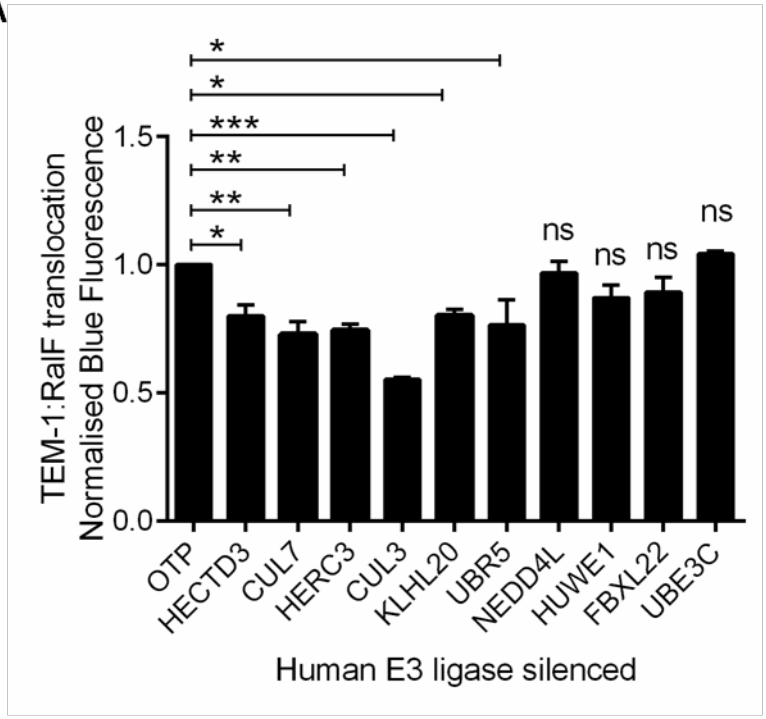
TEM-1:RalF translocation
Normalised Blue Fluorescence
1.5
1.0
0.5
0.0
*
*
***
**
**
*
ns
ns
ns
ns
OTP
HECTD3
CUL7
HERC3
CUL3
KLHL20
UBR5
NEDD4L
HUWE1
FBXL22
UBE3C
Human E3 ligase silenced

B

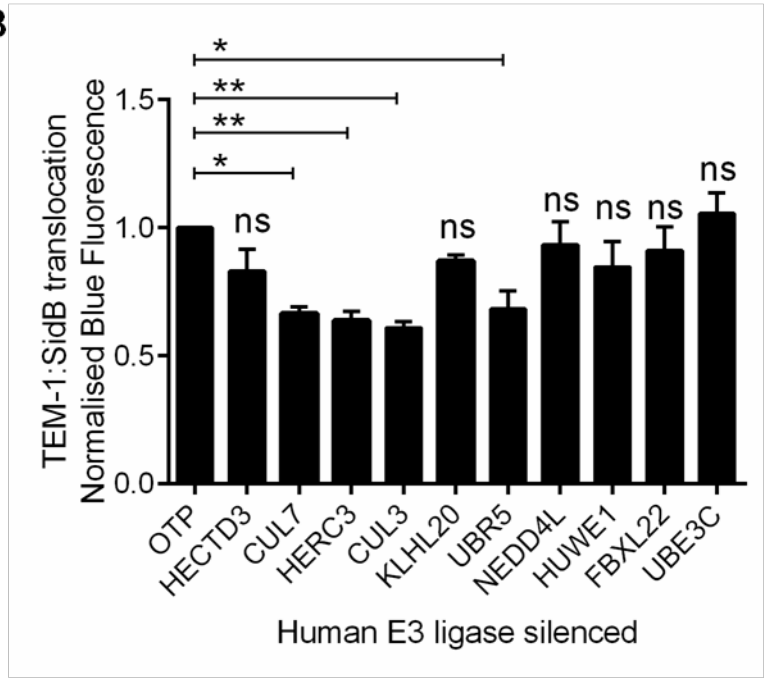
TEM-1:SidB translocation
Normalised Blue Fluorescence
1.5
1.0
0.5
0.0
*
**
**
*
ns
ns
ns
ns
ns
ns
OTP
HECTD3
CUL7
HERC3
CUL3
KLHL20
UBR5
NEDD4L
HUWE1
FBXL22
UBE3C
Human E3 ligase silenced

Figure 5.3 Effects of silencing gene expression of ten E3 ubiquitin ligases on translocation of RalF and SidB

HeLa229 cells were transfected with siRNA targeting HECTD3, CUL7, HERC3, CUL3, KLHL20, UBR5, NEDD4L, FBXL22, UBE3C or non-targeting OTP before infected with *L. pneumophila* carrying pXDC61:RalF (**A**) or pXDC61:SidB (**B**). The TEM-1 β-lactamase assay was then performed and the blue fluorescence levels quantified for each were normalised to that of control cells (OTP). Results are the mean ± SEM of four independent experiments carried out in duplicates.*Significantly different to OTP control (*$p \leq 0.05$, **$p \leq 0.01$, ***$p \leq 0.001$ one way ANOVA with Dunnett post test).

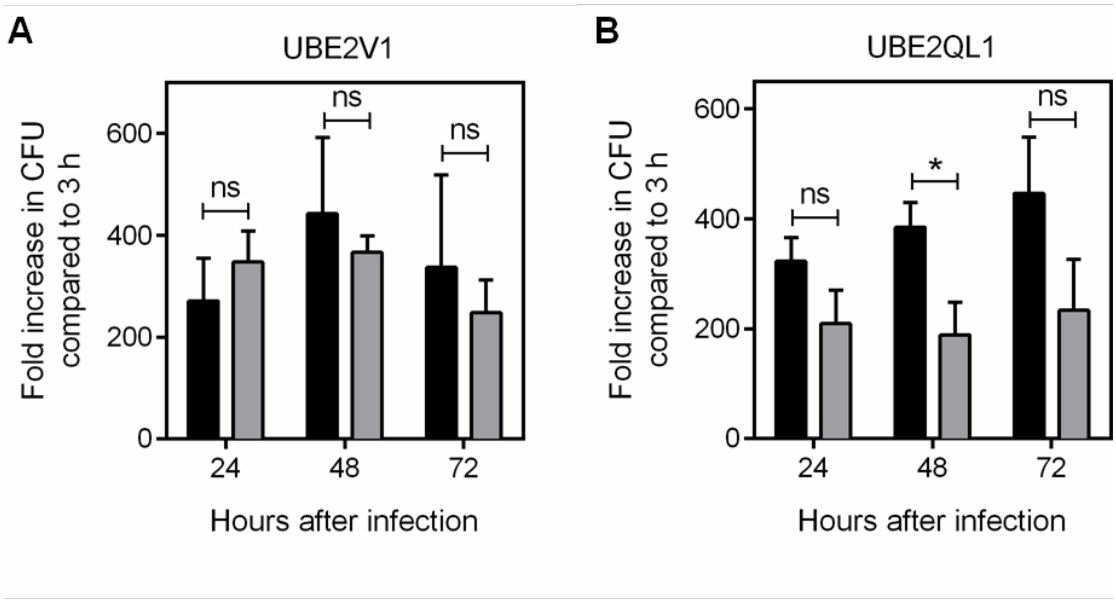

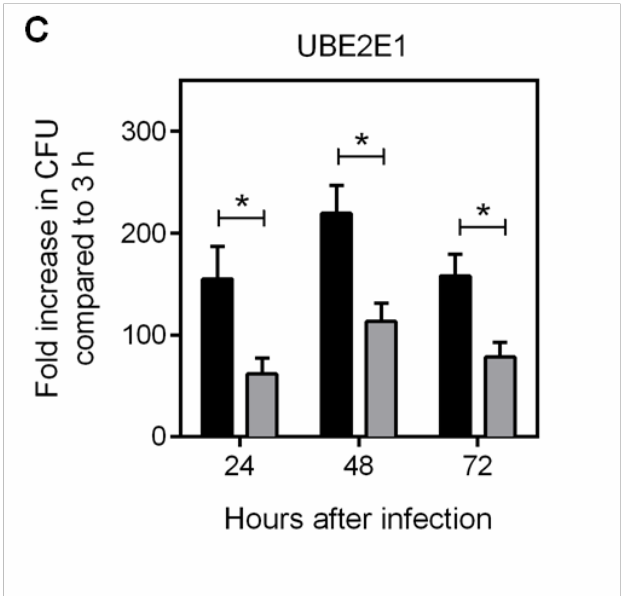

Figure 5.4 Replication of *L. pneumophila* in HeLa229 cells treated with siRNA to silence UBE2E1, UBE2V1 and UBE2QL1

HeLa229 cells were transfected with siRNA (▭) targeting UBE2V1 (**A**), UBE2QL1 (**B**) or UBE2E1 (**C**) before infection with *L. pneumophila* 130b. HeLa229 cells transfected with non-targeting OTP (■) were included as controls. 3 h, 24 h, 48 h and 72 h later, cells were lysed and bacterial CFU at the 3 latter time-points normalised to that of 3 h to obtain the fold increase of bacteria number. Results are the mean ± SEM of four independent experiments carried out in duplicate. *Significantly different to OTP control (*$p \leq 0.05$, **$p \leq 0.01$, ***$p \leq 0.001$, ns = $p > 0.05$ one way ANOVA with Dunnett post test).

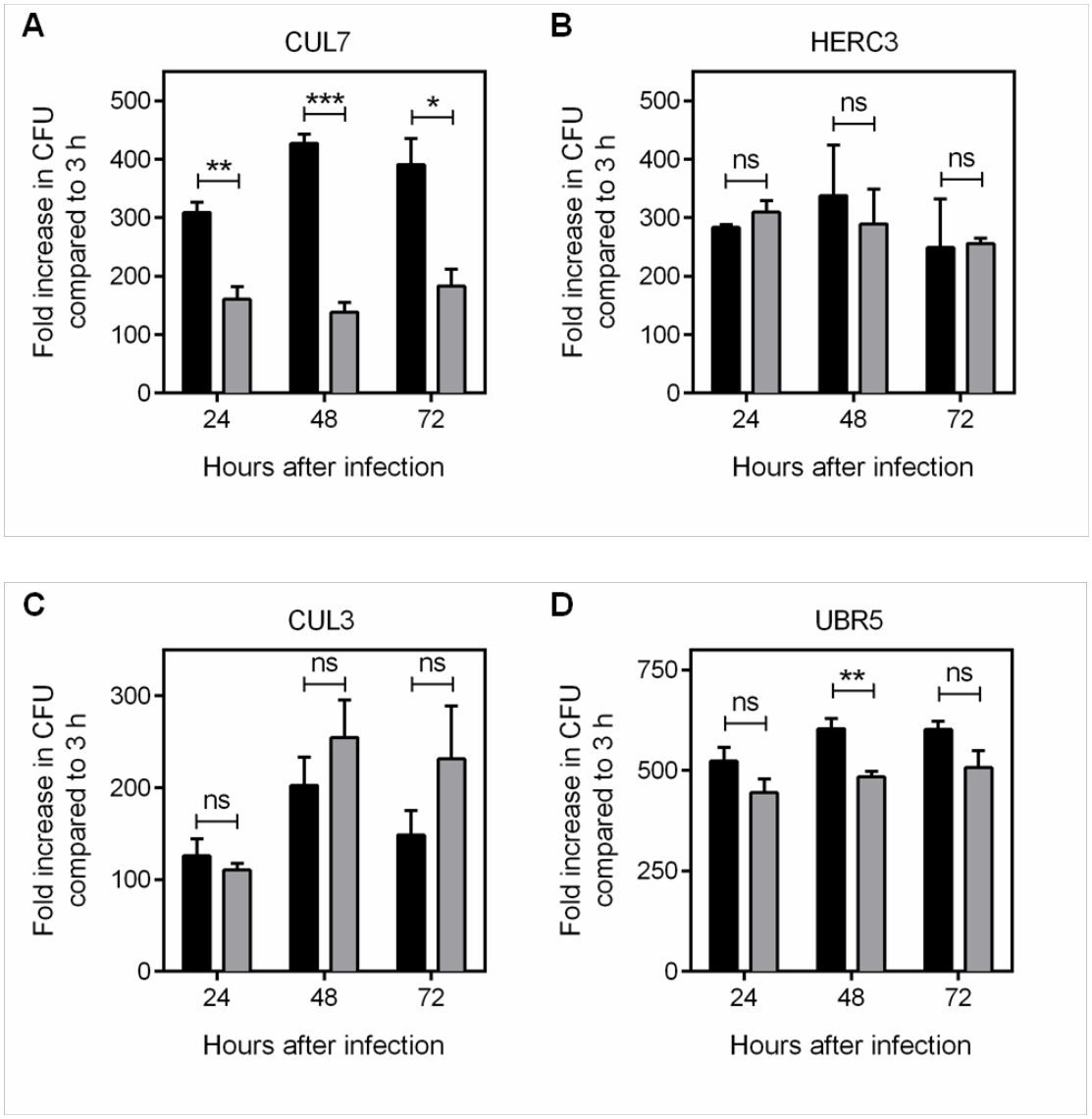

Figure 5.5 Replication of *L. pneumophila* in HeLa229 cells treated with siRNA to silence expression of selected E3 ubiquitin ligases

HeLa229 cells were transfected with siRNA (▭) targeting CUL7 (**A**), HERC3 (**B**), CUL3 (**C**) or UBR5 (**D**) before infection with *L. pneumophila* 130b. HeLa229 cells transfected with non-targeting OTP (■) were included as controls. 3 h, 24 h, 48 h and 72 h later, cells were lysed and bacterial CFU at the 3 latter time-points normalised to that of 3 h to obtain the fold increase of bacteria number. Results are the mean ± SEM of four independent experiments carried out in duplicates. *Significantly different to OTP control (*$p \leq 0.05$, **$p \leq 0.01$, ***$p \leq 0.001$, ns = $p > 0.05$ one way ANOVA with Dunnett post test).

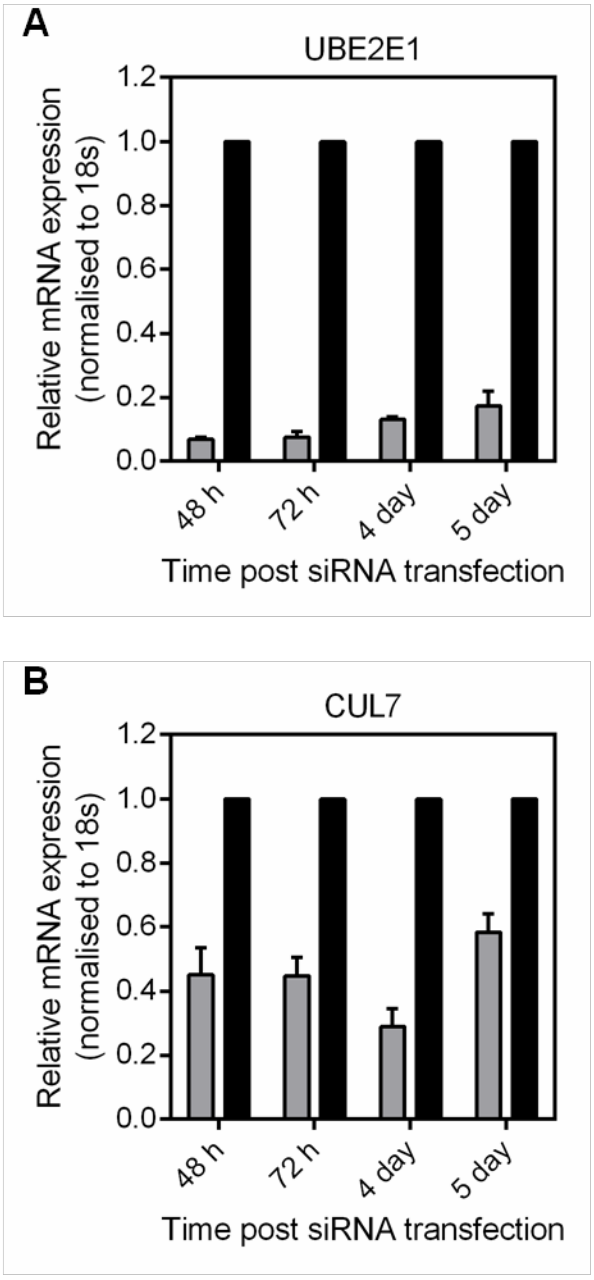

Figure 5.6 Analysis of target gene expression levels after siRNA treatment

HeLa229 cells were transfected with siRNA (▭) targeting UBE2E1 (**A**) or CUL7 (**B**). HeLa229 cells transfected with non-targeting OTP (■) were included as controls. 48 h, 72 h, 4 day and 5 day later, qRT-PCR was subsequently performed where expression levels of each target gene was quantified. This was normalised to expression levels of the housekeeping gene, 18s, and finally expressed as relative to the OTP control to indicate efficiency of gene knock-down. Results are the mean ± SEM of four independent experiments carried out in duplicates.

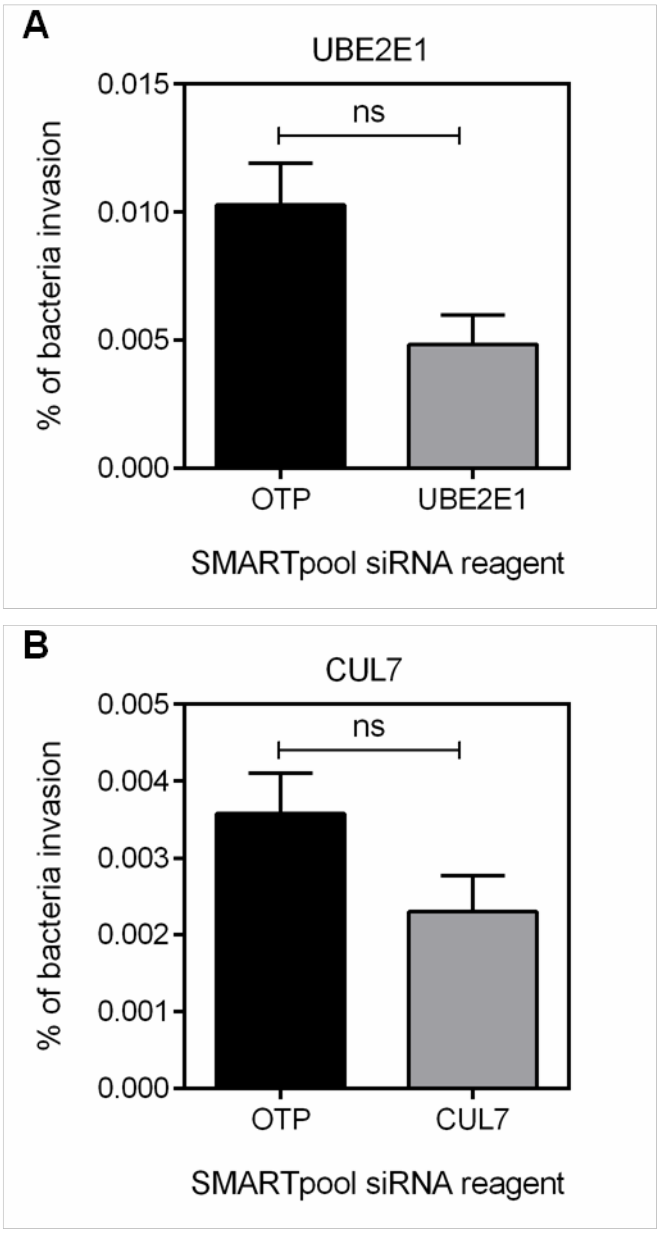

Figure 5.7 Bacterial invasion in the absence of UBE2E1 and CUL7

HeLa229 cells were transfected with siRNA (▭) targeting UBE2E1 (**A**) or CUL7 (**B**) before infection with *L. pneumophila* 130b. HeLa229 cells transfected with non-targeting OTP (■) were included as controls. 3 h later, cells were lysed and bacterial CFUs enumerated. This was divided by the bacterial inoculum and expressed as a percentage to indicate levels of successful bacterial invasion. Results are the mean ± SEM of four independent experiments carried out in duplicates. *ns = Not significantly different to OTP control ($p > 0.05$, one way ANOVA with Dunnett post test).

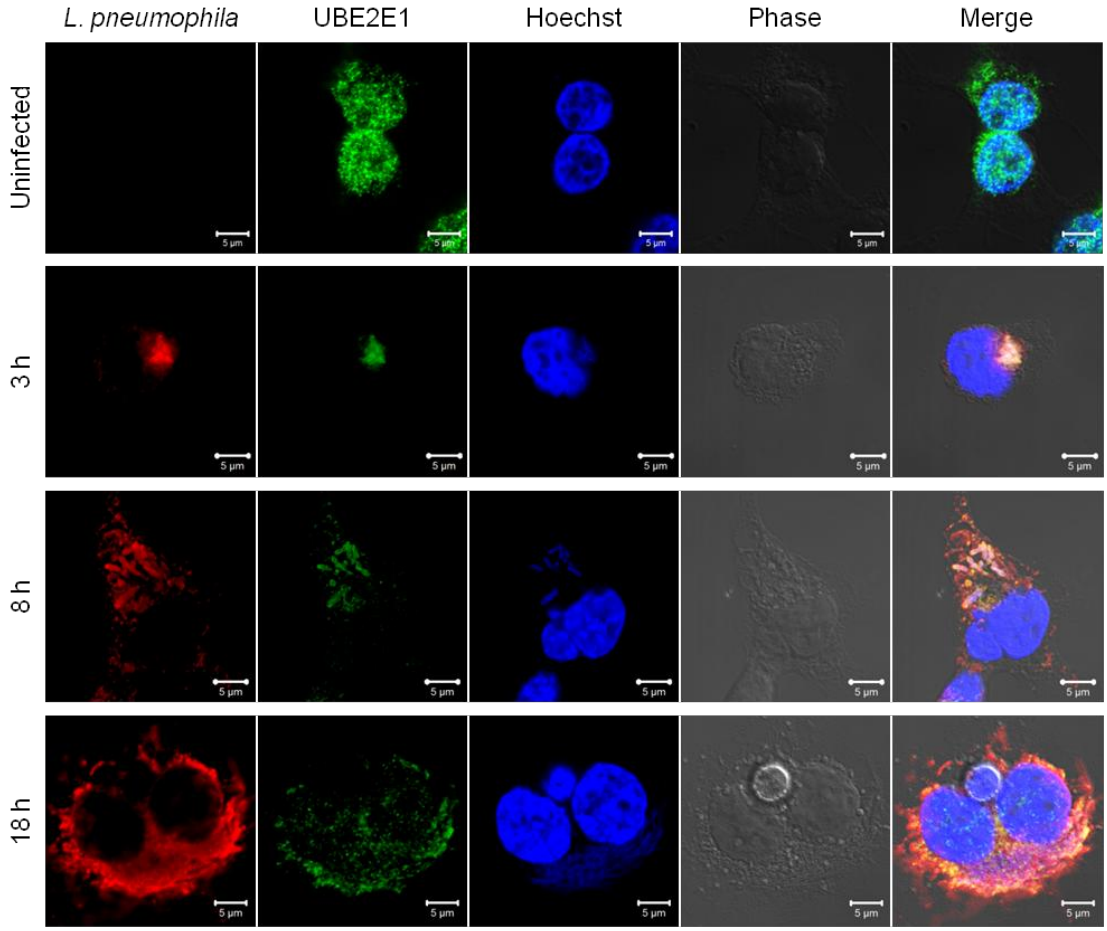

Figure 5.8 Association of endogenous UBE2E1 with *L. pneumophila* during infection

Representative immunofluorescence fields showing HekFcγR-expressing cells infected with *L. pneumophila* 130b for 3 h, 8 h or 18 h. Cells were stained with anti-UBE2E1 for localisation of endogenous UBE2E1 protein and Hoechst for cell nuclei. *L. pneumophila* was visualised using anti-*L. pneumophila* antibody.

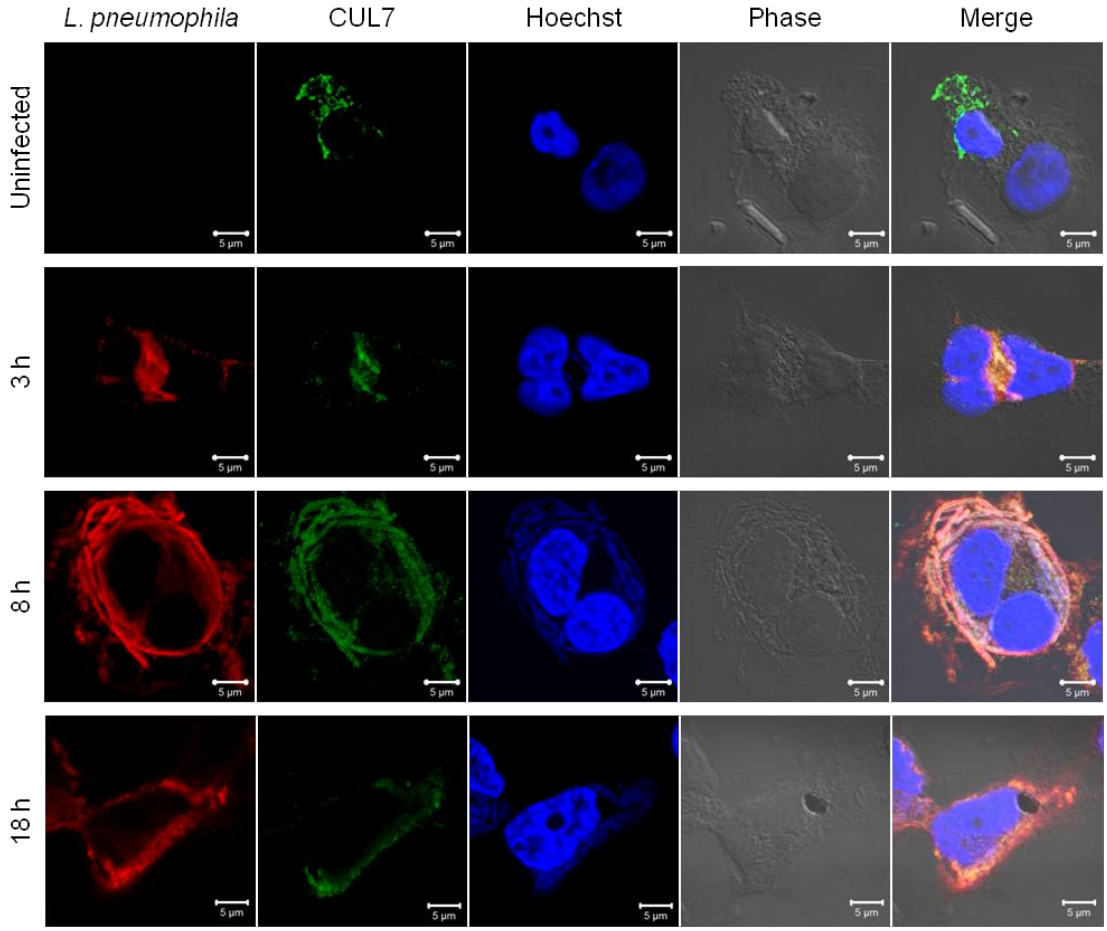

Figure 5.9 Association of endogenous CUL7 with *L. pneumophila* during infection

Representative immunofluorescence fields showing HekFcγR-expressing cells infected with *L. pneumophila* 130b for 3 h, 8 h or 18 h. Cells were stained with anti-CUL7 for localisation of endogenous CUL7 protein and Hoechst for cell nuclei. *L. pneumophila* was visualised using anti-*L. pneumophila* antibody.

CHAPTER 6: Perspective

Legionnaires' disease is a substantially underdiagnosed and under-reported infection caused by *Legionella* spp. Even with an estimated 200% increase in reported Legionnaires' cases in the USA from 2000 – 2009, it is still believed to be < 5% of actual cases (434, 435). The exact incidence worldwide is vague due to different awareness programs, reporting standards and diagnostic methods for each country (435). Accurate diagnosis is also often compounded by the strikingly similar clinical manifestations of Legionnaires' disease to other forms of pneumonia (436, 437). Moreover, most individuals are able to either self-resolve or effectively recover from *Legionella* infection without too many complications or medical attention. Hence, these cases are neither clinically diagnosed nor reported. However, in a small number of infected individuals, especially those who are immunocompromised, clinical symptoms can disseminate to outside of the lungs, resulting in fatality (438). For some Legionnaires' survivors, recovery can be slow with neurological complications and even chronic fatigue and posttraumatic stress disorder (439). While it is clearly difficult to pinpoint the true economic and health burdens of Legionnaires' disease worldwide, it is undoubtedly a bigger threat than currently recognised. Indeed Legionnaires' disease is considered to be the second highest disease burden for acute respiratory diseases, coming just behind influenza in the Netherlands (440).

To successfully replicate in eukaryotic cells, *L. pneumophila* has evolved mechanisms to manipulate host cell processes during infection. Manipulating host cell biology for survival and virulence is commonly observed in pathogenic bacteria; many of which do this through the actions of secreted toxins, such as *V. cholerae* and *Bordetella pertussis*, or translocated effector proteins (441). Unlike toxins which undergo series of trafficking events before gaining access to the host cell cytosol to exert their functions, effector proteins are typically delivered directly into cytosol of the host cells via dedicated bacterial protein secretion systems (441). During *L. pneumophila* infection, the Dot/Icm system translocates > 300 bacterial effector proteins into host cells. Many of these effector proteins play important roles in facilitating *L. pneumophila* pathogenesis, such as remodeling the host cell environment to create an intracellular replicative vacuole. Analysis of these effector proteins found an unusually high number of eukaryotic-like proteins, leading to speculation that they were acquired through horizontal gene transfer and recombination events as

L. pneumophila co-evolved with environmental protozoa (379, 442). In particular, the Dot/Icm system is a pivotal virulence factor of *L. pneumophila* that appears to be highly regulated as it is only 'turned on' in the event that the bacteria interact with a eukaryotic host. What regulates effector secretion is still yet to be elucidated. However, given that many aspects of *L. pneumophila* infection involve host factors such as bacterial entry into host cells, intracellular replication and eventual egress; we expected that host factors also play a role in regulating the function of the Dot/Icm system.

To test this idea, we established and performed a genome-wide siRNA screen to identify host factors that influenced Dot/Icm effector translocation. Since the discovery that RNAi can be artificially induced in cell lines or whole organisms using reagents such as siRNA or shRNA, researchers have exploited this technique to study host-pathogen interactions (334). Here, we used siRNA to individually silence each gene in the human genome before infection with a *L. pneumophila* strain that harbours the Dot/Icm effector, RalF, fused to a TEM-1 β-lactamase reporter, enabling us to measure the levels of blue fluorescence emitted when CCF2-AM is cleaved by TEM-1 β-lactamase. This serves as a quantitative indicator of RalF translocation into host cells during infection. Results from our genome-wide screen in HeLa cells confirmed that host factors indeed influenced the translocation of Dot/Icm effector proteins. Interestingly, host factors were identified that both enhanced and inhibited effector protein translocation. In this study, we focused solely on host factors that facilitated effector protein translocation. In particular, we found a significant over-representation of genes functioning in the eukaryotic ubiquitination system. Using siRNA to transiently knock-down the expression of genes encoding five E2-conjugating enzymes and 10 E3 ligases, we observed up to 30% reduction in translocation of the effector proteins RalF and SidB. While it remains to be proven, we hypothesise that Ub assists in the translocation of effectors across the ER-like membrane of the LCV.

The eukaryotic ubiquitination system is an extremely complex network and is involved in almost all aspects of cellular biology. Our findings suggested that the host ubiquitination system is a process and/or ubiquitin itself is possibly exploited by *L. pneumophila* for effector protein translocation. This corroborates and supplements previous findings that found *L. pneumophila* utilised the host ubiquitination system for intracellular survival and replication. Indeed many Dot/Icm effectors play a role in

ubiquitination as E3 ligases. Kubori *et al*. first described LubX as an effector protein that functions as an E3 ligase, spatially regulating the expression of another effector protein, SidH. More recently, the N-terminus of LubX was found to also activate several host E2-conjugating enzymes, such as UBE2W, UBEL6 and all members within the UBE2E and UBE2D families. Qiu *et al*. showed that *L. pneumophila* effector protein, SdeA, is a mono-ADP-ribosyltransferase that activates ubiquitin via ADP-ribosylation and subsequently ubiquitinates multiple Rab proteins associated with the ER (443). Astonishingly, SdeA achieved this without the requirement of E1-activating or E2-conjugating enzymes (443). More recently, Kotewicz *et. al*. found that *L. pneumophila* Sde proteins mediate ubiquitination of the host tubular ER protein, reticulon 4 (Rtn4), resulting in tubular rearrangements to initiate bacterial intracellular replication (444). In addition to being an ADP-ribosyltransferase, Sde proteins also possess nucleotidase/phosphohydrolase activity, thus allowing either the ubiquitination of Rtn4 or phosphoribosylation of Ub if a target protein is not available (444). This non-canonical ubiquitination mechanism which is independent of the host ubiquitination machinery is a novel finding. It highlights the extensive ability of *L. pneumophila* to modulate and hijack ubiquitination to remodel the host cell. It is also possible that Dot/Icm effector E3 ligases, similar to host E3 ligases, assist effector translocation for optimal remodelling of the LCV.

Modulating the host ubiquitination system via the actions of effector proteins is not exclusive to *L. pneumophila* and is in fact also seen in bacterial pathogens that utilise other secretion systems (257). During infection, the SopA effector protein of *S*. Typhimurium is ubiquitinated by the host factor, HsRMA, a process necessary for the bacteria to successfully escape the vacuole and disseminate during infection (445). SopA itself was characterised as a HECT-type E3 ligase (271). Interestingly, its E3 ligase activity appeared to not be involved in bacterial escape from the vacuole, but was important for neutrophil migration during infection (271). IpaH effectors of *S. flexneri* were the first characterised bacterial E3 ligases that appeared to modulate host inflammatory pathways during infection (446). For instance, IpaH9.8 degrades NEMO (NF-κB essential modulator), dampening NF-κB inflammatory response, thereby promoting bacterial replication compared to *Shigella* expressing catalytically inactive IpaH9.8 (447). Another member of the IpaH family of E3 ligases, IpaH7.8 is involved in bacterial escape from the endocytic vacuoles of macrophages, allowing

bacterial replication (446, 448). Suzuki *et al*. later found that IpaH7.8 targets glomulin, an inflammasome inhibitor, for degradation (449). This activates the inflammasome, promoting macrophage cell death and eventually facilitating bacterial dissemination (449). Lastly, almost all members of the family of NleG effectors found in pathogenic strains of enteropathogenic *E*. *coli* (EPEC) and enterohemorrhagic *E*. *coli* (EHEC) possess a conserved motif similar to eukaryotic RING/U-box domain that confers E3 ligase activity (446, 450-452). Indeed, NleG2-3, NleG5-1, NleG6-2 and NleG9 were experimentally shown to have E3 ligase activity *in vitro* (451). Even though the exact mechanism in which NleG effectors modulate host cellular environment is yet to be elucidated, it is suggested that they mimic host ubiquitination to increase pathogenicity (446). The multiple functions of effector E3 ligases highlights that the interplay between bacterial pathogens and the host ubiquitination system is highly complex and there is still much to learn.

C. *burnetii* is a gram-negative obligate intracellular bacterium that is phylogenetically related to *L*. *pneumophila* (453). *C*. *burnetii* causes Q-fever, which like Legionnaires' disease, is typically also transmitted via inhalation of contaminated aerosols (453). *C*. *burnetii* is considered one of the most infectious organisms known as it has an extremely low infectious dose (as low as one organism is required), and thus humans are highly susceptible (454). Like *L*. *pneumophila*, *C*. *burnetii* also possesses a Dot/Icm secretion system, which is vital for intracellular replication of the bacteria (455). Functionally, it is analogous to the Dot/Icm system found in *L*. *pneumophila* (456), and translocates around 130 different bacterial effector proteins into host cells during infection (457). Newton *et al*. observed that these effector proteins are first detected in the cytoplasm of HeLa cells only after 16 h infection with *C*. *burnetii* once the bacteria are in a lysosomal environment (458). This delay in effector protein translocation is in stark contrast to *L*. *pneumophila* where robust levels of effector translocation occur within 1 h of infection. These differences in activation of Dot/Icm effector translocation again suggest that the function of the Dot/Icm system is highly regulated.

To identify host factors that are important for Dot/Icm mediated effector protein translocation in *C*. *burnetii*, a similar genome-wide RNAi screen was recently performed in HeLa cells whereby translocation levels of the effector protein CBU0077 were evaluated (Newton *et*. *al*. personal communication). Interestingly, a

very different set of genes were identified. In particular, lysosomal proteins were found to contribute significantly to effector protein translocation in *C. burnetii*. Silencing the expression of host genes involved in maintenance of lysosomes, such as the lysosomal ATPase that generates and regulates the pH of lysosome, resulted in at least 25% reduction in CBU0077 translocation (459). In addition, reduction in CBU0077 translocation was also seen when the expression of enzymes found in lysosomes, such as cathepsin proteases was silenced with siRNA (Newton *et. al*. personal communication). Not detecting lysosomal proteins in our study was perhaps an expected result as *L. pneumophila* actively avoids the lysosomal endocytic pathway during establishment of the LCV. In contrast, the *Coxiella* containing vacuole (CCV) first fuses with autophagosomes and then lysosomes to form the mature CCV where the bacteria replicate (324). The findings of this screen suggested that host ubiquitination appeared to not be involved in effector protein translocation by *C. burnetii*. These studies also suggest that Dot/Icm effector translocation is indeed regulated by various host factors that reflect the biogenesis of each replicative vacuole.

Comparing the *L. pneumophila* and *C. burnetii* screens also proved that RNAi screen coupled with the TEM-1 β-lactamase effector reporter assay was a powerful way to identify host factors that contribute to the function of the Dot/Icm system. Prior to the development of this fluorescence-based TEM-1 β-lactamase reporter assay, a Cya-based cAMP assay was frequently used to quantify effector protein translocation during *L. pneumophila* infection (113). While sensitive, the Cya-based assay is impractical for use in a high-throughput methodology as it is time-consuming and involves multiple processing steps to extract the intracellular cAMP for quantification via ELISA (419). Comparatively, the fluorescence readout assay was rapid, reliable and sensitive, and hence suitable for high-throughput screening. Nevertheless, we still cannot discount possible weaknesses of an RNAi approach such as missing targets due to false negatives and RNAi induced cell death. As such, newer genome editing tools such as CRISPR/Cas9 could be considered for future functional genomics screens. Compared to RNAi, not only is CRISPR/Cas9 reported to be less prone to off-target effects, it also creates a knock-out instead of a knock-down of gene expression (460, 461). Hence, using CRISPR/Cas9 to create a knock-out cell line of a specific gene of interest can be useful for studying phenotypes that were previously limited by the duration of gene expression knock-down, such as longer bacterial

replication assays. This new technology may uncover novel host targets that regulate bacterial infection at various stages.

In recent times, more emphasis has been placed on studying how specific host cell factors influence *L. pneumophila* infection. Despite being able to replicate within alveolar macrophages, *L. pneumophila* does not replicate in other immune cell types (224). For example, during *L. pneumophila* lung infection, monocyte-derived cells are bactericidal in a IFNγ-dependent manner (224). However, IFNγ did not appear to dictate how alveolar macrophages respond to *L. pneumophila* infection *in vivo* (224). Hence, a host factor can restrict *L. pneumophila* infection in one cell type but not in another. It will be interesting to investigate the host factors identified from our study in other cell types, such as macrophages and amoebae. This might provide better insight into the relationship between specific host factors and the virulence of *L. pneumophila*.

In summary, given that the Dot/Icm system only translocates effector proteins when *L. pneumophila* is cultured in the presence of a host cell, understanding how recognition of this environment occurs will add valuable knowledge to the complex interactions between *L. pneumophila* and eukaryotic cells. In addition, as Dot/Icm effector proteins contribute to the pathogenesis of *L. pneumophila* infections, understanding the molecular mechanism of effector translocation may contribute to the development of new drug interventions during human infection and/or the control of *L. pneumophila* in environmental amoebae.

REFERENCES

1. **Fraser DW, Tsai TR, Orenstein W, Parkin WE, Beecham HJ, Sharrar RG, Harris J, Mallison GF, Martin SM, McDade JE, Shepard CC, Brachman PS.** 1977. Legionnaires' disease: description of an epidemic of pneumonia. N Engl J Med **297:**1189-1197.
2. **McDade JE, Shepard CC, Fraser DW, Tsai TR, Redus MA, Dowdle WR.** 1977. Legionnaires' disease: isolation of a bacterium and demonstration of its role in other respiratory disease. N Engl J Med **297:**1197-1203.
3. **Brenner DJ, Steigerwalt AG, McDade JE.** 1979. Classification of the Legionnaires' disease bacterium: *Legionella pneumophila*, genus novum, species nova, of the family Legionellaceae, familia nova. Ann Intern Med **90:**656-658.
4. **Thacker SB, Bennett JV, Tsai TF, Fraser DW, McDade JE, Shepard CC, Williams KH, Jr., Stuart WH, Dull HB, Eickhoff TC.** 1978. An outbreak in 1965 of severe respiratory illness caused by the Legionnaires' disease bacterium. J Infect Dis **138:**512-519.
5. **Glick TH, Gregg MB, Berman B, Mallison G, Rhodes WW, Jr., Kassanoff I.** 1978. Pontiac fever. An epidemic of unknown etiology in a health department: I. Clinical and epidemiologic aspects. Am J Epidemiol **107:**149-160.
6. **Feeley JC, Gibson RJ, Gorman GW, Langford NC, Rasheed JK, Mackel DC, Baine WB.** 1979. Charcoal-yeast extract agar: primary isolation medium for *Legionella pneumophila*. J Clin Microbiol **10:**437-441.
7. **McDade JE, Shepard CC.** 1979. Virulent to avirulent conversion of Legionnaires' disease bacterium (*Legionella pneumophila*)--its effect on isolation techniques. J Infect Dis **139:**707-711.
8. **Fry NK, Warwick S, Saunders NA, Embley TM.** 1991. The use of 16S ribosomal RNA analyses to investigate the phylogeny of the family Legionellaceae. J Gen Microbiol **137:**1215-1222.
9. **Weisburg WG, Dobson ME, Samuel JE, Dasch GA, Mallavia LP, Baca O, Mandelco L, Sechrest JE, Weiss E, Woese CR.** 1989. Phylogenetic diversity of the Rickettsiae. J Bacteriol **171:**4202-4206.
10. **Gomez-Valero L, Rusniok C, Rolando M, Neou M, Dervins-Ravault D, Demirtas J, Rouy Z, Moore RJ, Chen H, Petty NK, Jarraud S, Etienne J, Steinert M, Heuner K, Gribaldo S, Medigue C, Glockner G, Hartland EL, Buchrieser C.** 2014. Comparative analyses of *Legionella* species identifies genetic features of strains causing Legionnaires' disease. Genome Biol **15:**505.
11. **Yang G, Benson RF, Ratcliff RM, Brown EW, Steigerwalt AG, Thacker WL, Daneshvar MI, Morey RE, Saito A, Fields BS.** 2012. *Legionella nagasakiensis* sp. nov., isolated from water samples and from a patient with pneumonia. Int J Syst Evol Microbiol **62:**284-288.
12. **Neblett TR, Riddle JM, Dumoff M.** 1979. Surface topography and fine structure of the Legionnaires' disease bacterium. A study of six isolates from hospitalized patients. Ann Intern Med **90:**648-651.
13. **Chandler FW, Cole RM, Hicklin MD, Blackmon JA, Callaway CS.** 1979. Ultrastructure of the Legionnaires' disease bacterium. A study using transmission electron microscopy. Ann Intern Med **90:**642-647.
14. **Rodgers FG, Greaves PW, Macrae AD, Lewis MJ.** 1980. Electron microscopic evidence of flagella and pili on *Legionella pneumophila*. J Clin Pathol **33:**1184-1188.
15. **Thomason BM, Chandler FW, Hollis DG.** 1979. Flagella on Legionnaires' disease bacteria: an interim report. Ann Intern Med **91:**224-226.
16. **Fields BS, Benson RF, Besser RE.** 2002. *Legionella* and Legionnaires' disease: 25 years of investigation. Clin Microbiol Rev **15:**506-526.

17. **Yu VL, Plouffe JF, Pastoris MC, Stout JE, Schousboe M, Widmer A, Summersgill J, File T, Heath CM, Paterson DL, Chereshsky A.** 2002. Distribution of *Legionella* species and serogroups isolated by culture in patients with sporadic community-acquired legionellosis: an international collaborative survey. J Infect Dis **186:**127-128.
18. **Lanser JA, Adams M, Doyle R, Sangster N, Steele TW.** 1990. Genetic relatedness of *Legionella longbeachae* isolates from human and environmental sources in Australia. Appl Environ Microbiol **56:**2784-2790.
19. **Cameron S, Roder D, Walker C, Feldheim J.** 1991. Epidemiological characteristics of *Legionella* infection in South Australia: implications for disease control. Aust N Z J Med **21:**65-70.
20. **Howden BP, Stuart RL, Tallis G, Bailey M, Johnson PD.** 2003. Treatment and outcome of 104 hospitalized patients with legionnaires' disease. Intern Med J **33:**484-488.
21. **Marston BJ, Lipman HB, Breiman RF.** 1994. Surveillance for Legionnaires' disease. Risk factors for morbidity and mortality. Arch Intern Med **154:**2417-2422.
22. **Shachor-Meyouhas Y, Kassis I, Bamberger E, Nativ T, Sprecher H, Levy I, Srugo I.** 2010. Fatal hospital-acquired *Legionella pneumonia* in a neonate. Pediatr Infect Dis J **29:**280-281.
23. **Yu VL, Lee TC.** 2010. Neonatal legionellosis: the tip of the iceberg for pediatric hospital-acquired pneumonia? Pediatr Infect Dis J **29:**282-284.
24. **Sopena N, Sabria-Leal M, Pedro-Botet ML, Padilla E, Dominguez J, Morera J, Tudela P.** 1998. Comparative study of the clinical presentation of *Legionella pneumonia* and other community-acquired pneumonias. Chest **113:**1195-1200.
25. **Cunha BA.** 2006. Hypophosphatemia: diagnostic significance in Legionnaires' disease. Am J Med **119:**e5-6.
26. **Swanson MS, Hammer BK.** 2000. *Legionella pneumophila* pathogesesis: a fateful journey from amoebae to macrophages. Annu Rev Microbiol **54:**567-613.
27. **Tossa P, Deloge-Abarkan M, Zmirou-Navier D, Hartemann P, Mathieu L.** 2006. Pontiac fever: an operational definition for epidemiological studies. BMC Public Health **6:**112.
28. **Luttichau HR, Vinther C, Uldum SA, Moller J, Faber M, Jensen JS.** 1998. An outbreak of Pontiac fever among children following use of a whirlpool. Clin Infect Dis **26:**1374-1378.
29. **Girod JC, Reichman RC, Winn WC, Jr., Klaucke DN, Vogt RL, Dolin R.** 1982. Pneumonic and nonpneumonic forms of legionellosis. The result of a common-source exposure to *Legionella pneumophila*. Arch Intern Med **142:**545-547.
30. **Benin AL, Benson RF, Arnold KE, Fiore AE, Cook PG, Williams LK, Fields B, Besser RE.** 2002. An outbreak of travel-associated Legionnaires disease and Pontiac fever: the need for enhanced surveillance of travel-associated legionellosis in the United States. J Infect Dis **185:**237-243.
31. **Thomas DL, Mundy LM, Tucker PC.** 1993. Hot tub legionellosis. Legionnaires' disease and Pontiac fever after a point-source exposure to *Legionella pneumophila*. Arch Intern Med **153:**2597-2599.
32. **Murdoch DR.** 2003. Diagnosis of *Legionella* infection. Clin Infect Dis **36:**64-69.
33. **Wever PC, Yzerman EP, Kuijper EJ, Speelman P, Dankert J.** 2000. Rapid diagnosis of Legionnaires' disease using an immunochromatographic assay for *Legionella pneumophila* serogroup 1 antigen in urine during an outbreak in the Netherlands. J Clin Microbiol **38:**2738-2739.
34. **Kashuba AD, Ballow CH.** 1996. *Legionella* urinary antigen testing: potential impact on diagnosis and antibiotic therapy. Diagn Microbiol Infect Dis **24:**129-139.

35. **Laussucq S, Schuster D, Alexander WJ, Thacker WL, Wilkinson HW, Spika JS.** 1988. False-positive DNA probe test for *Legionella* species associated with a cluster of respiratory illnesses. J Clin Microbiol **26:**1442-1444.
36. **Yang G, Benson R, Pelish T, Brown E, Winchell JM, Fields B.** 2010. Dual detection of *Legionella pneumophila* and *Legionella* species by real-time PCR targeting the 23S-5S rRNA gene spacer region. Clin Microbiol Infect **16:**255-261.
37. **Dedicoat M, Venkatesan P.** 1999. The treatment of Legionnaires' disease. J Antimicrob Chemother **43:**747-752.
38. **Pedro-Botet L, Yu VL.** 2006. *Legionella*: macrolides or quinolones? Clin Microbiol Infect **12 Suppl 3:**25-30.
39. **Sabria M, Pedro-Botet ML, Gomez J, Roig J, Vilaseca B, Sopena N, Banos V, Legionnaires Disease Therapy G.** 2005. Fluoroquinolones vs macrolides in the treatment of Legionnaires disease. Chest **128:**1401-1405.
40. **Blazquez Garrido RM, Espinosa Parra FJ, Alemany Frances L, Ramos Guevara RM, Sanchez-Nieto JM, Segovia Hernandez M, Serrano Martinez JA, Huerta FH.** 2005. Antimicrobial chemotherapy for Legionnaires disease: levofloxacin versus macrolides. Clin Infect Dis **40:**800-806.
41. **Griffin AT, Peyrani P, Wiemken T, Arnold F.** 2010. Macrolides versus quinolones in *Legionella pneumonia*: results from the Community-Acquired Pneumonia Organization international study. Int J Tuberc Lung Dis **14:**495-499.
42. **Yu VL, Greenberg RN, Zadeikis N, Stout JE, Khashab MM, Olson WH, Tennenberg AM.** 2004. Levofloxacin efficacy in the treatment of community-acquired legionellosis. Chest **125:**2135-2139.
43. **Stout JE, Yu VL.** 1997. Legionellosis. N Engl J Med **337:**682-687.
44. **Atlas RM.** 1999. *Legionella*: from environmental habitats to disease pathology, detection and control. Environ Microbiol **1:**283-293.
45. **Steele TW, Moore CV, Sangster N.** 1990. Distribution of *Legionella longbeachae* serogroup 1 and other legionellae in potting soils in Australia. Appl Environ Microbiol **56:**2984-2988.
46. **Fliermans CB, Cherry WB, Orrison LH, Smith SJ, Tison DL, Pope DH.** 1981. Ecological distribution of *Legionella pneumophila*. Appl Environ Microbiol **41:**9-16.
47. **Atlas RM, Williams JF, Huntington MK.** 1995. *Legionella* contamination of dental-unit waters. Appl Environ Microbiol **61:**1208-1213.
48. **Benkel DH, McClure EM, Woolard D, Rullan JV, Miller GB, Jr., Jenkins SR, Hershey JH, Benson RF, Pruckler JM, Brown EW, Kolczak MS, Hackler RL, Rouse BS, Breiman RF.** 2000. Outbreak of Legionnaires' disease associated with a display whirlpool spa. Int J Epidemiol **29:**1092-1098.
49. **Delia S, Lagana P, Minutoli E.** 2007. Occurrence of *Legionella* in beach shower facilities. J Prev Med Hyg **48:**114-117.
50. **Palmore TN, Stock F, White M, Bordner M, Michelin A, Bennett JE, Murray PR, Henderson DK.** 2009. A cluster of cases of nosocomial legionnaires disease linked to a contaminated hospital decorative water fountain. Infect Control Hosp Epidemiol **30:**764-768.
51. **Hanrahan JP, Morse DL, Scharf VB, Debbie JG, Schmid GP, McKinney RM, Shayegani M.** 1987. A community hospital outbreak of legionellosis. Transmission by potable hot water. Am J Epidemiol **125:**639-649.
52. **Hughes MS, Steele TW.** 1994. Occurrence and distribution of *Legionella* species in composted plant materials. Appl Environ Microbiol **60:**2003-2005.
53. **Rowbotham TJ.** 1980. Preliminary report on the pathogenicity of *Legionella pneumophila* for freshwater and soil amoebae. J Clin Pathol **33:**1179-1183.

54. **Moffat JF, Tompkins LS.** 1992. A quantitative model of intracellular growth of *Legionella pneumophila* in *Acanthamoeba castellanii*. Infect Immun **60:**296-301.
55. **Newsome AL, Baker RL, Miller RD, Arnold RR.** 1985. Interactions between *Naegleria fowleri* and *Legionella pneumophila*. Infect Immun **50:**449-452.
56. **Wadowsky RM, Wilson TM, Kapp NJ, West AJ, Kuchta JM, States SJ, Dowling JN, Yee RB.** 1991. Multiplication of *Legionella* spp. in tap water containing *Hartmannella vermiformis*. Appl Environ Microbiol **57:**1950-1955.
57. **Tyndall RL, Domingue EL.** 1982. Cocultivation of *Legionella pneumophila* and free-living amoebae. Appl Environ Microbiol **44:**954-959.
58. **Kwaik YA.** 1998. Fatal attraction of mammalian cells to *Legionella pneumophila*. Mol Microbiol **30:**689-695.
59. **Harb OS, Gao LY, Abu Kwaik Y.** 2000. From protozoa to mammalian cells: a new paradigm in the life cycle of intracellular bacterial pathogens. Environ Microbiol **2:**251-265.
60. **Segal G, Shuman HA.** 1999. *Legionella pneumophila* utilizes the same genes to multiply within *Acanthamoeba castellanii* and human macrophages. Infect Immun **67:**2117-2124.
61. **Miyake M, Watanabe T, Koike H, Molmeret M, Imai Y, Abu Kwaik Y.** 2005. Characterization of *Legionella pneumophila* pmiA, a gene essential for infectivity of protozoa and macrophages. Infect Immun **73:**6272-6282.
62. **Gao LY, Harb OS, Abu Kwaik Y.** 1997. Utilization of similar mechanisms by *Legionella pneumophila* to parasitize two evolutionarily distant host cells, mammalian macrophages and protozoa. Infect Immun **65:**4738-4746.
63. **Brieland JK, Fantone JC, Remick DG, LeGendre M, McClain M, Engleberg NC.** 1997. The role of *Legionella pneumophila*-infected *Hartmannella vermiformis* as an infectious particle in a murine model of Legionnaire's disease. Infect Immun **65:**5330-5333.
64. **Barker J, Brown MR.** 1995. Speculations on the influence of infecting phenotype on virulence and antibiotic susceptibility of *Legionella pneumophila*. J Antimicrob Chemother **36:**7-21.
65. **Mashiba K, Hamamoto T, Torikai K.** 1993. [A case of Legionnaires' disease due to aspiration of hot spring water and isolation of *Legionella pneumophila* from hot spring water]. Kansenshogaku Zasshi **67:**163-166.
66. **Bentham RH, Broadbent CR.** 1993. A model for autumn outbreaks of Legionnaires' disease associated with cooling towers, linked to system operation and size. Epidemiol Infect **111:**287-295.
67. **Mermel LA, Josephson SL, Giorgio CH, Dempsey J, Parenteau S.** 1995. Association of Legionnaires' disease with construction: contamination of potable water? Infect Control Hosp Epidemiol **16:**76-81.
68. **States SJ, Conley LF, Ceraso M, Stephenson TE, Wolford RS, Wadowsky RM, McNamara AM, Yee RB.** 1985. Effects of metals on *Legionella pneumophila* growth in drinking water plumbing systems. Appl Environ Microbiol **50:**1149-1154.
69. **Rogers J, Dowsett AB, Dennis PJ, Lee JV, Keevil CW.** 1994. Influence of temperature and plumbing material selection on biofilm formation and growth of *Legionella pneumophila* in a model potable water system containing complex microbial flora. Appl Environ Microbiol **60:**1585-1592.
70. **Smith AJ, Hood J, Bagg J, Burke FT.** 1999. Water, water everywhere but not a drop to drink? Br Dent J **186:**12-14.
71. **Temmerman R, Vervaeren H, Noseda B, Boon N, Verstraete W.** 2006. Necrotrophic growth of *Legionella pneumophila*. Appl Environ Microbiol **72:**4323-4328.

72. **Berk SG, Ting RS, Turner GW, Ashburn RJ.** 1998. Production of respirable vesicles containing live *Legionella pneumophila* cells by two *Acanthamoeba* spp. Appl Environ Microbiol **64:**279-286.
73. **Bruggemann H, Hagman A, Jules M, Sismeiro O, Dillies MA, Gouyette C, Kunst F, Steinert M, Heuner K, Coppee JY, Buchrieser C.** 2006. Virulence strategies for infecting phagocytes deduced from the in vivo transcriptional program of *Legionella pneumophila*. Cell Microbiol **8:**1228-1240.
74. **Byrne B, Swanson MS.** 1998. Expression of *Legionella pneumophila* virulence traits in response to growth conditions. Infect Immun **66:**3029-3034.
75. **Molofsky AB, Swanson MS.** 2004. Differentiate to thrive: lessons from the *Legionella pneumophila* life cycle. Mol Microbiol **53:**29-40.
76. **Hammer BK, Swanson MS.** 1999. Co-ordination of *Legionella pneumophila* virulence with entry into stationary phase by ppGpp. Mol Microbiol **33:**721-731.
77. **Molofsky AB, Swanson MS.** 2003. *Legionella pneumophila* CsrA is a pivotal repressor of transmission traits and activator of replication. Mol Microbiol **50:**445-461.
78. **Horwitz MA.** 1984. Phagocytosis of the Legionnaires' disease bacterium (*Legionella pneumophila*) occurs by a novel mechanism: engulfment within a pseudopod coil. Cell **36:**27-33.
79. **Bozue JA, Johnson W.** 1996. Interaction of *Legionella pneumophila* with *Acanthamoeba castellanii*: uptake by coiling phagocytosis and inhibition of phagosome-lysosome fusion. Infect Immun **64:**668-673.
80. **Payne NR, Horwitz MA.** 1987. Phagocytosis of *Legionella pneumophila* is mediated by human monocyte complement receptors. J Exp Med **166:**1377-1389.
81. **Reynolds HY, Newball HH.** 1974. Analysis of proteins and respiratory cells obtained from human lungs by bronchial lavage. J Lab Clin Med **84:**559-573.
82. **Khelef N, Shuman HA, Maxfield FR.** 2001. Phagocytosis of wild-type *Legionella pneumophila* occurs through a wortmannin-insensitive pathway. Infect Immun **69:**5157-5161.
83. **Weber SS, Ragaz C, Reus K, Nyfeler Y, Hilbi H.** 2006. *Legionella pneumophila* exploits PI(4)P to anchor secreted effector proteins to the replicative vacuole. PLoS Pathog **2:**e46.
84. **Tachado SD, Samrakandi MM, Cirillo JD.** 2008. Non-opsonic phagocytosis of *Legionella pneumophila* by macrophages is mediated by phosphatidylinositol 3-kinase. PLoS One **3:**e3324.
85. **Cirillo SL, Bermudez LE, El-Etr SH, Duhamel GE, Cirillo JD.** 2001. *Legionella pneumophila* entry gene rtxA is involved in virulence. Infect Immun **69:**508-517.
86. **Cirillo SL, Lum J, Cirillo JD.** 2000. Identification of novel loci involved in entry by *Legionella pneumophila*. Microbiology **146 (Pt 6):**1345-1359.
87. **Ridenour DA, Cirillo SL, Feng S, Samrakandi MM, Cirillo JD.** 2003. Identification of a gene that affects the efficiency of host cell infection by *Legionella pneumophila* in a temperature-dependent fashion. Infect Immun **71:**6256-6263.
88. **Isberg RR, O'Connor TJ, Heidtman M.** 2009. The *Legionella pneumophila* replication vacuole: making a cosy niche inside host cells. Nat Rev Microbiol **7:**13-24.
89. **Horwitz MA.** 1983. The Legionnaires' disease bacterium (*Legionella pneumophila*) inhibits phagosome-lysosome fusion in human monocytes. J Exp Med **158:**2108-2126.
90. **Horwitz MA, Maxfield FR.** 1984. *Legionella pneumophila* inhibits acidification of its phagosome in human monocytes. J Cell Biol **99:**1936-1943.
91. **Horwitz MA.** 1983. Formation of a novel phagosome by the Legionnaires' disease bacterium (*Legionella pneumophila*) in human monocytes. J Exp Med **158:**1319-1331.

92. **Swanson MS, Isberg RR.** 1995. Association of *Legionella pneumophila* with the macrophage endoplasmic reticulum. Infect Immun **63:**3609-3620.
93. **Horwitz MA, Silverstein SC.** 1980. Legionnaires' disease bacterium (*Legionella pneumophila*) multiples intracellularly in human monocytes. J Clin Invest **66:**441-450.
94. **Ninio S, Roy CR.** 2007. Effector proteins translocated by *Legionella pneumophila*: strength in numbers. Trends Microbiol **15:**372-380.
95. **Hay JC.** 2001. SNARE complex structure and function. Exp Cell Res **271:**10-21.
96. **Seabra MC, Mules EH, Hume AN.** 2002. Rab GTPases, intracellular traffic and disease. Trends Mol Med **8:**23-30.
97. **Derre I, Isberg RR.** 2004. *Legionella pneumophila* replication vacuole formation involves rapid recruitment of proteins of the early secretory system. Infect Immun **72:**3048-3053.
98. **Kagan JC, Stein MP, Pypaert M, Roy CR.** 2004. *Legionella* subvert the functions of Rab1 and Sec22b to create a replicative organelle. J Exp Med **199:**1201-1211.
99. **Allan BB, Moyer BD, Balch WE.** 2000. Rab1 recruitment of p115 into a cis-SNARE complex: programming budding COPII vesicles for fusion. Science **289:**444-448.
100. **Moyer BD, Allan BB, Balch WE.** 2001. Rab1 interaction with a GM130 effector complex regulates COPII vesicle cis--Golgi tethering. Traffic **2:**268-276.
101. **Hay JC, Chao DS, Kuo CS, Scheller RH.** 1997. Protein interactions regulating vesicle transport between the endoplasmic reticulum and Golgi apparatus in mammalian cells. Cell **89:**149-158.
102. **Zhang T, Wong SH, Tang BL, Xu Y, Hong W.** 1999. Morphological and functional association of Sec22b/ERS-24 with the pre-Golgi intermediate compartment. Mol Biol Cell **10:**435-453.
103. **Machner MP, Isberg RR.** 2007. A bifunctional bacterial protein links GDI displacement to Rab1 activation. Science **318:**974-977.
104. **Murata T, Delprato A, Ingmundson A, Toomre DK, Lambright DG, Roy CR.** 2006. The *Legionella pneumophila* effector protein DrrA is a Rab1 guanine nucleotide-exchange factor. Nat Cell Biol **8:**971-977.
105. **Neunuebel MR, Chen Y, Gaspar AH, Backlund PS, Jr., Yergey A, Machner MP.** 2011. De-AMPylation of the small GTPase Rab1 by the pathogen *Legionella pneumophila*. Science **333:**453-456.
106. **Muller MP, Peters H, Blumer J, Blankenfeldt W, Goody RS, Itzen A.** 2010. The *Legionella* effector protein DrrA AMPylates the membrane traffic regulator Rab1b. Science **329:**946-949.
107. **Ingmundson A, Delprato A, Lambright DG, Roy CR.** 2007. *Legionella pneumophila* proteins that regulate Rab1 membrane cycling. Nature **450:**365-369.
108. **Tan Y, Luo ZQ.** 2011. *Legionella pneumophila* SidD is a deAMPylase that modifies Rab1. Nature **475:**506-509.
109. **Mukherjee S, Liu X, Arasaki K, McDonough J, Galan JE, Roy CR.** 2011. Modulation of Rab GTPase function by a protein phosphocholine transferase. Nature **477:**103-106.
110. **Tan Y, Arnold RJ, Luo ZQ.** 2011. *Legionella pneumophila* regulates the small GTPase Rab1 activity by reversible phosphorylcholination. Proc Natl Acad Sci U S A **108:**21212-21217.
111. **Dorer MS, Kirton D, Bader JS, Isberg RR.** 2006. RNA interference analysis of *Legionella* in *Drosophila* cells: exploitation of early secretory apparatus dynamics. PLoS Pathog **2:**e34.
112. **Gao LY, Kwaik YA.** 2000. The mechanism of killing and exiting the protozoan host *Acanthamoeba polyphaga* by *Legionella pneumophila*. Environ Microbiol **2:**79-90.

113. **Chen J, de Felipe KS, Clarke M, Lu H, Anderson OR, Segal G, Shuman HA.** 2004. *Legionella* effectors that promote nonlytic release from protozoa. Science **303:**1358-1361.
114. **Alli OA, Gao LY, Pedersen LL, Zink S, Radulic M, Doric M, Abu Kwaik Y.** 2000. Temporal pore formation-mediated egress from macrophages and alveolar epithelial cells by *Legionella pneumophila*. Infect Immun **68:**6431-6440.
115. **Kirby JE, Vogel JP, Andrews HL, Isberg RR.** 1998. Evidence for pore-forming ability by *Legionella pneumophila*. Mol Microbiol **27:**323-336.
116. **Finsel I, Hilbi H.** 2015. Formation of a pathogen vacuole according to *Legionella pneumophila*: how to kill one bird with many stones. Cell Microbiol **17:**935-950.
117. **Abu-Zant A, Santic M, Molmeret M, Jones S, Helbig J, Abu Kwaik Y.** 2005. Incomplete activation of macrophage apoptosis during intracellular replication of *Legionella pneumophila*. Infect Immun **73:**5339-5349.
118. **Molmeret M, Zink SD, Han L, Abu-Zant A, Asari R, Bitar DM, Abu Kwaik Y.** 2004. Activation of caspase-3 by the Dot/Icm virulence system is essential for arrested biogenesis of the *Legionella*-containing phagosome. Cell Microbiol **6:**33-48.
119. **Abu-Zant A, Jones S, Asare R, Suttles J, Price C, Graham J, Kwaik YA.** 2007. Anti-apoptotic signalling by the Dot/Icm secretion system of *L. pneumophila*. Cell Microbiol **9:**246-264.
120. **Ge J, Xu H, Li T, Zhou Y, Zhang Z, Li S, Liu L, Shao F.** 2009. A *Legionella* type IV effector activates the NF-kappaB pathway by phosphorylating the IkappaB family of inhibitors. Proc Natl Acad Sci U S A **106:**13725-13730.
121. **Banga S, Gao P, Shen X, Fiscus V, Zong WX, Chen L, Luo ZQ.** 2007. *Legionella pneumophila* inhibits macrophage apoptosis by targeting pro-death members of the Bcl2 protein family. Proc Natl Acad Sci U S A **104:**5121-5126.
122. **Hsu F, Zhu W, Brennan L, Tao L, Luo ZQ, Mao Y.** 2012. Structural basis for substrate recognition by a unique *Legionella* phosphoinositide phosphatase. Proc Natl Acad Sci U S A **109:**13567-13572.
123. **Cambronne ED, Roy CR.** 2006. Recognition and delivery of effector proteins into eukaryotic cells by bacterial secretion systems. Traffic **7:**929-939.
124. **Backert S, Meyer TF.** 2006. Type IV secretion systems and their effectors in bacterial pathogenesis. Curr Opin Microbiol **9:**207-217.
125. **Newton HJ, Ang DK, van Driel IR, Hartland EL.** 2010. Molecular pathogenesis of infections caused by *Legionella pneumophila*. Clin Microbiol Rev **23:**274-298.
126. **Hales LM, Shuman HA.** 1999. *Legionella pneumophila* contains a type II general secretion pathway required for growth in amoebae as well as for secretion of the Msp protease. Infect Immun **67:**3662-3666.
127. **Soderberg MA, Dao J, Starkenburg SR, Cianciotto NP.** 2008. Importance of type II secretion for survival of *Legionella pneumophila* in tap water and in amoebae at low temperatures. Appl Environ Microbiol **74:**5583-5588.
128. **Cianciotto NP.** 2005. Type II secretion: a protein secretion system for all seasons. Trends Microbiol **13:**581-588.
129. **Rossier O, Starkenburg SR, Cianciotto NP.** 2004. *Legionella pneumophila* type II protein secretion promotes virulence in the A/J mouse model of Legionnaires' disease pneumonia. Infect Immun **72:**310-321.
130. **Liles MR, Edelstein PH, Cianciotto NP.** 1999. The prepilin peptidase is required for protein secretion by and the virulence of the intracellular pathogen *Legionella pneumophila*. Mol Microbiol **31:**959-970.
131. **Polesky AH, Ross JT, Falkow S, Tompkins LS.** 2001. Identification of *Legionella pneumophila* genes important for infection of amoebas by signature-tagged mutagenesis. Infect Immun **69:**977-987.

132. **Rossier O, Cianciotto NP.** 2001. Type II protein secretion is a subset of the PilD-dependent processes that facilitate intracellular infection by *Legionella pneumophila*. Infect Immun **69:**2092-2098.
133. **Soderberg MA, Cianciotto NP.** 2008. A *Legionella pneumophila* peptidyl-prolyl cis-trans isomerase present in culture supernatants is necessary for optimal growth at low temperatures. Appl Environ Microbiol **74:**1634-1638.
134. **DebRoy S, Dao J, Soderberg M, Rossier O, Cianciotto NP.** 2006. *Legionella pneumophila* type II secretome reveals unique exoproteins and a chitinase that promotes bacterial persistence in the lung. Proc Natl Acad Sci U S A **103:**19146-19151.
135. **Rossier O, Dao J, Cianciotto NP.** 2009. A type II secreted RNase of *Legionella pneumophila* facilitates optimal intracellular infection of *Hartmannella vermiformis*. Microbiology **155:**882-890.
136. **Rossier O, Dao J, Cianciotto NP.** 2008. The type II secretion system of *Legionella pneumophila* elaborates two aminopeptidases, as well as a metalloprotease that contributes to differential infection among protozoan hosts. Appl Environ Microbiol **74:**753-761.
137. **Aragon V, Rossier O, Cianciotto NP.** 2002. *Legionella pneumophila* genes that encode lipase and phospholipase C activities. Microbiology **148:**2223-2231.
138. **Soderberg MA, Rossier O, Cianciotto NP.** 2004. The type II protein secretion system of *Legionella pneumophila* promotes growth at low temperatures. J Bacteriol **186:**3712-3720.
139. **Banerji S, Bewersdorff M, Hermes B, Cianciotto NP, Flieger A.** 2005. Characterization of the major secreted zinc metalloprotease- dependent glycerophospholipid:cholesterol acyltransferase, PlaC, of *Legionella pneumophila*. Infect Immun **73:**2899-2909.
140. **Flieger A, Neumeister B, Cianciotto NP.** 2002. Characterization of the gene encoding the major secreted lysophospholipase A of *Legionella pneumophila* and its role in detoxification of lysophosphatidylcholine. Infect Immun **70:**6094-6106.
141. **Matthews M, Roy CR.** 2000. Identification and subcellular localization of the *Legionella pneumophila* IcmX protein: a factor essential for establishment of a replicative organelle in eukaryotic host cells. Infect Immun **68:**3971-3982.
142. **De Buck E, Maes L, Meyen E, Van Mellaert L, Geukens N, Anne J, Lammertyn E.** 2005. *Legionella pneumophila* Philadelphia-1 tatB and tatC affect intracellular replication and biofilm formation. Biochem Biophys Res Commun **331:**1413-1420.
143. **de Felipe KS, Glover RT, Charpentier X, Anderson OR, Reyes M, Pericone CD, Shuman HA.** 2008. *Legionella* eukaryotic-like type IV substrates interfere with organelle trafficking. PLoS Pathog **4:**e1000117.
144. **Jacobi S, Heuner K.** 2003. Description of a putative type I secretion system in *Legionella pneumophila*. Int J Med Microbiol **293:**349-358.
145. **Lammertyn E, Anne J.** 2004. Protein secretion in *Legionella pneumophila* and its relation to virulence. FEMS Microbiol Lett **238:**273-279.
146. **Rossier O, Cianciotto NP.** 2005. The *Legionella pneumophila* tatB gene facilitates secretion of phospholipase C, growth under iron-limiting conditions, and intracellular infection. Infect Immun **73:**2020-2032.
147. **De Buck E, Lebeau I, Maes L, Geukens N, Meyen E, Van Mellaert L, Anne J, Lammertyn E.** 2004. A putative twin-arginine translocation pathway in *Legionella pneumophila*. Biochem Biophys Res Commun **317:**654-661.
148. **De Buck E, Hoper D, Lammertyn E, Hecker M, Anne J.** 2008. Differential 2-D protein gel electrophoresis analysis of *Legionella pneumophila* wild type and Tat secretion mutants. Int J Med Microbiol **298:**449-461.

149. **Alvarez-Martinez CE, Christie PJ.** 2009. Biological diversity of prokaryotic type IV secretion systems. Microbiol Mol Biol Rev **73:**775-808.
150. **Juhas M, Crook DW, Hood DW.** 2008. Type IV secretion systems: tools of bacterial horizontal gene transfer and virulence. Cell Microbiol **10:**2377-2386.
151. **Cazalet C, Rusniok C, Bruggemann H, Zidane N, Magnier A, Ma L, Tichit M, Jarraud S, Bouchier C, Vandenesch F, Kunst F, Etienne J, Glaser P, Buchrieser C.** 2004. Evidence in the *Legionella pneumophila* genome for exploitation of host cell functions and high genome plasticity. Nat Genet **36:**1165-1173.
152. **Bandyopadhyay P, Liu S, Gabbai CB, Venitelli Z, Steinman HM.** 2007. Environmental mimics and the Lvh type IVA secretion system contribute to virulence-related phenotypes of *Legionella pneumophila*. Infect Immun **75:**723-735.
153. **Hilbi H, Segal G, Shuman HA.** 2001. Icm/dot-dependent upregulation of phagocytosis by *Legionella pneumophila*. Mol Microbiol **42:**603-617.
154. **Berger KH, Merriam JJ, Isberg RR.** 1994. Altered intracellular targeting properties associated with mutations in the *Legionella pneumophila* dotA gene. Mol Microbiol **14:**809-822.
155. **Swanson MS, Isberg RR.** 1996. Identification of *Legionella pneumophila* mutants that have aberrant intracellular fates. Infect Immun **64:**2585-2594.
156. **Marra A, Blander SJ, Horwitz MA, Shuman HA.** 1992. Identification of a *Legionella pneumophila* locus required for intracellular multiplication in human macrophages. Proc Natl Acad Sci U S A **89:**9607-9611.
157. **Brand BC, Sadosky AB, Shuman HA.** 1994. The *Legionella pneumophila* icm locus: a set of genes required for intracellular multiplication in human macrophages. Mol Microbiol **14:**797-808.
158. **Berger KH, Isberg RR.** 1993. Two distinct defects in intracellular growth complemented by a single genetic locus in *Legionella pneumophila*. Mol Microbiol **7:**7-19.
159. **Segal G, Shuman HA.** 1997. Characterization of a new region required for macrophage killing by *Legionella pneumophila*. Infect Immun **65:**5057-5066.
160. **Vogel JP, Andrews HL, Wong SK, Isberg RR.** 1998. Conjugative transfer by the virulence system of *Legionella pneumophila*. Science **279:**873-876.
161. **Segal G, Purcell M, Shuman HA.** 1998. Host cell killing and bacterial conjugation require overlapping sets of genes within a 22-kb region of the *Legionella pneumophila* genome. Proc Natl Acad Sci U S A **95:**1669-1674.
162. **Purcell M, Shuman HA.** 1998. The *Legionella pneumophila* icmGCDJBF genes are required for killing of human macrophages. Infect Immun **66:**2245-2255.
163. **Andrews HL, Vogel JP, Isberg RR.** 1998. Identification of linked *Legionella pneumophila* genes essential for intracellular growth and evasion of the endocytic pathway. Infect Immun **66:**950-958.
164. **Sexton JA, Pinkner JS, Roth R, Heuser JE, Hultgren SJ, Vogel JP.** 2004. The *Legionella pneumophila* PilT homologue DotB exhibits ATPase activity that is critical for intracellular growth. J Bacteriol **186:**1658-1666.
165. **Sexton JA, Yeo HJ, Vogel JP.** 2005. Genetic analysis of the *Legionella pneumophila* DotB ATPase reveals a role in type IV secretion system protein export. Mol Microbiol **57:**70-84.
166. **Roy CR, Isberg RR.** 1997. Topology of *Legionella pneumophila* DotA: an inner membrane protein required for replication in macrophages. Infect Immun **65:**571-578.
167. **Nagai H, Roy CR.** 2001. The DotA protein from *Legionella pneumophila* is secreted by a novel process that requires the Dot/Icm transporter. EMBO J **20:**5962-5970.

168. **Vincent CD, Friedman JR, Jeong KC, Buford EC, Miller JL, Vogel JP.** 2006. Identification of the core transmembrane complex of the *Legionella* Dot/Icm type IV secretion system. Mol Microbiol **62:**1278-1291.
169. **Kubori T, Koike M, Bui XT, Higaki S, Aizawa S, Nagai H.** 2014. Native structure of a type IV secretion system core complex essential for *Legionella* pathogenesis. Proc Natl Acad Sci U S A **111:**11804-11809.
170. **Raychaudhury S, Farelli JD, Montminy TP, Matthews M, Menetret JF, Dumenil G, Roy CR, Head JF, Isberg RR, Akey CW.** 2009. Structure and function of interacting IcmR-IcmQ domains from a type IVb secretion system in *Legionella pneumophila*. Structure **17:**590-601.
171. **Dumenil G, Montminy TP, Tang M, Isberg RR.** 2004. IcmR-regulated membrane insertion and efflux by the *Legionella pneumophila* IcmQ protein. J Biol Chem **279:**4686-4695.
172. **Ninio S, Zuckman-Cholon DM, Cambronne ED, Roy CR.** 2005. The *Legionella* IcmS-IcmW protein complex is important for Dot/Icm-mediated protein translocation. Mol Microbiol **55:**912-926.
173. **Vincent CD, Vogel JP.** 2006. The *Legionella pneumophila* IcmS-LvgA protein complex is important for Dot/Icm-dependent intracellular growth. Mol Microbiol **61:**596-613.
174. **Cambronne ED, Roy CR.** 2007. The *Legionella pneumophila* IcmSW complex interacts with multiple Dot/Icm effectors to facilitate type IV translocation. PLoS Pathog **3:**e188.
175. **Bartfeld S, Engels C, Bauer B, Aurass P, Flieger A, Bruggemann H, Meyer TF.** 2009. Temporal resolution of two-tracked NF-kappaB activation by *Legionella pneumophila*. Cell Microbiol **11:**1638-1651.
176. **Shin S, Case CL, Archer KA, Nogueira CV, Kobayashi KS, Flavell RA, Roy CR, Zamboni DS.** 2008. Type IV secretion-dependent activation of host MAP kinases induces an increased proinflammatory cytokine response to *Legionella pneumophila*. PLoS Pathog **4:**e1000220.
177. **Losick VP, Isberg RR.** 2006. NF-kappaB translocation prevents host cell death after low-dose challenge by *Legionella pneumophila*. J Exp Med **203:**2177-2189.
178. **Campodonico EM, Chesnel L, Roy CR.** 2005. A yeast genetic system for the identification and characterization of substrate proteins transferred into host cells by the *Legionella pneumophila* Dot/Icm system. Mol Microbiol **56:**918-933.
179. **Shohdy N, Efe JA, Emr SD, Shuman HA.** 2005. Pathogen effector protein screening in yeast identifies *Legionella* factors that interfere with membrane trafficking. Proc Natl Acad Sci U S A **102:**4866-4871.
180. **Luo ZQ, Isberg RR.** 2004. Multiple substrates of the *Legionella pneumophila* Dot/Icm system identified by interbacterial protein transfer. Proc Natl Acad Sci U S A **101:**841-846.
181. **Zhu W, Banga S, Tan Y, Zheng C, Stephenson R, Gately J, Luo ZQ.** 2011. Comprehensive identification of protein substrates of the Dot/Icm type IV transporter of *Legionella pneumophila*. PLoS One **6:**e17638.
182. **Heidtman M, Chen EJ, Moy MY, Isberg RR.** 2009. Large-scale identification of *Legionella pneumophila* Dot/Icm substrates that modulate host cell vesicle trafficking pathways. Cell Microbiol **11:**230-248.
183. **Burstein D, Zusman T, Degtyar E, Viner R, Segal G, Pupko T.** 2009. Genome-scale identification of *Legionella pneumophila* effectors using a machine learning approach. PLoS Pathog **5:**e1000508.
184. **Huang L, Boyd D, Amyot WM, Hempstead AD, Luo ZQ, O'Connor TJ, Chen C, Machner M, Montminy T, Isberg RR.** 2011. The E Block motif is associated with *Legionella pneumophila* translocated substrates. Cell Microbiol **13:**227-245.

185. **Bruggemann H, Cazalet C, Buchrieser C.** 2006. Adaptation of *Legionella pneumophila* to the host environment: role of protein secretion, effectors and eukaryotic-like proteins. Curr Opin Microbiol **9:**86-94.
186. **Nagai H, Cambronne ED, Kagan JC, Amor JC, Kahn RA, Roy CR.** 2005. A C-terminal translocation signal required for Dot/Icm-dependent delivery of the *Legionella* RalF protein to host cells. Proc Natl Acad Sci U S A **102:**826-831.
187. **Hubber A, Roy CR.** 2010. Modulation of host cell function by *Legionella pneumophila* type IV effectors. Annu Rev Cell Dev Biol **26:**261-283.
188. **Pan X, Luhrmann A, Satoh A, Laskowski-Arce MA, Roy CR.** 2008. Ankyrin repeat proteins comprise a diverse family of bacterial type IV effectors. Science **320:**1651-1654.
189. **Newton HJ, Sansom FM, Dao J, McAlister AD, Sloan J, Cianciotto NP, Hartland EL.** 2007. Sel1 repeat protein LpnE is a *Legionella pneumophila* virulence determinant that influences vacuolar trafficking. Infect Immun **75:**5575-5585.
190. **Weber SS, Ragaz C, Hilbi H.** 2009. The inositol polyphosphate 5-phosphatase OCRL1 restricts intracellular growth of *Legionella*, localizes to the replicative vacuole and binds to the bacterial effector LpnE. Cell Microbiol **11:**442-460.
191. **Franco IS, Shohdy N, Shuman HA.** 2012. The *Legionella pneumophila* effector VipA is an actin nucleator that alters host cell organelle trafficking. PLoS Pathog **8:**e1002546.
192. **Brumell JH, Scidmore MA.** 2007. Manipulation of rab GTPase function by intracellular bacterial pathogens. Microbiol Mol Biol Rev **71:**636-652.
193. **Nagai H, Kagan JC, Zhu X, Kahn RA, Roy CR.** 2002. A bacterial guanine nucleotide exchange factor activates ARF on *Legionella* phagosomes. Science **295:**679-682.
194. **Conover GM, Derre I, Vogel JP, Isberg RR.** 2003. The *Legionella pneumophila* LidA protein: a translocated substrate of the Dot/Icm system associated with maintenance of bacterial integrity. Mol Microbiol **48:**305-321.
195. **Machner MP, Isberg RR.** 2006. Targeting of host Rab GTPase function by the intravacuolar pathogen *Legionella pneumophila*. Dev Cell **11:**47-56.
196. **Derre I, Isberg RR.** 2005. LidA, a translocated substrate of the *Legionella pneumophila* type IV secretion system, interferes with the early secretory pathway. Infect Immun **73:**4370-4380.
197. **Ragaz C, Pietsch H, Urwyler S, Tiaden A, Weber SS, Hilbi H.** 2008. The *Legionella pneumophila* phosphatidylinositol-4 phosphate-binding type IV substrate SidC recruits endoplasmic reticulum vesicles to a replication-permissive vacuole. Cell Microbiol **10:**2416-2433.
198. **Brombacher E, Urwyler S, Ragaz C, Weber SS, Kami K, Overduin M, Hilbi H.** 2009. Rab1 guanine nucleotide exchange factor SidM is a major phosphatidylinositol 4-phosphate-binding effector protein of *Legionella pneumophila*. J Biol Chem **284:**4846-4856.
199. **Horenkamp FA, Mukherjee S, Alix E, Schauder CM, Hubber AM, Roy CR, Reinisch KM.** 2014. *Legionella pneumophila* subversion of host vesicular transport by SidC effector proteins. Traffic **15:**488-499.
200. **Hsu F, Luo X, Qiu J, Teng YB, Jin J, Smolka MB, Luo ZQ, Mao Y.** 2014. The *Legionella* effector SidC defines a unique family of ubiquitin ligases important for bacterial phagosomal remodeling. Proc Natl Acad Sci U S A **111:**10538-10543.
201. **Shen X, Banga S, Liu Y, Xu L, Gao P, Shamovsky I, Nudler E, Luo ZQ.** 2009. Targeting eEF1A by a *Legionella pneumophila* effector leads to inhibition of protein synthesis and induction of host stress response. Cell Microbiol **11:**911-926.
202. **Belyi Y, Niggeweg R, Opitz B, Vogelsgesang M, Hippenstiel S, Wilm M, Aktories K.** 2006. *Legionella pneumophila* glucosyltransferase inhibits host elongation factor 1A. Proc Natl Acad Sci U S A **103:**16953-16958.

203. **Hempstead AD, Isberg RR.** 2015. Inhibition of host cell translation elongation by *Legionella pneumophila* blocks the host cell unfolded protein response. Proc Natl Acad Sci U S A **112:**E6790-6797.
204. **Copenhaver AM, Casson CN, Nguyen HT, Duda MM, Shin S.** 2015. IL-1R signaling enables bystander cells to overcome bacterial blockade of host protein synthesis. Proc Natl Acad Sci U S A **112:**7557-7562.
205. **Vergne I, Chua J, Deretic V.** 2003. *Mycobacterium tuberculosis* phagosome maturation arrest: selective targeting of PI3P-dependent membrane trafficking. Traffic **4:**600-606.
206. **Ge J, Gong YN, Xu Y, Shao F.** 2012. Preventing bacterial DNA release and absent in melanoma 2 inflammasome activation by a *Legionella* effector functioning in membrane trafficking. Proc Natl Acad Sci U S A **109:**6193-6198.
207. **Laguna RK, Creasey EA, Li Z, Valtz N, Isberg RR.** 2006. A *Legionella pneumophila*-translocated substrate that is required for growth within macrophages and protection from host cell death. Proc Natl Acad Sci U S A **103:**18745-18750.
208. **O'Connor TJ, Adepoju Y, Boyd D, Isberg RR.** 2011. Minimization of the *Legionella pneumophila* genome reveals chromosomal regions involved in host range expansion. Proc Natl Acad Sci U S A **108:**14733-14740.
209. **Creasey EA, Isberg RR.** 2012. The protein SdhA maintains the integrity of the *Legionella*-containing vacuole. Proc Natl Acad Sci U S A **109:**3481-3486.
210. **Neild AL, Roy CR.** 2004. Immunity to vacuolar pathogens: what can we learn from *Legionella*? Cell Microbiol **6:**1011-1018.
211. **Medzhitov R.** 2007. Recognition of microorganisms and activation of the immune response. Nature **449:**819-826.
212. **Hawn TR, Verbon A, Lettinga KD, Zhao LP, Li SS, Laws RJ, Skerrett SJ, Beutler B, Schroeder L, Nachman A, Ozinsky A, Smith KD, Aderem A.** 2003. A common dominant TLR5 stop codon polymorphism abolishes flagellin signaling and is associated with susceptibility to legionnaires' disease. J Exp Med **198:**1563-1572.
213. **Girard R, Pedron T, Uematsu S, Balloy V, Chignard M, Akira S, Chaby R.** 2003. Lipopolysaccharides from *Legionella* and *Rhizobium* stimulate mouse bone marrow granulocytes via Toll-like receptor 2. J Cell Sci **116:**293-302.
214. **Hawn TR, Smith KD, Aderem A, Skerrett SJ.** 2006. Myeloid differentiation primary response gene (88)- and toll-like receptor 2-deficient mice are susceptible to infection with aerosolized *Legionella pneumophila*. J Infect Dis **193:**1693-1702.
215. **Archer KA, Roy CR.** 2006. MyD88-dependent responses involving toll-like receptor 2 are important for protection and clearance of *Legionella pneumophila* in a mouse model of Legionnaires' disease. Infect Immun **74:**3325-3333.
216. **Sporri R, Joller N, Albers U, Hilbi H, Oxenius A.** 2006. MyD88-dependent IFN-gamma production by NK cells is key for control of *Legionella pneumophila* infection. J Immunol **176:**6162-6171.
217. **Braedel-Ruoff S, Faigle M, Hilf N, Neumeister B, Schild H.** 2005. *Legionella pneumophila* mediated activation of dendritic cells involves CD14 and TLR2. J Endotoxin Res **11:**89-96.
218. **Mascarenhas DP, Pereira MS, Manin GZ, Hori JI, Zamboni DS.** 2015. Interleukin 1 receptor-driven neutrophil recruitment accounts to MyD88-dependent pulmonary clearance of *Legionella pneumophila* infection *in vivo*. J Infect Dis **211:**322-330.
219. **Shim HK, Kim JY, Kim MJ, Sim HS, Park DW, Sohn JW, Kim MJ.** 2009. *Legionella* lipoprotein activates toll-like receptor 2 and induces cytokine production and expression of costimulatory molecules in peritoneal macrophages. Exp Mol Med **41:**687-694.

220. **Smith KD, Andersen-Nissen E, Hayashi F, Strobe K, Bergman MA, Barrett SL, Cookson BT, Aderem A.** 2003. Toll-like receptor 5 recognizes a conserved site on flagellin required for protofilament formation and bacterial motility. Nat Immunol **4:**1247-1253.
221. **Tateda K, Matsumoto T, Ishii Y, Furuya N, Ohno A, Miyazaki S, Yamaguchi K.** 1998. Serum cytokines in patients with *Legionella pneumonia*: relative predominance of Th1-type cytokines. Clin Diagn Lab Immunol **5:**401-403.
222. **Medzhitov R, Janeway C, Jr.** 2000. The Toll receptor family and microbial recognition. Trends Microbiol **8:**452-456.
223. **Brieland JK, Remick DG, LeGendre ML, Engleberg NC, Fantone JC.** 1998. In vivo regulation of replicative *Legionella pneumophila* lung infection by endogenous interleukin-12. Infect Immun **66:**65-69.
224. **Brown AS, Yang C, Fung KY, Bachem A, Bourges D, Bedoui S, Hartland EL, van Driel IR.** 2016. Cooperation between Monocyte-Derived Cells and Lymphoid Cells in the Acute Response to a Bacterial Lung Pathogen. PLoS Pathog **12:**e1005691.
225. **Brieland JK, Jackson C, Hurst S, Loebenberg D, Muchamuel T, Debets R, Kastelein R, Churakova T, Abrams J, Hare R, O'Garra A.** 2000. Immunomodulatory role of endogenous interleukin-18 in gamma interferon-mediated resolution of replicative *Legionella pneumophila* lung infection. Infect Immun **68:**6567-6573.
226. **Byrd TF, Horwitz MA.** 1989. Interferon gamma-activated human monocytes downregulate transferrin receptors and inhibit the intracellular multiplication of *Legionella pneumophila* by limiting the availability of iron. J Clin Invest **83:**1457-1465.
227. **Horwitz MA, Silverstein SC.** 1981. Activated human monocytes inhibit the intracellular multiplication of Legionnaires' disease bacteria. J Exp Med **154:**1618-1635.
228. **Skerrett SJ, Martin TR.** 1996. Roles for tumor necrosis factor alpha and nitric oxide in resistance of rat alveolar macrophages to *Legionella pneumophila*. Infect Immun **64:**3236-3243.
229. **LeibundGut-Landmann S, Weidner K, Hilbi H, Oxenius A.** 2011. Nonhematopoietic cells are key players in innate control of bacterial airway infection. J Immunol **186:**3130-3137.
230. **Wright EK, Goodart SA, Growney JD, Hadinoto V, Endrizzi MG, Long EM, Sadigh K, Abney AL, Bernstein-Hanley I, Dietrich WF.** 2003. Naip5 affects host susceptibility to the intracellular pathogen *Legionella pneumophila*. Curr Biol **13:**27-36.
231. **Ren T, Zamboni DS, Roy CR, Dietrich WF, Vance RE.** 2006. Flagellin-deficient *Legionella* mutants evade caspase-1- and Naip5-mediated macrophage immunity. PLoS Pathog **2:**e18.
232. **Neild AL, Roy CR.** 2003. *Legionella* reveal dendritic cell functions that facilitate selection of antigens for MHC class II presentation. Immunity **18:**813-823.
233. **Nogueira CV, Lindsten T, Jamieson AM, Case CL, Shin S, Thompson CB, Roy CR.** 2009. Rapid pathogen-induced apoptosis: a mechanism used by dendritic cells to limit intracellular replication of *Legionella pneumophila*. PLoS Pathog **5:**e1000478.
234. **Susa M, Ticac B, Rukavina T, Doric M, Marre R.** 1998. *Legionella pneumophila* infection in intratracheally inoculated T cell-depleted or -nondepleted A/J mice. J Immunol **160:**316-321.
235. **Blander SJ, Breiman RF, Horwitz MA.** 1989. A live avirulent mutant *Legionella pneumophila* vaccine induces protective immunity against lethal aerosol challenge. J Clin Invest **83:**810-815.
236. **Breiman RF, Horwitz MA.** 1987. Guinea pigs sublethally infected with aerosolized *Legionella pneumophila* develop humoral and cell-mediated immune responses and

are protected against lethal aerosol challenge. A model for studying host defense against lung infections caused by intracellular pathogens. J Exp Med **165:**799-811.
237. **Horwitz MA, Silverstein SC.** 1981. Interaction of the legionnaires' disease bacterium (*Legionella pneumophila*) with human phagocytes. II. Antibody promotes binding of *L. pneumophila* to monocytes but does not inhibit intracellular multiplication. J Exp Med **153:**398-406.
238. **Hubber A, Kubori T, Nagai H.** 2013. Modulation of the ubiquitination machinery by *Legionella*. Curr Top Microbiol Immunol **376:**227-247.
239. **Hicke L, Dunn R.** 2003. Regulation of membrane protein transport by ubiquitin and ubiquitin-binding proteins. Annu Rev Cell Dev Biol **19:**141-172.
240. **Haglund K, Dikic I.** 2005. Ubiquitylation and cell signaling. EMBO J **24:**3353-3359.
241. **Haglund K, Dikic I.** 2012. The role of ubiquitylation in receptor endocytosis and endosomal sorting. J Cell Sci **125:**265-275.
242. **Ulrich HD, Walden H.** 2010. Ubiquitin signalling in DNA replication and repair. Nat Rev Mol Cell Biol **11:**479-489.
243. **Hershko A, Ciechanover A.** 1998. The ubiquitin system. Annu Rev Biochem **67:**425-479.
244. **Hershko A, Heller H, Elias S, Ciechanover A.** 1983. Components of ubiquitin-protein ligase system. Resolution, affinity purification, and role in protein breakdown. J Biol Chem **258:**8206-8214.
245. **Pickart CM, Eddins MJ.** 2004. Ubiquitin: structures, functions, mechanisms. Biochim Biophys Acta **1695:**55-72.
246. **Ashida H, Kim M, Sasakawa C.** 2014. Exploitation of the host ubiquitin system by human bacterial pathogens. Nat Rev Microbiol **12:**399-413.
247. **van Wijk SJ, Timmers HT.** 2010. The family of ubiquitin-conjugating enzymes (E2s): deciding between life and death of proteins. FASEB J **24:**981-993.
248. **Hutchins AP, Liu S, Diez D, Miranda-Saavedra D.** 2013. The repertoires of ubiquitinating and deubiquitinating enzymes in eukaryotic genomes. Mol Biol Evol **30:**1172-1187.
249. **Li W, Bengtson MH, Ulbrich A, Matsuda A, Reddy VA, Orth A, Chanda SK, Batalov S, Joazeiro CA.** 2008. Genome-wide and functional annotation of human E3 ubiquitin ligases identifies MULAN, a mitochondrial E3 that regulates the organelle's dynamics and signaling. PLoS One **3:**e1487.
250. **Ardley HC, Robinson PA.** 2005. E3 ubiquitin ligases. Essays Biochem **41:**15-30.
251. **Pickart CM.** 2001. Mechanisms underlying ubiquitination. Annu Rev Biochem **70:**503-533.
252. **Rotin D, Kumar S.** 2009. Physiological functions of the HECT family of ubiquitin ligases. Nat Rev Mol Cell Biol **10:**398-409.
253. **Reyes-Turcu FE, Ventii KH, Wilkinson KD.** 2009. Regulation and cellular roles of ubiquitin-specific deubiquitinating enzymes. Annu Rev Biochem **78:**363-397.
254. **Bhoj VG, Chen ZJ.** 2009. Ubiquitylation in innate and adaptive immunity. Nature **458:**430-437.
255. **Hayden MS, Ghosh S.** 2012. NF-kappaB, the first quarter-century: remarkable progress and outstanding questions. Genes Dev **26:**203-234.
256. **Rytkonen A, Holden DW.** 2007. Bacterial interference of ubiquitination and deubiquitination. Cell Host Microbe **1:**13-22.
257. **Angot A, Vergunst A, Genin S, Peeters N.** 2007. Exploitation of eukaryotic ubiquitin signaling pathways by effectors translocated by bacterial type III and type IV secretion systems. PLoS Pathog **3:**e3.
258. **Collins CA, Brown EJ.** 2010. Cytosol as battleground: ubiquitin as a weapon for both host and pathogen. Trends Cell Biol **20:**205-213.

259. **Ogawa M, Mimuro H, Yoshikawa Y, Ashida H, Sasakawa C.** 2011. Manipulation of autophagy by bacteria for their own benefit. Microbiol Immunol **55:**459-471.
260. **Canadien V, Tan T, Zilber R, Szeto J, Perrin AJ, Brumell JH.** 2005. Cutting edge: microbial products elicit formation of dendritic cell aggresome-like induced structures in macrophages. J Immunol **174:**2471-2475.
261. **Szeto J, Kaniuk NA, Canadien V, Nisman R, Mizushima N, Yoshimori T, Bazett-Jones DP, Brumell JH.** 2006. ALIS are stress-induced protein storage compartments for substrates of the proteasome and autophagy. Autophagy **2:**189-199.
262. **Mesquita FS, Thomas M, Sachse M, Santos AJ, Figueira R, Holden DW.** 2012. The *Salmonella* deubiquitinase SseL inhibits selective autophagy of cytosolic aggregates. PLoS Pathog **8:**e1002743.
263. **Zhou H, Monack DM, Kayagaki N, Wertz I, Yin J, Wolf B, Dixit VM.** 2005. *Yersinia* virulence factor YopJ acts as a deubiquitinase to inhibit NF-kappa B activation. J Exp Med **202:**1327-1332.
264. **Mittal R, Peak-Chew SY, McMahon HT.** 2006. Acetylation of MEK2 and I kappa B kinase (IKK) activation loop residues by YopJ inhibits signaling. Proc Natl Acad Sci U S A **103:**18574-18579.
265. **Mukherjee S, Keitany G, Li Y, Wang Y, Ball HL, Goldsmith EJ, Orth K.** 2006. *Yersinia* YopJ acetylates and inhibits kinase activation by blocking phosphorylation. Science **312:**1211-1214.
266. **Patel JC, Galan JE.** 2006. Differential activation and function of Rho GTPases during *Salmonella*-host cell interactions. J Cell Biol **175:**453-463.
267. **Steele-Mortimer O, Knodler LA, Marcus SL, Scheid MP, Goh B, Pfeifer CG, Duronio V, Finlay BB.** 2000. Activation of Akt/protein kinase B in epithelial cells by the *Salmonella* typhimurium effector sigD. J Biol Chem **275:**37718-37724.
268. **Patel JC, Hueffer K, Lam TT, Galan JE.** 2009. Diversification of a *Salmonella* virulence protein function by ubiquitin-dependent differential localization. Cell **137:**283-294.
269. **Pearce MJ, Mintseris J, Ferreyra J, Gygi SP, Darwin KH.** 2008. Ubiquitin-like protein involved in the proteasome pathway of *Mycobacterium tuberculosis*. Science **322:**1104-1107.
270. **Diao J, Zhang Y, Huibregtse JM, Zhou D, Chen J.** 2008. Crystal structure of SopA, a *Salmonella* effector protein mimicking a eukaryotic ubiquitin ligase. Nat Struct Mol Biol **15:**65-70.
271. **Zhang Y, Higashide WM, McCormick BA, Chen J, Zhou D.** 2006. The inflammation-associated *Salmonella* SopA is a HECT-like E3 ubiquitin ligase. Mol Microbiol **62:**786-793.
272. **Hicks SW, Galan JE.** 2010. Hijacking the host ubiquitin pathway: structural strategies of bacterial E3 ubiquitin ligases. Curr Opin Microbiol **13:**41-46.
273. **Rohde JR, Breitkreutz A, Chenal A, Sansonetti PJ, Parsot C.** 2007. Type III secretion effectors of the IpaH family are E3 ubiquitin ligases. Cell Host Microbe **1:**77-83.
274. **Haraga A, Miller SI.** 2006. A *Salmonella* type III secretion effector interacts with the mammalian serine/threonine protein kinase PKN1. Cell Microbiol **8:**837-846.
275. **Kubori T, Galan JE.** 2003. Temporal regulation of *Salmonella* virulence effector function by proteasome-dependent protein degradation. Cell **115:**333-342.
276. **Ivanov SS, Roy CR.** 2009. Modulation of ubiquitin dynamics and suppression of DALIS formation by the *Legionella pneumophila* Dot/Icm system. Cell Microbiol **11:**261-278.
277. **Lelouard H, Gatti E, Cappello F, Gresser O, Camosseto V, Pierre P.** 2002. Transient aggregation of ubiquitinated proteins during dendritic cell maturation. Nature **417:**177-182.

278. **Bruckert WM, Abu Kwaik Y.** 2015. Complete and ubiquitinated proteome of the *Legionella*-containing vacuole within human macrophages. J Proteome Res **14:**236-248.
279. **Al-Khodor S, Price CT, Habyarimana F, Kalia A, Abu Kwaik Y.** 2008. A Dot/Icm-translocated ankyrin protein of *Legionella pneumophila* is required for intracellular proliferation within human macrophages and protozoa. Mol Microbiol **70:**908-923.
280. **Price CT, Al-Khodor S, Al-Quadan T, Santic M, Habyarimana F, Kalia A, Kwaik YA.** 2009. Molecular mimicry by an F-box effector of *Legionella pneumophila* hijacks a conserved polyubiquitination machinery within macrophages and protozoa. PLoS Pathog **5:**e1000704.
281. **Lomma M, Dervins-Ravault D, Rolando M, Nora T, Newton HJ, Sansom FM, Sahr T, Gomez-Valero L, Jules M, Hartland EL, Buchrieser C.** 2010. The *Legionella pneumophila* F-box protein Lpp2082 (AnkB) modulates ubiquitination of the host protein parvin B and promotes intracellular replication. Cell Microbiol **12:**1272-1291.
282. **Price CT, Al-Quadan T, Santic M, Rosenshine I, Abu Kwaik Y.** 2011. Host proteasomal degradation generates amino acids essential for intracellular bacterial growth. Science **334:**1553-1557.
283. **Price CT, Al-Quadan T, Santic M, Jones SC, Abu Kwaik Y.** 2010. Exploitation of conserved eukaryotic host cell farnesylation machinery by an F-box effector of *Legionella pneumophila*. J Exp Med **207:**1713-1726.
284. **Price CT, Jones SC, Amundson KE, Kwaik YA.** 2010. Host-mediated post-translational prenylation of novel dot/icm-translocated effectors of *Legionella pneumophila*. Front Microbiol **1:**131.
285. **Bruckert WM, Price CT, Abu Kwaik Y.** 2014. Rapid nutritional remodeling of the host cell upon attachment of *Legionella pneumophila*. Infect Immun **82:**72-82.
286. **Ivanov SS, Roy CR.** 2013. Pathogen signatures activate a ubiquitination pathway that modulates the function of the metabolic checkpoint kinase mTOR. Nat Immunol **14:**1219-1228.
287. **Laplante M, Sabatini DM.** 2012. mTOR signaling in growth control and disease. Cell **149:**274-293.
288. **Bruckert WM, Abu Kwaik Y.** 2016. Lysine11-Linked Polyubiquitination of the AnkB F-Box Effector of Legionella pneumophila. Infect Immun **84:**99-107.
289. **Pandey AK, Sassetti CM.** 2008. Mycobacterial persistence requires the utilization of host cholesterol. Proc Natl Acad Sci U S A **105:**4376-4380.
290. **Daniel J, Maamar H, Deb C, Sirakova TD, Kolattukudy PE.** 2011. *Mycobacterium tuberculosis* uses host triacylglycerol to accumulate lipid droplets and acquires a dormancy-like phenotype in lipid-loaded macrophages. PLoS Pathog **7:**e1002093.
291. **Marrero J, Trujillo C, Rhee KY, Ehrt S.** 2013. Glucose phosphorylation is required for *Mycobacterium tuberculosis* persistence in mice. PLoS Pathog **9:**e1003116.
292. **McKinney JD, Honer zu Bentrup K, Munoz-Elias EJ, Miczak A, Chen B, Chan WT, Swenson D, Sacchettini JC, Jacobs WR, Jr., Russell DG.** 2000. Persistence of *Mycobacterium tuberculosis* in macrophages and mice requires the glyoxylate shunt enzyme isocitrate lyase. Nature **406:**735-738.
293. **Abu Kwaik Y, Bumann D.** 2013. Microbial quest for food in vivo: 'nutritional virulence' as an emerging paradigm. Cell Microbiol **15:**882-890.
294. **Sauer JD, Bachman MA, Swanson MS.** 2005. The phagosomal transporter A couples threonine acquisition to differentiation and replication of *Legionella pneumophila* in macrophages. Proc Natl Acad Sci U S A **102:**9924-9929.
295. **Eylert E, Herrmann V, Jules M, Gillmaier N, Lautner M, Buchrieser C, Eisenreich W, Heuner K.** 2010. Isotopologue profiling of *Legionella pneumophila*: role of serine and glucose as carbon substrates. J Biol Chem **285:**22232-22243.

296. **Price CT, Richards AM, Von Dwingelo JE, Samara HA, Abu Kwaik Y.** 2014. Amoeba host-*Legionella* synchronization of amino acid auxotrophy and its role in bacterial adaptation and pathogenic evolution. Environ Microbiol **16:**350-358.
297. **Yamanaka K, Sasagawa Y, Ogura T.** 2012. Recent advances in p97/VCP/Cdc48 cellular functions. Biochim Biophys Acta **1823:**130-137.
298. **Latterich M, Frohlich KU, Schekman R.** 1995. Membrane fusion and the cell cycle: Cdc48p participates in the fusion of ER membranes. Cell **82:**885-893.
299. **Rabouille C, Levine TP, Peters JM, Warren G.** 1995. An NSF-like ATPase, p97, and NSF mediate cisternal regrowth from mitotic Golgi fragments. Cell **82:**905-914.
300. **Partridge JJ, Lopreiato JO, Jr., Latterich M, Indig FE.** 2003. DNA damage modulates nucleolar interaction of the Werner protein with the AAA ATPase p97/VCP. Mol Biol Cell **14:**4221-4229.
301. **Dai RM, Li CC.** 2001. Valosin-containing protein is a multi-ubiquitin chain-targeting factor required in ubiquitin-proteasome degradation. Nat Cell Biol **3:**740-744.
302. **Hoppe T, Matuschewski K, Rape M, Schlenker S, Ulrich HD, Jentsch S.** 2000. Activation of a membrane-bound transcription factor by regulated ubiquitin/proteasome-dependent processing. Cell **102:**577-586.
303. **Ye Y, Meyer HH, Rapoport TA.** 2001. The AAA ATPase Cdc48/p97 and its partners transport proteins from the ER into the cytosol. Nature **414:**652-656.
304. **Jarosch E, Taxis C, Volkwein C, Bordallo J, Finley D, Wolf DH, Sommer T.** 2002. Protein dislocation from the ER requires polyubiquitination and the AAA-ATPase Cdc48. Nat Cell Biol **4:**134-139.
305. **Ye Y, Meyer HH, Rapoport TA.** 2003. Function of the p97-Ufd1-Npl4 complex in retrotranslocation from the ER to the cytosol: dual recognition of nonubiquitinated polypeptide segments and polyubiquitin chains. J Cell Biol **162:**71-84.
306. **Meyer HH, Shorter JG, Seemann J, Pappin D, Warren G.** 2000. A complex of mammalian ufd1 and npl4 links the AAA-ATPase, p97, to ubiquitin and nuclear transport pathways. EMBO J **19:**2181-2192.
307. **Castrejon-Jimenez NS, Leyva-Paredes K, Hernandez-Gonzalez JC, Luna-Herrera J, Garcia-Perez BE.** 2015. The role of autophagy in bacterial infections. Biosci Trends **9:**149-159.
308. **Deretic V.** 2005. Autophagy in innate and adaptive immunity. Trends Immunol **26:**523-528.
309. **Shaid S, Brandts CH, Serve H, Dikic I.** 2013. Ubiquitination and selective autophagy. Cell Death Differ **20:**21-30.
310. **Behrends C, Fulda S.** 2012. Receptor proteins in selective autophagy. Int J Cell Biol **2012:**673290.
311. **Birmingham CL, Smith AC, Bakowski MA, Yoshimori T, Brumell JH.** 2006. Autophagy controls *Salmonella* infection in response to damage to the *Salmonella*-containing vacuole. J Biol Chem **281:**11374-11383.
312. **Perrin AJ, Jiang X, Birmingham CL, So NS, Brumell JH.** 2004. Recognition of bacteria in the cytosol of Mammalian cells by the ubiquitin system. Curr Biol **14:**806-811.
313. **van Wijk SJL, Fricke F, Herhaus L, Gupta J, Hotte K, Pampaloni F, Grumati P, Kaulich M, Sou YS, Komatsu M, Greten FR, Fulda S, Heilemann M, Dikic I.** 2017. Linear ubiquitination of cytosolic *Salmonella* Typhimurium activates NF-kappaB and restricts bacterial proliferation. Nat Microbiol **2:**17066.
314. **Zheng YT, Shahnazari S, Brech A, Lamark T, Johansen T, Brumell JH.** 2009. The adaptor protein p62/SQSTM1 targets invading bacteria to the autophagy pathway. J Immunol **183:**5909-5916.

315. **Wild P, Farhan H, McEwan DG, Wagner S, Rogov VV, Brady NR, Richter B, Korac J, Waidmann O, Choudhary C, Dotsch V, Bumann D, Dikic I.** 2011. Phosphorylation of the autophagy receptor optineurin restricts *Salmonella* growth. Science **333:**228-233.
316. **Castillo EF, Dekonenko A, Arko-Mensah J, Mandell MA, Dupont N, Jiang S, Delgado-Vargas M, Timmins GS, Bhattacharya D, Yang H, Hutt J, Lyons CR, Dobos KM, Deretic V.** 2012. Autophagy protects against active tuberculosis by suppressing bacterial burden and inflammation. Proc Natl Acad Sci U S A **109:**E3168-3176.
317. **Amer AO, Swanson MS.** 2005. Autophagy is an immediate macrophage response to *Legionella pneumophila*. Cell Microbiol **7:**765-778.
318. **Rolando M, Escoll P, Nora T, Botti J, Boitez V, Bedia C, Daniels C, Abraham G, Stogios PJ, Skarina T, Christophe C, Dervins-Ravault D, Cazalet C, Hilbi H, Rupasinghe TW, Tull D, McConville MJ, Ong SY, Hartland EL, Codogno P, Levade T, Naderer T, Savchenko A, Buchrieser C.** 2016. *Legionella pneumophila* S1P-lyase targets host sphingolipid metabolism and restrains autophagy. Proc Natl Acad Sci U S A **113:**1901-1906.
319. **Choy A, Dancourt J, Mugo B, O'Connor TJ, Isberg RR, Melia TJ, Roy CR.** 2012. The *Legionella* effector RavZ inhibits host autophagy through irreversible Atg8 deconjugation. Science **338:**1072-1076.
320. **Khweek AA, Caution K, Akhter A, Abdulrahman BA, Tazi M, Hassan H, Majumdar N, Doran A, Guirado E, Schlesinger LS, Shuman H, Amer AO.** 2013. A bacterial protein promotes the recognition of the *Legionella pneumophila* vacuole by autophagy. Eur J Immunol **43:**1333-1344.
321. **Ichimura Y, Kirisako T, Takao T, Satomi Y, Shimonishi Y, Ishihara N, Mizushima N, Tanida I, Kominami E, Ohsumi M, Noda T, Ohsumi Y.** 2000. A ubiquitin-like system mediates protein lipidation. Nature **408:**488-492.
322. **Kabeya Y, Mizushima N, Ueno T, Yamamoto A, Kirisako T, Noda T, Kominami E, Ohsumi Y, Yoshimori T.** 2000. LC3, a mammalian homologue of yeast Apg8p, is localized in autophagosome membranes after processing. EMBO J **19:**5720-5728.
323. **Gomez-Valero L, Rusniok C, Cazalet C, Buchrieser C.** 2011. Comparative and functional genomics of *Legionella* identified eukaryotic like proteins as key players in host-pathogen interactions. Front Microbiol **2:**208.
324. **van Schaik EJ, Chen C, Mertens K, Weber MM, Samuel JE.** 2013. Molecular pathogenesis of the obligate intracellular bacterium *Coxiella burnetii*. Nat Rev Microbiol **11:**561-573.
325. **Merriam JJ, Mathur R, Maxfield-Boumil R, Isberg RR.** 1997. Analysis of the *Legionella pneumophila* flil gene: intracellular growth of a defined mutant defective for flagellum biosynthesis. Infect Immun **65:**2497-2501.
326. **Engleberg NC, Drutz DJ, Eisenstein BI.** 1984. Cloning and expression of *Legionella pneumophila* antigens in *Escherichia coli*. Infect Immun **44:**222-227.
327. **Riedmaier P, Sansom FM, Sofian T, Beddoe T, Schuelein R, Newton HJ, Hartland EL.** 2014. Multiple ecto-nucleoside triphosphate diphosphohydrolases facilitate intracellular replication of *Legionella pneumophila*. Biochem J **462:**279-289.
328. **Charpentier X, Gabay JE, Reyes M, Zhu JW, Weiss A, Shuman HA.** 2009. Chemical genetics reveals bacterial and host cell functions critical for type IV effector translocation by *Legionella pneumophila*. PLoS Pathog **5:**e1000501.
329. **Fire A, Xu S, Montgomery MK, Kostas SA, Driver SE, Mello CC.** 1998. Potent and specific genetic interference by double-stranded RNA in *Caenorhabditis elegans*. Nature **391:**806-811.
330. **Urnov FD, Rebar EJ, Holmes MC, Zhang HS, Gregory PD.** 2010. Genome editing with engineered zinc finger nucleases. Nat Rev Genet **11:**636-646.

331. **Reyon D, Maeder ML, Khayter C, Tsai SQ, Foley JE, Sander JD, Joung JK.** 2013. Engineering customized TALE nucleases (TALENs) and TALE transcription factors by fast ligation-based automatable solid-phase high-throughput (FLASH) assembly. Curr Protoc Mol Biol **Chapter 12:**Unit 12 16.
332. **Mali P, Yang L, Esvelt KM, Aach J, Guell M, DiCarlo JE, Norville JE, Church GM.** 2013. RNA-guided human genome engineering via Cas9. Science **339:**823-826.
333. **Aagaard L, Rossi JJ.** 2007. RNAi therapeutics: principles, prospects and challenges. Adv Drug Deliv Rev **59:**75-86.
334. **Agrawal N, Dasaradhi PV, Mohmmed A, Malhotra P, Bhatnagar RK, Mukherjee SK.** 2003. RNA interference: biology, mechanism, and applications. Microbiol Mol Biol Rev **67:**657-685.
335. **Mohr SE, Smith JA, Shamu CE, Neumuller RA, Perrimon N.** 2014. RNAi screening comes of age: improved techniques and complementary approaches. Nat Rev Mol Cell Biol **15:**591-600.
336. **Bickle M, Djaballah H, Mayr LM.** 2015. The King Is Dead, Long Live the King! JBS Special Issue on Screening by RNAi and Precise Genome Editing Technologies. J Biomol Screen **20:**929-931.
337. **Jackson AL, Bartz SR, Schelter J, Kobayashi SV, Burchard J, Mao M, Li B, Cavet G, Linsley PS.** 2003. Expression profiling reveals off-target gene regulation by RNAi. Nat Biotechnol **21:**635-637.
338. **Zhou H, Xu M, Huang Q, Gates AT, Zhang XD, Castle JC, Stec E, Ferrer M, Strulovici B, Hazuda DJ, Espeseth AS.** 2008. Genome-scale RNAi screen for host factors required for HIV replication. Cell Host Microbe **4:**495-504.
339. **Brass AL, Dykxhoorn DM, Benita Y, Yan N, Engelman A, Xavier RJ, Lieberman J, Elledge SJ.** 2008. Identification of host proteins required for HIV infection through a functional genomic screen. Science **319:**921-926.
340. **Konig R, Zhou Y, Elleder D, Diamond TL, Bonamy GM, Irelan JT, Chiang CY, Tu BP, De Jesus PD, Lilley CE, Seidel S, Opaluch AM, Caldwell JS, Weitzman MD, Kuhen KL, Bandyopadhyay S, Ideker T, Orth AP, Miraglia LJ, Bushman FD, Young JA, Chanda SK.** 2008. Global analysis of host-pathogen interactions that regulate early-stage HIV-1 replication. Cell **135:**49-60.
341. **Bushman FD, Malani N, Fernandes J, D'Orso I, Cagney G, Diamond TL, Zhou H, Hazuda DJ, Espeseth AS, Konig R, Bandyopadhyay S, Ideker T, Goff SP, Krogan NJ, Frankel AD, Young JA, Chanda SK.** 2009. Host cell factors in HIV replication: meta-analysis of genome-wide studies. PLoS Pathog **5:**e1000437.
342. **Copenhaver AM, Casson CN, Nguyen HT, Fung TC, Duda MM, Roy CR, Shin S.** 2014. Alveolar macrophages and neutrophils are the primary reservoirs for *Legionella pneumophila* and mediate cytosolic surveillance of type IV secretion. Infect Immun **82:**4325-4336.
343. **Walz A, Nichterlein T, Hof H.** 1997. Excellent activity of newer quinolones on *Legionella pneumophila* in J774 macrophages. Zentralbl Bakteriol **285:**431-439.
344. **Higa F, Kusano N, Tateyama M, Shinzato T, Arakaki N, Kawakami K, Saito A.** 1998. Simplified quantitative assay system for measuring activities of drugs against intracellular *Legionella pneumophila*. J Clin Microbiol **36:**1392-1398.
345. **Charpentier X, Oswald E.** 2004. Identification of the secretion and translocation domain of the enteropathogenic and enterohemorrhagic *Escherichia coli* effector Cif, using TEM-1 beta-lactamase as a new fluorescence-based reporter. J Bacteriol **186:**5486-5495.
346. **Ensminger AW, Isberg RR.** 2009. *Legionella pneumophila* Dot/Icm translocated substrates: a sum of parts. Curr Opin Microbiol **12:**67-73.

347. **Aydin I, Weber S, Snijder B, Samperio Ventayol P, Kuhbacher A, Becker M, Day PM, Schiller JT, Kann M, Pelkmans L, Helenius A, Schelhaas M.** 2014. Large scale RNAi reveals the requirement of nuclear envelope breakdown for nuclear import of human papillomaviruses. PLoS Pathog **10:**e1004162.
348. **Somalinga BR, Day CE, Wei S, Roth MG, Thomas PJ.** 2012. TDP-43 identified from a genome wide RNAi screen for SOD1 regulators. PLoS One **7:**e35818.
349. **Price JV, Vance RE.** 2014. The macrophage paradox. Immunity **41:**685-693.
350. **Unanue ER.** 1984. Antigen-presenting function of the macrophage. Annu Rev Immunol **2:**395-428.
351. **Carralot JP, Kim TK, Lenseigne B, Boese AS, Sommer P, Genovesio A, Brodin P.** 2009. Automated high-throughput siRNA transfection in raw 264.7 macrophages: a case study for optimization procedure. J Biomol Screen **14:**151-160.
352. **De Arras L, Guthrie BS, Alper S.** 2014. Using RNA-interference to investigate the innate immune response in mouse macrophages. J Vis Exp doi:10.3791/51306**:**e51306.
353. **Zhang X, Edwards JP, Mosser DM.** 2009. The expression of exogenous genes in macrophages: obstacles and opportunities. Methods Mol Biol **531:**123-143.
354. **Marques JT, Williams BR.** 2005. Activation of the mammalian immune system by siRNAs. Nat Biotechnol **23:**1399-1405.
355. **Lee G, Santat LA, Chang MS, Choi S.** 2009. RNAi methodologies for the functional study of signaling molecules. PLoS One **4:**e4559.
356. **Hornung V, Guenthner-Biller M, Bourquin C, Ablasser A, Schlee M, Uematsu S, Noronha A, Manoharan M, Akira S, de Fougerolles A, Endres S, Hartmann G.** 2005. Sequence-specific potent induction of IFN-alpha by short interfering RNA in plasmacytoid dendritic cells through TLR7. Nat Med **11:**263-270.
357. **Sioud M.** 2005. Induction of inflammatory cytokines and interferon responses by double-stranded and single-stranded siRNAs is sequence-dependent and requires endosomal localization. J Mol Biol **348:**1079-1090.
358. **Karpala AJ, Doran TJ, Bean AG.** 2005. Immune responses to dsRNA: implications for gene silencing technologies. Immunol Cell Biol **83:**211-216.
359. **Kariko K, Bhuyan P, Capodici J, Ni H, Lubinski J, Friedman H, Weissman D.** 2004. Exogenous siRNA mediates sequence-independent gene suppression by signaling through toll-like receptor 3. Cells Tissues Organs **177:**132-138.
360. **Judge AD, Sood V, Shaw JR, Fang D, McClintock K, MacLachlan I.** 2005. Sequence-dependent stimulation of the mammalian innate immune response by synthetic siRNA. Nat Biotechnol **23:**457-462.
361. **Reynolds A, Anderson EM, Vermeulen A, Fedorov Y, Robinson K, Leake D, Karpilow J, Marshall WS, Khvorova A.** 2006. Induction of the interferon response by siRNA is cell type- and duplex length-dependent. RNA **12:**988-993.
362. **Zhou H, DeLoid G, Browning E, Gregory DJ, Tan F, Bedugnis AS, Imrich A, Koziel H, Kramnik I, Lu Q, Kobzik L.** 2012. Genome-wide RNAi screen in IFN-gamma-treated human macrophages identifies genes mediating resistance to the intracellular pathogen *Francisella tularensis*. PLoS One **7:**e31752.
363. **Cherry S.** 2008. Genomic RNAi screening in *Drosophila* S2 cells: what have we learned about host-pathogen interactions? Curr Opin Microbiol **11:**262-270.
364. **Ramet M, Manfruelli P, Pearson A, Mathey-Prevot B, Ezekowitz RA.** 2002. Functional genomic analysis of phagocytosis and identification of a *Drosophila* receptor for *E. coli*. Nature **416:**644-648.
365. **Ramet M, Pearson A, Manfruelli P, Li X, Koziel H, Gobel V, Chung E, Krieger M, Ezekowitz RA.** 2001. *Drosophila* scavenger receptor CI is a pattern recognition receptor for bacteria. Immunity **15:**1027-1038.

366. **Pearson AM, Baksa K, Ramet M, Protas M, McKee M, Brown D, Ezekowitz RA.** 2003. Identification of cytoskeletal regulatory proteins required for efficient phagocytosis in *Drosophila*. Microbes Infect **5:**815-824.
367. **Clemens JC, Worby CA, Simonson-Leff N, Muda M, Maehama T, Hemmings BA, Dixon JE.** 2000. Use of double-stranded RNA interference in *Drosophila* cell lines to dissect signal transduction pathways. Proc Natl Acad Sci U S A **97:**6499-6503.
368. **De Jesus DA, O'Connor TJ, Isberg RR.** 2013. Analysis of *Legionella* infection using RNAi in *Drosophila* cells. Methods Mol Biol **954:**251-264.
369. **Wendler F, Gillingham AK, Sinka R, Rosa-Ferreira C, Gordon DE, Franch-Marro X, Peden AA, Vincent JP, Munro S.** 2010. A genome-wide RNA interference screen identifies two novel components of the metazoan secretory pathway. EMBO J **29:**304-314.
370. **Jolly AL, Luan CH, Dusel BE, Dunne SF, Winding M, Dixit VJ, Robins C, Saluk JL, Logan DJ, Carpenter AE, Sharma M, Dean D, Cohen AR, Gelfand VI.** 2016. A Genome-wide RNAi Screen for Microtubule Bundle Formation and Lysosome Motility Regulation in *Drosophila* S2 Cells. Cell Rep **14:**611-620.
371. **Misselwitz B, Dilling S, Vonaesch P, Sacher R, Snijder B, Schlumberger M, Rout S, Stark M, von Mering C, Pelkmans L, Hardt WD.** 2011. RNAi screen of *Salmonella* invasion shows role of COPI in membrane targeting of cholesterol and Cdc42. Mol Syst Biol **7:**474.
372. **Dreyfus LA.** 1987. Virulence associated ingestion of *Legionella pneumophila* by HeLa cells. Microb Pathog **3:**45-52.
373. **Garduno RA, Quinn FD, Hoffman PS.** 1998. HeLa cells as a model to study the invasiveness and biology of *Legionella pneumophila*. Can J Microbiol **44:**430-440.
374. **Garduno RA, Garduno E, Hiltz M, Hoffman PS.** 2002. Intracellular growth of *Legionella pneumophila* gives rise to a differentiated form dissimilar to stationary-phase forms. Infect Immun **70:**6273-6283.
375. **Gu S, Rossi JJ.** 2005. Uncoupling of RNAi from active translation in mammalian cells. RNA **11:**38-44.
376. **Chien M, Morozova I, Shi S, Sheng H, Chen J, Gomez SM, Asamani G, Hill K, Nuara J, Feder M, Rineer J, Greenberg JJ, Steshenko V, Park SH, Zhao B, Teplitskaya E, Edwards JR, Pampou S, Georghiou A, Chou IC, Iannuccilli W, Ulz ME, Kim DH, Geringer-Sameth A, Goldsberry C, Morozov P, Fischer SG, Segal G, Qu X, Rzhetsky A, Zhang P, Cayanis E, De Jong PJ, Ju J, Kalachikov S, Shuman HA, Russo JJ.** 2004. The genomic sequence of the accidental pathogen *Legionella pneumophila*. Science **305:**1966-1968.
377. **Cazalet C, Gomez-Valero L, Rusniok C, Lomma M, Dervins-Ravault D, Newton HJ, Sansom FM, Jarraud S, Zidane N, Ma L, Bouchier C, Etienne J, Hartland EL, Buchrieser C.** 2010. Analysis of the *Legionella longbeachae* genome and transcriptome uncovers unique strategies to cause Legionnaires' disease. PLoS Genet **6:**e1000851.
378. **Kozak NA, Buss M, Lucas CE, Frace M, Govil D, Travis T, Olsen-Rasmussen M, Benson RF, Fields BS.** 2010. Virulence factors encoded by *Legionella longbeachae* identified on the basis of the genome sequence analysis of clinical isolate D-4968. J Bacteriol **192:**1030-1044.
379. **Gomez-Valero L, Rusniok C, Jarraud S, Vacherie B, Rouy Z, Barbe V, Medigue C, Etienne J, Buchrieser C.** 2011. Extensive recombination events and horizontal gene transfer shaped the *Legionella pneumophila* genomes. BMC Genomics **12:**536.
380. **Ensminger AW.** 2016. *Legionella pneumophila*, armed to the hilt: justifying the largest arsenal of effectors in the bacterial world. Curr Opin Microbiol **29:**74-80.

381. **Qiu J, Luo ZQ.** 2017. Legionella and Coxiella effectors: strength in diversity and activity. Nat Rev Microbiol **15:**591-605.
382. **Ensminger AW, Isberg RR.** 2010. E3 ubiquitin ligase activity and targeting of BAT3 by multiple *Legionella pneumophila* translocated substrates. Infect Immun **78:**3905-3919.
383. **Birmingham A, Selfors LM, Forster T, Wrobel D, Kennedy CJ, Shanks E, Santoyo-Lopez J, Dunican DJ, Long A, Kelleher D, Smith Q, Beijersbergen RL, Ghazal P, Shamu CE.** 2009. Statistical methods for analysis of high-throughput RNA interference screens. Nat Methods **6:**569-575.
384. **Rotty JD, Wu C, Haynes EM, Suarez C, Winkelman JD, Johnson HE, Haugh JM, Kovar DR, Bear JE.** 2015. Profilin-1 serves as a gatekeeper for actin assembly by Arp2/3-dependent and -independent pathways. Dev Cell **32:**54-67.
385. **Scheffzek K, Ahmadian MR.** 2005. GTPase activating proteins: structural and functional insights 18 years after discovery. Cell Mol Life Sci **62:**3014-3038.
386. **Amor JC, Swails J, Zhu X, Roy CR, Nagai H, Ingmundson A, Cheng X, Kahn RA.** 2005. The structure of RalF, an ADP-ribosylation factor guanine nucleotide exchange factor from *Legionella pneumophila*, reveals the presence of a cap over the active site. J Biol Chem **280:**1392-1400.
387. **Sjolinder M, Uhlmann J, Ponstingl H.** 2004. Characterisation of an evolutionary conserved protein interacting with the putative guanine nucleotide exchange factor DelGEF and modulating secretion. Exp Cell Res **294:**68-76.
388. **Sjolinder M, Uhlmann J, Ponstingl H.** 2002. DelGEF, a homologue of the Ran guanine nucleotide exchange factor RanGEF, binds to the exocyst component Sec5 and modulates secretion. FEBS Lett **532:**211-215.
389. **Marzioch M, Henthorn DC, Herrmann JM, Wilson R, Thomas DY, Bergeron JJ, Solari RC, Rowley A.** 1999. Erp1p and Erp2p, partners for Emp24p and Erv25p in a yeast p24 complex. Mol Biol Cell **10:**1923-1938.
390. **Otte S, Belden WJ, Heidtman M, Liu J, Jensen ON, Barlowe C.** 2001. Erv41p and Erv46p: new components of COPII vesicles involved in transport between the ER and Golgi complex. J Cell Biol **152:**503-518.
391. **Jung CH, Ro SH, Cao J, Otto NM, Kim DH.** 2010. mTOR regulation of autophagy. FEBS Lett **584:**1287-1295.
392. **Weiss WA, Taylor SS, Shokat KM.** 2007. Recognizing and exploiting differences between RNAi and small-molecule inhibitors. Nat Chem Biol **3:**739-744.
393. **Echeverri CJ, Beachy PA, Baum B, Boutros M, Buchholz F, Chanda SK, Downward J, Ellenberg J, Fraser AG, Hacohen N, Hahn WC, Jackson AL, Kiger A, Linsley PS, Lum L, Ma Y, Mathey-Prevot B, Root DE, Sabatini DM, Taipale J, Perrimon N, Bernards R.** 2006. Minimizing the risk of reporting false positives in large-scale RNAi screens. Nat Methods **3:**777-779.
394. **Parsons BD, Schindler A, Evans DH, Foley E.** 2009. A direct phenotypic comparison of siRNA pools and multiple individual duplexes in a functional assay. PLoS One **4:**e8471.
395. **Zhang XD, Kuan PF, Ferrer M, Shu X, Liu YC, Gates AT, Kunapuli P, Stec EM, Xu M, Marine SD, Holder DJ, Strulovici B, Heyse JF, Espeseth AS.** 2008. Hit selection with false discovery rate control in genome-scale RNAi screens. Nucleic Acids Res **36:**4667-4679.
396. **Zhang XD.** 2008. Novel analytic criteria and effective plate designs for quality control in genome-scale RNAi screens. J Biomol Screen **13:**363-377.
397. **International Human Genome Sequencing C.** 2004. Finishing the euchromatic sequence of the human genome. Nature **431:**931-945.

398. **Jensen ON.** 2004. Modification-specific proteomics: characterization of post-translational modifications by mass spectrometry. Curr Opin Chem Biol **8:**33-41.
399. **Beadle GW, Tatum EL.** 1941. Genetic Control of Biochemical Reactions in Neurospora. Proc Natl Acad Sci U S A **27:**499-506.
400. **Jensen ON.** 2006. Interpreting the protein language using proteomics. Nat Rev Mol Cell Biol **7:**391-403.
401. **Walsh CT, Garneau-Tsodikova S, Gatto GJ, Jr.** 2005. Protein posttranslational modifications: the chemistry of proteome diversifications. Angew Chem Int Ed Engl **44:**7342-7372.
402. **Michard C, Doublet P.** 2015. Post-translational modifications are key players of the *Legionella pneumophila* infection strategy. Front Microbiol **6:**87.
403. **Ribet D, Cossart P.** 2010. Pathogen-mediated posttranslational modifications: A re-emerging field. Cell **143:**694-702.
404. **Soufi B, Krug K, Harst A, Macek B.** 2015. Characterization of the *E. coli* proteome and its modifications during growth and ethanol stress. Front Microbiol **6:**103.
405. **Grangeasse C, Stulke J, Mijakovic I.** 2015. Regulatory potential of post-translational modifications in bacteria. Front Microbiol **6:**500.
406. **Li H, Xu H, Zhou Y, Zhang J, Long C, Li S, Chen S, Zhou JM, Shao F.** 2007. The phosphothreonine lyase activity of a bacterial type III effector family. Science **315:**1000-1003.
407. **Brennan DF, Barford D.** 2009. Eliminylation: a post-translational modification catalyzed by phosphothreonine lyases. Trends Biochem Sci **34:**108-114.
408. **Mazurkiewicz P, Thomas J, Thompson JA, Liu M, Arbibe L, Sansonetti P, Holden DW.** 2008. SpvC is a *Salmonella* effector with phosphothreonine lyase activity on host mitogen-activated protein kinases. Mol Microbiol **67:**1371-1383.
409. **Gomez-Valero L, Buchrieser C.** 2013. Genome dynamics in *Legionella*: the basis of versatility and adaptation to intracellular replication. Cold Spring Harb Perspect Med **3**.
410. **Lin YH, Doms AG, Cheng E, Kim B, Evans TR, Machner MP.** 2015. Host Cell-catalyzed S-Palmitoylation Mediates Golgi Targeting of the *Legionella* Ubiquitin Ligase GobX. J Biol Chem **290:**25766-25781.
411. **Ribet D, Cossart P.** 2010. Post-translational modifications in host cells during bacterial infection. FEBS Lett **584:**2748-2758.
412. **Hochstrasser M.** 2009. Origin and function of ubiquitin-like proteins. Nature **458:**422-429.
413. **Randow F, Lehner PJ.** 2009. Viral avoidance and exploitation of the ubiquitin system. Nat Cell Biol **11:**527-534.
414. **Hamilton MJ, Lee M, Le Roch KG.** 2014. The ubiquitin system: an essential component to unlocking the secrets of malaria parasite biology. Mol Biosyst **10:**715-723.
415. **Jiang X, Chen ZJ.** 2011. The role of ubiquitylation in immune defence and pathogen evasion. Nat Rev Immunol **12:**35-48.
416. **Cui J, Yao Q, Li S, Ding X, Lu Q, Mao H, Liu L, Zheng N, Chen S, Shao F.** 2010. Glutamine deamidation and dysfunction of ubiquitin/NEDD8 induced by a bacterial effector family. Science **329:**1215-1218.
417. **Sheedlo MJ, Qiu J, Tan Y, Paul LN, Luo ZQ, Das C.** 2015. Structural basis of substrate recognition by a bacterial deubiquitinase important for dynamics of phagosome ubiquitination. Proc Natl Acad Sci U S A **112:**15090-15095.
418. **Price CT, Richards AM, Abu Kwaik Y.** 2014. Nutrient generation and retrieval from the host cell cytosol by intra-vacuolar *Legionella pneumophila*. Front Cell Infect Microbiol **4:**111.

419. **Bardill JP, Miller JL, Vogel JP.** 2005. IcmS-dependent translocation of SdeA into macrophages by the *Legionella pneumophila* type IV secretion system. Mol Microbiol **56:**90-103.
420. **Holen T, Amarzguioui M, Wiiger MT, Babaie E, Prydz H.** 2002. Positional effects of short interfering RNAs targeting the human coagulation trigger Tissue Factor. Nucleic Acids Res **30:**1757-1766.
421. **Edelstein PH, Edelstein MA, Higa F, Falkow S.** 1999. Discovery of virulence genes of *Legionella pneumophila* by using signature tagged mutagenesis in a guinea pig pneumonia model. Proc Natl Acad Sci U S A **96:**8190-8195.
422. **Harb OS, Abu Kwaik Y.** 2000. Essential role for the *Legionella pneumophila* rep helicase homologue in intracellular infection of mammalian cells. Infect Immun **68:**6970-6978.
423. **Mintz CS, Chen JX, Shuman HA.** 1988. Isolation and characterization of auxotrophic mutants of *Legionella pneumophila* that fail to multiply in human monocytes. Infect Immun **56:**1449-1455.
424. **Thornbrough JM, Hundley T, Valdivia R, Worley MJ.** 2012. Human genome-wide RNAi screen for host factors that modulate intracellular *Salmonella* growth. PLoS One **7:**e38097.
425. **David Y, Ziv T, Admon A, Navon A.** 2010. The E2 ubiquitin-conjugating enzymes direct polyubiquitination to preferred lysines. J Biol Chem **285:**8595-8604.
426. **Jung P, Verdoodt B, Bailey A, Yates JR, 3rd, Menssen A, Hermeking H.** 2007. Induction of cullin 7 by DNA damage attenuates p53 function. Proc Natl Acad Sci U S A **104:**11388-11393.
427. **Celli J, Tsolis RM.** 2015. Bacteria, the endoplasmic reticulum and the unfolded protein response: friends or foes? Nat Rev Microbiol **13:**71-82.
428. **Mori K.** 2009. Signalling pathways in the unfolded protein response: development from yeast to mammals. J Biochem **146:**743-750.
429. **Christianson JC, Ye Y.** 2014. Cleaning up in the endoplasmic reticulum: ubiquitin in charge. Nat Struct Mol Biol **21:**325-335.
430. **Meyer H, Bug M, Bremer S.** 2012. Emerging functions of the VCP/p97 AAA-ATPase in the ubiquitin system. Nat Cell Biol **14:**117-123.
431. **Lencer WI.** 2001. Microbes and microbial Toxins: paradigms for microbial-mucosal toxins. *V. Cholera*: invasion of the intestinal epithelial barrier by a stably folded protein toxin. Am J Physiol Gastrointest Liver Physiol **280:**G781-786.
432. **Rodighiero C, Tsai B, Rapoport TA, Lencer WI.** 2002. Role of ubiquitination in retro-translocation of cholera toxin and escape of cytosolic degradation. EMBO Rep **3:**1222-1227.
433. **Schmitz A, Herrgen H, Winkeler A, Herzog V.** 2000. Cholera toxin is exported from microsomes by the Sec61p complex. J Cell Biol **148:**1203-1212.
434. **Centers for Disease C, Prevention.** 2011. Legionellosis --- United States, 2000-2009. MMWR Morb Mortal Wkly Rep **60:**1083-1086.
435. **Cunha BA, Burillo A, Bouza E.** 2016. Legionnaires' disease. Lancet **387:**376-385.
436. **Mulazimoglu L, Yu VL.** 2001. Can Legionnaires disease be diagnosed by clinical criteria? A critical review. Chest **120:**1049-1053.
437. **Cunha BA.** 2010. Legionnaires' disease: clinical differentiation from typical and other atypical pneumonias. Infect Dis Clin North Am **24:**73-105.
438. **Weisenburger DD, Helms CM, Renner ED.** 1981. Sporadic Legionnaires' disease. A pathologic study of 23 fatal cases. Arch Pathol Lab Med **105:**130-137.
439. **Lettinga KD, Verbon A, Nieuwkerk PT, Jonkers RE, Gersons BP, Prins JM, Speelman P.** 2002. Health-related quality of life and posttraumatic stress disorder among survivors of an outbreak of Legionnaires disease. Clin Infect Dis **35:**11-17.

440. **van Lier A, McDonald SA, Bouwknegt M, group EPI, Kretzschmar ME, Havelaar AH, Mangen MJ, Wallinga J, de Melker HE.** 2016. Disease Burden of 32 Infectious Diseases in the Netherlands, 2007-2011. PLoS One **11:**e0153106.
441. **Williams JM, Tsai B.** 2016. Intracellular trafficking of bacterial toxins. Curr Opin Cell Biol **41:**51-56.
442. **Nora T, Lomma M, Gomez-Valero L, Buchrieser C.** 2009. Molecular mimicry: an important virulence strategy employed by *Legionella pneumophila* to subvert host functions. Future Microbiol **4:**691-701.
443. **Qiu J, Sheedlo MJ, Yu K, Tan Y, Nakayasu ES, Das C, Liu X, Luo ZQ.** 2016. Ubiquitination independent of E1 and E2 enzymes by bacterial effectors. Nature **533:**120-124.
444. **Kotewicz KM, Ramabhadran V, Sjoblom N, Vogel JP, Haenssler E, Zhang M, Behringer J, Scheck RA, Isberg RR.** 2017. A Single *Legionella* Effector Catalyzes a Multistep Ubiquitination Pathway to Rearrange Tubular Endoplasmic Reticulum for Replication. Cell Host Microbe **21:**169-181.
445. **Zhang Y, Higashide W, Dai S, Sherman DM, Zhou D.** 2005. Recognition and ubiquitination of *Salmonella* type III effector SopA by a ubiquitin E3 ligase, HsRMA1. J Biol Chem **280:**38682-38688.
446. **Maculins T, Fiskin E, Bhogaraju S, Dikic I.** 2016. Bacteria-host relationship: ubiquitin ligases as weapons of invasion. Cell Res **26:**499-510.
447. **Ashida H, Kim M, Schmidt-Supprian M, Ma A, Ogawa M, Sasakawa C.** 2010. A bacterial E3 ubiquitin ligase IpaH9.8 targets NEMO/IKKgamma to dampen the host NF-kappaB-mediated inflammatory response. Nat Cell Biol **12:**66-73; sup pp 61-69.
448. **Fernandez-Prada CM, Hoover DL, Tall BD, Hartman AB, Kopelowitz J, Venkatesan MM.** 2000. *Shigella flexneri* IpaH(7.8) facilitates escape of virulent bacteria from the endocytic vacuoles of mouse and human macrophages. Infect Immun **68:**3608-3619.
449. **Suzuki S, Mimuro H, Kim M, Ogawa M, Ashida H, Toyotome T, Franchi L, Suzuki M, Sanada T, Suzuki T, Tsutsui H, Nunez G, Sasakawa C.** 2014. *Shigella* IpaH7.8 E3 ubiquitin ligase targets glomulin and activates inflammasomes to demolish macrophages. Proc Natl Acad Sci U S A **111:**E4254-4263.
450. **Aravind L, Koonin EV.** 2000. The U box is a modified RING finger - a common domain in ubiquitination. Curr Biol **10:**R132-134.
451. **Wu B, Skarina T, Yee A, Jobin MC, Dileo R, Semesi A, Fares C, Lemak A, Coombes BK, Arrowsmith CH, Singer AU, Savchenko A.** 2010. NleG Type 3 effectors from enterohaemorrhagic *Escherichia coli* are U-Box E3 ubiquitin ligases. PLoS Pathog **6:**e1000960.
452. **Hatakeyama S, Nakayama KI.** 2003. U-box proteins as a new family of ubiquitin ligases. Biochem Biophys Res Commun **302:**635-645.
453. **Sauer JD, Shannon JG, Howe D, Hayes SF, Swanson MS, Heinzen RA.** 2005. Specificity of *Legionella pneumophila* and *Coxiella burnetii* vacuoles and versatility of *Legionella pneumophila* revealed by coinfection. Infect Immun **73:**4494-4504.
454. **Tigertt WD, Benenson AS, Gochenour WS.** 1961. Airborne Q fever. Bacteriol Rev **25:**285-293.
455. **Carey KL, Newton HJ, Luhrmann A, Roy CR.** 2011. The *Coxiella burnetii* Dot/Icm system delivers a unique repertoire of type IV effectors into host cells and is required for intracellular replication. PLoS Pathog **7:**e1002056.
456. **McDonough JA, Newton HJ, Roy CR.** 2012. *Coxiella burnetii* secretion systems. Adv Exp Med Biol **984:**171-197.
457. **Moffatt JH, Newton P, Newton HJ.** 2015. *Coxiella burnetii*: turning hostility into a home. Cell Microbiol **17:**621-631.

458. **Newton HJ, McDonough JA, Roy CR.** 2013. Effector protein translocation by the *Coxiella burnetii* Dot/Icm type IV secretion system requires endocytic maturation of the pathogen-occupied vacuole. PLoS One **8:**e54566.
459. **Mindell JA.** 2012. Lysosomal acidification mechanisms. Annu Rev Physiol **74:**69-86.
460. **Smith C, Gore A, Yan W, Abalde-Atristain L, Li Z, He C, Wang Y, Brodsky RA, Zhang K, Cheng L, Ye Z.** 2014. Whole-genome sequencing analysis reveals high specificity of CRISPR/Cas9 and TALEN-based genome editing in human iPSCs. Cell Stem Cell **15:**12-13.
461. **Veres A, Gosis BS, Ding Q, Collins R, Ragavendran A, Brand H, Erdin S, Cowan CA, Talkowski ME, Musunuru K.** 2014. Low incidence of off-target mutations in individual CRISPR-Cas9 and TALEN targeted human stem cell clones detected by whole-genome sequencing. Cell Stem Cell **15:**27-30.

APPENDIX 1

List of genes that were analysed in secondary screen

Gene ID	Gene Symbol	Gene Full Name	Robust z-score
51248	PDZK11	PDZ domain containing 11	-5.73
5054	SERPINE1	serpin family E member 1	-5.23
342897	NCCRP1	non-specific cytotoxic cell receptor protein 1 homolog (zebrafish)	-5.14
286151	FBXO43	F-box protein 43	-4.89
340061	TMEM173	transmembrane protein 173	-4.89
25871	NEPRO	nucleolus and neural progenitor protein	-4.89
23142	DCUN1D4	defective in cullin neddylation 1 domain containing 4	-4.81
137682	NDUFAF6	NADH:ubiquinone oxidoreductase complex assembly factor 6	-4.72
7431	VIM	vimentin	-4.64
9503	XAGE1D	X antigen family, member 1D	-4.64
51667	NUB1	negative regulator of ubiquitin-like proteins 1	-4.55
55174	INTS10	integrator complex subunit 10	-4.55
81493	SYNC	syncoilin, intermediate filament protein	-4.55
253143	PRR14L	proline rich 14-like	-4.55
162461	TMEM92	transmembrane protein 92	-4.47
81610	FAM83D	family with sequence similarity 83 member D	-4.47
120379	PIH1D2	PIH1 domain containing 2	-4.38
148581	UBE2U	ubiquitin-conjugating enzyme E2U (putative)	-4.38
51465	UBE2J1	ubiquitin-conjugating enzyme E2 J1	-4.38
23322	RPGRIP1L	RPGRIP1-like	-4.38
84886	C1orf198	chromosome 1 open reading frame 198	-4.38
55627	SMPD4	sphingomyelin phosphodiesterase 4	-4.38
134111	UBE2QL1	ubiquitin-conjugating enzyme E2Q family-like 1	-4.3
23220	DTX4	deltex E3 ubiquitin ligase 4	-4.3
136332	LRGUK	leucine-rich repeats and guanylate kinase domain containing	-4.3
131118	DNAJC19	DnaJ heat shock protein family (Hsp40) member C19	-4.3
51335	NGRN	neugrin, neurite outgrowth associated	-4.3
83953	FCAMR	Fc fragment of IgA and IgM receptor	-4.3
388960	C2orf78	chromosome 2 open reading frame 78	-4.3
51619	UBE2D4	ubiquitin-conjugating enzyme E2D 4 (putative)	-4.22
55332	DRAM1	DNA-damage regulated autophagy modulator 1	-4.13
80224	NUBPL	nucleotide binding protein-like	-4.13
115939	TSR3	TSR3, acp transferase ribosome maturation factor	-4.13
7337	UBE3A	ubiquitin protein ligase E3A	-4.13
144203	OVOS2	ovostatin 2	-4.05
7335	UBE2V1	ubiquitin-conjugating enzyme E2 V1	-4.05
10477	UBE2E3	ubiquitin-conjugating enzyme E2 E3	-4.05
7320	UBE2B	ubiquitin-conjugating enzyme E2 B	-4.05
55832	CAND1	cullin-associated and neddylation dissociated 1	-4.05
23014	FBXO21	F-box protein 21	-4.05
84678	KDM2B	lysine demethylase 2B	-4.05
8835	SOCS2	suppressor of cytokine signaling 2	-4.05
126433	FBXO27	F-box protein 27	-4.05

Gene ID	Gene Symbol	Gene Full Name	Robust z-score
170392	OIT3	oncoprotein induced transcript 3	-4.05
151790	WDR49	WD repeat domain 49	-4.05
83986	FAM234A	family with sequence similarity 234 member A	-4.05
9136	RRP9	ribosomal RNA processing 9, small subunit (SSU) processome component, homolog (yeast)	-4.05
79091	METTL22	methyltransferase like 22	-4.05
126526	C19orf47	chromosome 19 open reading frame 47	-4.05
27076	LYPD3	LY6/PLAUR domain containing 3	-4.05
256987	SERINC5	serine incorporator 5	-4.05
347404	LANCL3	LanC like 3	-4.05
23371	TNS2	tensin 2	-3.96
79176	FBXL15	F-box and leucine-rich repeat protein 15	-3.96
90864	SPSB3	splA/ryanodine receptor domain and SOCS box containing 3	-3.96
54850	FBXL12	F-box and leucine-rich repeat protein 12	-3.96
10616	RBCK1	RANBP2-type and C3HC4-type zinc finger containing 1	-3.96
5608	MAP2K6	mitogen-activated protein kinase kinase 6	-3.88
4172	MCM3	minichromosome maintenance complex component 3	-3.88
84926	SPRYD3	SPRY domain containing 3	-3.88
164668	APOBEC3H	apolipoprotein B mRNA editing enzyme catalytic subunit 3H	-3.88
84975	MFSD5	major facilitator superfamily domain containing 5	-3.88
23327	NEDD4L	neural precursor cell expressed, developmentally down-regulated 4-like, E3 ubiquitin protein ligase	-3.88
9870	AREL1	apoptosis resistant E3 ubiquitin protein ligase 1	-3.88
7326	UBE2G1	ubiquitin-conjugating enzyme E2 G1	-3.88
140459	ASB6	ankyrin repeat and SOCS box containing 6	-3.88
80028	FBXL18	F-box and leucine-rich repeat protein 18	-3.88
84676	TRIM63	tripartite motif containing 63	-3.88
84219	WDR24	WD repeat domain 24	-3.88
84759	PCGF1	polycomb group ring finger 1	-3.88
10446	LRRN2	leucine rich repeat neuronal 2	-3.88
8642	DCHS1	dachsous cadherin-related 1	-3.88
84286	TMEM175	transmembrane protein 175	-3.88
64855	FAM129B	family with sequence similarity 129 member B	-3.88
134553	C5orf24	chromosome 5 open reading frame 24	-3.88
9980	DOPEY2	dopey family member 2	-3.88
64062	RBM26	RNA binding motif protein 26	-3.79
26190	FBXW2	F-box and WD repeat domain containing 2	-3.79
55700	MAP7D1	MAP7 domain containing 1	-3.79
55084	SOBP	sine oculis binding protein homolog	-3.79
255403	ZNF718	zinc finger protein 718	-3.79
83401	ELOVL3	ELOVL fatty acid elongase 3	-3.71
83460	EMC6	ER membrane protein complex subunit 6	-3.71
221718	LINC00518	long intergenic non-protein coding RNA 518	-3.71
56943	ENY2	ENY2, transcription and export complex 2 subunit	-3.71
23194	FBXL7	F-box and leucine-rich repeat protein 7	-3.71
200933	FBXO45	F-box protein 45	-3.71
353145	LCE3E	late cornified envelope 3E	-3.71

Gene ID	Gene Symbol	Gene Full Name	Robust z-score
55634	KRBOX4	KRAB box domain containing 4	-3.71
51534	VTA1	vesicle trafficking 1	-3.71
54958	TMEM160	transmembrane protein 160	-3.71
80213	TM2D3	TM2 domain containing 3	-3.71
80774	LIMD2	LIM domain containing 2	-3.71
83941	TM2D1	TM2 domain containing 1	-3.71
9370	ADIPOQ	adiponectin, C1Q and collagen domain containing	-3.71
441282	AKR1B15	aldo-keto reductase family 1 member B15	-3.71
169200	TMEM64	transmembrane protein 64	-3.71
843	CASP10	caspase 10	-3.71
146330	FBXL16	F-box and leucine-rich repeat protein 16	-3.71
90011	KIR3DX1	killer cell immunoglobulin like receptor, three Ig domains X1	-3.71
54737	MPHOSPH8	M-phase phosphoprotein 8	-3.63
79654	HECTD3	HECT domain containing 3	-3.63
7324	UBE2E1	ubiquitin-conjugating enzyme E2 E1	-3.63
64750	SMURF2	SMAD specific E3 ubiquitin protein ligase 2	-3.63
8450	CUL4B	cullin 4B	-3.63
374986	MIGA1	mitoguardin 1	-3.63
80143	SIKE1	suppressor of IKBKE 1	-3.63
286097	MICU3	mitochondrial calcium uptake family member 3	-3.63
286336	FAM78A	family with sequence similarity 78, member A	-3.63
79729	SH3D21	SH3 domain containing 21	-3.63
25764	HYPK	huntingtin interacting protein K	-3.54
85455	DISP2	dispatched RND transporter family member 2	-3.54
10961	ERP29	endoplasmic reticulum protein 29	-3.54
8916	HERC3	HECT and RLD domain containing E3 ubiquitin protein ligase 3	-3.54
10075	HUWE1	HECT, UBA and WWE domain containing 1, E3 ubiquitin protein ligase	-3.54
9039	UBA3	ubiquitin-like modifier activating enzyme 3	-3.54
57520	HECW2	HECT, C2 and WW domain containing E3 ubiquitin protein ligase 2	-3.54
150726	FBXO41	F-box protein 41	-3.54
140456	ASB11	ankyrin repeat and SOCS box containing 11	-3.54
8945	BTRC	beta-transducin repeat containing E3 ubiquitin protein ligase	-3.54
23291	FBXW11	F-box and WD repeat domain containing 11	-3.54
118430	MUCL1	mucin like 1	-3.54
54862	CC2D1A	coiled-coil and C2 domain containing 1A	-3.54
145497	LRRC74A	leucine rich repeat containing 74A	-3.54
152519	NIPAL1	NIPA-like domain containing 1	-3.54
149345	SHISA4	shisa family member 4	-3.54
79637	ARMC7	armadillo repeat containing 7	-3.54
29071	C1GALT1C1	C1GALT1-specific chaperone 1	-3.54
284948	SH2D6	SH2 domain containing 6	-3.54
85377	MICALL1	MICAL-like 1	-3.54
64342	HS1BP3	HCLS1 binding protein 3	-3.54
389792	IER5L	immediate early response 5-like	-3.54
84304	NUDT22	nudix hydrolase 22	-3.54
114932	MRFAP1L1	Morf4 family associated protein 1 like 1	-3.54

Gene ID	Gene Symbol	Gene Full Name	Robust z-score
389610	XKR5	XK related 5	-3.54
51249	TMEM69	transmembrane protein 69	-3.54
7318	UBA7	ubiquitin like modifier activating enzyme 7	-3.46
163782	KANK4	KN motif and ankyrin repeat domains 4	-3.46
493860	CCDC73	coiled-coil domain containing 73	-3.46
57465	TBC1D24	TBC1 domain family member 24	-3.46
81794	ADAMTS10	ADAM metallopeptidase with thrombospondin type 1 motif 10	-3.46
8452	CUL3	cullin 3	-3.46
83737	ITCH	itchy E3 ubiquitin protein ligase	-3.46
7323	UBE2D3	ubiquitin-conjugating enzyme E2 D3	-3.46
143279	HECTD2	HECT domain E3 ubiquitin protein ligase 2	-3.46
142686	ASB14	ankyrin repeat and SOCS box containing 14	-3.46
56995	TULP4	tubby like protein 4	-3.46
63891	RNF123	ring finger protein 123	-3.46
23295	MGRN1	mahogunin ring finger 1	-3.46
283742	FAM98B	family with sequence similarity 98 member B	-3.46
140700	SAMD10	sterile alpha motif domain containing 10	-3.46
79149	ZSCAN5A	zinc finger and SCAN domain containing 5A	-3.46
22982	DIP2C	disco interacting protein 2 homolog C	-3.46
23059	CLUAP1	clusterin associated protein 1	-3.46
92610	TIFA	TRAF interacting protein with forkhead associated domain	-3.46
256710	GLIPR1L1	GLI pathogenesis related 1 like 1	-3.46
9887	SMG7	SMG7, nonsense mediated mRNA decay factor	-3.46
138724	C9orf131	chromosome 9 open reading frame 131	-3.46
79780	CCDC82	coiled-coil domain containing 82	-3.46
85407	NKD1	naked cuticle homolog 1	-3.37
1302	COL11A2	collagen type XI alpha 2 chain	-3.37
144983	HNRNPA1L2	heterogeneous nuclear ribonucleoprotein A1-like 2	-3.37
256979	SUN3	Sad1 and UNC84 domain containing 3	-3.37
132299	OCIAD2	OCIA domain containing 2	-3.37
29070	CCDC113	coiled-coil domain containing 113	-3.37
388646	GBP7	guanylate binding protein 7	-3.37
92181	UBTD2	ubiquitin domain containing 2	-3.37
132228	LSMEM2	leucine rich single-pass membrane protein 2	-3.37
9476	NAPSA	napsin A aspartic peptidase	-3.37
7874	USP7	ubiquitin specific peptidase 7	-3.37
29089	UBE2T	ubiquitin-conjugating enzyme E2 T	-3.37
11059	WWP1	WW domain containing E3 ubiquitin protein ligase 1	-3.37
8451	CUL4A	cullin 4A	-3.37
26223	FBXL21	F-box and leucine-rich repeat protein 21 (gene/pseudogene)	-3.37
140461	ASB8	ankyrin repeat and SOCS box containing 8	-3.37
55272	IMP3	IMP3, U3 small nucleolar ribonucleoprotein	-3.37
124817	CNTD1	cyclin N-terminal domain containing 1	-3.37
125150	ZSWIM7	zinc finger SWIM-type containing 7	-3.37
56889	TM9SF3	transmembrane 9 superfamily member 3	-3.37
132660	LIN54	lin-54 DREAM MuvB core complex component	-3.37
55726	ASUN	asunder, spermatogenesis regulator	-3.37

Gene ID	Gene Symbol	Gene Full Name	Robust z-score
90381	TICRR	TOPBP1 interacting checkpoint and replication regulator	-3.37
9725	TMEM63A	transmembrane protein 63A	-3.37
140465	MYL6B	myosin light chain 6B	-3.37
84548	TMEM185A	transmembrane protein 185A	-3.37
84319	CMSS1	cms1 ribosomal small subunit homolog (yeast)	-3.37
121274	ZNF641	zinc finger protein 641	-3.37
157680	VPS13B	vacuolar protein sorting 13 homolog B	-3.37
90693	CCDC126	coiled-coil domain containing 126	-3.37
84247	LDOC1L	leucine zipper down-regulated in cancer 1-like	-3.37
80304	WDCP	WD repeat and coiled coil containing	-3.37
6738	TROVE2	TROVE domain family member 2	-3.37
54830	NUP62CL	nucleoporin 62 C-terminal like	-3.37
338773	TMEM119	transmembrane protein 119	-3.37
51274	KLF3	Kruppel like factor 3	-3.29
64900	LPIN3	lipin 3	-3.29
11009	IL24	interleukin 24	-3.29
64766	S100PBP	S100P binding protein	-3.29
55262	C7orf43	chromosome 7 open reading frame 43	-3.29
164284	APCDD1L	APC down-regulated 1 like	-3.29
54790	TET2	tet methylcytosine dioxygenase 2	-3.29
223075	CCDC129	coiled-coil domain containing 129	-3.29
57095	PITHD1	PITH domain containing 1	-3.29
116135	LRRC3B	leucine rich repeat containing 3B	-3.29
53616	ADAM22	ADAM metallopeptidase domain 22	-3.29
26168	SENP3	SUMO1/sentrin/SMT3 specific peptidase 3	-3.29
201456	FBXO15	F-box protein 15	-3.29
9655	SOCS5	suppressor of cytokine signaling 5	-3.29
8269	TMEM187	transmembrane protein 187	-3.29
79877	DCAKD	dephospho-CoA kinase domain containing	-3.29
55171	TBCCD1	TBCC domain containing 1	-3.29
340252	ZNF680	zinc finger protein 680	-3.29
116224	FAM122A	family with sequence similarity 122A	-3.29
122961	ISCA2	iron-sulfur cluster assembly 2	-3.29
23302	WSCD1	WSC domain containing 1	-3.29
84337	ELOF1	elongation factor 1 homolog	-3.29
55779	CFAP44	cilia and flagella associated protein 44	-3.29
51108	METTL9	methyltransferase like 9	-3.29
401944	LDLRAD2	low density lipoprotein receptor class A domain containing 2	-3.29
55249	YY1AP1	YY1 associated protein 1	-3.29
390927	ZNF793	zinc finger protein 793	-3.29
65084	TMEM135	transmembrane protein 135	-3.29
10603	SH2B2	SH2B adaptor protein 2	-3.29
151742	PPM1L	protein phosphatase, Mg2+/Mn2+ dependent 1L	-3.2
3688	ITGB1	integrin subunit beta 1	-3.2
349149	GJC3	gap junction protein gamma 3	-3.2
57691	KIAA1586	KIAA1586	-3.2
51330	TNFRSF12A	tumor necrosis factor receptor superfamily member 12A	-3.2

Gene ID	Gene Symbol	Gene Full Name	Robust z-score
144193	AMDHD1	amidohydrolase domain containing 1	-3.2
163259	DENND2C	DENN domain containing 2C	-3.2
55323	LARP6	La ribonucleoprotein domain family member 6	-3.2
63929	XPNPEP3	X-prolyl aminopeptidase 3	-3.2
4326	MMP17	matrix metallopeptidase 17	-3.2
1540	CYLD	CYLD lysine 63 deubiquitinase	-3.2
11085	ADAM30	ADAM metallopeptidase domain 30	-3.2
3250	HPR	haptoglobin-related protein	-3.2
51366	UBR5	ubiquitin protein ligase E3 component n-recognin 5	-3.2
25831	HECTD1	HECT domain E3 ubiquitin protein ligase 1	-3.2
7322	UBE2D2	ubiquitin-conjugating enzyme E2 D2	-3.2
84166	NLRC5	NLR family CARD domain containing 5	-3.2
84961	FBXL20	F-box and leucine-rich repeat protein 20	-3.2
10966	RAB40B	RAB40B, member RAS oncogene family	-3.2
151525	WDSUB1	WD repeat, sterile alpha motif and U-box domain containing 1	-3.2
158506	ZNF645	zinc finger protein 645	-3.2
55282	LRRC36	leucine rich repeat containing 36	-3.2
54414	SIAE	sialic acid acetylesterase	-3.2
26059	ERC2	ELKS/RAB6-interacting/CAST family member 2	-3.2
54360	CYTL1	cytokine-like 1	-3.2
63901	FAM111A	family with sequence similarity 111 member A	-3.2
285852	TREML4	triggering receptor expressed on myeloid cells like 4	-3.2
79073	TMEM109	transmembrane protein 109	-3.2
114769	CARD16	caspase recruitment domain family member 16	-3.2
146845	CFAP52	cilia and flagella associated protein 52	-3.2
4641	MYO1C	myosin IC	-3.12
9821	RB1CC1	RB1 inducible coiled-coil 1	-3.12
339231	ARL16	ADP ribosylation factor like GTPase 16	-3.12
85016	C11orf70	chromosome 11 open reading frame 70	-3.12
29895	MYLPF	myosin light chain, phosphorylatable, fast skeletal muscle	-3.12
1803	DPP4	dipeptidyl peptidase 4	-3.12
25825	BACE2	beta-site APP-cleaving enzyme 2	-3.12
55284	UBE2W	ubiquitin-conjugating enzyme E2 W (putative)	-3.12
9820	CUL7	cullin 7	-3.12
4734	NEDD4	neural precursor cell expressed, developmentally down-regulated 4, E3 ubiquitin protein ligase	-3.12
79754	ASB13	ankyrin repeat and SOCS box containing 13	-3.12
10612	TRIM3	tripartite motif containing 3	-3.12
85449	KIAA1755	KIAA1755	-3.12
54812	AFTPH	aftiphilin	-3.12
144809	FAM216B	family with sequence similarity 216 member B	-3.12
26099	SZRD1	SUZ RNA binding domain containing 1	-3.12
148304	C1orf74	chromosome 1 open reading frame 74	-3.12
153339	TMEM167A	transmembrane protein 167A	-3.12
26071	FAM127B	family with sequence similarity 127 member B	-3.12
57863	CADM3	cell adhesion molecule 3	-3.12
10068	IL18BP	interleukin 18 binding protein	-3.04

Gene ID	Gene Symbol	Gene Full Name	Robust z-score
6348	CCL3	C-C motif chemokine ligand 3	-3.04
54865	GPATCH4	G-patch domain containing 4	-3.04
5199	CFP	complement factor properdin	-3.04
57719	ANO8	anoctamin 8	-3.04
400757	C1orf141	chromosome 1 open reading frame 141	-3.04
112936	VPS26B	VPS26, retromer complex component B	-3.04
54942	FAM206A	family with sequence similarity 206 member A	-3.04
51027	BOLA1	bolA family member 1	-3.04
27252	KLHL20	kelch like famile member 20	-3.04
345062	PRSS48	protease, serine 48	-3.04
9159	PCSK7	proprotein convertase subtilisin/kexin type 7	-3.04
5122	PCSK1	proprotein convertase subtilisin/kexin type 1	-3.04
7512	XPNPEP2	X-prolyl aminopeptidase 2	-3.04
11330	CTRC	chymotrypsin C	-3.04
3093	UBE2K	ubiquitin-conjugating enzyme E2 K	-3.04
54165	DCUN1D1	defective in cullin neddylation 1 domain containing 1	-3.04
65264	UBE2Z	ubiquitin-conjugating enzyme E2 Z	-3.04
7332	UBE2L3	ubiquitin-conjugating enzyme E2 L3	-3.04
55008	HERC6	HECT and RLD domain containing E3 ubiquitin protein ligase family member 6	-3.04
7321	UBE2D1	ubiquitin-conjugating enzyme E2 D1	-3.04
9320	TRIP12	thyroid hormone receptor interactor 12	-3.04
26091	HERC4	HECT and RLD domain containing E3 ubiquitin protein ligase 4	-3.04
26261	FBXO24	F-box protein 24	-3.04
6468	FBXW4	F-box and WD repeat domain containing 4	-3.04
440730	TRIM67	tripartite motif containing 67	-3.04
117584	RFFL	ring finger and FYVE like domain containing E3 ubiquitin protein ligase	-3.04
157769	FAM91A1	family with sequence similarity 91 member A1	-3.04
64773	PCED1A	PC-esterase domain containing 1A	-3.04
54831	BEST2	bestrophin 2	-3.04
124842	TMEM132E	transmembrane protein 132E	-3.04
158431	ZNF782	zinc finger protein 782	-3.04
84923	FAM104A	family with sequence similarity 104 member A	-3.04
220001	VWCE	von Willebrand factor C and EGF domains	-3.04
342510	CD300E	CD300e molecule	-3.04
81037	CLPTM1L	CLPTM1 like	-3.04
29789	OLA1	Obg like ATPase 1	-3.04
119710	C11orf74	chromosome 11 open reading frame 74	-3.04
388581	FAM132A	family with sequence similarity 132 member A	-3.04
5822	PWP2	PWP2 periodic tryptophan protein homolog (yeast)	-3.04
113277	TMEM106A	transmembrane protein 106A	-3.04
55112	WDR60	WD repeat domain 60	-3.04
51290	ERGIC2	ERGIC and golgi 2	-3.04
126119	JOSD2	Josephin domain containing 2	-3.04
389860	PAGE2B	PAGE family member 2B	-3.04
84191	FAM96A	family with sequence similarity 96 member A	-3.04
80173	IFT74	intraflagellar transport 74	-3.04
57655	GRAMD1A	GRAM domain containing 1A	-3.04

Gene ID	Gene Symbol	Gene Full Name	Robust z-score
144348	ZNF664	zinc finger protein 664	-3.04
146713	RBFOX3	RNA binding protein, fox-1 homolog 3	-3.04
283377	SPRYD4	SPRY domain containing 4	-3.04
9636	ISG15	ISG15 ubiquitin-like modifier	-3.04
221294	NT5DC1	5'-nucleotidase domain containing 1	-3.04
339500	ZNF678	zinc finger protein 678	-3.04
84296	GINS4	GINS complex subunit 4	-3.04
200205	IBA57	IBA57 homolog, iron-sulfur cluster assembly	-3.04
79074	C2orf49	chromosome 2 open reading frame 49	-3.04
6447	SCG5	secretogranin V	-3.04
84260	TCHP	trichoplein keratin filament binding	-3.04
23550	PSD4	pleckstrin and Sec7 domain containing 4	-2.95
84727	SPSB2	splA/ryanodine receptor domain and SOCS box containing 2	-2.95
51665	ASB1	ankyrin repeat and SOCS box containing 1	-2.95
6048	RNF5	ring finger protein 5	-2.95
8453	CUL2	cullin 2	-2.87
84259	DCUN1D5	defective in cullin neddylation 1 domain containing 5	-2.87
55293	UEVLD	UEV and lactate/malate dehyrogenase domains	-2.87
7329	UBE2I	ubiquitin-conjugating enzyme E2 I	-2.87
54926	UBE2R2	ubiquitin-conjugating enzyme E2 R2	-2.87
9690	UBE3C	ubiquitin protein ligase E3C	-2.87
84893	FBXO18	F-box protein, helicase, 18	-2.87
9306	SOCS6	suppressor of cytokine signaling 6	-2.87
6502	SKP2	S-phase kinase associated protein 2	-2.87
222235	FBXL13	F-box and leucine-rich repeat protein 13	-2.87
283807	FBXL22	F-box and leucine-rich repeat protein 22	-2.87
51676	ASB2	ankyrin repeat and SOCS box containing 2	-2.87
9978	RBX1	ring-box 1	-2.87
4302	MLLT6	MLLT6, PHD finger domain containing	-2.87
283450	HECTD4	HECT domain E3 ubiquitin protein ligase 4	-2.78
7336	UBE2V2	ubiquitin-conjugating enzyme E2 V2	-2.78
27338	UBE2S	ubiquitin-conjugating enzyme E2 S	-2.78
9021	SOCS3	suppressor of cytokine signaling 3	-2.78
92591	ASB16	ankyrin repeat and SOCS box containing 16	-2.78
140460	ASB7	ankyrin repeat and SOCS box containing 7	-2.78
9744	ACAP1	ArfGAP with coiled-coil, ankyrin repeat and PH domains 1	-2.78
29922	NME7	NME/NM23 family member 7	-2.78
11065	UBE2C	ubiquitin-conjugating enzyme E2 C	-2.7
57154	SMURF1	SMAD specific E3 ubiquitin protein ligase 1	-2.7
7334	UBE2N	ubiquitin-conjugating enzyme E2 N	-2.7
51191	HERC5	HECT and RLD domain containing E3 ubiquitin protein ligase 5	-2.7
63893	UBE2O	ubiquitin-conjugating enzyme E2 O	-2.7
51725	FBXO40	F-box protein 40	-2.7
899	CCNF	cyclin F	-2.7
554251	FBXO48	F-box protein 48	-2.7
26231	LRRC29	leucine rich repeat containing 29	-2.7
26118	WSB1	WD repeat and SOCS box containing 1	-2.7

Gene ID	Gene Symbol	Gene Full Name	Robust z-score
22992	KDM2A	lysine demethylase 2A	-2.7
26271	FBXO5	F-box protein 5	-2.7
140458	ASB5	ankyrin repeat and SOCS box containing 5	-2.7
84261	FBXW9	F-box and WD repeat domain containing 9	-2.7
26233	FBXL6	F-box and leucine-rich repeat protein 6	-2.7
140825	NEURL2	neuralized E3 ubiquitin protein ligase 2	-2.7
26224	FBXL3A	F-box and leucine-rich repeat protein 3	-2.7
26267	FBXO10	F-box protein 10	-2.7
399664	MEX3D	mex-3 RNA binding family member D	-2.7
22893	BAHD1	bromo adjacent homology domain containing 1	-2.7
5216	PFN1	profilin 1	-2.7
26297	SERGEF	secretion regulating guanine nucleotide exchange factor	-2.7
91807	MYLK3	myosin light chain kinase 3	-2.7
8925	HERC1	HECT and RLD domain containing E3 ubiquitin protein ligase family member 1	-2.61
7328	UBE2H	ubiquitin-conjugating enzyme E2 H	-2.61
23403	FBXO46	F-box protein 46	-2.61
79876	UBA5	ubiquitin-like modifier activating enzyme 5	-2.53
55208	DCUN1D2	defective in cullin neddylation 1 domain containing 2	-2.53
64400	AKTIP	AKT interacting protein	-2.53
11060	WWP2	WW domain containing E3 ubiquitin protein ligase 2	-2.53
54455	FBXO42	F-box protein 42	-2.53
80176	SPSB1	splA/ryanodine receptor domain and SOCS box containing 1	-2.53
23219	FBXO28	F-box protein 28	-2.53
81545	FBXO38	F-box protein 38	-2.53
127247	ASB17	ankyrin repeat and SOCS box containing 17	-2.53
51666	ASB4	ankyrin repeat and SOCS box containing 4	-2.53
9781	RNF144A	ring finger protein 144A	-2.53
26524	LATS2	large tumor suppressor kinase 2	-2.61
9064	MAP3K6	mitogen-activated protein kinase kinase kinase 6	-2.61
7084	TK2	thymidine kinase 2, mitochondrial	-2.53
65125	WNK1	WNK lysine deficient protein kinase 1	-2.53
92912	UBE2Q2	ubiquitin-conjugating enzyme E2 Q2	-2.36
55585	UBE2Q1	ubiquitin-conjugating enzyme E2 Q1	-1.94
51729	WBP11	WW domain binding protein 11	3.04
84919	PPP1R15B	protein phosphatase 1 regulatory subunit 15B	3.04
4218	RAB8A	RAB8A, member RAS oncogene family	3.04
5467	PPARD	peroxisome proliferator activated receptor delta	3.04
9360	PPIG	peptidylprolyl isomerase G	3.04
165530	CLEC4F	C-type lectin domain family 4 member F	3.04
7568	ZNF20	zinc finger protein 20	3.04
1994	ELAVL1	ELAV like RNA binding protein 1	3.04
10687	PNMA2	paraneoplastic Ma antigen 2	3.04
134829	CLVS2	clavesin 2	3.04
89890	KBTBD6	kelch repeat and BTB domain containing 6	3.04
84654	SPZ1	spermatogenic leucine zipper 1	3.04
5733	PTGER3	prostaglandin E receptor 3	3.04
11163	NUDT4	nudix hydrolase 4	3.04

Gene ID	Gene Symbol	Gene Full Name	Robust z-score
553128	KIR2DL5B	killer cell immunoglobulin like receptor, two Ig domains and long cytoplasmic tail 5B	3.04
4067	LYN	LYN proto-oncogene, Src family tyrosine kinase	3.12
152926	PPM1K	protein phosphatase, Mg2+/Mn2+ dependent 1K	3.12
2519	FUCA2	fucosidase, alpha-L- 2, plasma	3.12
91603	ZNF830	zinc finger protein 830	3.12
202018	TAPT1	transmembrane anterior posterior transformation 1	3.12
27199	OXGR1	oxoglutarate receptor 1	3.12
9248	GPR50	G protein-coupled receptor 50	3.12
3117	HLA-DQA1	major histocompatibility complex, class II, DQ alpha 1	3.12
10929	SRSF8	serine and arginine rich splicing factor 8	3.12
8019	BRD3	bromodomain containing 3	3.2
225689	MAPK15	mitogen-activated protein kinase 15	3.2
5481	PPID	peptidylprolyl isomerase D	3.2
10499	NCOA2	nuclear receptor coactivator 2	3.2
112703	FAM71E1	family with sequence similarity 71 member E1	3.2
10360	NPM3	nucleophosmin/nucleoplasmin 3	3.2
55777	MBD5	methyl-CpG binding domain protein 5	3.2
11094	CACFD1	calcium channel flower domain containing 1	3.2
139425	DCAF8L1	DDB1 and CUL4 associated factor 8 like 1	3.2
51537	MTFP1	mitochondrial fission process 1	3.2
84878	ZBTB45	zinc finger and BTB domain containing 45	3.2
400673	VMAC	vimentin-type intermediate filament associated coiled-coil protein	3.2
58508	KMT2C	lysine methyltransferase 2C	3.2
2852	GPER1	G protein-coupled estrogen receptor 1	3.2
8811	GALR2	galanin receptor 2	3.2
4158	MC2R	melanocortin 2 receptor	3.2
139378	ADGRG4	adhesion G protein-coupled receptor G4	3.2
5414	SEPT4	septin 4	3.29
114815	SORCS1	sortilin related VPS10 domain containing receptor 1	3.29
2867	FFAR2	free fatty acid receptor 2	3.29
162083	C16orf82	chromosome 16 open reading frame 82	3.29
6305	SBF1	SET binding factor 1	3.37
26051	PPP1R16B	protein phosphatase 1 regulatory subunit 16B	3.37
80824	DUSP16	dual specificity phosphatase 16	3.37
7915	ALDH5A1	aldehyde dehydrogenase 5 family member A1	3.37
79154	DHRS11	dehydrogenase/reductase 11	3.37
5198	PFAS	phosphoribosylformylglycinamidine synthase	3.37
80168	MOGAT2	monoacylglycerol O-acyltransferase 2	3.37
23054	NCOA6	nuclear receptor coactivator 6	3.37
3092	HIP1	huntingtin interacting protein 1	3.37
79679	VTCN1	V-set domain containing T cell activation inhibitor 1	3.37
55559	HAUS7	HAUS augmin like complex subunit 7	3.37
123920	CMTM3	CKLF like MARVEL transmembrane domain containing 3	3.37
57506	MAVS	mitochondrial antiviral signaling protein	3.37
399693	CCDC187	coiled-coil domain containing 187	3.37

Gene ID	Gene Symbol	Gene Full Name	Robust z-score
1352	COX10	COX10, heme A:farnesyltransferase cytochrome c oxidase assembly factor	3.46
8976	WASL	Wiskott-Aldrich syndrome-like	3.46
84440	RAB11FIP4	RAB11 family interacting protein 4	3.46
553158	PRR5-ARHGAP8	PRR5-ARHGAP8 readthrough	3.46
5297	PI4KA	phosphatidylinositol 4-kinase alpha	3.54
8497	PPFIA4	PTPRF interacting protein alpha 4	3.54
8697	CDC23	cell division cycle 23	3.54
83855	KLF16	Kruppel like factor 16	3.54
25792	CIZ1	CDKN1A interacting zinc finger protein 1	3.54
5145	PDE6A	phosphodiesterase 6A	3.54
6642	SNX1	sorting nexin 1	3.54
124460	SNX20	sorting nexin 20	3.54
10978	CLP1	cleavage and polyadenylation factor I subunit 1	3.54
29083	GTPBP8	GTP-binding protein 8 (putative)	3.54
10277	UBE4B	ubiquitination factor E4B	3.54
27198	HCAR1	hydroxycarboxylic acid receptor 1	3.54
10316	NMUR1	neuromedin U receptor 1	3.54
1880	GPR183	G protein-coupled receptor 183	3.54
51163	DBR1	debranching RNA lariats 1	3.63
2882	GPX7	glutathione peroxidase 7	3.71
55346	TCP11L1	t-complex 11 like 1	3.71
8464	SUPT3H	SPT3 homolog, SAGA and STAGA complex component	3.79
8501	SLC43A1	solute carrier family 43 member 1	3.79
9716	AQR	aquarius intron-binding spliceosomal factor	3.79
1580	CYP4B1	cytochrome P450 family 4 subfamily B member 1	3.88
4247	MGAT2	mannosyl (alpha-1,6-)-glycoprotein beta-1,2-N-acetylglucosaminyltransferase	3.88
23035	PHLPP2	PH domain and leucine rich repeat protein phosphatase 2	3.88
116328	C8orf34	chromosome 8 open reading frame 34	3.88
136	ADORA2B	adenosine A2b receptor	3.88
8326	FZD9	frizzled class receptor 9	3.88
6899	TBX1	T-box 1	3.96
26298	EHF	ETS homologous factor	3.96
6869	TACR1	tachykinin receptor 1	3.96
5510	PPP1R7	protein phosphatase 1 regulatory subunit 7	4.05
248	ALPI	alkaline phosphatase, intestinal	4.05
9441	MED26	mediator complex subunit 26	4.05
10370	CITED2	Cbp/p300-interacting transactivator with Glu/Asp-rich carboxy-terminal domain, 2	4.05
143686	SESN3	sestrin 3	4.13
3355	HTR1F	5-hydroxytryptamine receptor 1F	4.13
4881	NPR1	natriuretic peptide receptor 1	4.13
832	CAPZB	capping actin protein of muscle Z-line beta subunit	4.3
50717	DCAF8	DDB1 and CUL4 associated factor 8	4.3
8729	GBF1	golgi brefeldin A resistant guanine nucleotide exchange factor 1	4.38
348738	C2orf48	chromosome 2 open reading frame 48	4.38

Gene ID	Gene Symbol	Gene Full Name	Robust z-score
56413	LTB4R2	leukotriene B4 receptor 2	4.38
10383	TUBB4B	tubulin beta 4B class IVb	4.47
5788	PTPRC	protein tyrosine phosphatase, receptor type C	4.72
27241	BBS9	Bardet-Biedl syndrome 9	4.72
91526	ANKRD44	ankyrin repeat domain 44	4.72
3613	IMPA2	inositol monophosphatase 2	4.89
8761	PABPC4	poly(A) binding protein cytoplasmic 4	4.89
91147	TMEM67	transmembrane protein 67	4.89
166979	CDC20B	cell division cycle 20B	4.89
613212	CTXN3	cortexin 3	4.89
8467	SMARCA5	SWI/SNF related, matrix associated, actin dependent regulator of chromatin, subfamily a, member 5	5.14
5536	PPP5C	protein phosphatase 5 catalytic subunit	5.31
151242	PPP1R1C	protein phosphatase 1 regulatory inhibitor subunit 1C	5.4
57408	LRTM1	leucine-rich repeats and transmembrane domains 1	5.48
8612	PLPP2	phospholipid phosphatase 2	5.65
55034	MOCOS	molybdenum cofactor sulfurase	7.76

Non-highlighted entries refer to genes that led to reduction in RalF translocation when silenced. Highlighted entries refer to genes that led to increase in RalF translocation when silenced.

APPENDIX 2

Complete list of secondary screening results

Gene ID	Gene Symbol	No. of validated duplex
51248	PDZK11	3
5054	SERPINE1	0
342897	NCCRP1	3
286151	FBXO43	1
340061	TMEM173	0
25871	NEPRO	1
23142	DCUN1D4	2
137682	NDUFAF6	2
7431	VIM	2
9503	XAGE1D	0
51667	NUB1	3
55174	INTS10	3
81493	SYNC	1
253143	PRR14L	0
162461	TMEM92	0
81610	FAM83D	1
120379	PIH1D2	1
148581	UBE2U	2
51465	UBE2J1	1
23322	RPGRIP1L	1
84886	C1orf198	1
55627	SMPD4	1
134111	UBE2QL1	3
23220	DTX4	0
136332	LRGUK	1
131118	DNAJC19	0
51335	NGRN	1
83953	FCAMR	2
388960	C2orf78	1
51619	UBE2D4	0
55332	DRAM1	1
80224	NUBPL	0
115939	TSR3	0
7337	UBE3A	4
144203	OVOS2	1
7335	UBE2V1	2
10477	UBE2E3	2
7320	UBE2B	1
55832	CAND1	0

Gene ID	Gene Symbol	No. of validated duplex
23014	FBXO21	2
84678	KDM2B	1
8835	SOCS2	1
126433	FBXO27	1
170392	OIT3	0
151790	WDR49	2
83986	FAM234A	2
9136	RRP9	1
79091	METTL22	2
126526	C19orf47	1
27076	LYPD3	0
256987	SERINC5	1
347404	LANCL3	1
23371	TNS2	3
79176	FBXL15	0
90864	SPSB3	1
54850	FBXL12	0
10616	RBCK1	1
5608	MAP2K6	1
4172	MCM3	2
84926	SPRYD3	3
164668	APOBEC3H	2
84975	MFSD5	3
23327	NEDD4L	2
9870	AREL1	0
7326	UBE2G1	2
140459	ASB6	0
80028	FBXL18	0
84676	TRIM63	2
84219	WDR24	0
84759	PCGF1	1
10446	LRRN2	2
8642	DCHS1	0
84286	TMEM175	2
64855	FAM129B	0
134553	C5orf24	0
9980	DOPEY2	0
64062	RBM26	2
26190	FBXW2	0

Gene ID	Gene Symbol	No. of validated duplex
255403	ZNF718	0
83401	ELOVL3	2
83460	EMC6	1
221718	LINC00518	1
56943	ENY2	3
23194	FBXL7	0
200933	FBXO45	0
353145	LCE3E	2
55634	KRBOX4	1
51534	VTA1	2
54958	TMEM160	0
80213	TM2D3	1
80774	LIMD2	1
83941	TM2D1	0
9370	ADIPOQ	0
441282	AKR1B15	1
169200	TMEM64	1
843	CASP10	1
146330	FBXL16	0
90011	KIR3DX1	0
54737	MPHOSPH8	1
79654	HECTD3	2
7324	UBE2E1	2
64750	SMURF2	1
8450	CUL4B	0
374986	MIGA1	1
80143	SIKE1	2
286097	MICU3	0
286336	FAM78A	1
79729	SH3D21	1
25764	HYPK	1
85455	DISP2	2
10961	ERP29	2
8916	HERC3	2
10075	HUWE1	2
9039	UBA3	0
57520	HECW2	1
150726	FBXO41	1
140456	ASB11	1
8945	BTRC	1
55700	MAP7D1	2
55084	SOBP	1

Gene ID	Gene Symbol	No. of validated duplex
23291	FBXW11	0
118430	MUCL1	2
54862	CC2D1A	0
145497	LRRC74A	1
152519	NIPAL1	3
149345	SHISA4	0
79637	ARMC7	0
29071	C1GALT1C1	2
284948	SH2D6	2
85377	MICALL1	1
64342	HS1BP3	2
389792	IER5L	0
84304	NUDT22	1
114932	MRFAP1L1	2
389610	XKR5	1
51249	TMEM69	2
7318	UBA7	0
163782	KANK4	0
493860	CCDC73	1
57465	TBC1D24	2
81794	ADAMTS10	1
8452	CUL3	2
83737	ITCH	0
7323	UBE2D3	1
143279	HECTD2	1
142686	ASB14	0
56995	TULP4	0
63891	RNF123	0
23295	MGRN1	0
283742	FAM98B	1
140700	SAMD10	1
79149	ZSCAN5A	1
22982	DIP2C	1
23059	CLUAP1	2
92610	TIFA	2
256710	GLIPR1L1	0
9887	SMG7	2
138724	C9orf131	1
79780	CCDC82	1
85407	NKD1	3
1302	COL11A2	2
144983	HNRNPA1L2	1

Gene ID	Gene Symbol	No. of validated duplex
256979	SUN3	2
132299	OCIAD2	0
29070	CCDC113	1
388646	GBP7	1
92181	UBTD2	1
132228	LSMEM2	1
9476	NAPSA	1
7874	USP7	1
29089	UBE2T	0
11059	WWP1	0
8451	CUL4A	1
26223	FBXL21	1
140461	ASB8	0
55272	IMP3	0
124817	CNTD1	1
125150	ZSWIM7	2
56889	TM9SF3	0
132660	LIN54	0
55726	ASUN	0
90381	TICRR	2
9725	TMEM63A	1
140465	MYL6B	1
84548	TMEM185A	1
84319	CMSS1	0
121274	ZNF641	0
157680	VPS13B	0
90693	CCDC126	1
84247	LDOC1L	1
80304	WDCP	1
6738	TROVE2	1
54830	NUP62CL	0
338773	TMEM119	0
51274	KLF3	2
64900	LPIN3	2
11009	IL24	1
64766	S100PBP	1
55262	C7orf43	0
164284	APCDD1L	1
54790	TET2	1
223075	CCDC129	3
57095	PITHD1	1
116135	LRRC3B	2

Gene ID	Gene Symbol	No. of validated duplex
53616	ADAM22	0
26168	SENP3	1
201456	FBXO15	0
9655	SOCS5	1
8269	TMEM187	2
79877	DCAKD	2
55171	TBCCD1	1
340252	ZNF680	0
116224	FAM122A	0
122961	ISCA2	1
23302	WSCD1	0
84337	ELOF1	1
55779	CFAP44	0
51108	METTL9	0
401944	LDLRAD2	1
55249	YY1AP1	0
390927	ZNF793	0
65084	TMEM135	2
10603	SH2B2	1
151742	PPM1L	0
3688	ITGB1	1
349149	GJC3	1
57691	KIAA1586	1
51330	TNFRSF12A	0
144193	AMDHD1	0
163259	DENND2C	2
55323	LARP6	1
63929	XPNPEP3	3
4326	MMP17	0
1540	CYLD	0
11085	ADAM30	2
3250	HPR	0
51366	UBR5	2
25831	HECTD1	0
7322	UBE2D2	1
84166	NLRC5	0
84961	FBXL20	0
10966	RAB40B	0
151525	WDSUB1	1
158506	ZNF645	1
55282	LRRC36	3
54414	SIAE	0

Gene ID	Gene Symbol	No. of validated duplex
26059	ERC2	1
54360	CYTL1	1
63901	FAM111A	0
285852	TREML4	1
79073	TMEM109	1
114769	CARD16	1
146845	CFAP52	2
4641	MYO1C	2
9821	RB1CC1	3
339231	ARL16	1
85016	C11orf70	0
29895	MYLPF	2
1803	DPP4	0
25825	BACE2	1
55284	UBE2W	0
9820	CUL7	3
4734	NEDD4	0
79754	ASB13	1
10612	TRIM3	0
85449	KIAA1755	1
54812	AFTPH	2
144809	FAM216B	2
26099	SZRD1	1
148304	C1orf74	0
153339	TMEM167A	1
26071	FAM127B	2
57863	CADM3	0
10068	IL18BP	3
6348	CCL3	2
54865	GPATCH4	2
5199	CFP	1
57719	ANO8	0
400757	C1orf141	1
112936	VPS26B	1
54942	FAM206A	0
51027	BOLA1	1
27252	KLHL20	3
345062	PRSS48	1
9159	PCSK7	0
5122	PCSK1	0
7512	XPNPEP2	2
11330	CTRC	0

Gene ID	Gene Symbol	No. of validated duplex
3093	UBE2K	1
54165	DCUN1D1	0
65264	UBE2Z	0
7332	UBE2L3	0
55008	HERC6	0
7321	UBE2D1	0
9320	TRIP12	1
26091	HERC4	1
26261	FBXO24	1
6468	FBXW4	0
440730	TRIM67	0
117584	RFFL	0
157769	FAM91A1	0
64773	PCED1A	1
54831	BEST2	1
124842	TMEM132E	1
158431	ZNF782	2
84923	FAM104A	0
220001	VWCE	2
342510	CD300E	1
81037	CLPTM1L	0
29789	OLA1	0
119710	C11orf74	0
388581	FAM132A	0
5822	PWP2	1
113277	TMEM106A	1
55112	WDR60	1
51290	ERGIC2	0
126119	JOSD2	0
389860	PAGE2B	0
84191	FAM96A	1
80173	IFT74	0
57655	GRAMD1A	0
144348	ZNF664	0
146713	RBFOX3	0
283377	SPRYD4	1
9636	ISG15	0
221294	NT5DC1	1
339500	ZNF678	1
84296	GINS4	1
200205	IBA57	1
79074	C2orf49	1

Gene ID	Gene Symbol	No. of validated duplex
6447	SCG5	0
84260	TCHP	0
23550	PSD4	1
84727	SPSB2	1
51665	ASB1	1
6048	RNF5	0
8453	CUL2	1
84259	DCUN1D5	0
55293	UEVLD	0
7329	UBE2I	1
54926	UBE2R2	0
9690	UBE3C	2
84893	FBXO18	0
9306	SOCS6	0
6502	SKP2	1
222235	FBXL13	0
283807	FBXL22	2
51676	ASB2	1
9978	RBX1	0
4302	MLLT6	0
283450	HECTD4	0
7336	UBE2V2	0
27338	UBE2S	0
9021	SOCS3	2
92591	ASB16	2
140460	ASB7	0
9744	ACAP1	2
29922	NME7	2
11065	UBE2C	0
57154	SMURF1	0
7334	UBE2N	0
51191	HERC5	1
63893	UBE2O	0
51725	FBXO40	0
899	CCNF	0
554251	FBXO48	0
26231	LRRC29	1
26118	WSB1	0
22992	KDM2A	0
26271	FBXO5	1
140458	ASB5	2
84261	FBXW9	1

Gene ID	Gene Symbol	No. of validated duplex
26233	FBXL6	1
140825	NEURL2	1
26224	FBXL3A	0
26267	FBXO10	0
399664	MEX3D	0
22893	BAHD1	1
5216	PFN1	3
26297	SERGEF	3
91807	MYLK3	1
8925	HERC1	1
7328	UBE2H	1
23403	FBXO46	1
79876	UBA5	0
55208	DCUN1D2	0
64400	AKTIP	0
11060	WWP2	0
54455	FBXO42	0
80176	SPSB1	0
23219	FBXO28	0
81545	FBXO38	1
127247	ASB17	0
51666	ASB4	0
9781	RNF144A	1
26524	LATS2	0
9064	MAP3K6	0
7084	TK2	0
65125	WNK1	1
92912	UBE2Q2	0
55585	UBE2Q1	3
51729	WBP11	2
84919	PPP1R15B	0
4218	RAB8A	1
5467	PPARD	0
9360	PPIG	0
165530	CLEC4F	0
7568	ZNF20	1
1994	ELAVL1	2
10687	PNMA2	0
134829	CLVS2	0
89890	KBTBD6	0
84654	SPZ1	0
5733	PTGER3	3

Gene ID	Gene Symbol	No. of validated duplex
11163	NUDT4	2
553128	KIR2DL5B	0
4067	LYN	3
152926	PPM1K	3
2519	FUCA2	0
91603	ZNF830	0
202018	TAPT1	1
27199	OXGR1	2
9248	GPR50	3
3117	HLA-DQA1	1
10929	SRSF8	1
8019	BRD3	3
225689	MAPK15	3
5481	PPID	0
10499	NCOA2	1
112703	FAM71E1	0
10360	NPM3	0
55777	MBD5	0
11094	CACFD1	0
139425	DCAF8L1	0
51537	MTFP1	0
84878	ZBTB45	0
400673	VMAC	0
58508	KMT2C	1
2852	GPER1	2
8811	GALR2	2
4158	MC2R	2
139378	ADGRG4	2
5414	SEPT4	1
114815	SORCS1	3
2867	FFAR2	3
162083	C16orf82	0
6305	SBF1	4
26051	PPP1R16B	1
80824	DUSP16	2
7915	ALDH5A1	1
79154	DHRS11	3
5198	PFAS	0
80168	MOGAT2	0
23054	NCOA6	0
3092	HIP1	0

Gene ID	Gene Symbol	No. of validated duplex
79679	VTCN1	0
55559	HAUS7	0
123920	CMTM3	0
57506	MAVS	1
399693	CCDC187	0
1352	COX10	0
8976	WASL	0
84440	RAB11FIP4	0
553158	PRR5-ARHGAP8	0
5297	PI4KA	1
8497	PPFIA4	2
8697	CDC23	0
83855	KLF16	0
25792	CIZ1	0
5145	PDE6A	0
6642	SNX1	0
124460	SNX20	0
10978	CLP1	0
29083	GTPBP8	0
10277	UBE4B	1
27198	HCAR1	2
10316	NMUR1	2
1880	GPR183	1
51163	DBR1	2
2882	GPX7	0
55346	TCP11L1	0
8464	SUPT3H	1
8501	SLC43A1	0
9716	AQR	0
1580	CYP4B1	2
4247	MGAT2	0
23035	PHLPP2	1
116328	C8orf34	1
136	ADORA2B	4
8326	FZD9	2
6899	TBX1	0
26298	EHF	0
6869	TACR1	2
5510	PPP1R7	2
248	ALPI	3
9441	MED26	0

Gene ID	Gene Symbol	No. of validated duplex
10370	CITED2	2
143686	SESN3	0
3355	HTR1F	2
4881	NPR1	3
832	CAPZB	1
50717	DCAF8	0
8729	GBF1	0
348738	C2orf48	1
56413	LTB4R2	2
10383	TUBB4B	0
5788	PTPRC	1
27241	BBS9	0
91526	ANKRD44	0
3613	IMPA2	2
8761	PABPC4	0
91147	TMEM67	0
166979	CDC20B	0
613212	CTXN3	0
8467	SMARCA5	0
5536	PPP5C	2
151242	PPP1R1C	3
57408	LRTM1	0
8612	PLPP2	3
55034	MOCOS	1